Príloha č. 1.

Králová S. (2017) Role of fatty acids in cold adaptation of Antarctic psychrophilic *Flavobacterium* spp. *Syst. Appl. Microbiol.*, 40(6): 329-333. Doi: 10.1016/j.syapm.2017.06.001

Systematic and Applied Microbiology 40 (2017) 329–333

Contents lists available at ScienceDirect

Systematic and Applied Microbiology

journal homepage: www.elsevier.de/syapm

Role of fatty acids in cold adaptation of Antarctic psychrophilic *Flavobacterium* spp.

Stanislava Králová

Czech Collection of Microorganisms, Department of Experimental Biology, Faculty of Science, Masaryk University, Kamenice 5, 62500 Brno, Czech Republic

ARTICLE INFO

Article history:
Received 9 May 2017
Received in revised form 8 June 2017
Accepted 12 June 2017

Keywords:
Flavobacterium
Antarctic bacteria
Adaptation
Fatty acids
Cell membrane
Cold-shock

ABSTRACT

Cold-loving microorganisms developed numerous adaptation mechanisms allowing them to survive in extremely cold habitats, such as adaptation of the cell membrane. The focus of this study was on the membrane fatty acids of Antarctic *Flavobacterium* spp., and their adaptation response to cold-stress. Fatty acids and cold-response of Antarctic flavobacteria was also compared to mesophilic and thermophilic members of the genus *Flavobacterium*. The results showed that the psychrophiles produced more types of major fatty acids than meso- and thermophilic members of this genus, namely $C_{15:1}$ iso G, $C_{15:0}$ iso, $C_{15:0}$ anteiso, $C_{15:1}$ *ω6c*, $C_{15:0}$ iso 3OH, $C_{17:1}$ *ω6c*, $C_{16:0}$ iso 3OH and $C_{17:0}$ iso 3OH, summed features 3 ($C_{16:1}$ *ω7*cand/or $C_{16:1}$ *ω6c*) and 9 ($C_{16:0}$ 10-methyl and/or $C_{17:1}$ iso *ω9c*). It was shown that the cell membrane of psychrophiles was composed mainly of branched and unsaturated fatty acids. The results also implied that Antarctic flavobacteria mainly used two mechanisms of membrane fluidity alteration in their cold-adaptive response. The first mechanism was based on unsaturation of fatty acids, and the second mechanism on *de novo* synthesis of branched fatty acids. The alteration of the cell membrane was shown to be similar for all thermotypes of members of the genus *Flavobacterium*.

Introduction

Microscopic life in cold regions of the Earth is characterized by a high biodiversity comprised mainly of microorganisms such as bacteria, fungi and microalgae [6]. To survive in conditions typical of cold regions (cold temperature, a lack of water and/or nutrients, intense UV irradiation and/or higher salinity) various adaptation mechanisms are required [7]. Of these conditions, cold temperatures strongly affect microbial cellular functions by influencing cell integrity, water viscosity, diffusion rates, the kinetics of enzyme reactions and membrane fluidity [7].

In recent years, researchers have intensively studied cold-adapted bacteria in order to determine the adaptations related to their cytoplasmic membrane [13]. The composition of the membrane fatty acids (FAs) strongly affects membrane properties by influencing fluidity and/or biological functions, such as solute uptake, nutrient transport, osmotic pressure and/or energy production [4]. These functions are directly associated with natural forms of biomembranes represented by the semi-liquid state of lipid structures. It is well known that environmental conditions and stresses strongly affect cell membrane structure, due to the cellular effort needed to maintain a liquid crystalline state [4,12,25,29,30]. The response of bacterial cells leading to maintenance of a fully functional cell membrane is termed homeoviscous adaptation.

Bacteria achieve homeoviscous adaptation to low temperatures (cold-shock) by using several mechanisms. These cold-induced responses are common among different bacterial groups and include an increase in FA unsaturation, FA methyl branching and/or increasing the *iso*/*anteiso*-branched FAs ratio [8,22–24]. Moreover, with a decrease in temperature, the average length of FAs, as well as the sterol/phospholipid ratio, have been shown to decrease [13,25]. These changes in different combinations and quantities allow bacteria to retain membrane function and fluidity [24] and thereby sustain the survival of these bacterial cells.

Previously, a number of bacterial species have been studied in order to characterize their membranes or the mechanisms of their membrane temperature adaptation. These studies were mainly focused on Gram-positive bacteria, such as members of the genera *Bacillus*, *Clostridium*, *Micrococcus* or *Listeria monocytogenes* [2,8,20,21,31]. Within the Gram-negative bacteria, the main object of chemotaxonomic studies has been the cell wall structure [10,14,15,19,27,29].

This current study focused on the cold-adapted *Flavobacterium* spp. isolated from Antarctica, and on their cell membrane properties. The aims of the study were: (i) to determine the FA composition

E-mail address: stanci@mail.muni.cz

http://dx.doi.org/10.1016/j.syapm.2017.06.001
0723-2020/

of Antarctic *Flavobacterium* spp., (ii) to determine their cold-adaptation mechanisms to low temperatures due to alteration of the FA composition, (iii) to compare the FAs of Antarctic flavobacteria to mesophilic and thermophilic reference strains of the genus *Flavobacterium*, and (iv) to compare the cold-shock response of all three of these thermotypes.

Materials and methods

Bacterial strains

Two groups of *Flavobacterium* spp. were used in this study. The first group included 28 unique psychrophilic gliding *Flavobacterium* spp. isolated from terrestrial abiotic sources in Antarctica (various water sources, rocks and regolith from James Ross Island). The strains used are listed and detailed in Table S1. These psychrophilic species exhibited the main characteristics of the genus *Flavobacterium*: Gram-negative rods with a yellow pigment exhibiting gliding motility. The assignment of these bacteria to the genus *Flavobacterium* was based on sequencing of their 16S rRNA gene and MALDI-TOF MS analysis (data not shown). All strains grew well under aerobic conditions at a temperature of 20 °C.

The second group was comprised of mesophilic flavobacteria reference cultures and one thermophilic reference culture of *Flavobacterium thermophilum* CCM 3694^T with optimal growth temperatures of 25–30 °C and 50 °C, respectively. The reference strains were obtained from the Czech Collection of Microorganisms (http://www.sci.muni.cz/ccm/) and are detailed in Table S2.

Cultivation for fatty acid methyl ester (FAME) analysis

All strains used in the study were cultured under optimal growth conditions for 48 h, and at temperatures that decreased by approximately 10 °C (for 48 or 72 h) in order to investigate the cold-shock response of their cell membranes. The psychrophilic strains used for FA analysis were grown on R2A agar at 20 ± 2 °C and 10 ± 2 °C for 48 and 72 h, respectively. The mesophilic reference strains used were grown on R2A agar at 30 ± 2 °C and 20 ± 2 °C, 25 ± 2 °C and 15 ± 2 °C for 48 h, and one thermophilic strain of *F. thermophilum* was grown at 50 ± 2 °C and 40 ± 2 °C for 48 h. Bacterial biomass was harvested from the third sector of growth on agar plates, where the cultures reached the late exponential growth phase, as previously described [26].

The FAME analysis

The extraction of fatty acid methyl esters was performed according to the standard protocol of the Sherlock® Microbial Identification System [26]. Cellular FA extracts were analysed by GC (model 7890B, Agilent) using the rapid Sherlock® Microbial Identification system (MIS, version 6.2B, MIDI database: RTSBA6, MIDI Inc.). Quantities of individual FAs are given as percentages of all named FAs. Randomly selected strains were tested three times in order to evaluate the reproducibility of the method.

Results and discussion

Reproducibility

Bacterial FA composition is influenced by several factors, including the culture medium, the incubation temperature and the culture's physiological age. It is well known that if standardized parameters are used for FAME analysis, highly reproducible patterns can be obtained [11,18]. In this part of the study, 5 psychrophilic strains, 4 mesophilic strains and *F. thermophilum* were re-cultivated three times and their FAs were analysed. The cultivation temperatures were initially set up according to optimal growth temperatures (20 °C, 25 °C, 30 °C and 50 °C) and, using standard deviation values, more stable FA profiles were obtained after cultivation for 48 h. The same process was repeated with the strains cultivated under lower cultivation temperatures (10 °C, 15 °C, 20 °C and 40 °C). In this case, the FA values varied less when the cultivation of Antarctic strains was prolonged for 72 h, since the growth rate decreased significantly at lower temperature. The indicator of the late exponential growth phase required for harvesting the bacterial biomass was confluent growth in the third sector of the agar plates, which was reached after 72 h cultivation. FA profiles of mesophilic flavobacteria and *F. thermophilum* CCM 3496^T were again most reproducible after cultivation for 48 h. In general, the FA amounts varied by less than 2%, which indicated high reproducibility and stability of FA composition patterns.

Fatty acid composition of Antarctic Flavobacterium *strains*

A total of 42 FAs were detected in the FAME profiles for all the 28 Antarctic flavobacteria cultivated under optimal growth conditions (20 ± 2 °C, 48 h). Nineteen FAs were uniformly present among all strains, with 10 of them present at values greater than 4% for most strains, and these were assigned as the main FAs of the Antarctic gliding *Flavobacterium* spp. (Fig. S1; bold emphasized in Table S3). According to Bernardet and Bowman [3], it is clear that members of the genus *Flavobacterium* have typically high amounts of $C_{15:0}$ iso, and significant amounts of $C_{15:0}$, $C_{15:0}$ iso 3OH, $C_{15:0}$ anteiso, $C_{15:1}$ iso G, $C_{15:1}$ *ω6c*, $C_{16:0}$ iso 3OH, $C_{17:0}$ iso 3OH, $C_{15:0}$ iso 2OH and/or $C_{16:1}$ *ω7c* and/or $C_{16:1}$ *ω7t*. In this study, the highest quantities were found among branched FAs, namely $C_{15:0}$ iso (18.6%), $C_{15:0}$ anteiso (6.0%), $C_{15:0}$ iso 3OH (8.4%), $C_{17:0}$ iso 3OH (8.2%), $C_{15:1}$ iso G (9.6%) and summed feature 3 containing $C_{16:1}$ *ω7c* and/or $C_{16:1}$ *ω6c* (12.6%). Slightly lower quantities were detected for $C_{17:1}$ *ω6c* (3.7%) and $C_{16:0}$ iso 3OH (5.3%). These major components matched the taxa-specific FAs mentioned above, except for summed feature 9 that included $C_{16:0}$ 10-methyl and/or $C_{17:1}$ iso *ω9c* (4.3%), which were found among all strains in quantities varying from 0.8 to 7.7%. These FAs made up approximately 83% of the overall FA membrane content. Thus, the results clearly showed that the cell membrane of the unique Antarctic flavobacteria was composed mainly of branched and unsaturated FAs that participated in fluidization of the cell membrane at low temperatures, thus maintaining and supporting the membrane's functionality [2,8,12,23].

Fatty acid composition of Antarctic Flavobacterium *spp. after temperature downshift*

The cold-shock response of the cell membrane and the composition of FAs was investigated by lowering the cultivation temperature to 10 ± 2 °C. A total of 42 fatty acids and one alcohol were detected in the FAME analysis of all 28 Antarctic *Flavobacterium* spp. cultivated at lower temperatures. Twenty-five FAs were uniformly present among these strains, with nine of them present at values greater than 4% in the majority of strains (Fig. S1; bold emphasized in Table S3).

Influence of low temperature on fatty acid composition of Antarctic flavobacteria

The most frequently recognized change due to lower temperatures is the unsaturation of FAs in bacterial membranes [23]. In aerobic bacterial species, this change is performed as an oxygen-dependent enzymatic modification of the already existing FAs [1]. In the group of 28 psychrophilic flavobacteria in this study, this trend was markedly obvious (Fig. 1). While the overall quantity

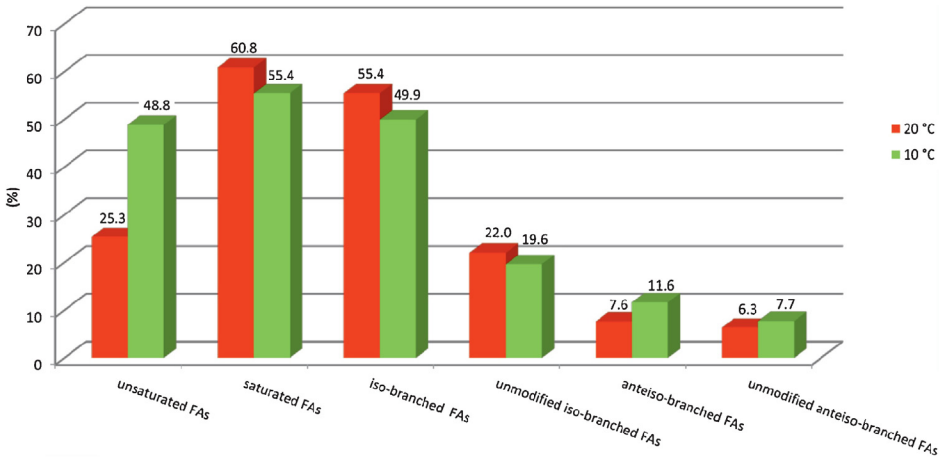

Fig. 1. Major changes in fatty acid composition among Antarctic flavobacteria cultivated at 20 ± 2 °C and 10 ± 2 °C.

of unsaturated FAs increased from 25.3% to 48.8%, the number of saturated FAs dropped at lower temperatures. The number of saturated straight FAs only decreased from 2.4% to 2.0%, but the overall content of saturated FAs decreased from 60.8% to 55.4%. Moreover, unsaturated $C_{17:1}$ anteiso *ω9c* was only detected after decreasing the temperature (Fig. S1), indicating its function in sustaining the membrane's semi-liquid state at low temperatures.

Another frequent change of membrane composition involves shortening of the fatty acid chain length [12,22]. This modification leads to a reduction of the Van der Waals interactions, thus reducing the viscosity of lipids and increasing the fluidity of membranes [22]. Some bacterial species have even been shown to regulate membrane fluidity by chain length alteration rather than unsaturation of FAs [9,23,21]. For Gram-negative bacteria, the shortening of $C_{18:1}$ to $C_{16:1}$ would be expected based on already known data [12]. Among the Antarctic strains in this current study, the long chain FAs with more than 18 carbons were detected only as $C_{18:1}$ *ω9c*, and the content of this FA indeed decreased with decreasing temperature, while the quantity of $C_{16:1}$ *ω5c* increased. However, this change occurred on such a small scale that it would only be speculation to consider this change as significant. In a previous study on *Bacillus megaterium*, the relative quantity of long chain FAs (C_{16}—C_{18}) increased significantly with increasing temperature and *vice versa* for short chain FAs (C_{14}—C_{15}) [20]. However, in the group of psychrophiles used in this study, no opposite trend could be found despite the expectations.

More important for these Antarctic flavobacterial strains was the branching of FAs. Branched FAs fluidize the cell membrane due to their lower melting temperatures (mostly *anteiso*-FAs) and significantly lower the phase transition temperatures (both *iso*,- and *anteiso*-FAs) [12,28]. This mechanism involves *de novo* synthesis of branched FAs and is usually connected to changes in the ratio of *iso*,- and *anteiso*-branched FAs [12]. The overall content of *iso*-branched FAs (modified with OH, a double bond, or unmodified) decreased from 55.4% to 49.9%, while the *anteiso*-branched FA contents increased from 7.6% to 11.6% (Fig. 1). The same trend was observed when only unmodified *iso/anteiso*-branched FAs were compared (Fig. 1). Although all branched FAs are known to participate in the fluidizing of the bacterial membrane, it seems that *anteiso*-FAs are more important for preventing the membrane transforming into a crystalline state [5,8,12]. This can be explained by the dual liquidising properties of *anteiso*-FAs, their lower melting temperatures and their lower phase transition temperatures [12].

Although other modifications in response to cold temperature have been described, such as hydroxylation, cyclization or isomerization of FAs [4,23,30], none of them were observed in the present study. Interestingly, it has also been described that Antarctic bacteria produce higher amounts of polyunsaturated FAs in order to maintain their membrane fluidity, such as was the case of the previously examined *Polaribacter glomeratus* [16]. However, the only polyunsaturated FAs detected among the Antarctic strains here were $C_{20:4}$ *ω6* and $C_{18:3}$ *ω6*. Additionally, $C_{20:4}$ *ω6* was only detected in five strains and only in trace amounts (<0.1%), and $C_{18:3}$ *ω6* was identified in one single strain. No correlation was observed between the temperature downshift and production of these polyunsaturated FAs, even though *P. glomeratus* is known to have a close phylogenetic relationship with the genus *Flavobacterium* and a similar response could be expected.

Fatty acid composition of mesophilic reference flavobacteria species and F. thermophilum *CCM 3496^T*

A total of 46 FAs were detected in the FAME analysis of ten mesophilic flavobacteria cultivated under optimal growth conditions (30 ± 2 °C, and 25 ± 2 °C for 48 h). Seventeen FAs were uniformly present among these strains, with five of them present in most strains at values greater than 4%. These five FAs were considered to be the main FAs of mesophilic *Flavobacterium* spp. (bold emphasized in Fig. S2; Table S4). After the temperature downshift to 20 ± 2 °C and 15 ± 2 °C, a total of 45 FAs were detected and 12 of them were uniform among all the analysed strains (Fig. S2; Table S4).

When the reference strain *F. thermophilum* CCM 3496^T was cultivated at an optimal growth temperature of 50 ± 2 °C for 48 h, sixteen FAs were found in its FAME profile. The main FAs were $C_{16:0}$, $C_{15:0}$ iso, $C_{16:0}$ iso, $C_{17:0}$ anteiso, $C_{17:0}$ iso 3OH and summed feature 3 (Fig. S3; bold emphasized in Table S5). After the temperature downshift to 40 ± 2 °C, eighteen FAs were detected. Except for the aforementioned major FAs, the 4% cut-off value was also reached by $C_{17:0}$ iso and $C_{17:1}$ iso *ω5c* (emphasized in Table S5 and Fig. S3).

Comparison of fatty acid composition of psychrophilic to mesophilic and thermophilic species

To determine if the FA composition in cold-adapted flavobacteria from Antarctica was unique and specific, the mesophilic species of the genus *Flavobacterium* and thermophilic *F. thermophilum* were also analysed. The 4% cut-off value was reached by mesophiles for only five FAs compared to Antarctic strains, namely $C_{15:0}$ iso, $C_{15:0}$ iso 3OH, $C_{16:0}$ iso 3OH, $C_{17:0}$ iso 3OH and summed feature 3 containing $C_{16:1}$ *ω7c* and/or $C_{16:1}$ *ω6c* (Fig. S2). Together with the

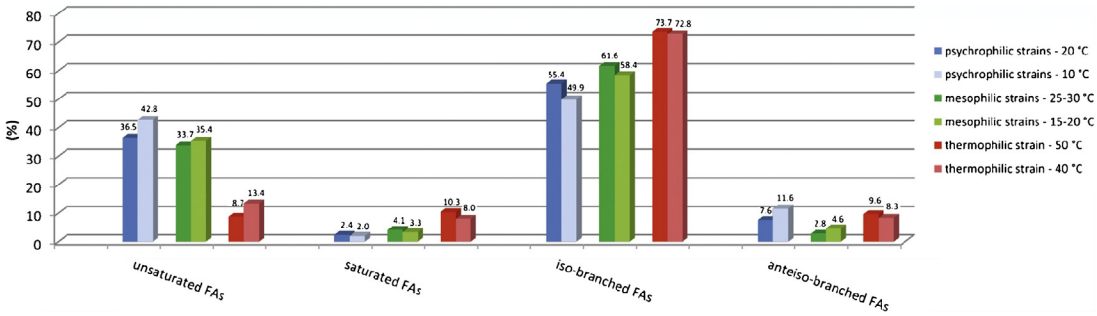

Fig. 2. Comparison of major changes in fatty acid composition among psychrophilic, mesophilic and thermophilic strains.

additional FA $C_{15:1}$ iso G (detected in 7/10 and 9/10 strains), these six FAs comprised approximately 71% of the overall FA content, and the remainder was covered by a number of minor FAs (Table S4). However, Antarctic flavobacteria possessed more branched and unsaturated FA types at values above 4%, which indicated the importance of these FAs for survival under extreme Antarctic conditions. These specific, additive compounds were $C_{15:1}$ *ω6c*, $C_{17:1}$ *ω6c*, $C_{15:0}$ anteiso, $C_{15:1}$ iso G and summed feature 9 ($C_{16:0}$ 10-methyl and/or $C_{17:1}$ iso *ω9c*) (Fig. S1, Table S3).

The FAME analysis of *F. thermophilum* showed an even more varied FA composition, expressing five FAs as major components. Out of these, only $C_{15:0}$ iso and $C_{17:0}$ iso 3OH (Fig. S3) were found to be major components similar to psychro- and mesophilic strains. The other three major FAs were saturated $C_{16:0}$, $C_{15:0}$ iso and $C_{17:0}$ anteiso (Fig. S3). Therefore, it was obvious that adaptation to higher temperatures was not only connected to higher quantities of saturated FAs, but also to *iso*-branched FAs, such as $C_{15:0}$ iso.

The temperature tolerance of the bacterial membrane can be evaluated based on the overall content of unsaturated FAs [5,9]. In this study, the content of unsaturated FAs decreased significantly from cold-adapted Antarctic flavobacteria (36.5%) to mesophilic species (33.7%) and *F. thermophilum* CCM 3496^T (8.7%) (Fig. 2). Moreover, after the temperature downshift, the content of unsaturated FAs increased in all three groups up to 42.8%, 35.4% and 13.4%, respectively (Fig. 2). This meant that adaptation to low temperatures in the genus *Flavobacterium* seemed to be associated at first with naturally higher quantities of unsaturated FAs in the membranes of cold-adapted species, but after cold stress also with active unsaturation of FAs.

Similarly, when the content of saturated FA was compared, significant differences were found. Antarctic strains possessed four types of unsaturated straight FAs comprising 2.4% of all FAs, whereas mesophilic species had 4.1% and *F. thermophilum* showed the highest amount with 10.3% (Fig. 2). Interestingly, after the temperature downshift, the decrease of these FAs was on a small-scale for psychro- and mesophilic strains (up to 2.0% and 3.3%, respectively), but was more significant for *F. thermophilum* (to 8%) with the entire loss of $C_{17:0}$ (Fig. S3; Table S5).

Regarding the chain length modification, neither mesophilic strains nor *F. thermophilum* CCM 3496^T were found to alter their FAs significantly. This mechanism therefore does not seem to be of great importance for *Flavobacterium* spp. as regards temperature adaptation compared to other Gram-negative bacteria [22,30]. However, one interesting correlation was found for *F. thermophilum* CCM 3496^T, the quantity of shorter $C_{16:0}$ iso decreased with decreasing temperature (from 12.7 to 10.5%) and the longer chain $C_{17:0}$ iso was only produced after cold-shock (Fig. S1), which is contrary to previous findings [17,31]. This was exactly opposite to the shortening of FAs at cold temperatures. This might be explained by the fact that $C_{17:0}$ iso possesses a lower phase transition temperature than $C_{16:0}$ iso [12], and it could have a greater impact on sustaining the membrane's semi-liquid state than shortening of the FAs has.

Finally, the presence of branched FAs was compared between all three flavobacterial thermotypes (Fig. 2). The overall content of *iso*-branched FAs was detected at high amounts in all three flavobacteria groups, with the lowest abundance occurring in psychrophilic strains (55.4%), and higher abundances occurring in mesophilic strains (61.6%) and *F. thermophilum* (73.7%). The values were lowered for all three thermotypes as temperatures decreased but were most significant for Antarctic strains (49.9%) and slightly less for mesophilic (58.4%) and thermophilic (72.8%) strains. The abundance of *anteiso*-branched FAs showed the opposite trend, with increases at lower temperatures for psychrophilic (from 7.6% up to 11.6%) and mesophilic (2.8% up to 4.6%) strains. However, this trend was not observed for *F. thermophilum*, where a decrease of *anteiso*-FAs was found (from 9.6 to 8.3%).

In conclusion, it was shown that psychrophilic flavobacteria produced more FA types (ten major FAs) in higher quantities than meso- and thermophilic members of this genus. It was proved that the cell membrane of Antarctic gliding flavobacteria was composed mainly of branched and unsaturated FAs, which might have direct impact on the fluidity of their membranes. Interestingly, the results implied that Antarctic flavobacteria mainly used two mechanisms for altering membrane fluidity in their cold-adaptive response. The first mechanism was based on unsaturation of their FAs and the second one on *de novo* synthesis of branched FAs. Based on the observations in this study, shortening the chain length seemed to be of lesser importance to the cold-adaptive response of Antarctic flavobacteria. In addition, no obvious modification regarding hydroxylation, cyclization, isomerization and/or polyunsaturated FAs was found among these strains. In this study, similar adaptation responses were found among psychrophilic, meso- and thermophilic strains, which suggested that the alteration of the cell membrane was similar for all thermotypes within the genus *Flavobacterium*, even when the overall abundance of different FA types was found to be different.

Funding

The author is grateful to the scientific infrastructure of the J.G. Mendel Czech Antarctic Station, which is part of the Czech Polar Research Infrastructure (CzechPolar2) supported by the Ministry of Education, Youth and Sports of the Czech Republic (LM2015078). Stanislava Králová is the holder of a Brno PhD Talent financial aid.

Appendix A. Supplementary data

Supplementary data associated with this article can be found, in the online version, at http://dx.doi.org/10.1016/j.syapm.2017.06.001.

References

[1] Aguilar, P.S., de Mendoza, D. (2006) Control of fatty acid desaturation: a mechanism conserved from bacteria to humans. Mol. Microbiol. 62, 1507–1514, http://dx.doi.org/10.1111/j.1365-2958.2006.05484.x.

[2] Annous, B.A., Becker, L.A., Bayles, D.O., Labeda, D.P., Wilkinson, B.J. (1997) Critical role of anteiso-$C_{15:0}$ fatty acid in the growth of *Listeria monocytogenes* at low temperatures. Appl. Environ. Microbiol. 63, 3887–3894.

[3] Bernardet, J.-F., Bowman, J.P. 2015 *Flavobacterium*. Bergey's manual of systematics of archaea and bacteria, John Wiley & Sons Ltd.

[4] Bin Haji Mohd Taha, A.I., Ahmed, R.Z., Motoigi, T., Watanabe, K., Kurosawa, N., Okuyama, H. (2013) Lipids in cold-adapted microorganisms. In: Yumoto, I. (Ed.), Cold-adapted microorganisms, Horizon Scientific Press, UK.

[5] Chan, M., Himes, R.H., Akagi, J.M. (1971) Fatty acid composition of thermophilic, mesophilic, and psychrophilic clostridia. J. Bacteriol. 106, 876–881.

[6] D'Amico, S., Collins, T., Marx, J.-C., Feller, G., Gerday, C. (2006) Psychrophilic microorganisms: challenges for life. EMBO Rep. 7, 385–389, http://dx.doi.org/10.1038/sj.embor.7400662.

[7] De Maayer, P., Anderson, D., Cary, C., Cowan, D.A. (2014) Some like it cold: understanding the survival strategies of psychrophiles. EMBO Rep. 15, 508–517, http://dx.doi.org/10.1002/embr.201338170.

[8] Diomandé, S.E., Nguyen-The, C., Guinebretière, M.-H., Broussolle, V., Brillard, J. (2015) Role of fatty acids in *Bacillus* environmental adaptation. Front. Microbiol 6, http://dx.doi.org/10.3389/fmicb.2015.00813.

[9] Evans, R.I., McClure, P.J., Gould, G.W., Russell, N.J. (1998) The effect of growth temperature on the phospholipid and fatty acyl compositions of non-proteolytic *Clostridium botulinum*. Int. J. Food Microbiol. 40, 159–167.

[10] Hirota, K., Nodasaka, Y., Orikasa, Y., Okuyama, H., Yumoto, I. (2005) *Shewanella pneumatophori* sp. nov., an eicosapentaenoic acid-producing marine bacterium isolated from the intestines of Pacific mackerel (*Pneumatophorus japonicus*). Int. J. Syst. Evol. Microbiol. 55, 2355–2359, http://dx.doi.org/10.1099/ijs.0.63804-0.

[11] Huys, G., Vancanneyt, M., Coopman, R., Janssen, P., Falsen, E., Altwegg, M., Kersters, K. (1994) Cellular fatty acid composition as a chemotaxonomic marker for the differentiation of phenospecies and hybridization groups in the genus *Aeromonas*. Int. J. Syst. Bacteriol. 44, 651–658, http://dx.doi.org/10.1099/00207713-44-4-651.

[12] Kaneda, T. (1991) Iso- and anteiso-fatty acids in bacteria: biosynthesis, function, and taxonomic significance. Microbiol. Rev. 55, 288–302.

[13] Könneke, M., Widdel, F. (2003) Effect of growth temperature on cellular fatty acids in sulphate-reducing bacteria. Environ. Microbiol. 5, 1064–1070.

[14] Margesin, R., Zhang, D.-C., Busse, H.-J. (2012) *Sphingomonas alpina* sp. nov., a psychrophilic bacterium isolated from alpine soil. J. Syst. Evol. Microbiol. 62, 1558–1563, http://dx.doi.org/10.1099/ijs.0. 035964-0.

[15] Morita, N., Gotoh, M., Okajima, N., Okuyama, H., Hayashi, H., Higashi, S., Murata, N. (1992) Both the anaerobic pathway and aerobic desaturation are involved in the synthesis of unsaturated fatty acids in *Vibrio* sp strain ABE-1. FEBS Lett. 297, 9–12.

[16] Nichols, D.S., Nichols, P.D., McMeekin, T.A. (1993) Polyunsaturated fatty acids in Antarctic bacteria. Antarct. Sci. 5, 149–160, http://dx.doi.org/10.1017/S0954102093000215.

[17] Oshima, M., Miyagawa, A. (1974) Comparative studies on the fatty acid composition of moderately and extremely thermophilic bacteria. Lipids 9, 476–480, http://dx.doi.org/10.1007/BF02534274.

[18] Osterhout, G.J., Shull, V.H., Dick, J.D. (1991) Identification of clinical isolates of Gram-negative nonfermentative bacteria by an automated cellular fatty acid identification system. J. Clin. Microbiol. 29, 1822–1830.

[19] Reddy, G.S., Aggarwal, R.K., Matsumoto, G.I., Shivaji, S. (2000) *Arthrobacter flavus* sp. nov., a psychrophilic bacterium isolated from a pond in McMurdo Dry Valley, Antarctica. Int. J. Syst. Evol. Microbiol. 50, 1553–1561, http://dx.doi.org/10.1099/00207713-50-4-1553.

[20] Rilfors, L., Wieslander, A., Ståhl, S. (1978) Lipid and protein composition of membranes of *Bacillus megaterium* variants in the temperature range 5 to 70 degrees C. J. Bacteriol. 135, 1043–1052.

[21] Russell, N.J. (1977) Desaturation of fatty acids by the psychrophilic bacterium *Micrococcus cryophilus*. Biochem. Soc. Trans. 5, 1492–1494, http://dx.doi.org/10.1042/bst0051492.

[22] Russell, N.J. (1984) The regulation of membrane fluidity in bacteria by acyl chain length changes. In: Kates, M., Manson, L.A. (Eds.), Membrane fluidity, Springer, US, pp. 329–347.

[23] Russell, N.J. (1984) Mechanisms of thermal adaptation in bacteria: blueprints for survival. Trends Biochem. Sci. 9, 108–112, http://dx.doi.org/10.1016/0968-0004(84)90106-3.

[24] Russell, N.J. (2008) Membrane components and cold sensing. In: Margesin, R., Schinner, F., Marx, J.-C., Gerday, C. (Eds.), Psychrophiles: from biodiversity to biotechnology, Springer Berlin Heidelberg, pp. 177–190.

[25] Russell, N.J., Evans, R.I., ter Steeg, P.F., Hellemons, J., Verheul, A., Abee, T. (1995) Membranes as a target for stress adaptation. Int. J. Food Microbiol. 28, 255–261, http://dx.doi.org/10.1016/0168-1605(95)00061-5.

[26] Sasser, M. (1990) MIDI technical note 101. Newark, Del: MIDI, Inc. Identification of bacteria by gas chromatography of cellular fatty acids, pp. 1–7.

[27] Seo, H.J., Bae, S.S., Lee, J.-H., Kim, S.-J. (2005) *Photobacterium frigidiphilum* sp. nov., a psychrophilic, lipolytic bacterium isolated from deep-sea sediments of Edison Seamount. Int. J. Syst. Evol. Microbiol. 55, 1661–1666, http://dx.doi.org/10.1099/ijs.0.63338-0.

[28] Silvius, J.R. (1982) Thermotropic phase transitions of pure lipids in model membranes and their modifications by membrane proteins. In: Jost, P.C., Griffith, O.H. (Eds.), Lipid–protein interactions, John Wiley & Sons Inc., New York, pp. 239–281.

[29] Sinensky, M. (1974) Homeoviscous adaptation—a homeostatic process that regulates the viscosity of membrane lipids in *Escherichia coli*. Proc. Natl. Acad. Sci. U. S. A. 71, 522–525.

[30] Suutari, M., Laakso, S. (1994) Microbial fatty acids and thermal adaptation. Crit. Rev. Microbiol. 20, 285–328, http://dx.doi.org/10.3109/10408419409113560.

[31] Weerkamp, A., Heinen, W. (1972) Effect of temperature on the fatty acid composition of the extreme thermophiles, *Bacillus caldolyticus* and *Bacillus caldotenax*. J. Bacteriol. 109, 443–446.

Supplementary Material

Title: Role of fatty acids in cold adaptation of Antarctic psychrophilic *Flavobacterium* spp.

Králová Stanislava[1]

[1]Czech Collection of Microorganisms, Department of Experimental Biology, Faculty of Science, Masaryk University, Kamenice 5, 62500, Brno, Czech Republic

Corresponding author: Králová Stanislava, ✉ stanci@mail.muni.cz, 00420 549 49 4897

Table S1. List of Antarctic *Flavobacterium* spp. used in this study

Table S2. List of reference cultures of *Flavobacterium* spp. used in this study.

Table S3. FA composition of 28 Antarctic *Flavobacterium* spp. cultivated at 20±2 °C and 10±2 °C.

Table S4. FA composition of 10 mesophilic *Flavobacterium* spp. cultivated at 30/25±2 °C and 25/15±2 °C.

Table S5. FA composition of *F. thermophilum* CCM 3496^T cultivated at 50±2 °C and 40±2 °C.

Figure S1. Major FAs and alterations in FA composition among 28 Antarctic *Flavobacterium* spp.

Figure S2. Major FAs and alterations in FA composition among mesophilic *Flavobacterium* spp.

Figure S3. Major FAs and alterations in FA composition of *F. thermophilum* CCM 3496^T

Table S1. List of Antarctic *Flavobacterium* spp. used in this study

Strain number	Source	Year	Locality
P2683	Regolith under the nest of skuas	2008	Berry Hill Meseta
P2759	Rocks	2008	Berry Hill, south base
P7679	Rocks	2009	Lachman Crags, west
P7681	Rocks	2009	Lachman Crags, west
P3177	Subglacial crushed rocks/regolith	2009	Lake, Panorama Pass
P3160	Rocks	2009	Devils Rocks
P3090	Rocks	2009	Wall of waterfall, Lachman Crags, west
P3596	Regolith	2010	Walls of Berry Hill
P3793	Rocks/regolith	2011	Rift in stone walls, Komarek Valley
P3932	Regolith	2011	Rift in stone walls, Komarek Valley
P3826	Regolith	2011	Halozetes Valley
P3764	Regolith	2011	Halozetes Valley
P4023	Material from the nest of skuas	2011	Lachman Crags
P4358	Rocks, regolith	2012	Komarek Valley
P4418	Rocks, regolith	2012	Komarek Valley
P4902	Rivulet water	2013	Interlagos
P4909	Creek water	2013	Left tributary of the Bohemia Stream
P4898	Creek water	2013	Mossy creek, J.G. Mendel Base
P4906	Creek water	2013	J.G. Mendel Base, source of drinking water
P4811	Creek water	2013	Confluence of creeks, J.G. Mendel Base
P4900	Lake water	2013	Temporary lake, Triangular Glacier
P4907	Creek water	2013	Mossy creek, J.G. Mendel Base
P5713	Rivulet water	2014	Halozetes Valley
P5700	Creek water	2014	Creek, up-river stream, Panorama Pass
P5908	Creek water	2014	Down-river stream of the Algal stream
P5953	Creek water	2014	Middle stream of the Dirty Stream
P6023	Creek water	2014	Up-river stream of the Bohemian Stream, by icefall
P5701	Puddle water	2014	Temporary puddle, Panorama Pass

Table S2. List of reference cultures of *Flavobacterium* spp. used in this study

Strain		Optimal growth temperature	Source
CCM 7424^T	*F. lindanitolerans*	30 °C	Soil, hexachlorocyclohexane-contaminated dumpsite
CCM 7847^T	*F. ummariense*	30 °C	HCH-contaminated soil in Lucknow, India
CCM 2847	*Flavobacterium* sp.	30 °C	Soil
CCM 7344^T	*F. mizutaii*	30 °C	Ventricular fluid
CCM 8409	*Flavobacterium* sp.	30 °C	Surface of a juvenile leech
CCM 8742^T	*F. akiainvivens*	28-30 °C	Decaying wood
CCM 8744^T	*F. cucumis*	30 °C	Greenhouse soil cultivated with cucumber
CCM 8745^T	*F. cutihirudinis*	28-30 °C	Skin of a juvenile medical leech
CCM 8746^T	*F. granuli*	30 °C	Granule sludge to treat wastewater
CCM 7939^T	*F. araucananum*	25 °C	Atlantic salmon
CCM 3496^T	*F. thermophilum*	50 °C	Hot spring near Alma-Ata

Table S3. FA composition[a,b] of 28 Antarctic *Flavobacterium* spp. cultivated at 20±2 °C and 10±2 °C

20±2 °C for 48 h				10±2 °C for 72 h			
Fatty acid[a]	**Frequency (%)**	**Mean value[c] (%)**	**Range (%)**	**Fatty acid[b]**	**Frequency (%)**	**Mean value[c] (%)**	**Range (%)**
Saturated FA				**Saturated FA**			
13:0	78.6	0.1	0.0-0.3	13:0	57.1	0.1	0.0-0.3
14:0	100.0	0.5	0.3-0.9	14:0	100.0	0.5	0.3-0.7
16:0	100.0	1.7	0.5-3.5	16:0	100.0	1.2	0.5-1.8
17:0	78.6	0.1	0.0-0.1	17:0	100.0	0.2	0.1-0.3
Unsaturated FA[d]				**Unsaturated FA[d]**			
13:1 at 12-13	28.6	0.2	0.0-1.0	13:1 at 12-13	82.1	0.1	0.0-0.4
15:1 *ω6c*	**100.0**	**6.2**	**3.4-20.2**	**15:1 *ω6c***	**100.0**	**5.2**	**1.8-20.8**
16:1 *ω5c*	71.4	0.3	0.0-0.8	16:1 ω5c	100.0	0.5	0.2-0.8
17:1 *ω8c*	100.0	0.5	0.4-0.7	17:1 ω8c	100.0	0.5	0.3-0.6
17:1 *ω6c*	**100.0**	**3.7**	**1.5-7.0**	17:1 ω6c	100.0	4.1	2.7-6.4
18:1 *ω9c*	100.0	0.3	0.1-0.5	18:1 ω9c	100.0	0.2	0.2-0.5
Hydroxy FA				**Hydroxy FA**			
15:0 2OH	100.0	1.0	0.5-1.3	15:0 2OH	100.0	0.9	0.5-1.0
15:0 3OH	75.0	2.5	0.0-3.3	15:0 3OH	67.9	2.2	0.0-3.4
16:0 3OH	100.0	2.2	1.0-3.7	16:0 3OH	100.0	2.4	0.9-3.8
17:0 2OH	100.0	1.5	0.3-2.7	17:0 2OH	100.0	1.5	0.5-2.5
17:0 3OH	100.0	0.3	0.2-0.6	17:0 3OH	96.4	0.2	0.0-0.3
***iso*-branched FA**				***iso*-branched FA**			
13:0 iso	92.9	0.3	0.0-0.7	13:0 iso	100.0	0.2	0.1-0.5
14:0 iso	92.9	0.8	0.0-3.2	14:0 iso	100.0	0.7	0.2-2.2
15:0 iso	**100.0**	**18.6**	**14.4-23.0**	**15:0 iso**	**100.0**	**16.7**	**9.2-19.6**
16:0 iso	100.0	2.1	0.8-2.8	16:0 iso	100.0	1.9	0.6-2.6
17:0 iso	92.9	0.2	0.0-0.3	17:0 iso	92.9	0.1	0.0-0.2
***anteiso*-branched FA**				***anteiso*-branched FA**			
13:0 anteiso	78.6	0.1	0.0-0.2	13:0 anteiso	96.4	0.1	0.0-0.2
15:0 anteiso	**100.0**	**6.0**	**3.8-9.0**	**15:0 anteiso**	**100.0**	**7.4**	**5.0-12.2**
	ND			16:0 anteiso	53.6	0.1	0.0-0.1
17:0 anteiso	92.9	0.2	0.0-0.3	17:0 anteiso	89.3	0.1	0.0-0.2
Branched hydroxy FA				**Branched hydroxy FA**			
14:0 iso 3OH	96.4	0.4	0.0-0.7	14:0 iso 3OH	100.0	0.3	0.2-0.4
15:0 iso 3OH	**100.0**	**8.4**	**5.6-12.9**	**15:0 iso 3OH**	**100.0**	**7.4**	**5.8-10.5**
16:0 iso 3OH	**100.0**	**5.3**	**2.4-8.8**	**16:0 iso 3OH**	**100.0**	**4.8**	**1.2-7.8**
17:0 iso 3OH	**100.0**	**8.2**	**3.6-11.0**	**17:0 iso 3OH**	**100.0**	**6.4**	**3.4-8.5**
Branched unsaturated FA				**Branched unsaturated FA**			
15:1 iso G[e]	**100.0**	**9.6**	**7.7-10.8**	**15:1 iso G[e]**	**100.0**	**10.2**	**7.8-12.2**
15:1 anteiso A	96.4	1.3	0.0-2.0	15:1 anteiso A	100.0	2.4	1.5-3.3
16:1 iso H	96.4	1.5	0.0-4.7	16:1 iso H	100.0	1.2	0.4-4.3
	ND			17:1 anteiso ω9c	14.3	1.5	0.0-2.5
Summed features[f]				**Summed features[f]**			
SF 2	32.1	0.5	0.0-1.1	SF 2	57.4	0.5	0.0-0.7
SF 3	**100.0**	**12.6**	**7.6-18.7**	**SF 3**	**100.0**	**16.9**	**5.9-31.3**
SF 8	10.7	0.3	0.1-0.6		ND		
SF 9	**100.0**	**4.3**	**0.8-7.7**	SF 9	100.0	3.6	1.1-6.5

[a] Eight FAs detected under 0.1% or in less than 5% of strains cultivated at 20±2 °C were excluded from the analysis: $C_{10:0}$ 3OH, $C_{12:0}$, $C_{17:1}$ anteiso *ω9c*, $C_{16:0}$ 2OH, $C_{18:3}$ *ω6c* (6,9,12), $C_{19:0}$ anteiso, $C_{20:4}$ *ω6,9,12,15c*, summed feature 5 ($C_{18:0}$ ante/$C_{18:2}$ *ω6,9c*).

[b] Seven FAs and one alcohol were detected under 0.1% or in less than 5% of strains cultivated at 10±2 °C and were excluded from the analysis: $C_{14:0}$ anteiso, $C_{17:1}$ anteiso A, $C_{16:1}$ 2OH, $C_{18:1}$ *ω7c* 11-methyl, $C_{20:4}$ *ω6,9,12,15c*, summed feature 5 ($C_{18:0}$ ante/$C_{18:2}$ *ω6,9c*), summed feature 8 ($C_{18:1}$ *ω7c* and/or $C_{18:1}$ *ω7c*) and $C_{16:0}$ N alcohol.

[c] Mean values were calculated for all FAs, regardless of the fact that some FAs were not detected in all strains.

[d] The position of a double bond in unsaturated FAs is counted from the methyl end (*ω*) of the carbon chain. *Cis* conformation is indicated by the suffix *c*.

[e] A capital letter indicates that the position of the double bond is unknown.

[f] Summed features represent groups of fatty acids that could not be separated by the Sherlock® Microbial Identification System. Summed feature 2 contains $C_{12:0}$ aldehyde, $C_{16:1}$ iso I, $C_{14:0}$ 3OH and/or an unknown fatty acid with an equivalent chain-length of 10.9525; summed feature 3 contains $C_{16:1}$ *ω7c* and/or $C_{16:1}$ *ω6c*; summed feature 8 contains $C_{18:1}$ *ω7c* and/or $C_{18:1}$ *ω7c*; summed feature 9 contains $C_{16:0}$ 10-methyl and/or $C_{17:1}$ iso *ω9c*.

ND – not detected

Table S4. FA composition[a,b] of 10 mesophilic *Flavobacterium* spp. cultivated at 30/25±2 °C and 25/15±2 °C

(25/30±2 °C for 48 h)				(15/20±2 °C for 48 h)			
Fatty acid[a]	**Frequency (%)**	**Mean value[c] (%)**	**Range (%)**	**Fatty acid[b]**	**Frequency (%)**	**Mean value[c] (%)**	**Range (%)**
Saturated FA				**Saturated FA**			
13:0	3/10	0.5	0.0-0.7	13:0	3/10	0.3	0.0-0.4
14:0	10/10	0.6	0.2-1.3	14:0	9/10	0.4	0.0-1.1
16:0	10/10	2.9	0.4-8.6	16:0	10/10	2.5	0.7-6.3
17:0	5/10	0.1	0.0-0.1	17:0	4/10	0.1	0.0-0.1
Unsaturated FA[d]				**Unsaturated FA[d]**			
13:1 at 12-13	5/10	0.4	0.2-1.0		ND		
14:1 w5c	3/10	0.1	0.0-0.1	14:1 w5c	3/10	0.1	0.0-0.1
15:1 w6c	10/10	3.5	0.3-16.9	15:1 w6c	9/10	3.7	0.0-14.3
	ND			16:1 w5c	3/10	0.5	0.3-0.7
17:1 w8c	9/10	0.8	0.0-2.2	17:1 w8c	9/10	0.8	0.0-1.9
17:1 w6c	7/10	2.2	0.0-7.0	17:1 w6c	9/10	2.7	0.0-8.5
18:1 w9c	10/10	0.6	0.3-0.8	18:1 w9c	9/10	0.6	0.0-1.6
Hydroxy FA				**Hydroxy FA**			
14:0 2OH	5/10	0.1	0.0-0.2		ND		
15:0 2OH	10/10	1.0	0.3-4.3	15:0 2OH	10/10	0.8	0.3-2.6
15:0 3OH	6/10	2.3	0.0-4.0	15:0 3OH	5/10	2.0	0.4-3.1
16:0 2OH	5/10	0.2	0.0-0.2	16:0 2OH	3/10	0.1	0.0-0.1
16:0 3OH	10/10	2.3	0.4-7.8	16:0 3OH	10/10	1.8	0.5-5.7
17:0 2OH	9/10	0.7	0.0-1.4	17:0 2OH	9/10	0.9	0.0-1.8
17:0 3OH	10/10	0.5	0.2-1.2	17:0 3OH	10/10	0.4	0.1-0.7
Unsaturated hydroxy FA				**Unsaturated hydroxy FA**			
16:1 2OH	3/10	0.2	0.0-0.2	16:1 2OH	3/10	0.1	0.0-0.2
***iso*-branched FA**				***iso*-branched FA**			
13:0 iso	10/10	0.4	0.2-1.0	13:0 iso	6/10	0.4	0.0-0.7
14:0 iso	5.10	3.0	0.0-5.0	14:0 iso	5/10	2.3	0.0-4.0
15:0 iso	**10/10**	**25.2**	**10.9-37.4**	**15:0 iso**	**10/10**	**22.4**	**6.0-43.7**
16:0 iso	10/10	2.7	0.4-8.6	16:0 iso	10/10	3.3	0.5-11.5
17:0 iso	10/10	0.3	0.1-0.5	17:0 iso	8/10	0.3	0.1-0.4
***anteiso*-branched FA**				***anteiso*-branched FA**			
15:0 anteiso	10/10	2.7	0.5-4.7	15:0 anteiso	10/10	3.9	2.0-6.0
17:0 anteiso	6/10	0.1	0.0-0.1	17:0 anteiso	6/10	0.1	0.0-0.2
Branched hydroxy FA				**Branched hydroxy FA**			
14:0 iso 3OH	5/10	1.2	0.0-3.5	14:0 iso 3OH	5/10	0.8	0.0-1.2
15:0 iso 3OH	**10/10**	**5.5**	**1.4-10.5**	**15:0 iso 3OH**	**10/10**	**4.9**	**1.5-8.8**
16:0 iso 3OH	**10/10**	**3.6**	**0.4-9.7**	**16:0 iso 3OH**	**10/10**	**4.0**	**0.5-11.5**
17:0 iso 3OH	**10/10**	**12.2**	**5.3-17.7**	**17:0 iso 3OH**	**10/10**	**11.2**	**5.2-17.7**
Branched unsaturated FA				**Branched unsaturated FA**			
15:1 iso G[e]	7/10	6.2	0.0-14.0	15:1 iso G[e]	9/10	6.9	0.0-11.1
	ND			15:1 anteiso A	8/10	0.6	0.0-1.1
16:1 iso H	6/10	1.3	0.0-3.0	16:1 iso H	9/10	1.9	0.0-5.7
Summed features[f]				**Summed features[f]**			
SF 1	3/10	0.7	0.0-0.9		ND		
SF 2	4/10	0.9	0.0-1.2		ND		
SF 3	**10/10**	**18.4**	**1.4-32.9**	**SF 3**	**10/10**	**17.9**	**7.5-32.6**
SF 4	3/10	0.8	0.0-1.1	SF 4	3/10	0.9	0.6-1.2
	ND			SF 8	3/10	0.2	0.0-0.2
	ND			**SF 9**	**10/10**	**5.8**	**2.5-17.6**

[a] Ten FAs detected under 0.1% or in less than three strains cultivated under optimal growth temperatures were excluded from the analysis: $C_{12:0}$, $C_{13:0}$ iso 3OH, $C_{13:0}$ anteiso, $C_{15:1}$ *ω8c*, $C_{15:1}$ anteiso A, $C_{15:1}$ iso F, $C_{18:0}$, $C_{20:4}$ *ω6,9,12,15c*, summed feature 5 ($C_{18:0}$ ante/$C_{18:2}$ ω6,9c) and summed feature 8 ($C_{18:1}$ *ω7c* and/or $C_{18:1}$ *ω7c*).

[b] Ten FAs detected under 0.1% or in less than three strains cultivated after the temperature downshift were excluded from the analysis: $C_{12:0}$ iso, $C_{13:0}$ anteiso, $C_{13:1}$ at 12-13, $C_{15:1}$ *ω8c*, $C_{14:0}$ 2OH, $C_{17:1}$ anteiso A, $C_{18:0}$, summed feature 1 ($C_{15:1}$ iso H/$C_{13:0}$ 3OH), summed feature 2 ($C_{12:0}$ aldehyde, $C_{16:1}$ iso I, $C_{14:0}$ 3OH and/or an unknown fatty acid with an equivalent chain-length of 10.9525) and summed feature 5 ($C_{18:0}$ ante/$C_{18:2}$ *ω6,9c*).

[c] Mean values were calculated for all FAs, regardless of the fact that some FAs were not detected in all strains.

[d] The position of a double bond in unsaturated FAs is counted from the methyl end (*ω*) of the carbon chain. *Cis* conformation is indicated by the suffix *c.*

[e] A capital letter indicates that the position of the double bond is unknown.

[f] Summed features represent groups of fatty acids that could not be separated by the Sherlock® Microbial Identification System. Summed feature 1 contains $C_{15:1}$ iso H and/or $C_{13:0}$ 3OH; summed feature 2 contains $C_{12:0}$ aldehyde, $C_{16:1}$ iso I, $C_{14:0}$ 3OH and/or an unknown fatty acid with an equivalent chain-length of 10.9525; summed feature 3 contains $C_{16:1}$ *ω7c* and/or $C_{16:1}$ *ω6c*; summed feature 4 contains $C_{17:1}$ iso I and/or $C_{17:1}$ anteiso B; summed feature 8 contains $C_{18:1}$ *ω7c* and/or $C_{18:1}$ *ω7c*; summed feature 9 contains $C_{16:0}$ 10-methyl and/or $C_{17:1}$ iso *ω9c*.

ND – not detected

Table S5. FA composition of *F. thermophilum* CCM 3496[T] cultivated at 50±2 °C and 40±2 °C

(50±2 °C for 48 h)		(40±2 °C for 48 h)	
Fatty acid	**Percentage[a] (%)**	**Fatty acid**	**Percentage[a] (%)**
Saturated FA		**Saturated FA**	
14:0	1.5	14:0	1.9
16:0	**8.0**	**16:0**	**5.7**
17:0	0.3	ND	
18:0	0.5	18:0	0.4
Unsaturated FA[b]		**Unsaturated FA[b]**	
18:1 *ω9c*	0.4	15:1 *ω6c*	0.7
ND		18:1 *ω9c*	0.3
Unsaturated hydroxy FA		**Unsaturated hydroxy FA**	
18:1 2OH	0.5	18:1 2OH	0.3
***iso*-branched FA**		***iso*-branched FA**	
ND		13:0 iso	0.3
14:0 iso	3.1	14:0 iso	3.7
15:0 iso	**44.8**	**15:0 iso**	**47.3**
16:0 iso	**12.7**	**16:0 iso**	**10.5**
ND		**17:0 iso**	**6.9**
***anteiso*-branched FA**		***anteiso*-branched FA**	
15:0 anteiso	3.4	15:0 anteiso	3.0
17:0 anteiso	**5.3**	**17:0 anteiso**	**3.5**
Branched hydroxy FA			
17:0 iso 3OH	**10.3**	ND	
Branched unsaturated FA		**Branched unsaturated FA**	
17:1 iso *ω5c*	2.8	**17:1 iso *ω5c***	**4.1**
17:1 anteiso A[c]	0.9	17:1 anteiso A[c]	1.8
Summed features[d]		**Summed features[d]**	
SF 2	1.5	SF2	3.3
SF 3	**4.1**	**SF 3**	**6.2**
ND		SF 5	0.3

[a] Percentage is the average value of three FAME analyses repeated under the same conditions.
[b] The position of a double bond in unsaturated FAs is counted from the methyl end (*ω*) of the carbon chain. *Cis* conformation is indicated by the suffix *c.*
[c] A capital letter indicates that the position of the double bond is unknown.
[d] Summed features represent groups of fatty acids that could not be separated by the Sherlock® Microbial Identification System. Summed feature 2 contains $C_{12:0}$ aldehyde, $C_{16:1}$ iso I, $C_{14:0}$ 3OH and/or an unknown fatty acid with an equivalent chain-length of 10.9525; summed feature 3 contains $C_{16:1}$ *ω7c* and/or $C_{16:1}$ *ω6c*; summed feature 5 contains $C_{18:0}$ ante and/or$C_{18:2}$ *ω6,9c*.
ND – not detected

Figure S1. Major FAs and alterations in FA composition among 28 Antarctic *Flavobacterium* spp.

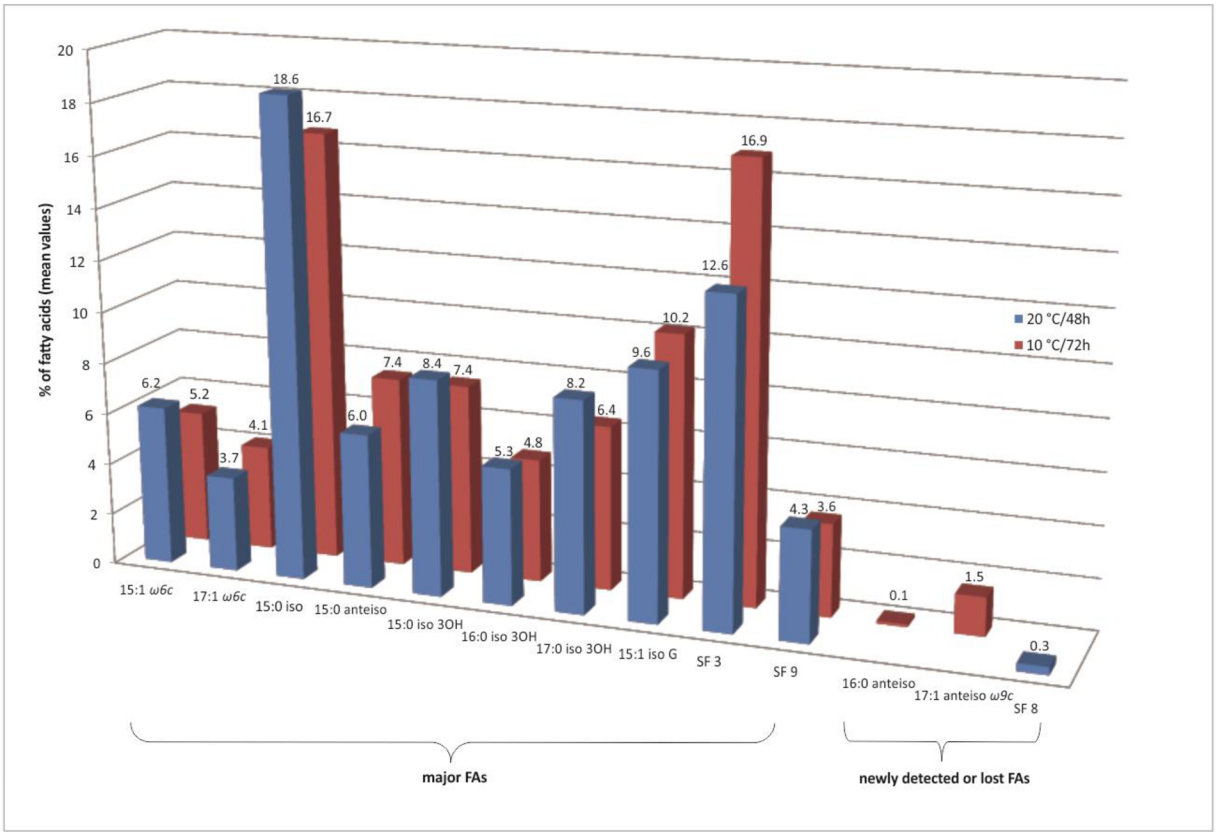

Figure S2. Major FAs and alterations in FA composition among mesophilic *Flavobacterium* spp.

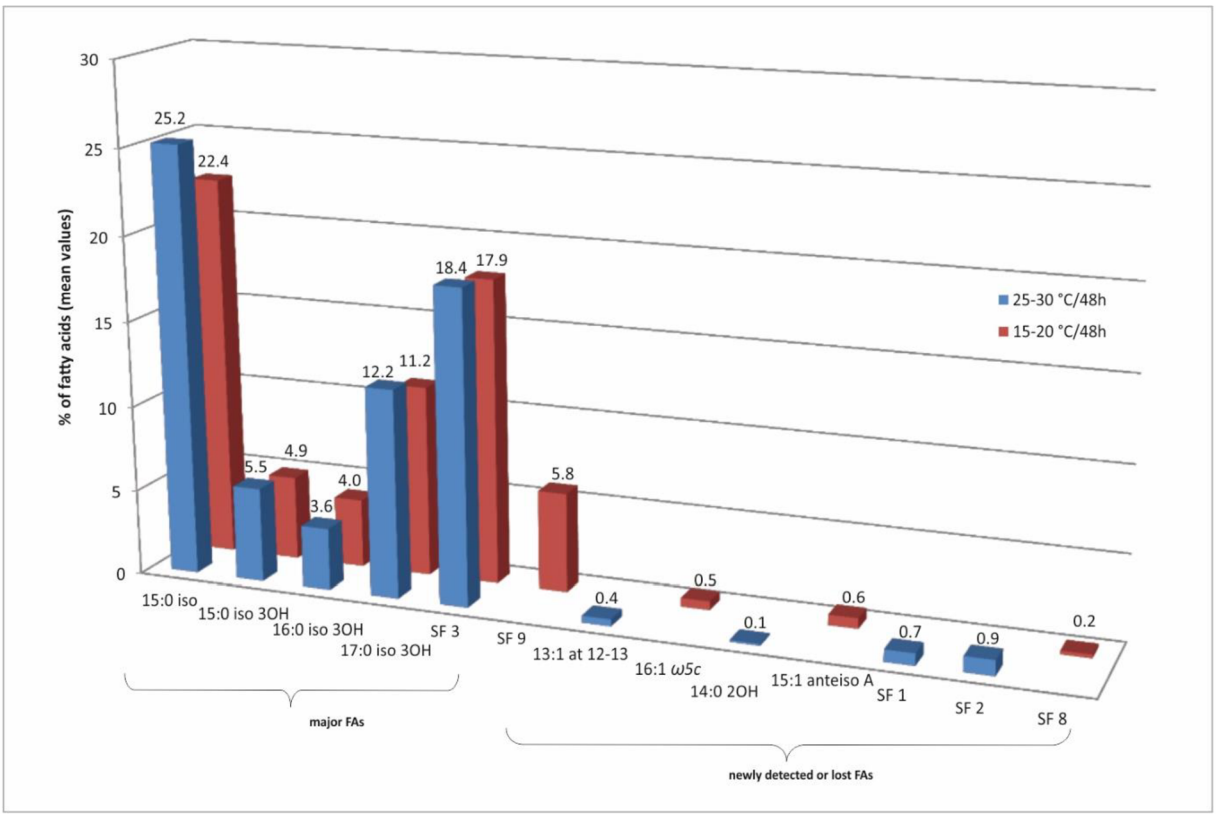

Figure S3. Major FAs and alterations in FA composition of *F. thermophilum* CCM 3496^{T}

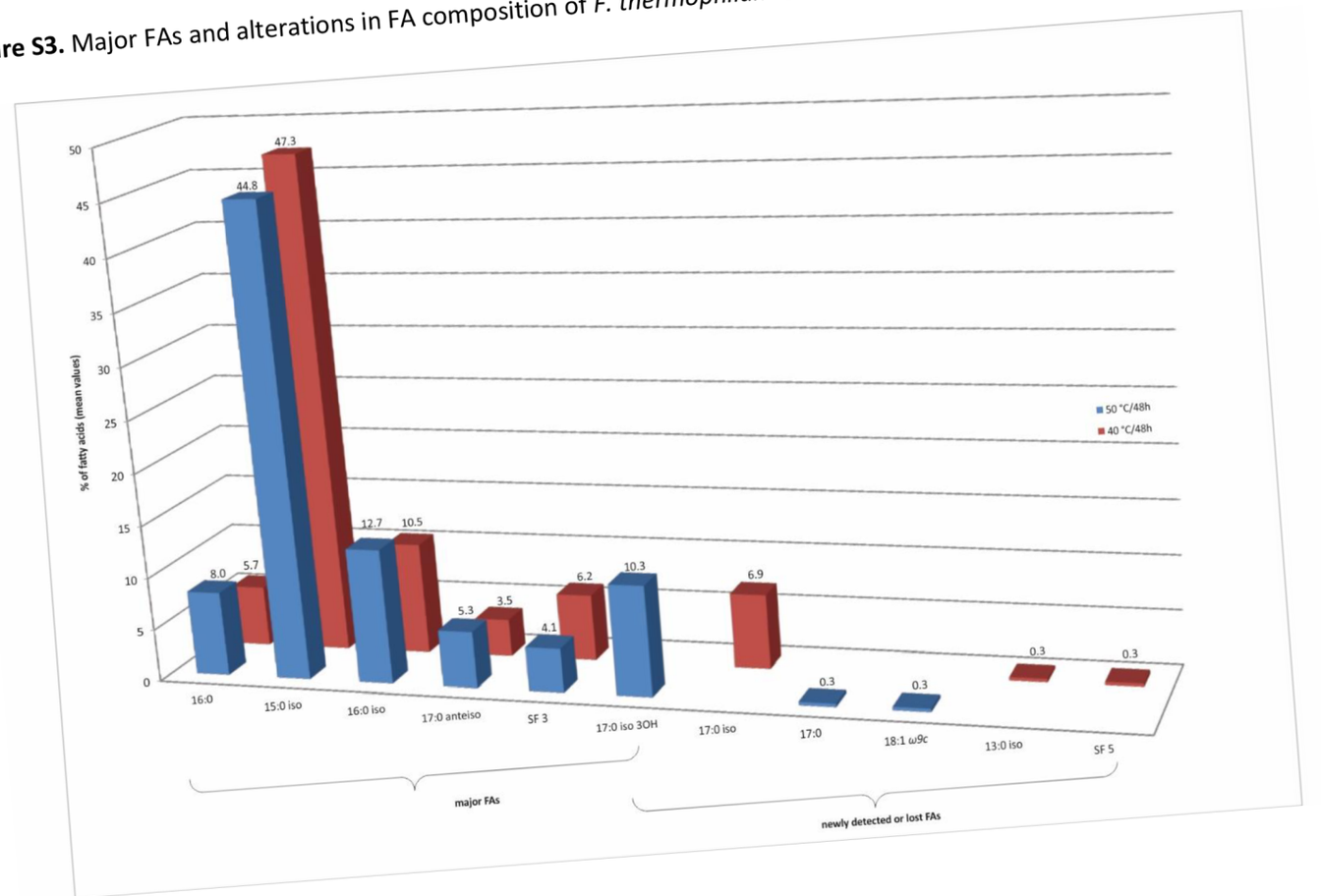

Príloha č. 2.

Švec P., Králová S., Busse H.-J., Kleinhagauer T., Pantůček R., Mašlaňová I., Cnockaert M., Vandamme P., Staňková E., Gelbíčová T., Holochová P., Barták M., Kýrová K., Sedláček I. (2017) *Pedobacter jamesrossensis* sp. nov., *Pedobacter lithocola* sp. nov., *Pedobacter mendelii* sp. nov. and *Pedobacter petrophilus* sp. nov., isolated from the Antarctic environment. *Int. J. Syst. Evol. Microbiol*. 67(5): 1499–507. Doi: 10.1099/ijsem.0.001749.

INTERNATIONAL JOURNAL OF SYSTEMATIC AND EVOLUTIONARY MICROBIOLOGY

NOTE

Švec *et al.*, *Int J Syst Evol Microbiol* 2017;67:1499–1507
DOI 10.1099/ijsem.0.001749

MICROBIOLOGY SOCIETY

Pedobacter jamesrossensis sp. nov., *Pedobacter lithocola* sp. nov., *Pedobacter mendelii* sp. nov. and *Pedobacter petrophilus* sp. nov., isolated from the Antarctic environment

Pavel Švec,[1,*] Stanislava Králová,[1] Hans-Jürgen Busse,[2] Tanita Kleinhagauer,[2] Roman Pantůček,[3] Ivana Mašlaňová,[3] Margo Cnockaert,[4] Peter Vandamme,[4] Eva Staňková,[1] Tereza Gelbíčová,[1] Pavla Holochová,[1] Miloš Barták,[5] Kamila Kýrová[1] and Ivo Sedláček[1]

Abstract

A taxonomic study performed on 17 Gram-stain-negative rod-shaped bacterial strains originating from the Antarctic environment is described. Initial phylogenetic analysis using 16S rRNA gene sequencing differentiated the strains into four groups belonging to the genus *Pedobacter* but they were separated from all hitherto described *Pedobacter* species. Group I (*n*=8) was closest to *Pedobacter aquatilis* (97.8 % 16S rRNA gene sequence similarity). Group II (*n*=2) and group III (*n*=4) were closely related (98.8 % 16S rRNA gene sequence similarity) and had *Pedobacter jejuensis* as their common nearest neighbour. Group IV (*n*=3) was distantly delineated from the remaining *Pedobacter* species. Differentiation of the analysed strains into four clusters was further confirmed by repetitive sequence-based PCR fingerprinting, ribotyping, DNA–DNA hybridization and phenotypic traits. Common to representative strains for the four groups were the presence of major menaquinone MK-7, *sym*-homospermidine as the major polyamine, phosphatidylethanolamine, two unidentified lipids (L2, L5) and an unidentified aminolipid (AL2) as the major polar lipids, presence of an alkali-stable lipid, and $C_{16:1}\omega7c/C_{16:1}\omega6c$ (summed feature 3), iso-$C_{15:0}$ and iso-$C_{17:0}$ 3-OH as the major fatty acids, which corresponded to characteristics of the genus *Pedobacter*. The obtained results showed that the strains analysed represent four novel species of the genus *Pedobacter*, for which the names *Pedobacter jamesrossensis* sp. nov. (type strain CCM 8689^T=LMG 29684^T), *Pedobacter lithocola* sp. nov. (CCM 8691^T=LMG 29685^T), *Pedobacter mendelii* sp. nov. (CCM 8685^T=LMG 29688^T) and *Pedobacter petrophilus* sp. nov. (CCM 8687^T=LMG 29686^T) are proposed.

The genus *Pedobacter* [1] represents strictly aerobic, Gram-stain-negative, rod-shaped bacteria. Phylogenetically, they belong to the family *Sphingobacteriaceae* within the phylum *Bacteroidetes*. Members of the genus *Pedobacter* exhibit catalase, oxidase and phosphatase activity but they typically do not reduce nitrate or exhibit urease activity. The presence of MK-7 as the major respiratory menaquinone, phosphatidylethanolamine as the major polar lipid, *sym*-homospermidine as the major polyamine and the presence of sphingolipids is typical for the genus [1, 2]. *Pedobacter* species have been isolated from different environmental, mainly terrestrial and aquatic, habitats worldwide, including Arctic and Antarctic regions (e.g. [3–5]).

The present study describes the taxonomic investigation of 17 *Pedobacter* strains isolated in the frame of a project dealing with the investigation of cultivable bacteria inhabiting the Antarctic environment and performed at the Johann Gregor Mendel Antarctic station situated on James Ross

Author affiliations: [1]Czech Collection of Microorganisms, Department of Experimental Biology, Faculty of Science, Masaryk University, Kamenice 5, 625 00 Brno, Czech Republic; [2]Institute of Microbiology, University of Veterinary Medicine Vienna, A-1210 Vienna, Austria; [3]Section of Genetics and Molecular Biology, Department of Experimental Biology, Faculty of Science, Masaryk University, Kotlářská 2, 611 37 Brno, Czech Republic; [4]Department of Biochemistry and Microbiology, Faculty of Sciences, Ghent University, K.L. Ledeganckstraat 35, 9000 Ghent, Belgium; [5]Section of Physiology and Anatomy of Plants, Department of Experimental Biology, Faculty of Science, Masaryk University, Kamenice 5, 625 00 Brno, Czech Republic.
***Correspondence:** Pavel Švec, mpavel@sci.muni.cz
Keywords: *Pedobacter jamesrossensis* sp. nov.; *Pedobacter lithocola* sp. nov.; *Pedobacter mendelii* sp. nov.; *Pedobacter petrophilus* sp. nov.; James Ross Island; Antarctica.
The GenBank/EMBL/DDBJ accession numbers for the 16S rRNA gene sequences obtained in this study are KX611467–KX611483: *Pedobacter jamesrossensis* sp. nov. strain CCM 8689^T, accesion number KX611467; CCM 8690, KX611474; P3164, KX611468; P3658, KX611469; P3679, KX611470; P3802, KX611471; P3824, KX611472; P4838, KX611473; *Pedobacter lithocola* sp. nov. CCM 8691^T, KX611475; P3926, KX611476; *Pedobacter mendelii* sp. nov. CCM 8685^T, KX611477; CCM 8686, KX611478; P2490, KX611479; P2749, KX611480; *Pedobacter petrophilus* sp. nov. CCM 8687^T, KX611481; CCM 8688, KX611482; P4106, KX611483.
Six supplementary figures and three supplementary tables are available with the online Supplementary Material.

Island near the Antarctic Peninsula. All strains were isolated from environmental materials sampled at James Ross Island (Table 1). Individual samples were suspended in sterile saline solution and 200 µl of the suspension was spread on R2A agar plates and cultivated at 15 °C for 5–7 days. Individual colonies were picked up, purified and pure cultures were maintained at R2A agar slant agars until transported and analysed.

Reference type strains *Pedobacter agri* CCM 8572^T, *Pedobacter alluvionis* CCM 8562^T, *Pedobacter aquatilis* CCM 7347^T, *Pedobacter borealis* CCM 8563^T, *Pedobacter ginsengiterrae* CCM 8571^T, *Pedobacter ginsenosidimutans* CCM 8564^T and *Pedobacter jejuensis* CCM 8565^T were obtained from the Czech Collection of Microorganisms and *Pedobacter sandarakinus* KCTC 12559^T was obtained from the Korean Collection for Type Cultures.

Genomic DNAs for 16S rRNA gene sequence analysis were extracted using a FastPrep Lysing Matrix type B and FastPrep Homogenizer (MP Biomedicals) and purified by using a High Pure PCR Template Preparation Kit (Roche Diagnostics). A fragment of the 16S rRNA gene corresponding to coordinates 8–1542 used for *Escherichia coli* was amplified by PCR with FastStart PCR Master (Roche Diagnostics) and conserved primers pA (AGAGTTTGATCCTGGCTCAG) and pH (AAGGAGGTGATCCAGCCGCA) described by Edwards *et al.* [6], and purified using a QIAquick PCR Purification Kit (Qiagen). Sequencing was performed using PCR primers and custom primers F1 (GTGGGGAKCRAACAGGATTAG), F2 (CGTCARGTCMTCATGGCCCTT), R1 (ATTACCGCGGCTGCTGGCAC) and R2 (CACATSMTCCMCCRCTTGT) in the Eurofins MWG Operon sequencing facility. Initial identification of the 16S rRNA gene sequences using the EzTaxon database [7] showed that all investigated strains are members of the genus *Pedobacter*. Strain CCM 8689^T (group I) was closest to *P. jejuensis* THG-DR3^T (98.6 % 16S rRNA gene sequence similarity) and *P. aquatilis* AR107^T (97.9 %); strain CCM 8691^T (group II) was closest to *P. jejuensis* THG-DR3^T (98.8 %), *P. aquatilis* AR107^T (97.6 %) and *P. alluvionis* NWER-II11^T (97.3 %); strain CCM 8685^T (group III) was closest to *P. aquatilis* AR107^T (97.8 %) and *P. jejuensis* THG-DR3^T (97.5 %); and strain CCM 8687^T (group IV) was closest to *P. agri* PB92^T (97.7 %), *P. borealis* DSM 19626^T (97.6 %), *P. alluvionis* NWER-II11^T (97.4 %), *P. ginsenosidimutans* THG-45^T (97.3 %) and *P. sandarakinus* DS-27^T (97.1 %). Except the similarity value between strain CCM 8691^T (group II) and *P. jejuensis* THG-DR3^T (98.8 %) all 16S rRNA gene sequence similarities were below the 98.7 % similarity threshold suggested by Stackebrandt and Ebers [8], who showed that two strain pairs with 16S rRNA gene sequence similarity of less than 98.7 % have DNA–DNA reassociation values of less than 70 %. Phylogenetic comparison of the obtained sequences with 16S rRNA gene sequences of validly named *Pedobacter* species retrieved from the GenBank database was performed using MEGA 6 software [9]. Genetic distances were corrected using Kimura's two-parameter model and the evolutionary history was inferred using the neighbour-joining, maximum-likelihood and maximum-parsimony methods. Sequence similarities between individual strains were calculated using Bionumerics 7.6 software (Applied Maths). Neighbour-joining clustering (Fig. 1)

Table 1. Origin of the analysed *Pedobacter* strains

Strain	Sample	Locality	Year	GPS
P. jamesrossensis sp. nov. (group I)				
CCM 8689^T	Stone fragments	Devils Rocks	2009	63° 51′ 41″ S 57° 49′ 10″ W
CCM 8690	Stone fragments	Lachman Crags	2012	63° 49′ 38″ S 57° 50′ 7.4′ W
P3164	Stone fragments	Devils Rocks	2009	63° 51′ 20″ S 57° 49′ 52″ W
P3658	Stone fragments	Lachman Crags	2010	63° 50′ 47.8″ S 57° 51′ 58.3″ W
P3679	Organo-mineral substrate	Berry Hill	2010	63° 48′ 30.7″ S 57° 49′ 30″ W
P3802	Stone fragments	Devils Rocks	2011	63° 50′ 4.9″ S 57° 50′ 43.7″ W
P3824	Stone fragments	Halozetes Valley	2011	63° 49′ 15″ S 57° 48′ 30″ W
P4838	Sandy soil	Big Lachman Lake	2013	63° 47′ 55″ S 57° 48′ 25″ W
P. lithocola sp. nov. (group II)				
CCM 8691^T	Stone fragments	Panorama Pass	2007	63° 48′ 52″ S 57° 50′ 36″ W
P3926	Stone fragments	Devils Rocks	2011	63° 47′ 59″ S 57° 50′ 43.8″ W
P. mendelii sp. nov. (group III)				
CCM 8685^T	Stone fragments	Lachman Crags	2010	63° 50′ 47.8″ S 57° 51′ 58.3″ W
CCM 8686	Stone fragments	Berry Hill	2008	63° 48′ 45″ S 57° 49′ 42″ W
P2490	Sandy soil	Crame Col	2007	63° 49′ 47″ S 57° 53′ 22″ W
P2749	Stone fragments	Berry Hill	2008	63° 48′ 52″ S 57° 49′ 25″ W
P. petrophilus sp. nov. (group IV)				
CCM 8687^T	Stone fragments	Devils Rocks	2009	63° 51′ 41″ S 57° 49′ 10″ W
CCM 8688	Stone fragments	Lachman Crags	2012	63° 49′ 45.5″ S 57° 50′ 14.8″ W
P4106	Organo-mineral substrate	Devils Rocks	2011	63° 49′ 52″ S 57° 50′ 27.6″ W

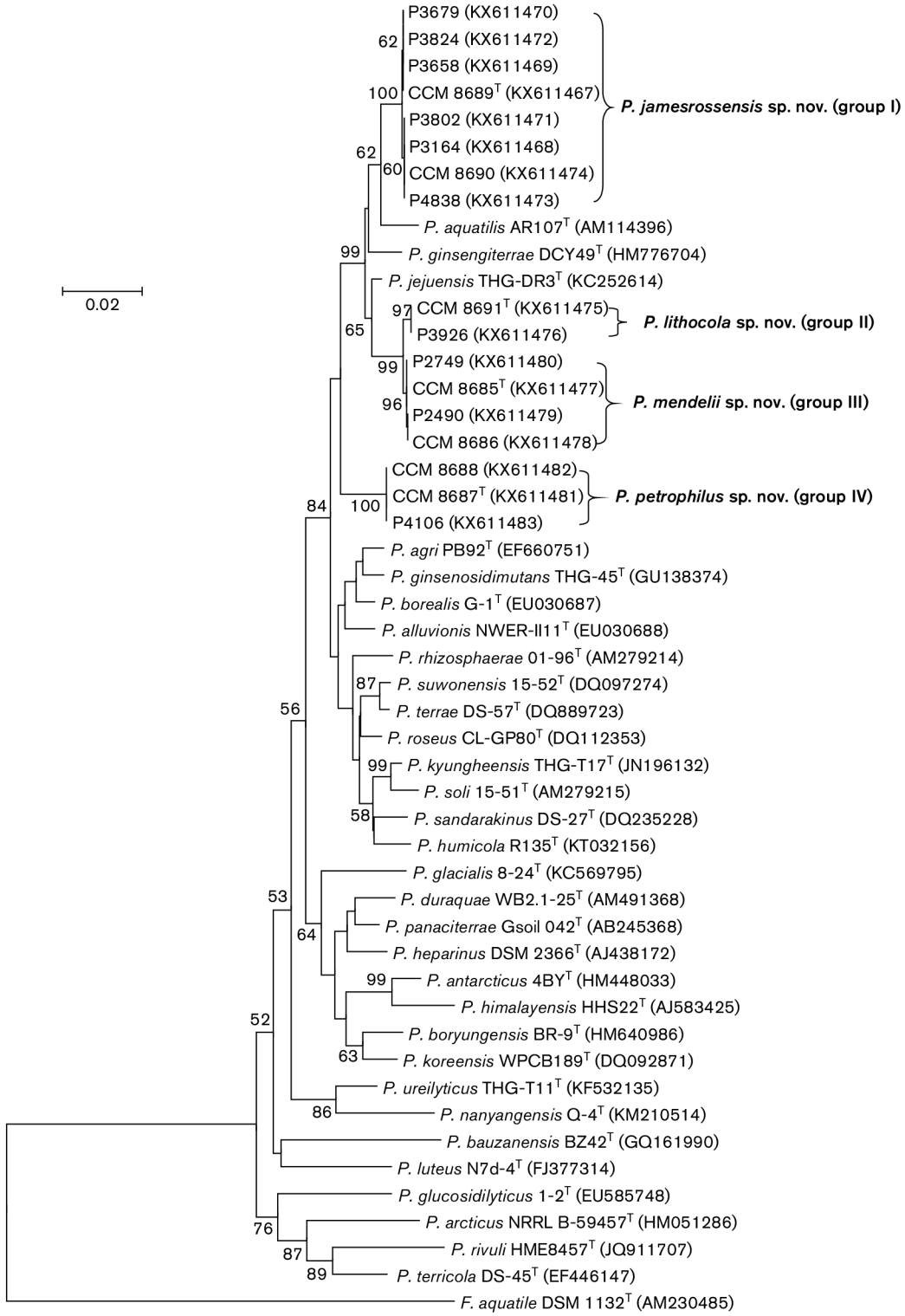

Fig. 1. Neighbour-joining phylogenetic tree based on 16S rRNA gene sequences, showing the position of groups I–IV strains within the genus *Pedobacter*. The evolutionary history was inferred by using the Kimura two-parameter model. Bootstrap probability values (percentages of 1000 tree replications) greater than 50 % are indicated at branch points. All positions with less than 95 % site coverage were eliminated. *Flavobacterium aquatile* DSM 1132^T (AM230485) was used as an outgroup. Bar, 0.02 substitutions per nucleotide position.

matched the tree topology obtained by the maximum-likelihood (Fig. S1, available in the online Supplementary Material) and maximum-parsimony analysis (Fig. S2) and separated the strains into four groups (I, II, III and IV) that were differentiated from established *Pedobacter* species. Group I consisted of eight strains sharing 99.9–100 % 16S rRNA gene sequence similarity. Isolates assigned to groups II, III and IV showed 100 % 16S rRNA gene sequence similarity within individual clusters. Phylogenetically, group I was closest to *P. aquatilis* AR107^T. Groups II and III were closely related to each other (98.8 % 16S rRNA gene sequence similarity) and had *P. jejuensis* THG-DR3^T as their closest phylogenetic neighbour. Group IV was most similar to, but only distantly related to, the *P. agri–P. borealis–P. ginsenosidimutans* cluster.

Repetitive sequence-based PCR (rep-PCR) fingerprinting using the $(GTG)_5$ primer and automated ribotyping with the *Eco*RI restriction enzyme were performed to assess the genetic variability between individual strains assigned to groups I–IV. rep-PCR fingerprinting with the $(GTG)_5$ primer was performed as described by Švec *et al.* [10]. The automatic ribotyping was performed using the RiboPrinter Microbial Characterization System (DuPont Qualicon) in accordance with the manufacturer's instructions. Numerical analysis and dendrogram construction was done using the BioNumerics 7.6 software (Applied Maths). The ribotype patterns were imported into the BioNumerics software using the load samples import script provided by the manufacturer. Numerical analysis of rep-PCR fingerprints showed a high genetic homogeneity within strains assigned to groups I–IV. Individual strains revealed visually similar fingerprints which clearly separated these groups from each other (Fig. S3). Heterogeneity was revealed only among group I strains due to a distinct fingerprint revealed by strain CCM 8690. In contrast, automated ribotyping using the *Eco*RI restriction enzyme showed closely similar ribotype patterns within all strains in group I and also confirmed the genetic homogeneity within groups II and IV. This method, however, separated group III strains into two subclusters (Fig. S4). Both DNA fingerprinting techniques also clearly differentiated groups I–IV from the type strains representing the phylogenetically closest *Pedobacter* species.

Total high-molar-mass genomic DNA extraction for the G+C content analysis and DNA–DNA hybridization experiments was performed as described by Cleenwerck *et al.* [11]. The DNA G+C content was determined using the HPLC method described by Mesbah and Whitman [12]. Strains CCM 8689^T (group I), CCM 8691^T (group II), CCM 8685^T (group III) and CCM 8687^T (group IV) revealed 36.2, 35.6, 35.5 and 38.8 mol% G+C genomic DNA content, respectively. DNA–DNA hybridization was done to confirm the differentiation of groups I, II and III from the phylogenetically nearest *Pedobacter* species and to confirm that the phylogenetically neighbouring groups II and III are representatives of different species. Group IV, which had a distinct phylogenetic position, was not included in DNA–DNA hybridization experiments. The method was performed using the microplate technique described by Ezaki *et al.* [13], according to the protocols described previously [11, 14]. DNA–DNA relatedness percentages were calculated as means based on at least three independent hybridizations. Reciprocal reactions were performed and also considered as independent experiments. The standard deviation between reciprocal reactions was approximately 7 %, as reported by Goris *et al.* [14]. The level of DNA–DNA hybridization obtained between strain CCM 8689^T (group I) and *P. aquatilis* CCM 7347^T and *P. jejuensis* CCM 8565^T was 21 and 15 %, respectively. The hybridization values between strains CCM 8691^T (group II) and CCM 8685^T (group III) and their phylogenetically nearest neighbours *P. jejuensis* CCM 8565^T and *P. aquatilis* CCM 7347^T were in the range from 15 to 20 %. DNA–DNA hybridization also showed that group II and group III strains represent different species because the hybridization value between strains CCM 8691^T and CCM 8685^T was 29 %. All DNA–DNA hybridization values obtained were well below the 70 % threshold [15], which confirmed that each of the strains analysed represented a novel species.

Phenotypic characteristics of all 17 strains and of the type strains of nearest neighbouring species *P. aquatilis* CCM 7347^T, *P. ginsengiterrae* CCM 8571^T and *P. jejuensis* CCM 8565^T were assessed by a set of key tests relevant for Gram-negative rod-shaped bacteria. Oxidase (OXItest; Erba-Lachema) and catalase (ID colour Catalase; bioMérieux) activity was verified according to the manufacturers' instructions. Cellular morphology was investigated by Gram staining [16] and transmission electron microscopy using a Morgagni 268D Philips (FEI Company) electron microscope (Fig. S5). Further tests for the following were done: oxidation-fermentation (OF) [17], urease [18], arginine dihydrolase, ornithine and lysine decarboxylase [19], hydrolysis of aesculin, starch [20], gelatin, Tween 80 [21], casein, tyrosine [22] and DNA (CM321; Oxoid), egg-yolk reaction [23], ONPG [24], nitrate and nitrite reduction, indol production, growth on Simmon's citrate agar [20], and utilization of acetamide [25] and sodium malonate [26]. Motility was observed in a glucose oxidation tube. Screening for flexirubin-type pigment production was done using a 20 % KOH test as described by Bernardet *et al.* [27]. Growth at different temperatures (5–35 °C in increments of 5.0 °C) and NaCl concentrations (0, 1, 2 and 3 %, w/v) was tested on R2A agar (Oxoid) adjusted accordingly. The pH range for growth was tested on R2A agar adjusted to pH 5.0–12.0 (in increments of 1 pH unit) by using the following buffer systems: pH 5.0–8.0, 0.1 M KH_2PO_4/0.1 M NaOH; pH 9.0–10.0, 0.1 M $NaHCO_3$/0.1 M Na_2CO_3; pH 11.0–12.0, 0.05 M Na_2HPO_4/0.1 M NaOH. The pH of the R2A agar was confirmed after autoclaving. Aerobic growth was tested on brain heart infusion agar (Oxoid), Columbia blood agar (Oxoid), MacConkey agar (Oxoid), nutrient agar (Oxoid), plate count agar (Oxoid), R2A agar (Oxoid) and tryptone soya agar (Oxoid) and anaerobic growth was tested on R2A agar using the Anaerocult A system (Merck). The aforementioned

biochemical and physiological tests were assessed using cells grown on R2A agar at 20 °C and read daily for up to 7 days with incubation at 20 °C. Phenotype screening showed that all strains were Gram-stain-negative, aerobic, non-fermenting, oxidase- and catalase-positive rods. Group I, II and III strains produced small red colonies and group IV strains produced pink colonies when cultivated on R2A agar plates at 20 °C. Further characterization using the Biolog system with the Gram-negative identification test panel GEN III MicroPlate (Biolog) and the API ZYM microtest system (bioMérieux) was done to obtain additional phenotypic data. Antibiotic resistance testing was done by the disc diffusion method on R2A agar (Oxoid). Sixteen antibiotic discs (Oxoid) relevant for Gram-negative rods [28, 29] were tested: ampicillin (10 µg), aztreonam (30 µg), carbenicillin (100 µg), cefixim (5 µg), ceftazidim (10 µg), cephalothin (30 µg), ciprofloxacin (5 µg), gentamicin (10 µg), chloramphenicol (30 µg), imipenem (10 µg), kanamycin (30 µg), cotrimoxazol (25 µg), piperacillin (30 µg), polymyxin B (300 U), streptomycin (10 µg) and tetracycline (30 µg). CLSI/EUCAST standards were followed for cultivation and inhibition zone diameter reading [28, 29]. The biochemical and physiological characteristics of group I–IV strains are listed in the species descriptions below. The tests distinguishing group I–IV strains and enabling their straightforward differentiation from their nearest neighbour species are shown in Table 2. Test results obtained with the GEN III MicroPlate test panel (Biolog) are listed in Table S1 and antibiotic susceptibility profiles of group I–IV strains are given in Table S2.

Table 2. Biochemical differentiation of *Pedobacter jamesrossensis* sp. nov., *Pedobacter lithocola* sp. nov., *Pedobacter mendelii* sp. nov. and *Pedobacter petrophilus* sp. nov. from phylogenetically related *Pedobacter* species

Taxa: 1, *P. jamesrossensis* sp. nov. (group I); 2, *P. lithocola* sp. nov. (group II); 3, *P. mendelii* sp. nov. (group III); 4, *P. petrophilus* sp. nov. (group IV); 5, *P. aquatilis* CCM 7347^T; 6, *P. ginsengiterrae* CCM 8571^T; 7, *P. jejuensis* CCM 8565^T. +, Positive; −, negative; w, weakly positive; d, strain dependent. All data were obtained in this study.

Characteristic	1	2	3	4	5	6	7
Growth on Simmon's citrate	−	−	−	−	−	−	+
Malonate	−	−	−	−	−	−	+
Hydrolysis of:							
Tween 80	−	−	d†	+	+	+	+
Gelatin	−	−	+	+	−	−	−
Aesculin	d*	+	+	+	+	+	+
Starch	+	+	+	−	+	+	+
Casein	−	−	+	+	−	−	−
DNA	+	+	+	−	−	w	w
Production of:							
α-Galactosidase	−	+	+	+	−	−	−
β-Galactosidase	+	+	+	+	−	−	−

*Two positive out of eight strains.

†Two positive out of four strains.

Chemotaxonomic analyses of the representative strains CCM 8689^T (group I), CCM 8691^T (group II), CCM 8685^T (group III) and CCM 8687^T (group IV) were performed to further characterize the analysed groups.

Analysis of fatty acid methyl esters was performed using an Agilent 7890B gas chromatograph according to the standard protocol of the Sherlock MIDI Identification System (MIDI Sherlock version 6.2, MIDI database RTSBA 6.21). Bacterial cells were grown on R2A agar (Oxoid) at 20±2 °C for 48 h, where the bacterial communities reached the late-exponential stage of growth according to the four quadrants streak method [30]. The predominant fatty acids of strains CCM 8689^T, CCM 8691^T, CCM 8685^T and CCM 8687^T were summed feature 3 ($C_{16:1}\omega7c/C_{16:1}\omega6c$), iso-$C_{15:0}$ and iso-$C_{17:0}$ 3-OH, which corresponded to the fatty acids typically found in other *Pedobacter* species [2]. The complete cellular fatty acid compositions of strains CCM 8689^T, CCM 8691^T, CCM 8685^T and CCM 8687^T and the type strains representing the nearest neighbour species are shown in Table S3.

Freeze-dried biomass for the following chemotaxonomic analyses was prepared from bacterial cells grown on R2A agar plates cultivated at 20 °C for 72 h. Quinones and polar lipids were extracted from freeze-dried biomass and analysed as described previously [31–34]. Analysis of all four strains revealed the presence of the major menaquinone MK-7 and minor amounts of MK-6 (CCM 8691^T: 90.9 % MK-7, 9.1 % MK-6; CCM 8687^T: 77.9 % MK-7; 22.1 % MK-6; CCM 8689^T: 91.4 % MK-7, 8.6 .% MK-6; CCM 8685^T: 97.7 % MK-7, 2.3 % MK-8). In the polar lipid profiles, common to all four strains were the major polar lipids phosphatidylethanolamine, the unidentified lipids L2 and L5 and the unidentified aminolipid AL2 (Fig. S6). The presence of the unidentified aminophospholipid APL1, the aminoglycolipid AGL1, the aminoglycophospholipid AGPL1, the glycolipid GL2, the aminolipid AL3 and the lipids L3 and L7 distinguished strain CCM 8687^T from the other three strains. Strain CCM 8689^T was distinguishable from the other three strains by the presence of lipids L8 and L9. The presence of glycolipid GL1 distinguished strain CCM 8685^T from strain CCM 8691^T and both strains showed a less complex polar lipid profile than the other two strains. The presence of alkali-stable lipids characteristic for sphingolipids in the analysed strains was investigated according to Kato *et al.* [35]. All four strains produced one alkali-stable lipid that was detected after staining with ninhydrin, but none of these was positive for the presence of a phosphate group after staining with molybdenum blue. Hence, the alkali-stable lipids detected are not sphingophospholipids as reported in members of the neighbouring genus *Sphingobacterium* [36]. Polyamines were extracted from freeze-dried biomass cultivated in PYE broth (0.3 % peptone from casein, 0.3 % yeast extract, pH 7.2) at 20 °C for 72 h as described previously [37]. HPLC conditions applied

for analyses of the polyamine patterns were as described by Busse *et al.* [38] and the HPLC apparatus was as described by Stolz *et al.* [32]. *sym*-Homospermidine was the major polyamine in all four strains, which is in accordance with the genus description [1]. Strain CCM 8689^T contained (per gram dry weight) 11.8 µmol *sym*-homospermidine, 0.1 µmol cadaverine and traces of putrescine and spermidine (<0.1 µmol); strain CCM 8691^T contained 14.9 µmol *sym*-homospermidine, 0.1 µmol spermidine and traces of putrescine, cadaverine and spermine (<0.1 µmol); strain CCM 8685^T contained 3.1 µmol *sym*-homospermidine and traces of cadaverine and spermidine (<0.1 µmol); strain CCM 8687^T contained 17.8 µmol *sym*-homospermidine, 0.2 µmol spermidine and traces of cadaverine and spermine (<0.1 µmol). The aforementioned chemotaxonomic characteristics of strains CCM 8689^T, CCM 8691^T, CCM 8685^T and CCM 8687^T corresponded with their assignment to the genus *Pedobacter* [1, 2].

All results obtained in the present study demonstrated that each of the groups I, II, III and IV represents a distinct novel species within the genus *Pedobacter*, for which the names *Pedobacter jamesrossensis* sp. nov., *Pedobacter lithocola* sp. nov., *Pedobacter mendelii* sp. nov. and *Pedobacter petrophilus* sp. nov., respectively, are proposed.

In each of the species descriptions, the numbers given in parentheses in strain-dependent test results show the number of strains revealing a positive reaction. Test results obtained using the Biolog GEN III MicroPlate test panel are given in Table S1. Antibiotic susceptibility profiles are given in Table S2.

PEDOBACTER JAMESROSSENSIS SP. NOV.

Pedobacter jamesrossensis (ja.mes.ross.en′sis. N.L. masc. adj. *jamesrossensis* pertaining to James Ross Island where the type strain was isolated).

Cells are Gram-stain-negative, short rods, 1–1.2×0.5 µm, occurring predominantly in pairs or in irregular clusters, non-motile and non-spore-forming. Colonies on R2A agar are reddish, circular, slightly convex, smooth and glistening with whole margins, and reach about 1–2 mm in diameter when cultivated at 20 °C for 5 days. Flexirubin-type pigments are absent. The species is aerobic; no anaerobic growth on R2A agar is detected. Aerobic but non-fermenting in the OF test. Grows at 1–30 °C, but not at 35 °C. Grows in the presence of up to 1 % (w/v) NaCl; growth in 2 % NaCl is strain dependent (4) and is inhibited in 3 % NaCl. Grows at pH 6–10; growth at pH 11 is strain dependent (3) and growth is not detected at pH 5 or 12. Most abundant growth is observed on R2A agar without NaCl, at pH 8.0 and at 20 °C. Fluorescein pigment is not produced on King B medium. Grows on plate count agar, tryptone soya agar, R2A agar, brain heart infusion agar and nutrient agar, but not on MacConkey agar. Positive reactions for catalase and oxidase, ONPG test and hydrolysis of starch and DNA. Aesculin hydrolysis is strain dependent (2). Negative for Simmon's citrate, sodium malonate, acetamide, hydrolysis of Tween 80, gelatin, casein, tyrosine and lecithin (egg-yolk reaction), production of indol, urease, arginine dihydrolase, lysine and ornithine decarboxylase and reduction of nitrate and nitrite. Enzymatic reactions tested by the API ZYM kit revealed positive test results for alkaline phosphatase, acid phosphatase, leucine arylamidase, valine arylamidase, trypsin, β-galactosidase, α-glucosidase, β-glucosidase, *N*-acetyl-β-glucosaminidase and α-mannosidase, and weakly positive for esterase lipase (C8); negative test results for lipase (C14), chymotrypsin, α-galactosidase, β-glucuronidase; and strain-dependent test results for esterase (C4) (1), cystine arylamidase (6), naphthol-AS-BI-phosphohydrolase (7) and α-fucosidase (7). Contains an alkali-stable lipid. The quinone system consists of the major menaquinone MK-7 and small amounts of MK-6. The polar lipid profile is composed of the major lipids phosphatidylethanolamine, the unidentified lipids L2 and L5 and the unidentified aminolipid AL2, and moderate to minor amounts of the unidentified lipids L1, L6, L8 and L9, glycolipid GL1 and aminolipid AL1. *sym*-Homospermidine is the major polyamine. iso-$C_{15:0}$, iso-$C_{17:0}$ 3-OH and summed feature 3 ($C_{16:1}\omega7c/C_{16:1}\omega6c$) are the major cellular fatty acids.

The type strain, CCM 8689^T (=LMG 29684^T), was isolated from stone fragments sampled at Devils Rocks locality at James Ross Island (Antarctica). The genomic DNA G+C content of the type strain is 36.2 mol%. Most characteristics of the type strain are in agreement with the general species description. The strain-dependent characteristics of the type strain are as follows: no hydrolysis of aesculin, no growth in 2 % (w/v) NaCl and at pH 11, no production of esterase (C4), cystine arylamidase or α-fucosidase, and weak production of naphthol-AS-BI-phosphohydrolase.

PEDOBACTER LITHOCOLA SP. NOV.

Pedobacter lithocola [li.tho′co.la. Gr. n. *lithos* stone, L. suff. -*cola* (from L. n. *incola*) inhabitant; N.L. masc. n. *lithocola* a dweller of stones].

Cells are Gram-stain-negative, short rods, 0.9–1.4×0.4–0.5 µm, occurring predominantly in pairs or in irregular clusters, non-motile and non-spore-forming. Colonies on R2A agar are reddish, circular, slightly convex, smooth and glistening with whole margins, and reach about 1–2 mm in diameter when cultivated at 20 °C for 5 days. Flexirubin-type pigments are absent. The species is aerobic; no anaerobic growth on R2A agar is detected. Aerobic but non-fermenting in OF test. Grows at 1–30 °C, but not at 35 °C. Grows in the presence of up to 1 % (w/v) NaCl; growth is inhibited with ≥2 % NaCl. Grows at pH 6–8; growth at pH 9 is strain dependent and growth is not detected at pH 5 or pH ≥10. Most abundant growth is observed on R2A agar without NaCl, at pH 8.0 and at 20 °C. Fluorescein pigment is not produced on King B medium. Grows on plate count agar, tryptone soya agar, R2A agar, brain heart infusion agar and nutrient agar, but not on MacConkey agar. Positive reactions for catalase and oxidase, ONPG test and hydrolysis of starch, aesculin and DNA. Negative for

Simmon's citrate, sodium malonate, acetamide, hydrolysis of Tween 80, gelatin, casein, tyrosine and lecithin (egg-yolk reaction), production of indol, urease, arginine dihydrolase, lysine and ornithine decarboxylase and reduction of nitrate and nitrite. Enzymatic reactions tested by the API ZYM kit revealed positive results for alkaline phosphatase, acid phosphatase, leucine arylamidase, valine arylamidase, trypsin, naphthol-AS-BI-phosphohydrolase, α-galactosidase, β-galactosidase, α-glucosidase, β-glucosidase, *N*-acetyl-β-glucosaminidase and α-mannosidase, and weakly positive for esterase lipase (C8) and cystine arylamidase. Negative test results for lipase (C14), chymotrypsin and β-glucuronidase; and strain dependent test results are detected for esterase (C4) and α-fucosidase. Contains an alkali-stable lipid. The quinone system consists of the major menaquinone MK-7 and small amounts of MK-6. The polar lipid profile is composed of the major lipids phosphatidylethanolamine, the unidentified lipids L2 and L5 and the unidentified aminolipid AL2, and minor amounts of unidentified aminolipid AL1. *sym*-Homospermidine is the major polyamine. iso-$C_{15:0}$, iso-$C_{17:0}$ 3-OH and summed feature 3 ($C_{16:1}\omega7c$/$C_{16:1}\omega6c$) are the major cellular fatty acids.

The type strain, CCM 8691^T (=LMG 29685^T), was isolated from stone fragments sampled at Panorama Pass locality at James Ross Island (Antarctica). The genomic DNA G+C content of the type strain is 35.6 mol%. Most characteristics of the type strain are in agreement with the general species description. The strain-dependent characteristics of the type strain are as follows: growth at pH 9, and no production of esterase (C4) or α-fucosidase.

PEDOBACTER MENDELII SP. NOV.

Pedobacter medelii (men.de'li.i. N.L. gen. n. *mendelii* of Mendel, named in honour of Johann Gregor Mendel, a pioneer of genetics, for his contribution to general genetics; the name also reflects the fact that the species was isolated near the Johann Gregor Mendel Antarctic station).

Cells are Gram-stain-negative, short rods, 1–1.3×0.5 µm, occurring predominantly in pairs or in irregular clusters, non-motile and non-spore-forming. Colonies on R2A agar are reddish, circular, slightly convex, smooth and glistening with whole margins, and reach about 1–2 mm in diameter when cultivated at 20 °C for 5 days. Flexirubin-type pigments are absent. The species is aerobic; no anaerobic growth on R2A agar is detected. Aerobic but non-fermenting in the OF test. Grows at 1–30 °C, but not at 35 °C. Grows in the presence of up to 2 % (w/v) NaCl; growth was inhibited in 3 % NaCl. Grows at pH 6–8; growth at pH 9 is strain dependent (1) and growth is not detected at pH 5 or pH ≥10. Most abundant growth is observed on R2A agar without NaCl, at pH 8.0 and at 20 °C. Fluorescein pigment is not produced on King B medium. Grows on plate count agar, tryptone soya agar, R2A agar, brain heart infusion agar and nutrient agar, but not on MacConkey agar. Positive reactions for catalase and oxidase, ONPG test and hydrolysis of gelatin, aesculin, starch, casein and DNA. Hydrolysis of Tween 80 is strain dependent (2). Negative for Simmon's citrate, sodium malonate, acetamide, hydrolysis of tyrosine and lecithin (egg-yolk reaction), production of indol, urease, arginine dihydrolase, lysine and ornithine decarboxylase and reduction of nitrate and nitrite. Enzymatic reactions tested by the API ZYM kit reveal positive test results for alkaline phosphatase, acid phosphatase, leucine arylamidase, valine arylamidase, trypsin, naphthol-AS-BI-phosphohydrolase, α-galactosidase, β-galactosidase, α-glucosidase, β-glucosidase, *N*-acetyl-β-glucosaminidase, α-mannosidase and α-fucosidase and weakly positive for esterase lipase (C8); negative test results for esterase (C4), lipase (C14), cystine arylamidase, chymotrypsin and β-glucuronidase. Contains an alkali-stable lipid. The quinone system consists of the major menaquinone MK-7 and small amounts of MK-6. The polar lipid profile is composed of the major lipids phosphatidylethanolamine, the unidentified lipids L2 and L5 and the unidentified aminolipid AL2, and moderate to minor amounts of the unidentified lipid L6, aminolipid AL1 and glycolipid GL1. *sym*-Homospermidine is the major polyamine. iso-$C_{15:0}$, iso-$C_{17:0}$ 3-OH and summed feature 3 ($C_{16:1}\omega7c$/$C_{16:1}\omega6c$) are major cellular fatty acids.

The type strain, CCM 8685^T (=LMG 29688^T), was isolated from stone fragments sampled at Lachman Crags locality at James Ross Island (Antarctica). The genomic DNA G+C content of the type strain is 35.5 mol%. Most characteristics of the type strain are in agreement with the general species description. The strain-dependent characteristics of the type strain are as follows: no growth at pH 9 and no Tween 80 hydrolysis.

PEDOBACTER PETROPHILUS SP. NOV.

Pedobacter petrophilus [pe.tro'phi.lus. Gr. n. *petra* rock; N.L. masc. adj. *philus* (from Gr. masc. adj. *philos*) friend, loving; N.L. masc. adj. *petrophilus*, rock loving].

Cells are Gram-stain-negative, short rods, 1.2–1.6×0.6 µm, occurring predominantly in pairs or in irregular clusters, non-motile and non-spore-forming. Colonies on R2A agar are pink, circular, slightly convex, smooth and glistening with whole margins, and reach about 1–2 mm in diameter when cultivated at 20 °C for 5 days. Flexirubin-type pigments are absent. The species is aerobic; no anaerobic growth on R2A agar is detected. Aerobic but non-fermenting in the OF test. Grows at 1–30 °C, but not at 35 °C. Grows in the presence of up to 2 % (w/v) NaCl; growth is inhibited with 3 % NaCl. Grows at a pH 6–9; growth at pH 10 is strain dependent (1) and growth is not detected at pH 5 or ≥11. Most abundant growth is observed on R2A agar without NaCl, at pH 8.0 and at 20 °C. Fluorescein pigment is not produced on King B medium. Grows on plate count agar, tryptone soya agar, R2A agar, brain heart infusion agar and nutrient agar, but not on MacConkey agar. Positive reactions for catalase and oxidase, ONPG test and hydrolysis of Tween 80, gelatin, aesculin and casein. Negative for Simmon's citrate, sodium malonate, acetamide, hydrolysis of starch, DNA, tyrosine and lecithin (egg-yolk

reaction), production of indol, urease, arginine dihydrolase, lysine and ornithine decarboxylase and reduction of nitrate and nitrite. Enzymatic reactions tested by the API ZYM kit revealed positive results for alkaline phosphatase, acid phosphatase, leucine arylamidase, valine arylamidase, trypsin, naphthol-AS-BI-phosphohydrolase, α-galactosidase, β-galactosidase, α-glucosidase, β-glucosidase, *N*-acetyl-β-glucosaminidase and α-mannosidase and weakly positive for esterase lipase (C8); negative test results for esterase (C4), lipase (C14), cystine arylamidase, chymotrypsin, β-glucuronidase and α-fucosidase. Contains an alkali-stable lipid. The quinone system consists of the major menaquinone MK-7 and small amounts of MK-6. The polar lipid profile is composed of the major lipids phosphatidylethanolamine, the unidentified lipids L2 and L5 and the unidentified aminolipid AL2, and moderate to minor amounts of the unidentified lipids L1, L3, L4, L6 and L7, glycolipid GL2, aminophospholipid APL1, aminoglycolipid AGL1, aminoglycophospholipid AGPL1 and aminolipid AL2. *sym*-Homospermidine is the major polyamine. iso-$C_{15:0}$, iso-$C_{17:0}$ 3-OH and summed feature 3 ($C_{16:1}\omega7c$/$C_{16:1}\omega6c$) are major cellular fatty acids.

The type strain, CCM 8687^T (=LMG 29686^T), was isolated from stone fragments sampled at Devils Rocks locality at James Ross Island (Antarctica). The genomic DNA G+C content of the type strain is 38.8 mol%. Most characteristics of the type strain are in agreement with the general species description. The strain-dependent characteristics of the type strain are as follows: weak growth at pH 10.

Funding information
We are grateful to the scientific infrastructure of the J. G. Mendel Czech Antarctic Station as a part of the Czech Polar Research Infrastructure (CzechPolar2) supported by the Ministry of Education, Youth and Sports of the Czech Republic (LM2015078). S. K. is a holder of Brno PhD Talent financial aid.

Acknowledgements
Dr Daniel Krsek (National Reference Laboratory for Diagnostic Electron Microscopy of Infectious Agents, National Institute of Public Health, Prague, Czech Republic) is acknowledged for transmission electron microscopy and Jana Bajerová (Czech Collection of Microorganisms, Masaryk University, Brno, Czech Republic) is acknowledged for excellent technical assistance.

Conflicts of interest
The authors declare that there are no conflicts of interest.

References

1. Steyn PL, Segers P, Vancanneyt M, Sandra P, Kersters K *et al.* Classification of heparinolytic bacteria into a new genus, *Pedobacter*, comprising four species: *Pedobacter heparinus* comb. nov., *Pedobacter piscium* comb. nov., *Pedobacter africanus* sp. nov. and *Pedobacter saltans* sp. nov. proposal of the family *Sphingobacteriaceae* fam. nov. *Int J Syst Bacteriol* 1998;48:165–177.
2. Margesin R, Shivaji S. Genus II. *Pedobacter* Steyn, Segers, Vancanneyt, Sandra, Kersters and Joubert 1998, 171^{VP}. In: Krieg NR, Staley JT, Brown DR, Hedlund BP, Paster BJ *et al.* (editors). *Bergey's Manual of Systematic Bacteriology The Bacteroidetes, Spirochaetes, Tenericutes (Mollicutes), Acidobacteria, Fibrobacteres, Fusobacteria, Dictyoglomi, Gemmatimonadetes, Lentisphaerae, Verrucomicrobia, Chlamydiae, and Planctomycetes*, vol. 4. New York, USA: Springer; 2010. pp. 339–351.
3. Da X, Jiang F, Chang X, Ren L, Qiu X *et al.* *Pedobacter ardleyensis* sp. nov., isolated from soil in Antarctica. *Int J Syst Evol Microbiol* 2015;65:3841–3846.
4. Qiu X, Qu Z, Jiang F, Ren L, Chang X *et al.* *Pedobacter huanghensis* sp. nov. and *Pedobacter glacialis* sp. nov., isolated from Arctic glacier foreland. *Int J Syst Evol Microbiol* 2014;64:2431–2436.
5. Zhou Z, Jiang F, Wang S, Peng F, Dai J *et al.* *Pedobacter arcticus* sp. nov., a facultative psychrophile isolated from Arctic soil, and emended descriptions of the genus *Pedobacter*, *Pedobacter heparinus*, *Pedobacter daechungensis*, *Pedobacter terricola*, *Pedobacter glucosidilyticus* and *Pedobacter lentus*. *Int J Syst Evol Microbiol* 2012;62:1963–1969.
6. Edwards U, Rogall T, Blöcker H, Emde M, Böttger EC. Isolation and direct complete nucleotide determination of entire genes. Characterization of a gene coding for 16S ribosomal RNA. *Nucleic Acids Res* 1989;17:7843–7853.
7. Kim OS, Cho YJ, Lee K, Yoon SH, Kim M *et al.* Introducing EzTaxon-e: a prokaryotic 16S rRNA gene sequence database with phylotypes that represent uncultured species. *Int J Syst Evol Microbiol* 2012;62:716–721.
8. Stackebrandt E, Ebers J. Taxonomic parameters revisited: tarnished gold standards. *Microbiol Today* 2006;8:152–155.
9. Tamura K, Stecher G, Peterson D, Filipski A, Kumar S. MEGA6: molecular Evolutionary genetics analysis version 6.0. *Mol Biol Evol* 2013;30:2725–2729.
10. Švec P, Nováková D, Žáčková L, Kukletová M, Sedláček I. Evaluation of $(GTG)_5$-PCR for rapid identification of *Streptococcus mutans*. *Antonie van Leeuwenhoek* 2008;94:573–579.
11. Cleenwerck I, Vandemeulebroecke K, Janssens D, Swings J. Re-examination of the genus *Acetobacter*, with descriptions of *Acetobacter cerevisiae* sp. nov. and *Acetobacter malorum* sp. nov. *Int J Syst Evol Microbiol* 2002;52:1551–1558.
12. Mesbah M, Whitman WB. Measurement of deoxyguanosine/thymidine ratios in complex mixtures by high-performance liquid chromatography for determination of the mole percentage guanine + cytosine of DNA. *J Chromatogr A* 1989;479:297–306.
13. Ezaki T, Hashimoto Y, Yabuuchi E. Fluorometric deoxyribonucleic acid-deoxyribonucleic acid hybridization in microdilution wells as an alternative to membrane filter hybridization in which radioisotopes are used to determine genetic relatedness among bacterial strains. *Int J Syst Bacteriol* 1989;39:224–229.
14. Goris J, Suzuki K-Ichiro, Vos PD, Nakase T, Kersters K. Evaluation of a microplate DNA–DNA hybridization method compared with the initial renaturation method. *Can J Microbiol* 1998;44:1148–1153.
15. Wayne LG, Moore WEC, Stackebrandt E, Kandler O, Colwell RR, Brenner DJ, Grimont PAD *et al.* Report of the ad hoc committee on reconciliation of approaches to bacterial systematics. *Int J Syst Evol Microbiol* 1987;37:463–464.
16. Atlas RM, Snyder JW. Reagents, stains, and media: Bacteriology. In: Versalovic J, Carroll KC, Funke G, Jorgensen JH, Landry ML*et al.* (editors). *Manual of Clinical Microbiology*, 10th ed, vol. 1. Washington: ASM Press; 2011. pp. 272–303.
17. Hugh R, Leifson E. The taxonomic significance of fermentative versus oxidative metabolism of carbohydrates by various Gram negative bacteria. *J Bacteriol* 1953;66:24–26.
18. Christensen WB. Urea decomposition as a means of differentiating *Proteus* and paracolon cultures from each other and from *Salmonella* and *Shigella* types. *J Bacteriol* 1946;52:461–466.
19. Brooks K, Sodeman T. A rapid method for determining decarboxylase and dihydrolase activity. *J Clin Pathol* 1974;27:148–152.
20. Barrow GI, Feltham RKA. *Cowan and Steel's Manual for the Identification of Medical Bacteria*, 3rd ed. Great Britain: Cambridge University Press; 1993.
21. Páčová Z, Kocur M. New medium for detection of esterase and gelatinase activity. *Zb Bakt Hyg* 1984;258:69–73.

22. **Kurup VP, Babcock JB.** Use of casein, tyrosine, and hypoxanthine in the identification of nonfermentative Gram-negative bacilli. *Med Microbiol Immunol* 1979;167:71–75.
23. **Owens JJ.** The egg yolk reaction produced by several species of bacteria. *J Appl Bacteriol* 1974;37:137–148.
24. **Lowe GH.** The rapid detection of lactose fermentation in paracolon organisms by the demonstration of beta-D-galactosidase. *J Med Lab Technol* 1962;19:21–25.
25. **Oberhofer TR, Rowen JW.** Acetamide agar for differentiation of nonfermentative bacteria. *Appl Microbiol* 1974;28:720–721.
26. **Ewing WH.** Enterobacteriaceae. Biochemical Methods for Group Differentation. Public Health Service Publication Nono 734 CDC, Atlanta. 1960.
27. **Bernardet JF, Nakagawa Y, Holmes B. Subcommittee on the taxonomy of *Flavobacterium Cytophaga*-like bacteria of the International Committee on Systematics of Prokaryotes.** Proposed minimal standards for describing new taxa of the family *Flavobacteriaceae* and emended description of the family. *Int J Syst Evol Microbiol* 2002;52:1049–1070.
28. **CLSI**. *Performance Standards for Antimicrobial Susceptibility Testing; Twenty-Fifth Informational Supplement (M100–s25)*. Vol. 35, No. 3. 2015.
29. **EUCAST.** 2015. European committee on antimicrobial susceptibility testing. EUCAST clinical breakpoints - bacteria (version 5.0). http://www.eucast.org.
30. **Sasser M.** *Identification of Bacteria by Gas Chromatography of Cellular Fatty Acids*, MIDI Technical Note 101. Newark,DE: Microbial ID, Inc; 1990.
31. **Altenburger P, Kämpfer P, Makristathis A, Lubitz W, Busse HJ.** Classification of bacteria isolated from a medieval wall painting. *J Biotechnol* 1996;47:39–52.
32. **Stolz A, Busse HJ, Kämpfer P.** *Pseudomonas knackmussii* sp. nov. *Int J Syst Evol Microbiol* 2007;57:572–576.
33. **Tindall BJ.** Lipid composition of *Halobacterium lacusprofundi*. *FEMS Microbiol Lett* 1990;66:199–202.
34. **Tindall BJ.** A comparative study of the lipid composition *of Halobacterium saccharovorum* from various sources. *Syst Appl Microbiol* 1990;13:128–130.
35. **Kato M, Muto Y, Tanaka-Bandoh K, Watanabe K, Ueno K.** Sphingolipid composition in *Bacteroides* species. *Anaerobe* 1995;1:135–139.
36. **Naka T, Fujiwara N, Yano I, Maeda S, Doe M *et al.*** Structural analysis of sphingophospholipids derived from *Sphingobacterium spiritivorum*, the type species of genus *Sphingobacterium*. *Biochim Biophys Acta* 2003;1635:83–92.
37. **Busse HJ, Auling G.** Polyamine pattern as a chemotaxonomic marker within the proteobacteria. *Syst Appl Microbiol* 1988;11:1–8.
38. **Busse HJ, Bunka S, Hensel A, Lubitz W.** Discrimination of members of the family *Pasteurellaceae* based on polyamine patterns. *Int J Syst Bacteriol* 1997;47:698–708.

International Journal of Systematic and Evolutionary Microbiology

Supplementary materials

Pedobacter jamesrossensis sp. nov., *Pedobacter lithocola* sp. nov., *Pedobacter mendelii* sp. nov., and *Pedobacter petrophilus* sp. nov., isolated from Antarctic environment

Pavel Švec[1,*], Stanislava Králová[1], Hans-Jürgen Busse[2], Tanita Kleinhagauer[2], Roman Pantůček[3], Ivana Mašlaňová[3], Margo Cnockaert[4], Peter Vandamme[4], Eva Staňková[1], Tereza Gelbíčová[1], Pavla Holochová[1], Miloš Barták[5], Kamila Kýrová[1], and Ivo Sedláček[1]

[1]Czech Collection of Microorganisms, Department of Experimental Biology, Faculty of Science, Masaryk University, Kamenice 5, 625 00 Brno, Czech Republic

[2]Institute of Microbiology, University of Veterinary Medicine Vienna, A-1210 Vienna, Austria

[3]Section of Molecular Biology, Department of Experimental Biology, Faculty of Science, Masaryk University, Kamenice 5, 625 00 Brno, Czech Republic

[4]Department of Biochemistry and Microbiology, Faculty of Sciences, Ghent University, K.L. Ledeganckstraat 35, 9000 Ghent, Belgium

[5]Section of Physiology and Anatomy of Plants, Department of Experimental Biology, Faculty of Science, Masaryk University, Kamenice 5, 625 00 Brno, Czech Republic

*Corresponding author: Pavel Švec, E-mail: mpavel@sci.muni.cz

Table S1. Test results obtained using the Biolog GEN III MicroPlate test panel from *P. jamesrossensis* sp. nov. (group I), *P. lithocola* sp. nov. (group II), *P. mendelii* sp. nov. (group III), *P. petrophilus* sp. nov. (group IV) and phylogenetically related *Pedobacter* spp.

All data were obtained in this study. +, Positive; -, negative; b, borderline reaction.

All strains were positive for utilization of dextrin, D-maltose, D-trehalose, D-cellobiose, gentiobiose, sucrose, D-turanose, D-raffinose, α-D-lactose, D-melibiose, β-methyl-D-glucoside, D-salicin, α-D-Glucose, D-mannose, D-fructose, D-galactose, gelatin, glycyl-L-proline, L-glutamic acid, pectin, D-galacturonic acid, L-galactonic acid, and lactone, and negative for utilization of N-acetyl-β-D-mannosamine, 3-methyl glucose, inosine, D-sorbitol, D-mannitol, glycerol, D-aspartic acid, D-serine, L-arginine, L-pyroglutamic acid, D-gluconic acid, mucic acid, quinic acid, D-saccharic acid, p-hydroxy-phenylacetic acid, methyl pyruvate, D-lactic acid methyl ester, L-lactic acid, citric acid, α-keto-glutaric acid, D-malic acid, bromo-succinic acid, γ amino-butryric acid, α-hydroxy-butyric acid, β-hydroxy-D,L-butyric acid, α-keto-butyric acid, propionic acid, and formic acid. All strains were inhibited by pH 5, 4 % and 8 % NaCl, fusidic acid, D-serine, troleandomycin, minocycline, lincomycin, niaproof 4, lithium chloride, potassium tellurite, sodium butyrate and sodium bromate, but they grew in the presence of tetrazolium blue and aztreonam.

Characteristic	Group I								Group II		Group III				Group IV			*P. jejuensis* CCM 8565^T	*P. ginsengiterrae* CCM 8571^T	*P. aquatilis* CCM 7347^T
	CCM 8689^T	CCM 8690	P3164	P3658	P3679	P3802	P3824	P4838	CCM 8691^T	P3926	CCM 8685^T	CCM 8686	P2490	P2749	CCM 8687^T	CCM 8688	P4106			
Utilization of																				
Stachyose	+	+	+	+	+	+	+	+	-	-	-	-	b	-	+	+	+	+	b	+
N-Acetyl-D-Glucosamine	+	+	+	+	+	+	+	+	+	-	b	+	+	b	+	b	+	+	+	+
N-Acetyl-D-Galactosamine	+	+	+	+	+	+	+	+	-	-	-	+	b	-	-	-	-	+	+	+
N-Acetyl Neuraminic Acid	-	-	-	-	-	-	-	-	-	-	-	-	-	-	-	-	-	-	+	-
D-Fucose	+	-	-	-	-	-	-	-	-	-	-	-	-	-	-	-	-	b	b	+
L-Fucose	-	-	-	-	-	-	-	-	-	-	-	-	-	-	+	b	b	+	+	+
L-Rhamnose	+	+	+	+	+	+	+	+	b	+	b	+	+	+	+	+	+	+	+	+
D-Arabitol	-	-	-	-	-	-	-	-	-	-	-	-	-	-	-	-	-	-	-	+
myo-Inositol	-	+	-	-	-	-	-	-	-	-	-	-	b	-	-	-	-	-	-	b
D-Glucose-6-PO4	+	+	b	b	b	b	+	b	-	-	-	-	b	-	-	-	-	+	b	+
D-Fructose-6-PO4	+	+	+	+	+	+	+	-	-	-	-	-	-	-	b	-	-	+	+	+
L-Alanine	-	-	-	-	-	-	-	-	-	-	-	+	-	b	-	-	-	-	-	b
L-Aspartic Acid	+	+	+	+	+	+	+	+	-	-	b	+	+	b	+	b	+	+	+	+
L-Glutamic Acid	+	+	+	+	+	+	+	+	+	+	+	+	+	+	+	+	+	+	+	+
L-Histidine	b	+	b	-	b	b	-	-	b	+	b	+	b	b	-	-	-	-	+	+
L-Serine	-	b	-	-	b	b	-	b	-	-	-	-	-	-	b	-	-	-	+	b
D-Glucuronic Acid	+	+	+	+	+	+	+	+	-	-	-	+	-	-	+	+	+	+	+	+
Glucuronamide	-	-	b	-	-	-	-	-	-	-	-	-	b	b	b	b	-	+	+	+
L-Malic Acid	-	-	-	-	-	-	-	-	-	-	-	-	-	-	+	+	+	-	-	-
Tween 40	-	+	-	-	b	-	-	+	-	-	-	-	-	-	-	-	-	-	-	-
Acetoacetic Acid	+	-	+	b	+	+	+	-	-	-	-	-	-	-	+	+	+	+	+	+
Acetic Acid	+	b	b	b	+	+	+	+	+	-	+	+	+	+	+	+	+	+	+	+
Sensitivity to																				
pH 6	-	-	-	-	-	-	-	-	-	b	b	+	-	b	b	+	-	-	-	-
1% NaCl	-	b	-	b	-	b	-	+	+	+	+	+	+	+	+	+	+	-	b	-
1% Sodium Lactate	-	b	b	-	-	-	-	b	+	+	+	+	+	+	+	+	+	-	-	-
Rifamycin SV	+	+	+	+	+	+	+	b	+	+	-	+	-	-	+	+	+	-	+	+
Guanidine HCl	+	+	+	+	+	+	+	+	+	+	+	+	+	+	+	+	+	-	+	+
Vancomycin	-	-	-	-	-	-	-	-	+	+	-	+	+	-	+	-	-	-	-	-
Tetrazolium Violet	-	+	-	-	-	-	-	b	b	b	b	b	+	b	+	b	b	-	-	b
Nalidixic Acid	b	-	b	b	b	b	b	-	-	-	-	-	-	-	b	+	+	-	-	-

Table S2. Antibiotic susceptibility profiles of analysed *Pedobacter* spp. strains

S, susceptible; R, resistant; I, intermediate

Strain	Ampicillin	Aztreonam	Carbenicillin	Cefixime	Ceftazidime	Cephalothin	Ciprofloxacin	Gentamicine	Chloramphenicol	Imipenem	Kanamycin	Cotrimoxazole	Piperacillin	Polymyxin B	Streptomycin	Tetracycline
***P. jamesrossensis* sp. nov. (group I)**																
CCM 8689^T	R	R	R	R	R	R	R	R	S	S	R	S	R	R	I	S
CCM 8690	R	R	R	R	R	R	R	R	S	I	R	S	R	R	I	S
P3164	R	R	R	R	R	R	R	R	S	S	R	S	R	R	I	S
P3658	R	R	R	R	R	R	R	R	S	S	R	S	R	R	R	S
P3679	R	R	R	R	R	R	R	R	S	S	R	S	R	R	S	S
P3802	R	R	R	R	R	R	R	R	S	S	R	S	R	R	S	S
P3824	R	R	R	R	R	R	R	R	S	S	R	S	R	R	S	S
P4838	R	R	R	R	R	R	R	R	S	S	I	S	R	R	S	S
***P. lithocola* sp. nov. (group II)**																
CCM 8691^T	S	R	S	R	R	R	R	R	S	S	S	S	R	S	S	S
P3926	R	R	S	R	R	R	S	R	S	S	S	S	R	S	S	S
***P. mendelii* sp. nov. (group III)**																
CCM 8685^T	R	I	S	R	R	R	S	R	S	S	S	S	R	R	S	S
CCM 8686	R	R	R	R	R	R	S	R	S	S	S	S	R	R	S	S
P2490	R	R	R	R	R	R	S	R	S	S	S	S	R	S	S	S
P2749	R	R	S	R	R	R	R	R	S	S	S	S	R	S	S	S
***P. petrophilus* sp. nov. (group IV)**																
CCM 8687^T	R	R	R	R	R	R	R	R	R	S	R	S	R	R	R	S
CCM 8688	R	R	R	R	R	R	R	R	R	S	R	S	R	R	R	S
P4106	R	R	R	R	R	R	R	R	R	S	R	S	R	R	I	S

Table S3. Cellular fatty acid composition (as a percentage of the total) of strains CCM 8689^T (group I), CCM 8691^T (group II), CCM 8685^T (group III), CCM 8687^T (group IV) and type strains of the phylogenetically nearest *Pedobacter* species.

All data were obtained in this study. Fatty acids revealing less than 1 % in all strains are not shown. ND, not detected; TR, trace amount (< 1 %).

Fatty acid	**CCM 8689^T (group I)**	**CCM 8691^T (group II)**	**CCM 8685^T (group III)**	**CCM 8687^T (group IV)**	***P. agri* CCM 8572^T**	***P. alluvionis* CCM 8562^T**	***P. aquatilis* CCM 7347^T**	***P. borealis* CCM 8563^T**	***P. ginsengiterrae* CCM 8571^T**	***P. ginsenosidimutans* CCM 8564^T**	***P. jejuensis* CCM 8565^T**	***P. sandarakinus* KCTC 12559^T**
$C_{11:0}$ anteiso	1.5	ND	TR	ND	ND	1.3	TR	ND	1.4	1.4	TR	TR
$C_{15:0}$ iso	12.0	8.4	10.2	17.9	18.8	19.5	15.3	18.5	15.4	19.0	18.4	14.6
$C_{15:0}$ anteiso	7.6	8.4	9.5	5.5	5.4	3.9	3.8	5.7	6.5	3.2	3.3	5.1
$C_{15:1}$ *ω6c*	TR	3.3	1.2	2.8	2.4	2.0	1.8	3.2	1.2	2.0	3.0	3.4
$C_{16:1}$ iso H	1.2	3.5	1.4	TR	TR	TR	TR	TR	TR	TR	1.2	2.3
$C_{16:0}$ iso	1.8	2.9	1.4	1.2	1.6	TR	1.1	TR	1.1	TR	1.6	5.6
$C_{16:1}$ *ω5c*	4.0	3.7	3.1	2.6	3.1	2.4	3.3	1.6	3.9	2.2	2.7	1.2
$C_{15:0}$ iso 3OH	1.4	1.4	1.3	2.3	1.7	2.8	2.0	2.2	1.8	2.6	2.1	1.6
$C_{15:0}$ 2OH	1.1	2.1	2.0	1.4	1.4	1.0	1.5	1.4	1.0	1.0	1.4	2.2
$C_{17:1}$ anteiso *ω9c*	1.3	3.3	2.9	ND	ND	ND	ND	ND	ND	ND	ND	ND
$C_{17:1}$ *ω8c*	TR	TR	TR	1.1	TR	TR	TR	TR	TR	TR	TR	1.6
$C_{17:1}$ *ω6c*	ND	1.4	ND	TR	TR	TR	1.0	1.1	TR	TR	1.1	1.7
$C_{16:0}$ iso 3OH	6.6	9.2	5.8	6.6	5.0	2.9	5.8	4.5	5.4	4.1	4.7	9.6
$C_{16:0}$ 3OH	1.9	1.1	1.1	TR	2.4	2.3	3.1	1.8	3.2	2.7	2.0	1.0
$C_{17:0}$ iso 3OH	11.4	7.7	12.4	14.8	13.3	15.7	14.4	14.3	12.3	15.8	15.0	11.0
$C_{17:0}$ 2OH	6.6	7.2	9.5	4.2	3.4	2.8	3.4	3.6	4.3	2.7	2.6	3.4
Summed Feature 3*	34.7	28.2	30.6	31.3	31.5	33.2	34.2	32.0	34.7	33.7	29.9	25.4
Summed Feature 9†	2.9	3.3	3.9	3.5	3.9	4.7	3.6	4.5	2.8	4.2	5.1	5.5

*$C_{16:1}$ *ω7c*/ $C_{16:1}$ *ω6c*; †$C_{16:0}$ 10-methyl/ $C_{17:1}$ iso *ω9c*

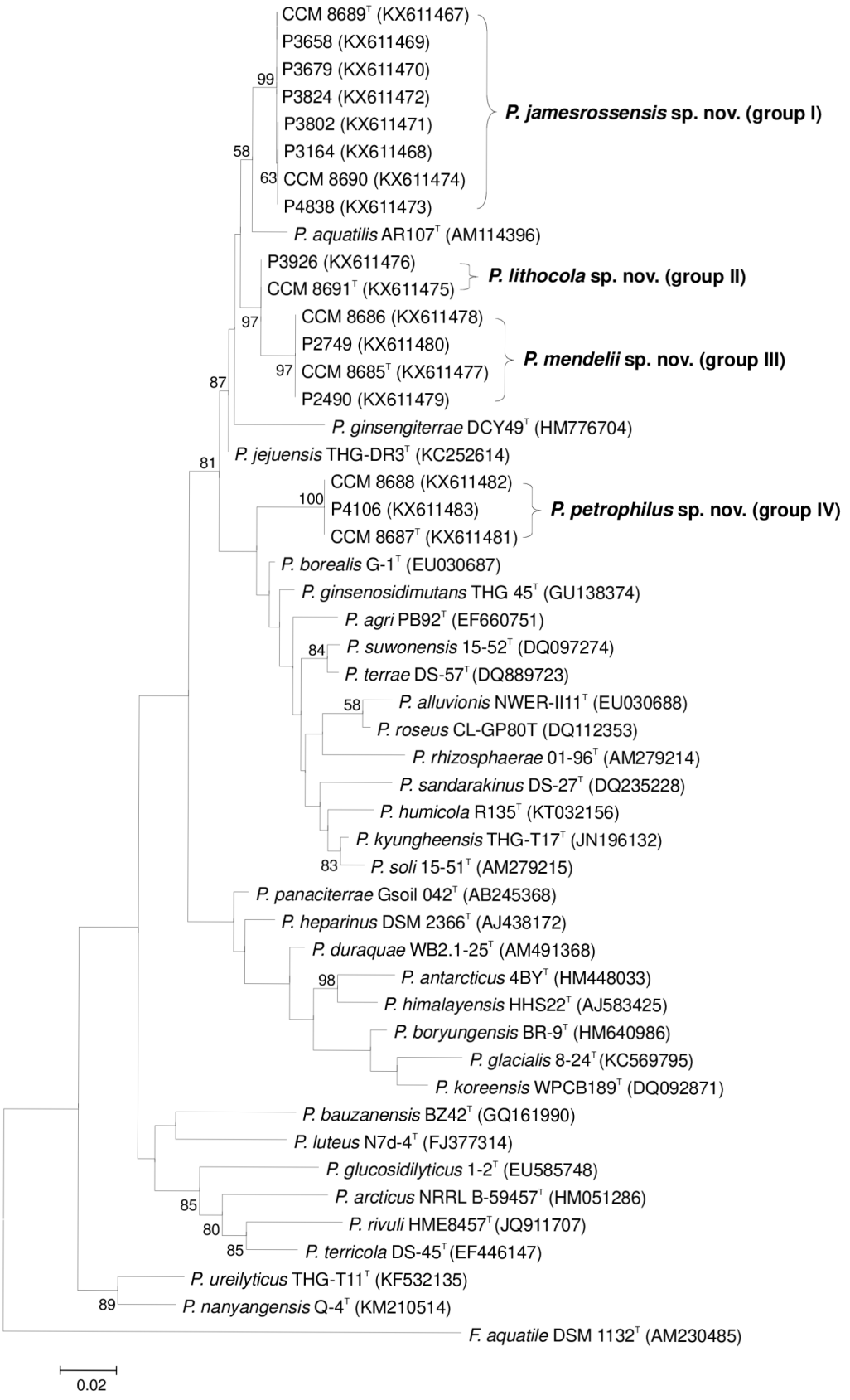

Fig. S1. Maximum Likelihood phylogenetic tree, based on 16S rRNA gene sequences, showing the phylogenetic position of groups I–IV strains within the genus *Pedobacter*. The evolutionary history was inferred by using the Kimura 2-parameter model. Bootstrap probability values (percentages of 1,000 tree replications) greater than 50 % are indicated at branch points. *Flavobacterium aquatile* DSM 1132^T (AM230485) was used as an outgroup. Bar, 0.02 substitutions per nucleotide position.

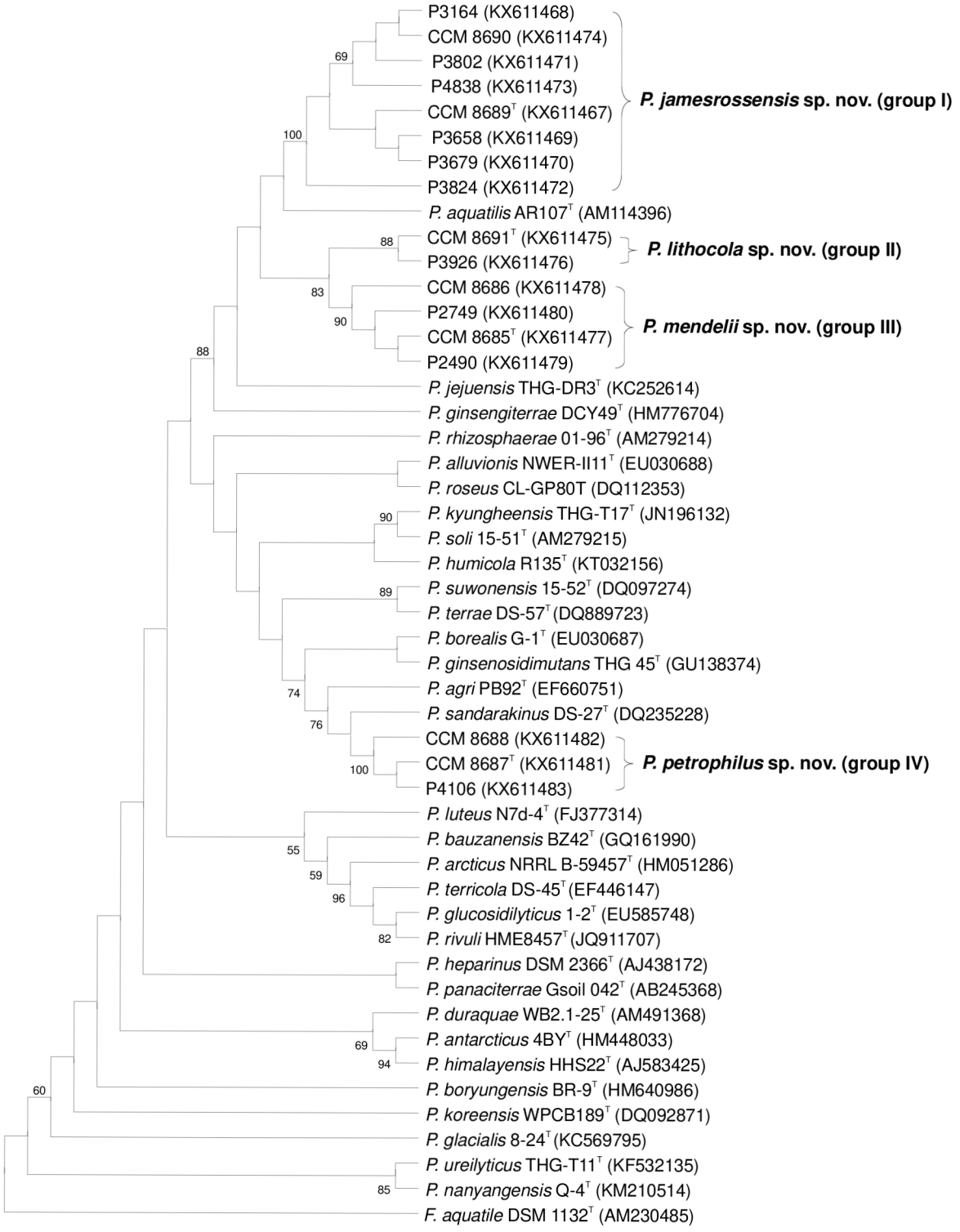

Fig. S2. Maximum Parsimony phylogenetic tree, based on 16S rRNA gene sequences, showing the phylogenetic position of groups I–IV strains within the genus *Pedobacter*. The most parsimonious tree with length = 1432 is shown. The consistency index is (0.338435), the retention index is (0.615802), and the composite index is 0.281006 (0.208409) for all sites and parsimony-informative sites (in parentheses). The percentage of replicate trees greater than 50 % in which the associated taxa clustered together in the bootstrap test (1000 replicates) are shown at branch points. The tree was obtained using the Subtree-Pruning-Regrafting (SPR) algorithm with search level 1 in which the initial trees were obtained by the random addition of sequences (10 replicates). There were a total of 1523 positions in the final dataset. *Flavobacterium aquatile* DSM 1132^T (AM230485) was used as an outgroup.

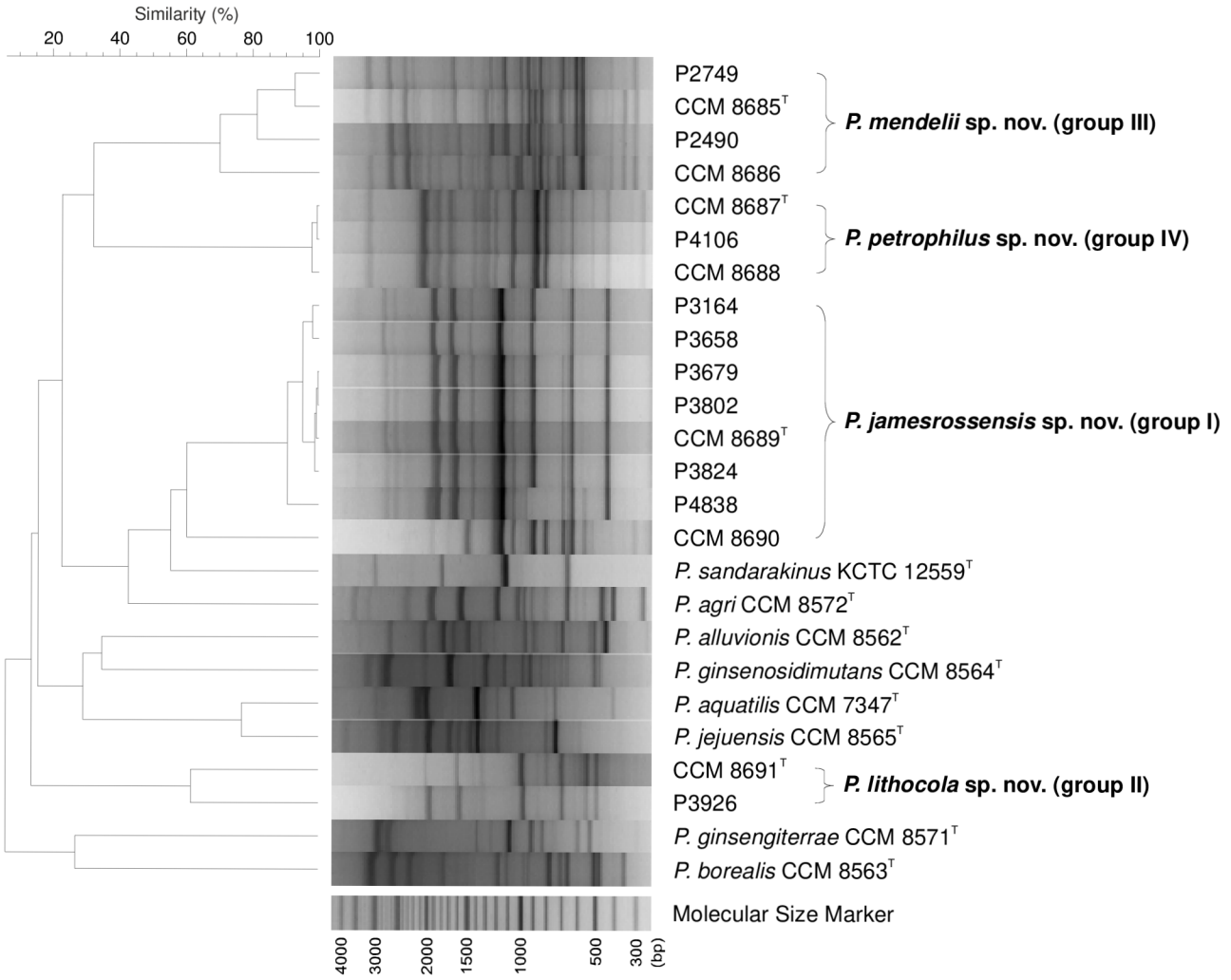

Fig. S3. Dendrogram based on cluster analysis of rep-PCR fingerprints obtained with $(GTG)_5$ primer from groups I–IV strains and the type strains of the phylogenetically nearly related species. The dendrogram was calculated with Pearson's correlation coefficients with UPGMA clustering method (*r*, expressed as percentage similarity values).

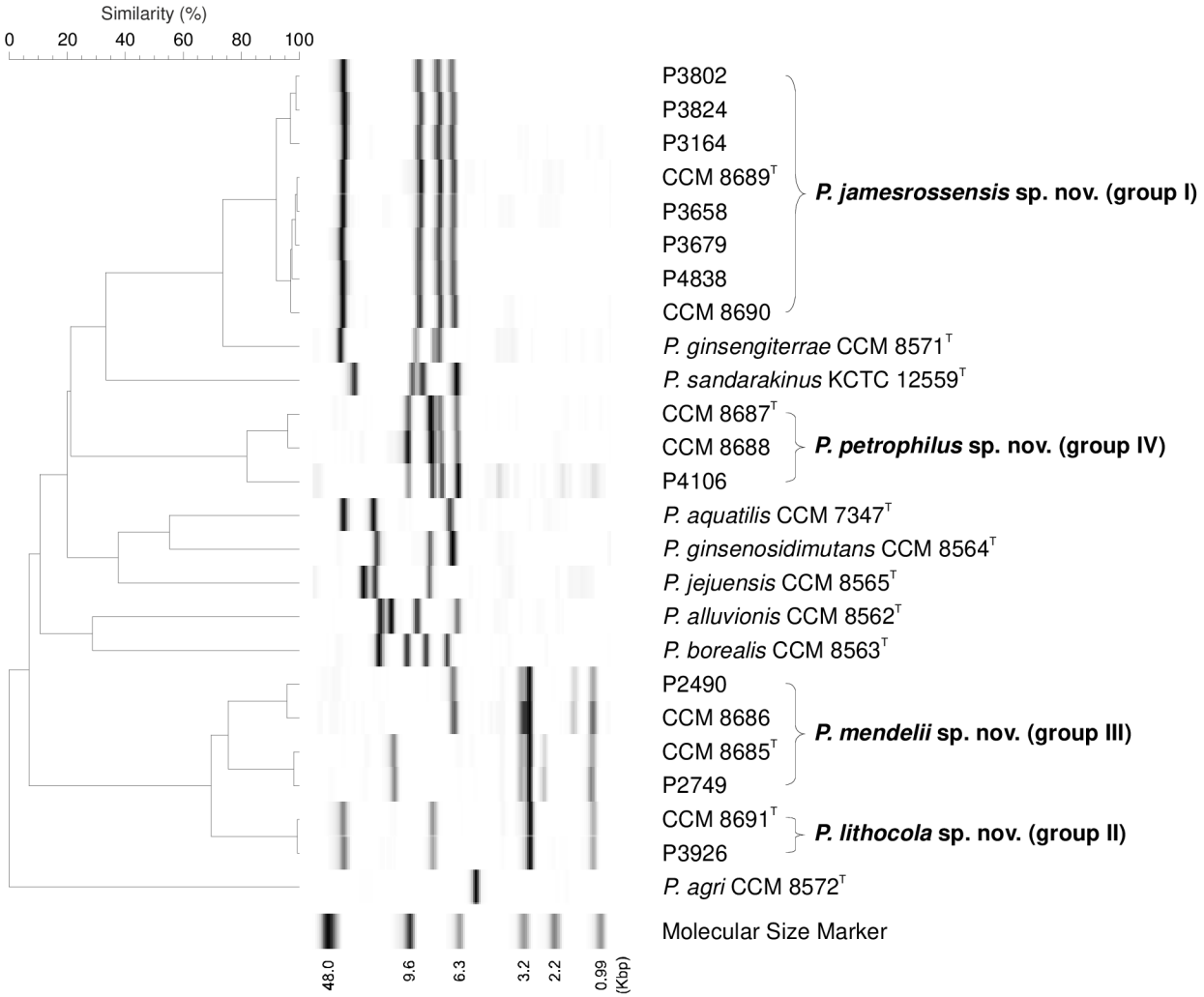

Fig. S4. Dendrogram based on cluster analysis of *Eco*RI ribotype patterns obtained using the RiboPrinter system from groups I–IV strains and the type strains of the phylogenetically nearly related species. The dendrogram was calculated with Pearson's correlation coefficients with UPGMA clustering method (*r*, expressed as percentage similarity values).

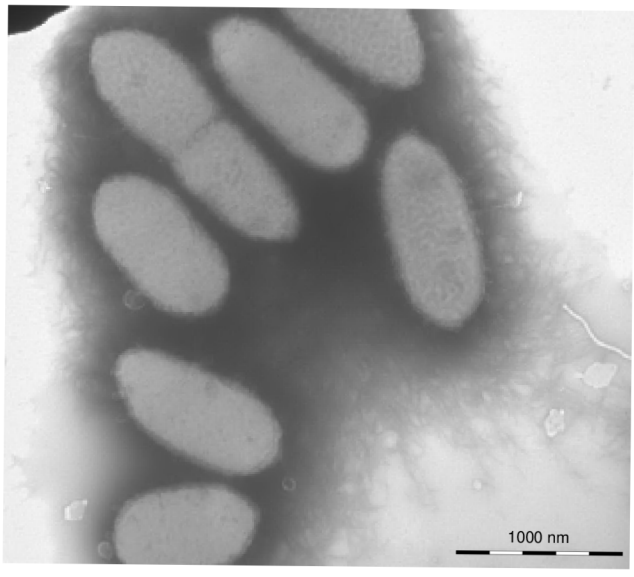

P. jamesrossensis sp. nov. CCM 8689^{T}

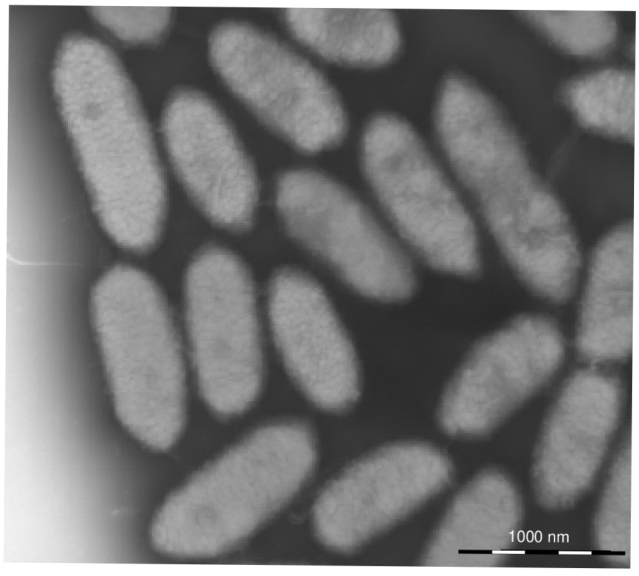

P. lithocola sp. nov. CCM 8691^{T}

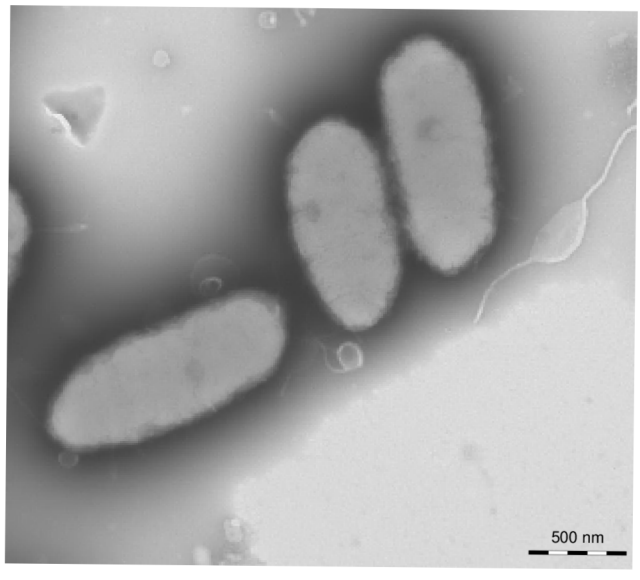

P. mendelii sp. nov. CCM 8685^{T}

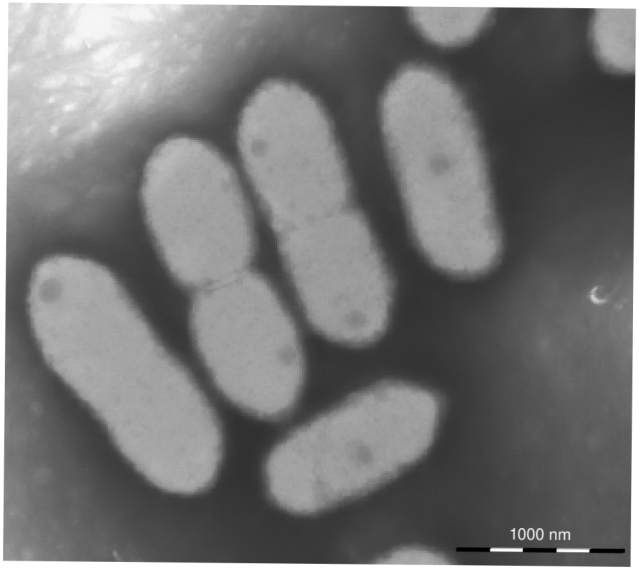

P. petrophilus sp. nov. CCM 8687^{T}

Fig. S5. Cellular morphology of strains CCM 8689^{T} (group I), CCM 8691^{T} (group II), CCM 8685^{T} (group III) and CCM 8687^{T} (group IV) cultivated on R2A agar (Oxoid). Images were obtained using transmission electron microscopy performed with a Morgagni 268D Philips (FEI Company, USA) electron microscope. Negative staining with 2% ammonium molybdate.

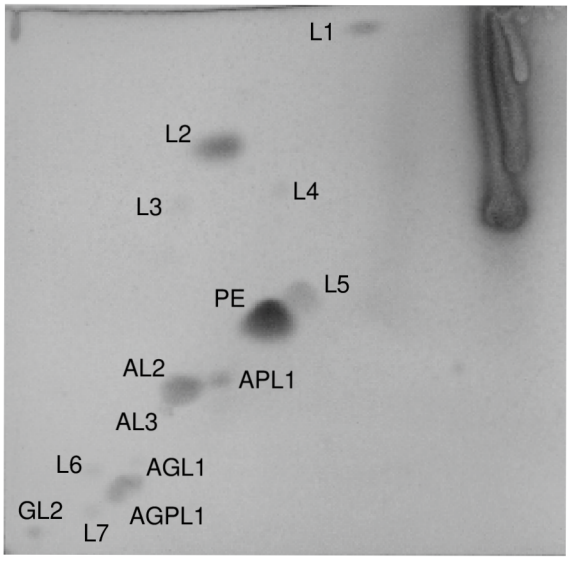

P. petrophilus sp. nov. CCM 8687^{T}

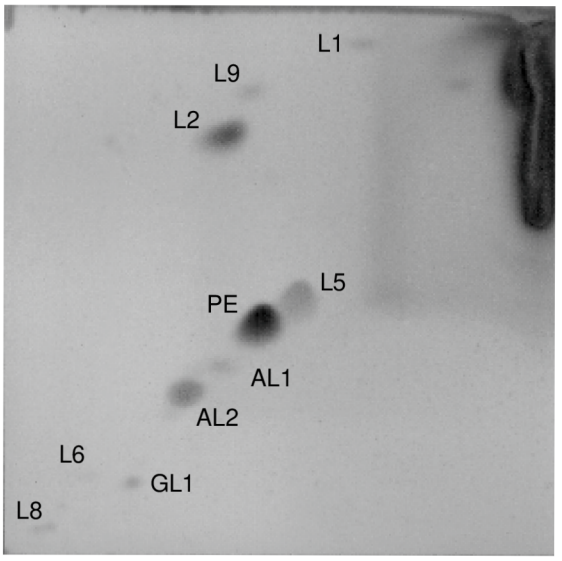

P. jamesrossensis sp. nov. CCM 8689^{T}

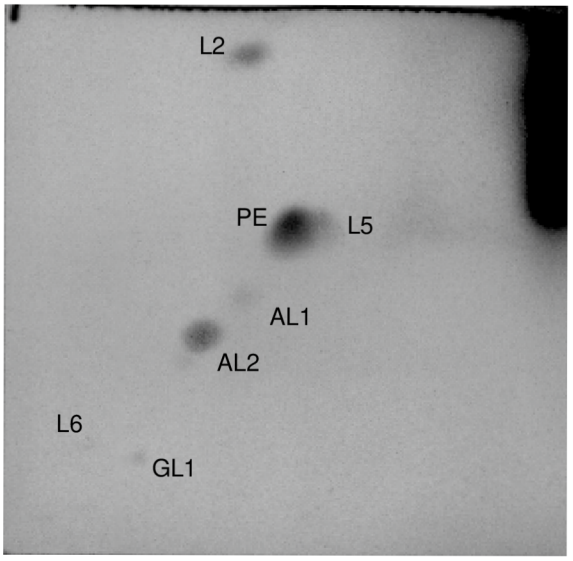

P. mendelii sp. nov. CCM 8685^{T}

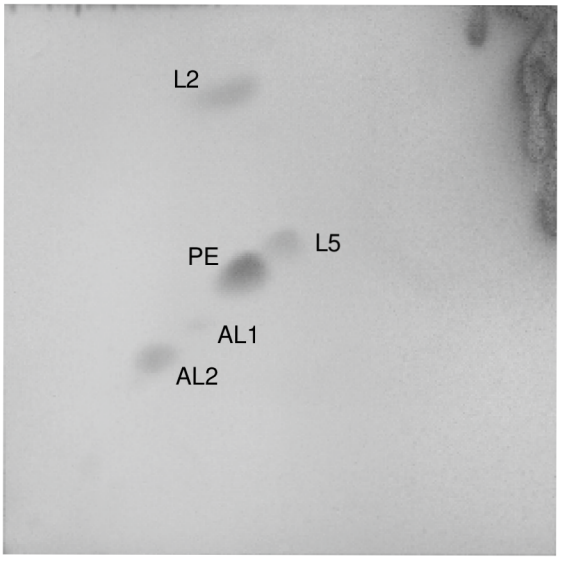

P. lithocola sp. nov. CCM 8691^{T}

Fig. S6. Two dimensional TLC showing the total polar lipids of strains CCM 8689^{T} (group I), CCM 8691^{T} (group II), CCM 8685^{T} (group III) and CCM 8687^{T} (group IV). Abbreviatons: L1-L9, unidentified polar lipids; AL1-AL3, unidentified aminolipids; GL1 and GL2, unidentified glycolipids; AGL1, unidentified aminoglykolipid; APL1, unidentified aminophospholipid; AGPL1, unidentified aminoglycophospholipid; PE, phosphatidylethanolamine.

Príloha č. 3.

Švec P., Králová S., Busse H.-J., Kleinhagauer T., Kýrová K., Pantůček R., Mašlaňová I., Staňková E., Němec M., Holochová P., Barták M., Sedláček I. (2017) *Pedobacter psychrophilus* sp. nov., isolated from Antarctic fragmentary rock. *Int. J. Syst. Evol. Microbiol*. 67(8): 2538-2543. Doi: 10.1099/ijsem.0.001962.

INTERNATIONAL JOURNAL OF SYSTEMATIC AND EVOLUTIONARY MICROBIOLOGY

TAXONOMIC DESCRIPTION
Švec *et al.*, *Int J Syst Evol Microbiol* 2017;67:2538–2543
DOI 10.1099/ijsem.0.001962

MICROBIOLOGY SOCIETY

Pedobacter psychrophilus sp. nov., isolated from fragmentary rock

Pavel Švec,[1,*] Stanislava Králová,[1] Hans-Jürgen Busse,[2] Tanita Kleinhagauer,[2] Kamila Kýrová,[1] Roman Pantůček,[3] Ivana Mašlaňová,[3] Eva Staňková,[1] Miroslav Němec,[4] Pavla Holochová,[1] Miloš Barták[5] and Ivo Sedláček[1]

Abstract

Strain P4487A^T was isolated during investigation of cultivable bacterial populations of environmental materials sampled at James Ross Island, Antarctica. It revealed Gram-stain-negative short rod-shaped cells producing a pink pigment. Phylogenetic analysis based on 16S rRNA gene sequences allocated strain P4487A^T to the genus *Pedobacter* but showed that the strain represents a distinct intrageneric phylogenetic lineage clearly separated from remaining *Pedobacter* species. Phylogenetically, strain P4487A^T formed a common branch with the *Pedobacter arcticus* and *Pedobacter lignilitoris* cluster while the highest value of 94.4 % 16S rRNA gene sequence similarity suggested that *Pedobacter lentus* is the most closely related species. Biochemical and physiological test results enabled the differentiation of strain P4487A^T from all phylogenetically closely related species. Chemotaxonomic analyses of strain P4487A^T showed MK-7 as the respiratory menaquinone, *sym*-homospermidine as the major polyamine, phosphatidylethanolamine and two unidentified lipids as the major polar lipids, presence of sphingolipids, and $C_{16:1}\omega7c/C_{16:1}\omega6c$ (summed feature 3), iso-$C_{15:0}$ and iso-$C_{17:0}$ 3-OH as the major fatty acids, all of which corresponded with characteristics of the genus *Pedobacter*. The results showed that strain P4487A^T represents a novel species within the genus *Pedobacter*, for which the name *Pedobacter psychrophilus* sp. nov. is proposed. The type strain is P4487A^T (=CCM 8644^T=LMG 29436^T).

The genus *Pedobacter* [1] represents a large group of species inhabiting different environmental, mainly terrestrial and aquatic, habitats worldwide. Members of the genus *Pedobacter* are Gram-stain-negative rod-shaped bacteria producing catalase, oxidase and phosphatase while being negative for the production of nitrate reductase and urease [2]. The presence of MK-7 as the major respiratory menaquinone, homospermidine as the major polyamine, phosphatidylethanolamine as the major polar lipid and presence of sphingolipids is typical for the genus *Pedobacter* [2]. The number of novel *Pedobacter* species with validly published names has increased significantly in recent years. At the time of writing, the genus *Pedobacter* harboured more than 60 recognized species [3].

The present taxonomic study deals with strain P4487A^T isolated in the framework of a project investigating bacterial populations inhabiting the Antarctic environment. The studied strain was isolated from fragmentary rock sampled at James Ross Island, Antarctica (GPS: 63° 49′ 20.316″ S, 57° 50′ 20.5404″ W). The sampling site was located at the north-east foot of the Lachman Crags mesa and formed a shallow depression filled by volcanic stones and rock fragments that ranged from 0.3 to 20.0 cm in size. The samples were taken from the south-facing side of an individual monolithic rock exhibiting a heavily fragmented surface caused by frost weathering. Therefore, the sampling site was a typical shaded habitat with a lower surface temperature than sunlit surfaces of the monolith. The sample was suspended in sterile saline solution, and 200 µl of the suspension was spread on R2A agar plates and cultivated at 15 °C for 5–7 days. Individual colonies were picked up, purified and pure cultures were maintained at −70 °C until analysed.

Author affiliations: [1]Czech Collection of Microorganisms, Department of Experimental Biology, Faculty of Science, Masaryk University, Kamenice 5, 625 00 Brno, Czech Republic; [2]Institute of Microbiology, University of Veterinary Medicine Vienna, A-1210 Vienna, Austria; [3]Section of Molecular Biology, Department of Experimental Biology, Faculty of Science, Masaryk University, Kamenice 5, 625 00 Brno, Czech Republic; [4]Section of Microbiology and Molecular Biotechnology, Department of Experimental Biology, Faculty of Science, Masaryk University, Kamenice 5, 625 00 Brno, Czech Republic; [5]Section of Physiology and Anatomy of Plants, Department of Experimental Biology, Faculty of Science, Masaryk University, Kamenice 5, 625 00 Brno, Czech Republic.
***Correspondence:** Pavel Švec, mpavel@sci.muni.cz
Keywords: *Pedobacter psychrophilus* sp. nov.; Antarctica; James Ross Island; taxonomy.
Abbreviation: WGS, whole genome sequencing.
The GenBank/EMBL/DDBJ accession number for the 16S rRNA gene sequence of strain CCM 8644^T (=P4487A^T) is KX113374. The Whole Genome Shotgun projects have been deposited at DDBJ/EMBL/GenBank under accession LWHJ00000000. The version described in this paper is LWHJ01000000.
Four supplementary figures and one supplementary table are available with the online Supplementary Material.

The analysed strain, designated P4487A^T, was deposited in the Czech Collection of Microorganisms and BCCM/LMG Bacteria Collection under accession numbers CCM 8644^T and LMG 29436^T, respectively. Reference strain *Pedobacter arcticus* CCTCC AB 2010223^T was obtained from the China Center for Type Culture Collection and *Pedobacter lentus* KCTC 12875^T was obtained from the Korean Collection for Type Cultures.

DNA for 16S rRNA gene sequence analysis was extracted by using a FastPrep Lysing Matrix type B and FastPrep Homogenizer (MP Biomedicals) and purified via a High Pure PCR Template Preparation Kit (Roche Diagnostics). A fragment of the 16S rRNA gene corresponding to positions 8–1542 used for *Escherichia coli* was amplified by PCR with FastStart PCR Master (Roche Diagnostics) and conserved primers pA (AGAGTTTGATCCTGGCTCAG) and pH (AAGGAGGTGATCCAGCCGCA) described by Edwards *et al.* [4], and purified using a QIAquick PCR Purification Kit (Qiagen). Sequencing was performed using PCR primers and custom primers F1 (GTGGGGAKCRAACAGGA TTAG), F2 (CGTCARGTCMTCATGGCCCTT), R1 (A TTACCGCGGCTGCTGGCAC) and R2 (CACATSMTCC MCCRCTTGT) in the Eurofins MWG Operon sequencing facility. The obtained sequence was identified via the EzTaxon database [5] which showed the type strain of *P. lentus* (accession no. EF446146) as its closest neighbour with a 16S rRNA gene sequence similarity value of 94.4 %, followed by those of *Pedobacter terricola* (94.3 %) and *Pedobacter daechungensis* (94.1 %). To characterize strain P4487A^T in more detail, whole genome sequencing (WGS) was performed. The purified genomic DNA was used for 400 bp sequencing library preparation as described previously [6]. The sample was loaded on a 316v2 chip and sequenced using an Ion PGM Hi-Q sequencing kit (Life Technologies) on an Ion PGM system (Life Technologies). Quality trimming and error correction of the reads were performed with the Ion Torrent Suite Software (v5.0.2). The assembly computation was performed using the plug-in Assembler SPAdes (v5.0.0). The total length of the assembly comprised 3 999 136 bp. Assembled contigs larger than 500 bp were used for subsequent analysis. To estimate the DNA G+C content, the draft genome sequence was used. The DNA G+C content of strain P4487A^T was 46.3 mol%. The complete 16S rRNA gene sequence extracted from WGS data using the RNAmmer 1.2. server [7] showed similarity with that obtained by Sanger sequencing and therefore was used for further phylogenetic comparison with 16S rRNA gene sequences from recognized species of the genus *Pedobacter* retrieved from the GenBank/EMBL/DDBJ database. Phylogenetic analysis was performed using MEGA v6 software [8]. Genetic distances were corrected using Kimura's two-parameter model and the evolutionary history was inferred using the maximum-likelihood and neighbour-joining methods. Comparative analysis of the 16S rRNA gene assigned strain P4487A^T to the genus *Pedobacter* but it was distantly separated from remaining *Pedobacter* species. The trees reconstructed using the maximum-likelihood (Fig. 1) and neighbour-joining (Fig. S1, available in the online Supplementary Material) clustering methods showed robust clustering (>80 % bootstrap value) of strain P4487A^T with the cluster comprising the type strains of *P. arcticus* and *Pedobacter lignilitoris*.

The phenotypic profile of strain P4487A^T was assessed by a set of key tests relevant for Gram-negative rod-shaped bacteria. *P. arcticus* CCTCC AB 2010223^T and *P. lentus* KCTC 12875^T were used as reference strains for evaluation of phenotypic test results obtained under the same conditions as for strain P4487A^T. Oxidase (OXItest; Erba-Lachema) and catalase (ID colour Catalase; bioMérieux) activities were determined according to the manufacturers' instructions. Further tube and plate conventional tests for urease, oxidation-fermentation (OF) test, motility, arginine dihydrolase, ornithine decarboxylase and lysine decarboxylase, hydrolysis of casein, DNA, aesculin, gelatin, lecithin (egg-yolk reaction), ONPG, starch, Tween 80 and tyrosine, acid production from fructose, maltose, mannitol and xylose, nitrate and nitrite reduction, indol production, and Simmons citrate, acetamide and sodium malonate utilization tests were done as described previously [9–11]. The temperature range for growth (1, 5, 10, 15, 20, 25, 30 and 35 °C) and NaCl concentration tolerance (0, 1, 2 and 3 %, w/v) were tested on R2A agar (Oxoid) adjusted accordingly. The pH range for growth was tested on R2A agar adjusted to pH 5.0–10.0 (in increments of 1 pH unit) by using the following buffer systems: pH 5.0–8.0, 0.1 M KH_2PO_4/0.1 M NaOH; pH 9.0–10.0, 0.1 M $NaHCO_3$/0.1 M Na_2CO_3. The pH of the R2A agar was confirmed after autoclaving. Aerobic growth of strain P4487A^T was assessed on brain heart infusion agar, Columbia blood agar, MacConkey agar, nutrient agar, plate count agar, R2A agar and tryptone soya agar (all from Oxoid) and anaerobic growth was tested on R2A agar using the Anaerocult A system (Merck). Biochemical and growth tests were carried out using cells grown on R2A agar at 20 °C and read daily for up to 7 days with incubation at 20 °C. Cellular morphology was further investigated by transmission electron microscopy using a Morgagni 268D Philips (FEI) electron microscope (Fig. S2). Phenotypic screening showed that strain P4487A^T was Gram-stain-negative, rod-shaped, aerobic, non-fermenting, and oxidase- and catalase-positive. It revealed small pink colonies when cultivated on R2A agar plates at 20 °C. The colonies became dark red–orange after the cultivation was prolonged for more than 1 week. Further extensive phenotypic characterization using the Biolog system with the Gram-negative identification test panel GN2 MicroPlate (Biolog) and API ZYM (bioMérieux) was done according to the manufacturers' instructions. Screening for flexirubin-type pigment production was done using a 20 % KOH test as described by Bernardet *et al.* [12]. Gliding motility was assessed by a direct microscopic examination of cell colonies grown on the agar surface as well as using a hanging drop method as suggested by Bernardet *et al.* [12]. The antibiotic resistance pattern was obtained by the disc diffusion method on R2A agar (Oxoid). Sixteen antibiotic discs (Oxoid) relevant for Gram-

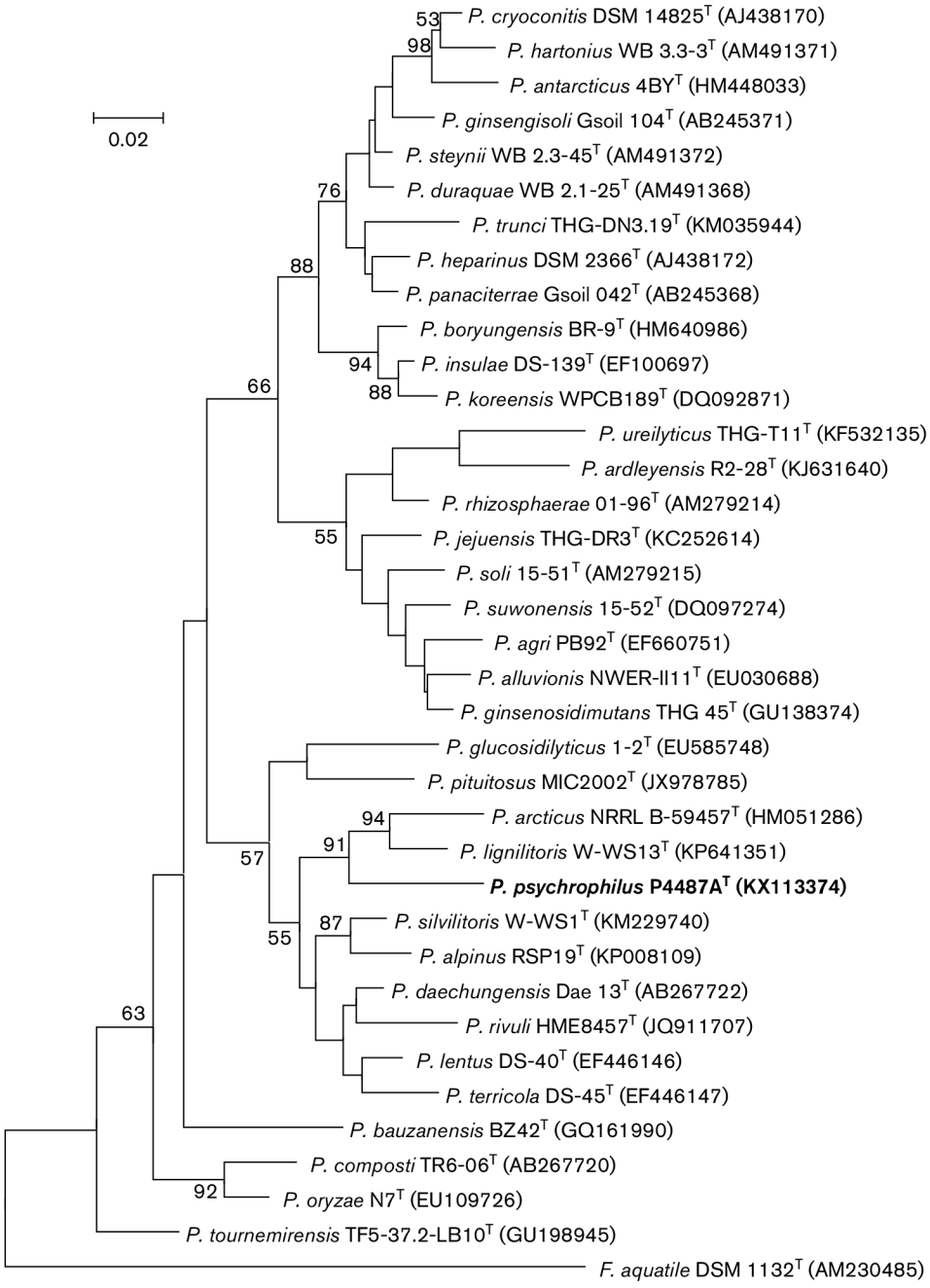

Fig. 1. Phylogenetic tree based on 16S rRNA gene sequences showing the position of strain P4487A^T within the genus *Pedobacter*. The evolutionary history was inferred by using the maximum-likelihood method based on the Kimura two-parameter model. Bootstrap probability values (percentages of 1000 tree replications) greater than 50 % are indicated at branch points. There were a total of 1523 positions in the final dataset. *Flavobacterium aquatile* DSM 1132^T (AM230485) was used as an outgroup. Bar, 0.02 substitutions per nucleotide position.

negative rods [13, 14] were tested: ampicillin (10 µg), aztreonam (30 µg), carbenicillin (100 µg), cefixim (5 µg), ceftazidim (10 µg), cephalothin (30 µg), ciprofloxacin (5 µg), gentamicin (10 µg), chloramphenicol (30 µg), imipenem (10 µg), kanamycin (30 µg), cotrimoxazol (25 µg), piperacillin (30 µg), polymyxin B (300 U), streptomycin (10 µg) and tetracycline (30 µg). CLSI/EUCAST standards were followed for cultivation and inhibition zone diameter reading. The biochemical and physiological characteristics and antibiotic susceptibility pattern of strain P4487A^T are

given in the species description below. The tests distinguishing strain P4487A^T from phylogenetically closest related *Pedobacter* species are shown in Table 1.

Spectrophotometric characterization of the produced pigment(s) was done from cells grown on R2A agar for 72 h at 20 °C. Cells were washed off and rinsed twice using 0.1 M phosphate buffer (pH 7.2). Harvested cells were suspended in an extraction mixture composed of equal volumes of acetone, ether and ethanol (96 %). Extraction was done in a shaker for 120 min at 4 °C (shaking interval: 120 swings min^{-1}) and centrifuged at 5000 *g* at 4 °C for 20 min. The supernatant was evaporated in vacuum at room temperature and the evaporation residue was diluted in hexane. A Cary 100Bio (Agilent) spectrophotometer was used for the measurement of spectra. The extracted pigment showed a whole absorbance spectrum with a typical major peak at 479 nm and less distinct peaks at 450 and 509 nm. Another major peak was observed at 270 nm (Fig. S3). The obtained spectrum resembled that of β-carotene as described by Burns *et al.* [15].

Analysis of fatty acid methyl esters was performed using an Agilent 7890B gas chromatograph according to the standard protocol of the Sherlock MIDI Identification System (MIDI Sherlock version 6.2, MIDI database RTSBA 6.21). *P. arcticus* CCTCC AB 2010223^T and *P. lentus* KCTC 12875^T were used for comparison of fatty acid analysis results of strain P4487A^T obtained under the same laboratory conditions. The strains were grown on R2A agar (Oxoid) at 20 ±2 °C for 72 h (except *P. lentus* KCTC 12875^T, which was cultivated for 7 days), where the bacterial communities reached the late-exponential stage of growth according to the four quadrants streak method [16]. The predominant fatty acids of strain P4487A^T were summed feature 3 ($C_{16:1}$ $\omega7c$/$C_{16:1}$ $\omega6c$) (21.0 %), iso-$C_{15:0}$ (15.4 %) and iso-$C_{17:0}$ 3-OH (11.6 %), which corresponded with those typically found in *P. arcticus* CCTCC AB 2010223^T, *P. lentus* KCTC 12875^T and *Pedobacter heparinus* DSM 2366^T (Table S1) as well as in other *Pedobacter* species [2].

Quinones and polar lipids were extracted from freeze-dried biomass grown on R2A agar at 20 °C for 72 h and analysed as described previously [17–20]. The analysis of strain P4487A^T revealed MK-7 as the respiratory quinone (100 %). The major polar lipid was phosphatidylethanolamine, followed by three unknown polar lipids (L1, L2, and L5) and an unknown aminolipid (AL2). Moderate amounts of five unknown polar lipids (L3, L4, L6–L8), an unknown aminolipid (AL1) and an unknown aminoglycolipid (AGL1) were detected (Fig. S4). The presence of phosphatidylethanolamine and lipid L2 was reported in the close relatives of strain P4487A^T, namely *P. arcticus*,*P. lignilitoris* and *P. lentus* [21, 22]. On the other hand, the presence of aminolipids corresponding chromatographically to AL2 was reported for *P. arcticus* and *P. lignilitoris* but not for *P. lentus*. However, the presence of the unidentified aminoglycolipid AGL1 and lipid L1 in addition to some minor lipids clearly distinguished stain P4487A^T from its close relatives. Mild alkaline hydrolysis of the total polar lipid extract [23] of strain P4487A^T revealed the presence of an aminolipid

Table 1. Differentiation of strain P4487A^T from phylogenetically related *Pedobacter* species

Taxa: 1, strain P4487A^T; 2, *P. alpinus;* 3, *P. arcticus*; 4, *P. daechungensis*; 5, *P. glucosidilyticus*; 6, *P. lentus*; 7, *P. lignilitoris*; 8, *P. rivuli*; 9, *P. silvilitoris*; 10, *P. terricola*. +, Positive; −, negative; W, weakly positive; D, strain-dependent. Data for strain P4487A^T, *P. arcticus* CCTCC AB 2010223^T and *P. lentus* KCTC 12875^T were obtained in this study; data for the remaining *Pedobacter* species were retrieved from Yoon *et al.* [27], An *et al.* [28], Luo *et al.* [29], Kang *et al.* [30], Li *et al.* [31] and Park *et al.* [22, 32].

Characteristic	1	2	3	4	5	6	7	8	9	10
Growth at 30 °C	−	−	−	+	+	+	+	+	+	+
Enzyme activities:										
α-Glucosidase	+	D	+*	−	+	+	+	+	−	+
β-Galactosidase	+	+	+	−	+	+	−	+	−	+
Acid phosphatase	+	+	+	−	+	+	+	+	+	+
Naphthol-AS-BI-phosphohydrolase	+	+	+	−	+	+	+	−	+	+
Valine arylamidase	+	+	+	+	+	+	W	+	−	+
α-Fucosidase	−	−	+*	−	+	−	−	−	−	−
α-Galactosidase	−	−	−	−	−	−	−	−	+	−
β-Glucosidase	−	−	+	+	+	+†	+	−	+	−
Arginine dihydrolase	−	−	+	+	−	−	−	−	−	−
Cystine arylamidase	−	+	−	+	+	+	W	+	−	+
Chymotrypsin	−	−	−	−	−	+	−	−	−	+
N-Acetyl-β glucosaminidase	−	+	+	−	+	+	+	+	+	+

*Opposite results were reported by Zhou *et al.* [21].

†Opposite results were reported by Yoon *et al.* [27].

that did not stain positive for phosphate. Hence, it is clear that this alkali-stable lipid is not a sphingophospholipid as reported to be present in members of the neighbouring genus *Sphingobacterium* [24] or more distantly related genera such as *Bacteroides* and *Prevotella* [23] but might show a chemical structure similar to sphingosine and dihydrosphingosine, which do not contain phosphate. However, this observation does not conflict with the characteristics of other *Pedobacter* species, which were reported to contain sphingolipid(s), but none of them was reported to contain a sphingophospholipid. Biomass for the detection of polyamines was harvested from cells grown on R2A agar at 20 °C for 72 h (late exponential growth phase). Extraction and analysis was done as described previously [20, 25, 26]. Strain P4487A^T contained *sym*-homospermidine as the major polyamine. Both the presence of a quinone system with MK-7 predominating and the major polyamine *sym*-homospermidine are in line with the characteristics listed in the description of the family *Sphingobacteriaceae* [1].

The results obtained in this study demonstrated that strain P4487A^T represents a novel *Pedobacter* species for which the name *Pedobacter psychrophilus* sp. nov. is proposed.

DESCRIPTION OF *PEDOBACTER PSYCHROPHILUS* SP. NOV.

Pedobacter psychrophilus (psy.chro′phi.lus. Gr. adj. *psychros* cold; Gr. adj. *philos* liking, loving; N.L. masc. adj. *psychrophilus* cold-loving).

Cells are Gram-stain-negative, short rods, occurring predominantly in pairs or in irregular clusters, non-motile and non-spore-forming. Colonies on R2A agar are pink, circular, slightly convex, smooth and glistening with whole margins, and reach about 1 mm in diameter when cultivated at 20 °C for 5 days. Produces carotenoid pigment. Flexirubin-type pigments are absent. Aerobic; no anaerobic growth on R2A agar is detected. Aerobic but non-fermenting in the oxidative-fermentative (OF) test. Grows at 5–25 °C. Growth does not occur at 1, 30 or 35 °C. Grows in the presence of up to 2 % (w/v) NaCl and at pH 6–9. Most abundant growth is observed on R2A agar without NaCl, at pH 8.0 and at 20 °C. No fluorescein pigment on King B medium. Grows on plate count agar and R2A agar, but not on tryptone soya agar, brain heart infusion agar, MacConkey agar, Columbia blood agar or nutrient agar. Positive for production of catalase, oxidase (weak), DNase, esterase (C4), esterase lipase (C8) (weak), leucine arylamidase, valine arylamidase, naphthol-AS-BI-phosphohydrolase, β-galactosidase, α-glucosidase, alkaline phosphatase and acid phosphatase. Negative for production of urease, arginine dihydrolase, lysine decarboxylase, ornithine decarboxylase, lipase (C14), cystine arylamidase, trypsin, chymotrypsin, β-glucuronidase, β-glucosidase, α-galactosidase, *N*-acetyl-β-glucosaminidase, α-mannosidase, α-fucosidase, nitrate reduction and nitrite reduction. Aesculine, ONPG and starch hydrolysis are positive. Negative for indole production, Simmons citrate, sodium malonate, acetamide and hydrolysis of gelatin, Tween 80, tyrosine, caseine and lecithin (egg-yolk reaction). Acid is produced from xylose and maltose, but not from fructose or mannitol. Sensitive to ampicillin, carbenicillin, ceftazidim, cephalothin, ciprofloxacin, gentamicin, chloramphenicol, imipenem, kanamycin, cotrimoxazol, piperacillin, polymyxin B, streptomycin and tetracycline, but resistant to aztreonam and cefixim. Carbon source utilization ability via respiration, determined in Biolog GN2 MicroPlate test panels, is positive for α-cyclodextrin, dextrin, glycogen, *N*-acetyl-D-glucosamine, cellobiose, gentiobiose, α-D-glucose, lactose, maltose, melibiose, turanose, α-ketobutyric acid, L-glutamic acid and glycyl L-glutamic acid but negative for Tween 40, Tween 80, *N*-acetyl-D-galactosamine, adonitol, L-arabinose D-arabitol, erythritol, D-fructose, L-fucose, D-galactose, *myo*-inositol, lactulose, D-mannitol, D-mannose, methyl β-D-glucoside, D-psicose, raffinose, L-rhamnose, D-sorbitol, sucrose, trehalose, xylitol, pyruvic acid methyl ester, succinic acid monomethyl ester, acetic acid, *cis*-aconitic acid, citric acid, formic acid, D-galactonic acid lactone, D-galacturonic acid, D-gluconic acid, D-glucosaminic acid, D-glucuronic acid, α-hydroxybutyric acid, β-hydroxybutyric acid, γ-hydroxybutyric acid, *p*-hydroxyphenylacetic acid, itaconic acid, α-ketoglutaric acid, α-ketovaleric acid, DL-lactic acid, malonic acid, propionic acid, quinic acid, D-saccharic acid, sebacic acid, succinic acid, bromosuccinic acid, succinamic acid, glucuronamide, L-alaninamide, D-alanine, L-alanine, L-alanyl glycine, L-asparagine, L-aspartic acid, glycyl L-aspartic acid, L-histidine, hydroxy-L-proline, L-leucine, L-ornithine, L-phenylalanine, L-proline, L-pyroglutamic acid, D-serine, L-serine, L-threonine, DL-carnitine, γ-aminobutyric acid, urocanic acid, inosine, uridine, thymidine, phenylethylamine, putrescine, 2-aminoethanol, 2,3-butanediol, glycerol, DL-α-glycerol phosphate, α-D-glucose 1-phosphate and D-glucose 6-phosphate. Contains an alkaline stable lipid lacking a phosphate group, MK-7 as the respiratory quinone, phosphatidylethanolamine as the major polar lipid, *sym*-homospermidine as the major polyamine and iso-$C_{15:0}$, iso-$C_{17:0}$ 3-OH and summed feature 3 ($C_{16:1}\omega7c$/$C_{16:1}\omega6c$) as major cellular fatty acids.

The type strain, P4487A^T (=CCM 8644^T=LMG 29436^T), was isolated from fragmentary rock sampled at James Ross Island, Antarctica. The genomic DNA G+C content of the type strain is 46.3 mol%.

Funding information
This study was supported by the Ministry of Education, Youth and Sports of the Czech Republic project LM2015078.

Conflicts of interest
The authors report that there are no conflicts of interest.

Acknowledgements
We thank the scientific infrastructure of the J. G. Mendel Czech Antarctic Station as a part of the Czech Polar Research Infrastructure (CzechPolar2) and its crew for their assistance, supported by the Ministry of Education, Youth and Sports of the Czech Republic (LM2015078). S.K. is a holder of Brno PhD Talent financial aid. Dr Daniel Krsek (National Reference Laboratory for Diagnostic Electron Microscopy of Infectious Agents, National Institute of Public Health,

Prague, Czech Republic) is acknowledged for transmission electron microscopy and Jana Bajerová (Czech Collection of Microorganisms, Masaryk University, Brno, Czech Republic) for excellent technical assistance. We thank the Korean Collection for Type Cultures (KCTC) and China Center for Type Culture Collection (CCTCC) for providing *Pedobacter* spp. reference strains.

References

1. **Steyn PL, Segers P, Vancanneyt M, Sandra P, Kersters K *et al.*** Classification of heparinolytic bacteria into a new genus, *Pedobacter*, comprising four species: *Pedobacter heparinus* comb. nov., *Pedobacter piscium* comb. nov., *Pedobacter africanus* sp. nov. and *Pedobacter saltans* sp. nov. proposal of the family *Sphingobacteriaceae* fam. nov. *Int J Syst Bacteriol* 1998;48:165–177.
2. **Margesin R, Shivaji S.** Genus II. *Pedobacter* Steyn, Segers, Vancanneyt, Sandra, Kersters and Joubert 1998, 171VP. In: Krieg NR, Staley JT, Brown DR, Hedlund BP, Paster BJ (editors). *Bergey's Manual of Systematic Bacteriology the Bacteroidetes, Spirochaetes, Tenericutes (Mollicutes), Acidobacteria, Fibrobacteres, Fusobacteria, Dictyoglomi, Gemmatimonadetes, Lentisphaerae, Verrucomicrobia, Chlamydiae, and Planctomycetes*, vol. 4. New York, USA: Springer; 2010. pp. 339–351.
3. **Parte AC.** LPSN–list of prokaryotic names with standing in nomenclature. *Nucleic Acids Res* 2014;42:D613–D616. http://www.bacterio.net
4. **Edwards U, Rogall T, Blöcker H, Emde M, Böttger EC.** Isolation and direct complete nucleotide determination of entire genes. Characterization of a gene coding for 16S ribosomal RNA. *Nucleic Acids Res* 1989;17:7843–7853.
5. **Kim OS, Cho YJ, Lee K, Yoon SH, Kim M *et al.*** Introducing EzTaxon-e: a prokaryotic 16S rRNA gene sequence database with phylotypes that represent uncultured species. *Int J Syst Evol Microbiol* 2012;62:716–721.
6. **Sedláček I, Kwon SW, Švec P, Mašlaňová I, Kýrová K *et al.*** *Aquitalea pelogenes* sp. nov., isolated from mineral peloid. *Int J Syst Evol Microbiol* 2016;66:962–967.
7. **Lagesen K, Hallin PF, Rødland E, Stærfeldt HH, Rognes T *et al.*** RNammer: consistent annotation of rRNA genes in genomic sequences. *Nucleic Acids Res* 2007;35:3100–3108.
8. **Tamura K, Stecher G, Peterson D, Filipski A, Kumar S.** MEGA6: molecular evolutionary Genetics analysis version 6.0. *Mol Biol Evol* 2013;30:2725–2729.
9. **Barrow GI, Feltham RKA.** *Cowan and Steel's Manual for the Identification of Medical Bacteria*, 3rd ed. Great Britain: Cambridge University Press; 1993.
10. **Atlas RM.** *Handbook of Microbiological Media*, 4th ed. Washington, DC: ASM Press; 2010.
11. **Kosina M, Barták M, Mašlaňová I, Vávrová Pascutti A, Šedo O *et al.*** *Pseudomonas prosekii* sp. nov., a novel psychrotrophic bacterium from Antarctica. *Curr Microbiol* 2013;67:637–646.
12. **Bernardet JF, Nakagawa Y, Holmes B, Subcommittee on the taxonomy of *Flavobacterium* and *Cytophaga*-like bacteria of the International Committee on Systematics of Prokaryotes.** Proposed minimal standards for describing new taxa of the family *Flavobacteriaceae* and emended description of the family. *Int J Syst Evol Microbiol* 2002;52:1049–1070.
13. **CLSI.** *Performance Standards for Antimicrobial Susceptibility Testing; Twenty-Fifth Informational Supplement (M100-S25*, vol. 35, No. 3, ISBN 1-56238-989-0. 2015.
14. **EUCAST.** European Committee on Antimicrobial susceptibility testing. EUCAST clinical breakpoints - bacteria. 2015. version 5.0 http://www.eucast.org (accessed May 2016).
15. **Burns J, Fraser PD, Bramley PM.** Identification and quantification of carotenoids, tocopherols and chlorophylls in commonly consumed fruits and vegetables. *Phytochemistry* 2003;62:939–947.
16. **Sasser M.** *Identification of bacteria by gas chromatography of cellular fatty acids,* MIDI Technical Note 101. Newark, DE, USA: Microbial ID, Inc; 1990.
17. **Altenburger P, Kämpfer P, Makristathis A, Lubitz W, Busse H-J.** Classification of bacteria isolated from a medieval wall painting. *J Biotechnol* 1996;47:39–52.
18. **Tindall BJ.** Lipid composition of *Halobacterium lacusprofundi*. *FEMS Microbiol Lett* 1990;66:199–202.
19. **Tindall BJ.** A comparative study of the lipid composition *of Halobacterium saccharovorum* from various sources. *Syst Appl Microbiol* 1990;13:128–130.
20. **Stolz A, Busse HJ, Kämpfer P.** *Pseudomonas knackmussii* sp. nov. *Int J Syst Evol Microbiol* 2007;57:572–576.
21. **Zhou Z, Jiang F, Wang S, Peng F, Dai J *et al.*** *Pedobacter arcticus* sp. nov., a facultative psychrophile isolated from Arctic soil, and emended descriptions of the genus *Pedobacter*, *Pedobacter heparinus*, *Pedobacter daechungensis*, *Pedobacter terricola*, *Pedobacter glucosidilyticus* and *Pedobacter lentus*. *Int J Syst Evol Microbiol* 2012;62:1963–1969.
22. **Park S, Park JM, Jung YT, Won SM, Yoon JH.** *Pedobacter lignilitoris* sp. nov., isolated from wood falls. *Int J Syst Evol Microbiol* 2015; 65:3481–3486.
23. **Kato M, Muto Y, Tanaka-Bandoh K, Watanabe K, Ueno K.** Sphingolipid composition in *Bacteroides* species. *Anaerobe* 1995;1:135–139.
24. **Naka T, Fujiwara N, Yano I, Maeda S, Doe M *et al.*** Structural analysis of sphingophospholipids derived from *Sphingobacterium spiritivorum*, the type species of genus *Sphingobacterium*. *Biochim Biophys Acta* 2003;1635:83–92.
25. **Busse J, Auling G.** Polyamine pattern as a chemotaxonomic marker within the *Proteobacteria*. *Syst Appl Microbiol* 1988;11:1–8.
26. **Busse H-J, Bunka S, Hensel A, Lubitz W.** Discrimination of members of the Family *Pasteurellaceae* based on polyamine patterns. *Int J Syst Bacteriol* 1997;47:698–708.
27. **Yoon JH, Kang SJ, Park S, Oh TK.** *Pedobacter lentus* sp. nov. and *Pedobacter terricola* sp. nov., isolated from soil. *Int J Syst Evol Microbiol* 2007;57:2089–2095.
28. **An DS, Kim SG, Ten LN, Cho CH.** *Pedobacter daechungensis* sp. nov., from freshwater lake sediment in South Korea. *Int J Syst Evol Microbiol* 2009;59:69–72.
29. **Luo X, Wang Z, Dai J, Zhang L, Li J *et al.*** *Pedobacter glucosidilyticus* sp. nov., isolated from dry riverbed soil. *Int J Syst Evol Microbiol* 2010;60:229–233.
30. **Kang H, Kim H, Joung Y, Joh K.** *Pedobacter rivuli* sp. nov., isolated from a freshwater stream. *Int J Syst Evol Microbiol* 2014;64:4073–4078.
31. **Li AH, Liu HC, Zhou YG.** *Pedobacter alpinus* sp. nov., isolated from a plateau lake in China. *Int J Syst Evol Microbiol* 2015;65:3782–3787.
32. **Park S, Jung YT, Park JM, Won SM, Yoon JH.** *Pedobacter silvilitoris* sp. nov., isolated from wood falls. *Int J Syst Evol Microbiol* 2015; 65:1284–1289.

International Journal of Systematic and Evolutionary Microbiology

Supplementary materials

Pedobacter psychrophilus sp. nov., isolated from Antarctic fragmentary rock

Pavel Švec[1,*], Stanislava Králová[1], Hans-Jürgen Busse[2], Tanita Kleinhagauer[2], Kamila Kýrová[1], Roman Pantůček[3], Ivana Mašlaňová[3], Eva Staňková[1], Miroslav Němec[4], Pavla Holochová[1], Miloš Barták[5] and Ivo Sedláček[1]

[1]Czech Collection of Microorganisms, Department of Experimental Biology, Faculty of Science, Masaryk University, Kamenice 5, 625 00 Brno, Czech Republic

[2]Institute of Microbiology, University of Veterinary Medicine Vienna, A-1210 Vienna, Austria

[3]Section of Molecular Biology, Department of Experimental Biology, Faculty of Science, Masaryk University, Kamenice 5, 625 00 Brno, Czech Republic

[4]Section of Microbiology and Molecular Biotechnology, Department of Experimental Biology, Faculty of Science, Masaryk University, Kamenice 5, 625 00 Brno, Czech Republic

[5]Section of Physiology and Anatomy of Plants, Department of Experimental Biology, Faculty of Science, Masaryk University, Kamenice 5, 625 00 Brno, Czech Republic

*Corresponding author:
Pavel Švec: E-mail: mpavel@sci.muni.cz

Table S1. Cellular fatty acid composition (as a percentage of the total) of strain P4487A^T, *P. arcticus* CCTCC AB 2010223^T, *P. lentus* KCTC 12875^T and *P. heparinus* DSM 2366^T.

Strains: 1, P4487A^T; 2, *P. arcticus* CCTCC AB 2010223^T; 3, *P. lentus* KCTC 12875^T; 4, *P. heparinus* DSM 2366^T. TR, trace values (< 1 %); ND, not detected. Values of less than 1 % are not shown. Data for strain P4487A^T, *P. arcticus* CCTCC AB 2010223^T and *P. lentus* KCTC 12875^T were obtained in this study; data for *P. heparinus* DSM 2366^T were obtained from Zhou *et al*. (2012).

Fatty acid	**1**	**2**	**3**	**4**
Summed Feature 3*	21.0	20.1	25.8	19.0
C $_{15:0}$ iso	15.4	28.4	23.6	26.4
C $_{17:0}$ iso 3OH	11.6	12.3	15.9	16.1
C $_{15:0}$ anteiso	8.7	5.8	5.0	TR
C $_{15:1}$ *ω6c*	7.8	11.0	1.1	TR
C $_{16:0}$ iso 3OH	6.3	3.0	2.3	1.2
C $_{17:0}$ 2OH	5.6	2.3	2.0	3.6
Summed Feature 9†	5.1	1.8	3.4	ND
C $_{17:1}$ anteiso *ω9c*	3.6	ND	ND	ND
C $_{15:0}$ 2OH	2.4	1.4	1.7	TR
C $_{15:0}$ iso 3OH	2.3	3.8	3.0	3.9
C $_{16:1}$ iso H	1.6	TR	TR	ND
C $_{17:1}$ *ω8c*	1.7	1.0	TR	TR
C $_{16:0}$ iso	1.2	TR	1.5	TR
C $_{17:1}$ *ω6c*	1.1	1.0	TR	TR
C $_{16:0}$ 3OH	1.00	1.4	1.7	TR
C $_{16:1}$ *ω5c*	1.00	2.5	4.4	1.1

*C $_{16:1}$ *ω7c*/ C $_{16:1}$ *ω6c*; †C $_{16:0}$ 10-methyl/ C $_{17:1}$ iso *ω9c*

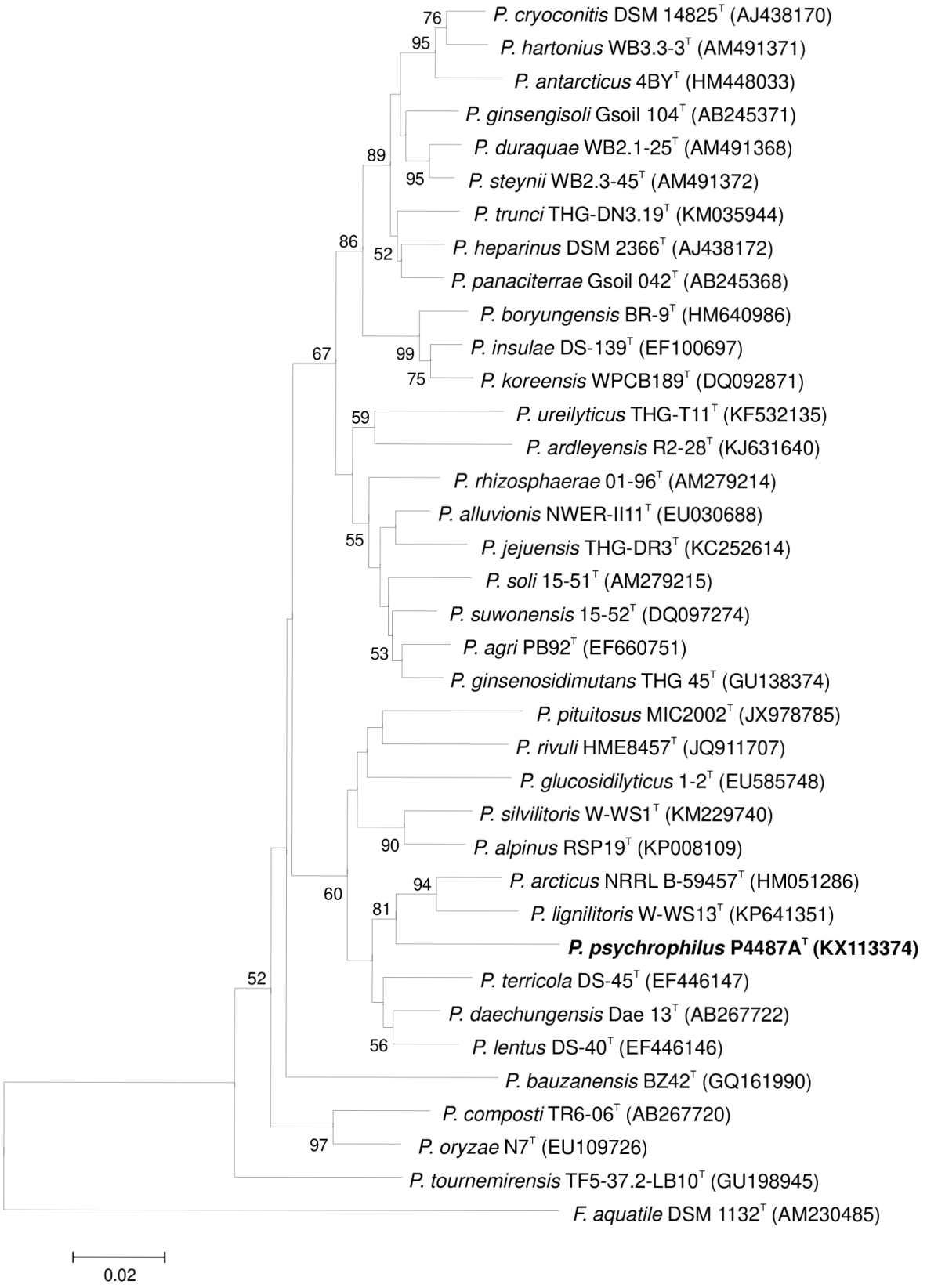

Fig. S1. Phylogenetic tree based on 16S rRNA gene sequences comparison showing the phylogenetic position of strain P4487A^{T}within the genus *Pedobacter*. The evolutionary history was inferred by using the Neighbor-Joining method based on the Kimura 2-parameter model. All positions with less than 95% site coverage were eliminated. Bootstrap probability values (percentages of 1,000 tree replications) greater than 50 % are indicated at branch points. There were a total of 1368 positions in the final dataset. *Flavobacterium aquatile* DSM 1132^T (AM230485) was used as an outgroup. Bar, 0.02 substitutions per nucleotide position.

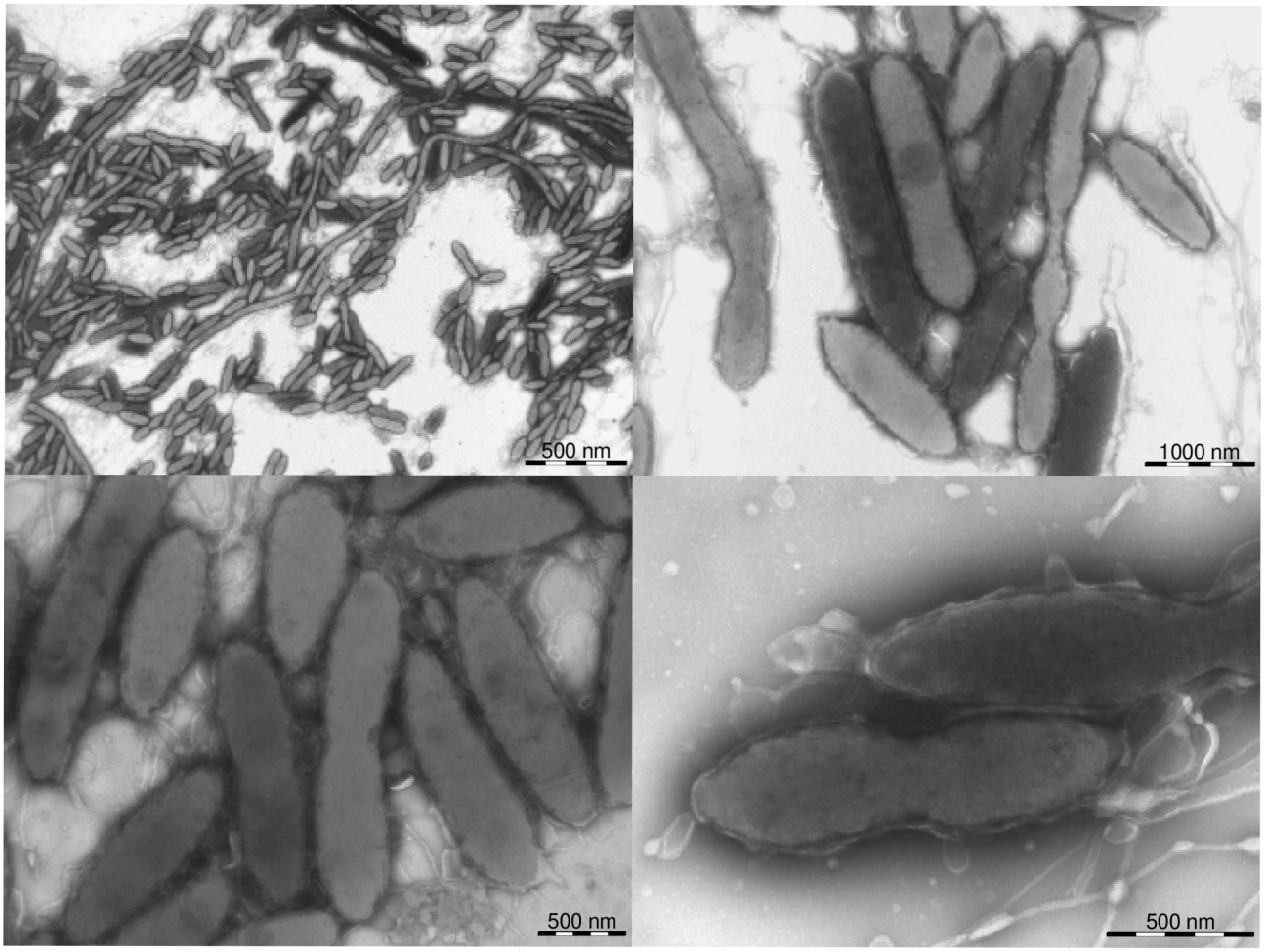

Fig. S2. Cellular morphology of strain P4487A^{T} cultivated on R2A agar (Oxoid). Images were obtained using transmission electron microscopy performed with a Morgagni 268D Philips (FEI Company, USA) electron microscope. Negative staining with 2% ammonium molybdate.

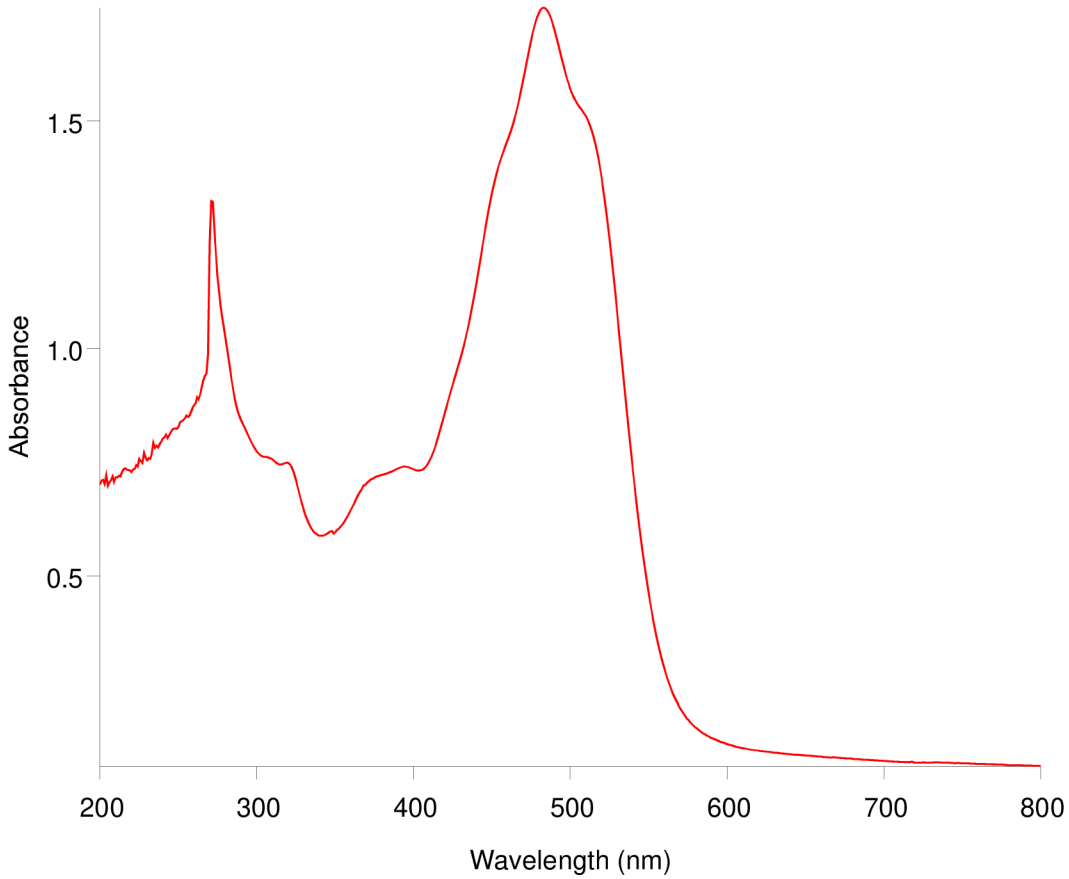

Fig. S3. Whole absorbance spectrum of hexane eluted pigment(s) produced by strain P4487A^{T}.

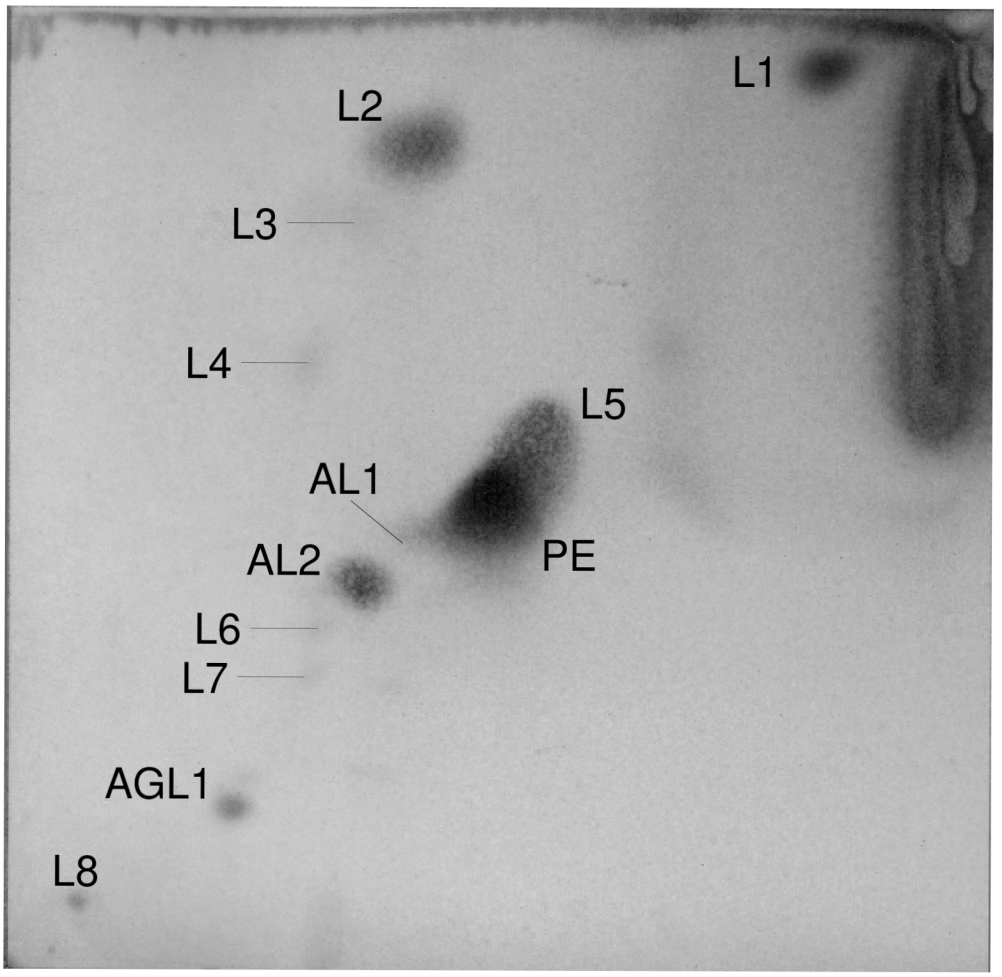

Fig. S4. Two dimensional thin layer chromatogram showing the total polar lipids of strain P4487A^{T}. PE, phosphatidylethanolamine; L1-L8, unknown polar lipids; AL1 and AL2, unknown aminolipids; AGL1, unknown aminoglykolipid.

Príloha č. 4.

Sedláček I., Králová S., Kýrová K., Mašlaňová I., Busse H.-J., Staňková E., Vrbovská V., Němec M., Barták M., Holochová P., Švec P., Pantůček R. (2017) Red-pink pigmented *Hymenobacter coccineus* sp. nov., *Hymenobacter lapidarius* sp. nov. and *Hymenobacter glacialis* sp. nov., isolated from rocks in Antarctica. *Int. J. Syst. Evol. Microbiol*. 67(6): 1975–83. Doi: 10.1099/ijsem.0.001898.

INTERNATIONAL JOURNAL OF SYSTEMATIC AND EVOLUTIONARY MICROBIOLOGY

TAXONOMIC DESCRIPTION

Sedláček *et al.*, *Int J Syst Evol Microbiol* 2017;67:1975–1983

DOI 10.1099/ijsem.0.001898

MICROBIOLOGY SOCIETY

Red-pink pigmented *Hymenobacter coccineus* sp. nov., *Hymenobacter lapidarius* sp. nov. and *Hymenobacter glacialis* sp. nov., isolated from rocks in Antarctica

Ivo Sedláček,[1,*] Stanislava Králová,[1] Kamila Kýrová,[1] Ivana Mašlaňová,[2] Hans-Jürgen Busse,[3] Eva Staňková,[1] Veronika Vrbovská,[1,2] Miroslav Němec,[4] Miloš Barták,[5] Pavla Holochová,[1] Pavel Švec[1] and Roman Pantůček[2]

Abstract

Four rod–shaped and Gram-stain-negative bacterial strains, CCM 8647, CCM 8649^T, CCM 8643^T and CCM 8648^T, were isolated from rock samples collected on James Ross Island, Antarctica. Extensive biotyping, fatty acid profiling, chemotaxonomy, 16S rRNA gene sequencing and whole-genome sequencing was applied to isolates to clarify their taxonomic position. Phylogenetic analysis based on 16S rRNA gene sequencing indicated that all four isolates belonged to the genus *Hymenobacter*. Strains CCM 8649^T and CCM 8647 were most closely related to *Hymenobacter arizonensis* OR362-8^T (94.4 % 16S rRNA gene sequence similarity), strain CCM 8643^T to *Hymenobacter terrae* DG7A^T (96.3 %) and strain CCM 8648^T to *Hymenobacter glaciei* VUG-A130^T (96.3 %). The predominant fatty acids of CCM 8649^T and CCM 8647 were summed feature 3 ($C_{16:1}\omega7c/C_{16:1}\omega6c$), $C_{16:1}\omega5c$ and iso-$C_{15:0}$, whereas those of CCM 8643^T and CCM 8648^T were summed feature 3 ($C_{16:1}\omega7c/C_{16:1}\omega6c$) and $C_{16:1}\omega5c$. The quinone systems contained exclusively menaquinone MK-7. The major polyamine was *sym*-homospermidine. All four strains contained the major polar lipid phosphatidylethanolamine. The G+C content of genomic DNA ranged from 60–63 mol%. Whole-genome sequencing data supported the finding that isolates represented distinct species of the genus *Hymenobacter*. On the basis of the results obtained, three novel species are proposed for which the names *Hymenobacter coccineus* sp. nov., *Hymenobacter lapidarius* sp. nov. and *Hymenobacter glacialis* sp. nov. are suggested, with the type strains CCM 8649^T (=LMG 29441^T=P5239^T), CCM 8643^T (=LMG 29435^T=P3150^T) and CCM 8648^T (=LMG 29440^T=P5086^T), respectively.

Recently, many novel species of the genus *Hymenobacter* have been discovered worldwide among environmental psychrotolerant bacteria [1–9]. The genus *Hymenobacter* was proposed almost twenty years ago [10], and the genus description was afterwards emended by Buczolits *et al.* [11] and Han *et al.* [3]. Based on phylogenetic analysis of species of the genus *Hymenobacter*, three phylogenetic clades were defined and two new genera, *Siccationidurans* and *Parahymenobacter*, were proposed [12], but these names have not been validly published yet. At the time of writing, the genus *Hymenobacter* represents a member of the family *Cytophagaceae*, order *Cytophagales*, class *Cytophagia*, phylum *Bacteroidetes* [13] and is comprised of 36 species with validly published names (LPSN, www.bacterio.net/hymenobacter.html; accessed August, 2016) [14]. All species are brick-red, red–pink or pink pigmented with many shades of colours [15]. Representatives of species of the genus *Hymenobacter* have been isolated from various habitats from the environment, e.g. sediment in the permafrost [3, 8], Antarctic soils [10], polluted soil and water [9, 16], arid lands [7], air [17], glacial till [1] or glacier ice [5]. Some hymenobacters are radiation-resistant [18–20] or UV-resistant

Author affiliations: [1]Czech Collection of Microorganisms, Department of Experimental Biology, Faculty of Science, Masaryk University, Kamenice 5, 625 00 Brno, Czech Republic; [2]Section of Genetics and Molecular Biology, Department of Experimental Biology, Faculty of Science, Masaryk University, Kotlářská 2, 611 37 Brno, Czech Republic; [3]Institut für Bakteriology, Mykology und Hygiene, Veterinärmedizinische Universität Wien, Veterinärplatz 1, A-1210 Wien, Austria; [4]Section of Microbiology and Molecular Biotechnology, Department of Experimental Biology, Faculty of Science, Masaryk University, Kamenice 5, 625 00 Brno, Czech Republic; [5]Section of Plant Physiology and Anatomy, Department of Experimental Biology, Faculty of Science, Masaryk University, Kamenice 5, 625 00 Brno, Czech Republic.
***Correspondence:** Ivo Sedláček, ivo@sci.muni.cz
Keywords: *Hymenobacter*; taxonomy; species description; James Ross Island.
Abbreviations: ANI, average nucleotide identity; dDDH, digital DNA-DNA hybridization; FAME, fatty acid methyl ester; OF, oxidation-fermentation; ONPG, *O*-nitrophenyl-b-D-galactopyranoside.
The GenBank/EMBL/DDBJ accession numbers for the 16S rRNA gene sequences of *Hymenobacter coccineus* CCM 8649^T, *H. coccineus* CCM 8647, *Hymenobacter lapidarius* CCM 8643^T and *Hymenobacter glacialis* CCM 8648^T are KX611463-KX611466, respectively. The whole-genome shotgun projects have been deposited at DDBJ/EMBL/GenBank under the accession numbers MDZA00000000 (CCM 8649^T), MDZB00000000 (CCM 8643^T) and MDZC00000000 (CCM 8648^T). The versions described in this paper are versions MDZA01000000, MDZB01000000 and MDZC01000000, respectively.
Two supplementary figures and one supplementary table are available with the online Supplementary Material.

(254 nm) [2]. In the present study, the classification of three novel species of the genus *Hymenobacter* isolated from rocks in Antarctica is reported. Strains designated CCM 8649^T, CCM 8647, CCM 8643^T and CCM 8648^T were subjected to a further taxonomic investigation.

Sampling was carried out by dispersing 1 g of rock sample in 5 ml sterile saline solution, and 200 µl of the suspension was spread on an R2A agar plate (Oxoid) and cultivated at 15 °C for 5 days. Afterwards, individual red–pink pigmented colonies were picked up, purified by repeated streaking on R2A medium at 15 °C, and the resulting pure cultures were maintained in R2A broth supplemented with 15 % (v/v) glycerol and stored at −70 °C until analysed. Strain CCM 8649^T was isolated from a stone surface covered by lichens (*Usnea antarctica*) at the Panorama Pass locality (GPS position: 57° 50′ 45″ W 63° 48′ 54″ S) in 2013 and strain CCM 8647 was retrieved from stone fragments near Big Lachman Lake (GPS position: 57° 48′ 32″ W 63° 47′ 34″ S) in 2013. Strain CCM 8643^T was isolated from small stones in Marsovske valley (GPS position: 57° 49′ 33″ W 63° 48′ 36″ S) in 2009, and the last isolate, CCM 8648^T, was obtained from volcanic tuff in a hill above Cape Lachman (GPS position: 57° 47′ 11″ W 63° 46′ 58″ S) in 2013. All sampling sites are situated in a deglaciated northern part of James Ross Island, Antarctica.

Reference strains of the phylogenetic relatives, namely *Hymenobacter arizonensis* CCM 8581^T, *Hymenobacter antarcticus* CCM 8582^T, *Hymenobacter glaciei* CCM 8583^T, *Hymenobacter ruber* KCTC 32477^T, *Hymenobacter soli* KCTC 12607^T and *Hymenobacter terrae* KCTC 32554^T were obtained from the Czech Collection of Microorganisms (www.sci.muni.cz/ccm/), and the Korean Collection for Type Cultures (https://kctc.kribb.re.kr) and used for subsequent comparison. Unless stated otherwise, all strains were routinely cultivated on R2A agar for 48–72 h at 15 °C.

DNA for molecular analyses was extracted by using FastPrep Lysing Matrix type B and a FastPrep Homogenizer (MP Biomedicals) and purified by using the High Pure PCR Template Preparation kit (Roche Diagnostics). A fragment of the 16S rRNA gene corresponding to co-ordinates 8–1542 used for *Escherichia coli* was amplified by PCR with FastStart PCR Master (Roche Diagnostics) and conserved forward primer pA (AGAGTTTGATCCTGGCTCAG) and reverse primer pH (AAGGAGGTGATCCAGCCGCA) [21], and purified using a QIAquick PCR Purification kit (Qiagen). Sequencing was performed using the PCR primers and custom primers F1 (GTGGGGAKCRAACAGGATTAG), F2 (CGTCARGTC MTCATGGCCCTT), R1 (ATTACCGCGGCTGCTGGCAC) and R2 (CACATSMTCCMCCRCTTGT) at the Eurofins MWG Operon sequencing facility (Ebersberg, Germany). The sequences obtained were identified using the EzBioCloud database [22]. The 16S rRNA gene sequence analysis placed the isolates within the genus *Hymenobacter*. Strains CCM 8649^T and CCM 8647 revealed identical 16S rRNA gene sequences, and *H. arizonensis* OR362-8^T was the closest relative with 94.4 % 16S rRNA gene sequence similarity. Strain CCM 8643^T showed *H. terrae* DG7A^T as the closest phylogenetic relative with 96.3 % 16S rRNA gene sequence similarity, and CCM 8648^T was most closely related to *H. glaciei* VUG-A130^T with 96.3 % 16S rRNA gene similarity. Moreover, isolates CCM 8643^T and CCM 8648^T were related, having 97.6 % 16S rRNA gene sequence similarity reciprocally.

Phylogenetic analysis was performed using MEGA version 7 software [23]. Genetic distances were corrected using Kimura's 2-parameter model. 16S rRNA gene sequences of other taxa of the genus *Hymenobacter* retrieved from the GenBank/EMBL/DDJB database, as denoted in the List of Prokaryotic Names with Standing in Nomenclature [14], were used for the phylogenetic analysis. The evolutionary history was inferred using the neighbour-joining and maximum-likelihood methods, using a bootstrap test based on 1000 replications. Phylogenetic analysis based on the neighbour-joining method (Fig. 1) showed that all strains analysed belonged to the *H. soli* phylogenetic clade. The maximum-likelihood method confirmed their phylogenetic position (Fig. 1).

Whole-genome sequencing was performed to determine the faultless taxonomic position of strains CCM 8649^T, CCM 8643^T and CCM 8648^T in more detail. The purified genomic DNA of isolates CCM 8649^T, CCM 8643^T and CCM 8648^T was used for 400 bp sequencing library preparation as described previously [24]. The samples were loaded on a 318v2 chip and sequenced using the Ion PGM Hi-Q View sequencing kit (Thermo Fisher Scientific) on the Ion PGM system (Life Technologies). Quality trimming and error correction of the reads were performed with the Ion Torrent Suite Software (version 5.0.4). The assembly computation was performed using the plug-in Assembler SPAdes (version 3.1.0). The total length of assembly contained 5 720 607 bp (CCM 8649^T), 4 682 061 bp (CCM 8643^T) and 4 268 822 bp (CCM 8648^T). Assembled contigs larger than 200 bp were used for subsequent analysis.

To evaluate the mean level of nucleotide sequence similarity at the genome level among the isolates CCM 8649^T, CCM 8643^T and CCM 8648^T, an average nucleotide identity (ANI) and a digital DNA–DNA hybridization (dDDH) were determined. The dDDH values were calculated using the web-based genome-to-genome distance calculator (GGDC) version 2.1 [25], and the recommended formula 2 was taken into account to interpret the results. To calculate the ANI value, the algorithm implemented at the EzGenome server was used (www.ezbiocloud.net/tools/ani) [26]. The dDDH value between closely related isolates CCM 8643^T and CCM 8648^T was 40.3 %, and the ANI value between the aforementioned isolates was 89.8896 %, reciprocal value 90.0045 %. Both values were well below the proposed cut-off values recommended for species delineation (70 % and 95–96 %, respectively) [27, 28]. The dDDH values between CCM 8649^T and CCM 8643^T, and CCM 8649^T and CCM 8648^T were 22.3 and 22.4 %, respectively, and the ANI values were 76.683 and 76.4533 %, respectively. Thus, these results proved the genomic dissimilarity of isolates CCM 8649^T,

CCM 8643^T and CCM 8648^T and showed that they are members of three different species, as implied by the 16S rRNA gene sequencing results.

To estimate the DNA G+C content, the draft genome sequences were used. The DNA G+C content of CCM 8649^T, CCM 8643^T and CCM 8648^T was 63.1, 61.0, and 60.5 mol%, respectively. The DNA G+C values fell in the range of 55–70 mol% observed in other species of the genus *Hymenobacter* [3, 13].

Phenotype testing was performed using cells grown at 20 °C for 48–72 h on R2A agar (Oxoid). Liquid cultures were not used because of the poor growth of these isolates in broth medium, which is a common feature of many species of the genus *Hymenobacter* [5]. Morphology of cells was noted under light microscopy using a BX53 microscope (Olympus). Gram staining was confirmed by using the KOH lysis test method [29]. The morphology of strains CCM 8649^T, CCM 8643^T and CCM 8648^T was observed by transmission electron microscopy (Morgagni 268D Philips, FEI) using samples stained with 2 % ammonium molybdate (Fig. S1, available in the online Supplementary Material). The gliding motility test was done using a hanging-drop method as described by Bernardet *et al.* [30].

The presence of flexirubin-type pigments was investigated using a 20 % (w/v) KOH solution [30]. Spectrophotometric characterization of carotenoid pigments was done from cells grown on R2A agar for 72 h at 20 °C. The cells were washed off and rinsed two times using 0.1 M phosphate buffer (pH 7.2). Harvested cells were suspended in an extraction solution composed of equal volumes of acetone, ether and ethanol (96 %). Extraction was done in a shaker for 120 min at 4 °C with a shaking interval of 120 swings per minute, and the solution was then centrifuged at 5000 g at 4 °C for 20 min. Supernatant was evaporated in a vacuum at ambient temperature, and the evaporation residue was diluted in hexane. A spectrophotometer (Cary 100Bio, Agilent) was used for the spectra measurements. The pigments extracted showed whole-absorbance spectra with two typical major peaks at 275 and 475 nm for strain CCM 8649^T and at 275 and 480 nm for strain CCM 8647 (data not shown). Strain CCM 8643^T had two similar major peaks at 275 and 475 nm, and a less distinct peak at 385 nm. Strain CCM 8648^T showed major peaks at 270

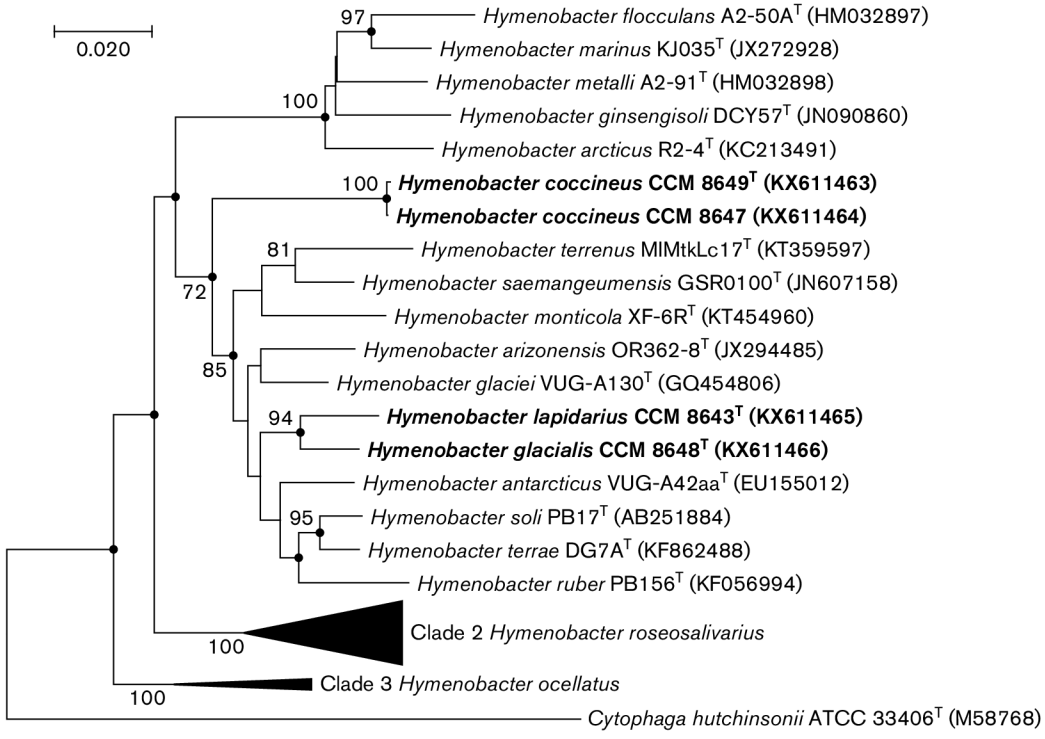

Fig. 1. Unrooted neighbour-joining tree based on 16S rRNA gene sequences comparison showing the phylogenetic position of strains CCM 8647, CCM 8649^T, CCM 8643^T and CCM 8648^T within the *H. soli* phylogenetic clade. Bootstrap probability values (percentages of 1000 tree replications) greater than 70 % are shown at branch points. The evolutionary distances are in the units of the number of base substitutions per site. The analysis involved 46 nucleotide sequences. All ambiguous positions were removed for each sequence pair. There were a total of 1579 positions in the final dataset. Filled circles indicate that the corresponding nodes are also obtained in the maximum-likelihood tree. *Cytophaga hutchinsonii* was used as an outgroup. GenBank accession numbers of 16S rRNA gene sequences are given in parentheses. Bar, 0.02 substitutions per nucleotide position.

and 480 nm, with a less distinct peak at 380 nm. The spectra obtained resembled those of β-carotene as described by Burns *et al.* [31]. The UV-resistance test was performed as described by Hirsch *et al.* [32] with minor modifications (UVC lamp, R2A agar plates exposed for 5 and 20 min at a distance of 15 cm to a lamp, *Serratia rubidaea* CCM 4684 was used as a control).

Growth on several media such as plate count agar (PCA; Oxoid), tryptone soya agar (TSA; Oxoid), nutrient agar CM03 (Oxoid), MacConkey agar (Becton Dickinson) and brain heart infusion agar (BHI; Oxoid) at 15 °C was evaluated. Anaerobic growth on R2A agar (Oxoid) was tested at 15 °C for 72 h using the Anaerocult A system (Merck) and compared with growth of those bacteria cultivated in ambient atmosphere. Growth at different temperatures (1, 5, 10, 15, 20, 25, 30, 35 and 37 °C) and tolerance to various concentrations of NaCl (0.5, 1, 2, 3, 4 and 5 %, w/v) were determined based on cultivation on R2A agar plates for up to 6 days. The pH range for growth was tested for 1 week at 20 °C on R2A agar plates adjusted to pH 5.0–10.0, at intervals of 1 pH unit, by using the following buffer systems: pH 5.0–8.0, 0.1 M KH_2PO_4/0.1 M NaOH; pH 9.0–10.0, 0.1 M $NaHCO_3$/0.1 M Na_2CO_3[33]. The basic phenotypic classification was performed using traditional key tests applicable for Gram-negative rods. Oxidase (OXItest, Erba-Lachema) and catalase (ID colour Catalase, bioMérieux) activity was tested according to the manufacturers' instructions. Further tests were done as follows: oxidation–fermentation (OF) test [34], urease [35], arginine dihydrolase, ornithine and lysine decarboxylase [36], hydrolysis of aesculin, starch [37], gelatin, Tween 80 [38], casein, tyrosine [39] and DNA (CM321, Oxoid), egg-yolk reaction [40], *O*-nitrophenyl-β-D-galactopyranoside (ONPG) [41], nitrate and nitrite reduction, growth on Simmons' citrate agar [37], and utilization of acetamide [42] and sodium malonate [43]. Motility was observed in a glucose oxidation tube. Further extended phenotyping using identification test kits, GN2 MicroPlate (Biolog), API 50 CH and API ZYM (bioMérieux) according to the manufacturer's instructions, enabled detailed characterization of isolates. Inoculated kits were incubated at 20 °C, and the results were read after 18 h (API ZYM) or 24–48 h (GN2 MicroPlate) or 2–8 days (API 50 CH).

Differences in the antibiotic resistance patterns were tested by the disc diffusion method on R2A agar for 2 days at 20 °C. Sixteen antibiotic discs generally used for Gram-negative rods [44, 45] were chosen: ampicillin (10 µg), aztreonam (30 µg), carbenicillin (100 µg), cefixim (5 µg), ceftazidime (10 µg), cefalotin (30 µg), ciprofloxacin (5 µg), gentamicin (10 µg), chloramphenicol (30 µg), imipenem (10 µg), kanamycin (30 µg), kotrimoxazol (25 µg), piperacillin (30 µg), polymyxin B (300 U), streptomycin (10 µg) and tetracycline (30 µg). EUCAST/CLSI standards were followed strictly for cultivation and reading of the inhibition zone diameter.

The comprehensive morphological and biochemical/physiological traits of CCM 8649^T, CCM 8647, CCM 8643^T and CCM 8648^T are summarized in the species descriptions. The tests distinguishing the suggested novel species from the phylogenetically closest species of the genus *Hymenobacter* are shown in Table 1.

Fatty acids methyl ester (FAME) analysis was performed with cells growing on R2A agar (Difco) incubated at 20 °C ±2 °C for 72 h, where the bacterial communities reached the late-exponential stage of growth according to the four quadrants streak method [46]. Extraction of FAMEs was performed according to the standard protocol of the Sherlock Microbial Identification System (MIDI) [46]. Cellular fatty acid extracts were analysed by a gas chromatograph (model 7890B, Agilent) according to the standard protocol of the Sherlock MIDI Identification system (MIS, version 6.2, MIDI database: RTSBA 6.21.). The predominant fatty acids of CCM 8649^T and CCM 8647 were summed feature 3 ($C_{16:1}$ $\omega7c$/$C_{16:1}\omega6c$) (37–39 %), $C_{16:1}\omega5c$ (20 %) and iso-$C_{15:0}$ (14 %), whereas the predominant fatty acids of CCM 8643^T and CCM 8648^T were summed feature 3 ($C_{16:1}\omega7c$/$C_{16:1}$ $\omega6c$) (34 and 25 %, respectively) and $C_{16:1}\omega5c$ (15 and 17%, respectively). The complete cellular fatty acids compositions of strains CCM 8647, CCM 8649^T, CCM 8643^T and CCM 8648^T and of the respective closest phylogenetic neighbours are given in Table S1. The FAME profiles obtained corresponded to those typically found in other species of the genus *Hymenobacter* [8, 11, 13]. In comparison with the closest phylogenetic neighbours, strains CCM 8647, CCM 8649^T, CCM 8643^T and CCM 8648^T contained lower amounts of anteiso-$C_{15:0}$, whereas the amounts of predominant fatty acids, namely iso-$C_{15:0}$, $C_{16:1}\omega5c$ and summed feature 3, were similar to those of their closest neighbours.

Quinones and polar lipids were extracted from freeze-dried biomass grown on R2A medium and analysed as described previously [47–50]. The major respiratory quinone of strains CCM 8647, CCM 8649^T, CCM 8643^T and CCM 8648^T was unanimously menaquinone MK-7, which is in agreement with the description of the genus *Hymenobacter* [13]. In all four strains, the predominant polar lipid was phosphatidylethanolamine (Fig. S2). All strains also contained moderate to minor amounts of phosphatidylserine, unidentified lipids L1-L5 and unidentified phospholipid PL1. Additionally strain CCM 8643^T contained moderate to minor amounts of six unidentified lipids lacking a functional group (L6-L8, L12-L14), two unidentified glycolipids (GL1, GL2), an unidentified aminoglycolipid (AGL1) and an unidentified aminolipid (AL1). Additional components in strain CCM 8649^T were lipids L10 and L11, the unidentified aminophospholipids APL1 and APL2, unidentified aminolipids AL1 and AL2, and unidentified phospholipids PL2 and PL3. The polar lipid profile of strain CCM 8647 differed from that of CCM 8649^T qualitatively only by the absence of the minor lipids L10 and L11. These data corresponded again with classification of the genus *Hymenobacter* as mentioned by Buczolits *et al.* [11].

Biomass subjected to polyamine analysis was grown on R2A agar, scraped off the surface, freeze dried and then extracted according to the method of Busse and Auling [51] and

Table 1. Phenotypic characteristics that differentiate strains CCM 8649^T, CCM 8647, CCM 8643^T and CCM 8648^T from closely related species of the genus *Hymenobacter*

Strains: 1, CCM 8649^T and CCM 8647; 2, CCM 8643^T; 3, CCM 8648^T; 4, *H. arizonensis* CCM 8581^T; 5, *H. antarcticus* CCM 8582^T; 6, *H. glaciei* CCM 8583^T; 7, *H. ruber* KCTC 32477^T; 8, *H. soli* KCTC 12607^T; 9, *H. terrae* KCTC 32554^T. +, Positive; w, weakly positive; –, negative; all data were taken from this study.

Characteristic	1	2	3	4	5	6	7	8	9
Growth at 5 °C	+	+	+	–	w	+	w	–	w
Growth with 1 % NaCl	–	–	–	+	–	–	–	–	–
Hydrolysis of:									
Gelatin	–	w	w	+	–	–	+	w	+
Tween 80	–	–	+	+	–	–	–	–	–
DNA	–	–	+	+	–	–	+	–	–
Starch	–	–	+	w	w	w	+	–	w
ONPG	+	–	–	+	–	–	+	w	+
Casein	–	w	+	–	+	+	+	+	+

analysed by HPLC as reported by Busse *et al.* [52]. The HPLC equipment used was described by Stolz *et al.* [48]. In all four strains, *sym*-homospermidine was found to be the major polyamine. However, compared with other species of the genus *Hymenobacter* [11], the polyamine content was significantly lower [0.11–3.33 μmol (g dry weight)$^{-1}$]. However, these results are in line with the results from polyamine analyses of other bacterial strains grown on agar media, which also showed significantly lower polyamine contents in contrast to those of strains grown in liquid media (H.-J. Busse, unpublished results).

Strains CCM 8643^T, CCM 8647, CCM 8648^T and CCM 8649^T represented psychrophilic, Gram-stain-negative, aerobic, catalase-positive and oxidase-negative, non-fermenting rods with red carotenoid pigments. Subsequently, 16S rRNA gene sequence analysis placed all four strains within the genus *Hymenobacter* and EZ taxon showed *H arizonensis* OR362-8^T as the most closely related species, having 16S rRNA gene sequence similarity below 97 %.

Polyphasic investigation of strains CCM 8643^T, CCM 8647, CCM 8648^T and CCM 8649^T using 16S rRNA gene sequencing, chemotaxonomy analysis (polyamines, menaquinone, polar lipids and FAMEs) and extended phenotyping differentiated the aforementioned strains from the type strains representing hitherto described species of the genus *Hymenobacter*. The results demonstrated that strains CCM 8643^T, CCM 8647, CCM 8648^T and CCM 8649^T isolated from the rock environment in Antarctica represented three distinct species of the genus *Hymenobacter* for which the names *Hymenobacter coccineus* sp. nov., *Hymenobacter lapidarius* sp. nov., and *Hymenobacter glacialis* sp. nov. are proposed.

DESCRIPTION OF *HYMENOBACTER COCCINEUS* SP. NOV.

Hymenobacter coccineus sp. nov. (coc.ci′ne.us. L. adj. *coccineus* reddish coloured).

Description of the species is based on two strains. Cells are Gram-stain-negative, non-spore-forming rods, non-motile and non-gliding, sporadically longer, occurring predominantly separately or in irregular clusters. Colonies on R2A agar (Oxoid) are circular with entire margin, flat, smooth, glistening, reddish-pigmented and 1–2 mm in diameter after 3 days of cultivation at 15 °C. Carotenoid pigments are produced while flexirubin-type pigments are absent. Resistant to UVC irradiation. Growth occurs on R2A agar and weakly on PCA agar in an aerobic atmosphere. No growth is observed on TSA, BHI, MacConkey agar or nutrient agar at 15 °C. There is no growth on R2A agar under anaerobic conditions. Growth is observed at temperatures between 5 and 20 °C, but not at 25 °C. Cells grow at pH 7.0 only. Good growth on R2A medium in the presence of 0.5 % NaCl (w/v); however, the presence of 1 % NaCl inhibits growth. Glucose is not fermented to acid in OF test medium. Catalase, phosphatase, leucine arylamidase, valine arylamidase, α-galactosidase, β-galactosidase, α-glucosidase, β-glucosidase and *N*-acetyl-β-glucosaminidase are positive by API ZYM. Urease, oxidase, lysine and ornithine decarboxylase, arginine dihydrolase, esterase (C4), esterase lipase (C8), lipase (C14), cystine arylamidase, trypsin, chymotrypsin, naphthol-AS-BI-phosphohydrolase, β-glucuronidase, α-mannosidase and α-fucosidase are negative by API ZYM. Aesculin and ONPG hydrolysis is positive. Nitrate and nitrite reduction, fluorescein (King B medium), Simmons' citrate, acetamide and malonate utilization are negative. Hydrolysis of Tween 80, gelatin, starch, casein, tyrosine, lecithin and DNA is negative. Acid is produced (API 50 CH) from galactose, D-glucose, D-mannose, cellobiose, maltose, lactose, sucrose, trehalose, β-gentiobiose and 5 ketogluconate. Acid is not produced (API 50 CH) from glycerol, erythritol, ribose, D-xylose, L-xylose, adonitol, methyl β-D-xyloside, D-fructose, sorbose, rhamnose, dulcitol, inositol, mannitol, sorbitol, methyl α-D-mannoside, methyl α-D-glucoside, *N*-acetylglucosamine, amygdalin, arbutin, melibiose, inulin, melezitose, raffinose, starch, glycogen, xylitol, turanose, D-lyxose, D-tagatose, D-fucose, L-fucose, D-arabitol, L-arabitol,

gluconate or 2 ketogluconate. Variable phenotypical reactions of *H. coccineus* isolates are mentioned within the type strain description.

Utilizes (Biolog GN2 Micro Plate) the following carbon sources via respiration: dextrin, cellobiose, gentiobiose, α-D-glucose, lactose, lactulose, maltose, methyl β-D-glucoside, sucrose, trehalose, turanose and acetic acid. Negative for utilization of α-cyclodextrin, glycogen, Tween 40, Tween 80, *N*-acetyl-D-galactosamine, *N*-acetyl-D-glucosamine, adonitol, D-arabitol, erythritol, D-fructose, L-fucose, *myo*-inositol, D-mannitol, melibiose, D-psicose, raffinose, L-rhamnose, xylitol, pyruvic acid methyl ester, succinic acid monomethyl ester, *cis*-aconitic acid, formic acid, D-galactonic acid lactone, D-galacturonic acid, D-glucosaminic acid, D-glucuronic acid, α-hydroxybutyric acid, β-hydroxybutyric acid, γ-hydroxybutyric acid, *p*-hydroxyphenylacetic acid, itaconic acid, α-ketobutyric acid, α-ketoglutaric acid, α-ketovaleric acid, D,L-lactic acid, malonic acid, propionic acid, quinic acid, D-saccharic acid, sebacic acid, succinic acid, bromosuccinic acid, succinamic acid, glucuronamide, L-alaninamide, D-alanine, L-alanine, L-alanyl-glycine, L-asparagine, L-aspartic acid, L-glutamic acid, glycyl-L-aspartic acid, glycyl-L-glutamic acid, L-histidine, hydroxy-L-proline, L-leucine, L-ornithine, L-phenylalanine, L-proline, L-pyroglutamic acid, D-serine, L-serine, L-threonine, D,L-carnitine, γ-aminobutyric acid, urocanic acid, inosine, thymidine, uridine, phenyethylamine, putrescine, 2-aminoethanol, 2,3-butanediol, glycerol, α-D,L-glycerol phosphate and D-glucose 6-phosphate. Variable results of *H. coccineus* strains obtained in Biolog GN2 Micro Plate are indicated in the type strain description. Sensitive to ampicillin, carbenicillin, cefalotin, ciprofloxacin, chloramphenicol, imipenem, kotrimoxazol, piperacillin, streptomycin and tetracycline. Resistant to aztreonam, cefixim, ceftazidime, gentamicin and kanamycin. Sensitivity or resistance to polymyxin B is strain dependent.

Contains summed feature 3 ($C_{16:1}\omega7c/C_{16:1}\omega6c$), $C_{16:1}\omega5c$ and iso-$C_{15:0}$ as major cellular fatty acids. The polar lipid profile contains phosphatidylethanolamine as the major compound and moderate to minor amounts of phosphatidylserine, five unidentified lipids (L1-L5), two unidentified aminophospholipids (APL1, APL2), two unidentified aminolipids (AL1, AL2) and three unidentified phospholipids (PL1-PL3). Two additional lipids may be present (L10, L11). The quinone system contains predominantly menaquinone MK-7, and the major polyamine is *sym*-homospermidine.

The type strain is CCM 8649^T (=LMG 29441^T=P5239^T). The DNA G+C content of the type strain is 63.1 mol%. Almost all characteristics of the type strain CCM 8649^T are in agreement with the species description. The strain-dependent test results of CCM 8649^T are as follows: acid is produced from D-arabinose and salicin; no growth at 1 °C; negative for acid production from L-arabinose; sensitive to polymyxin B. On the Biolog GN2 MicroPlate, the type strain CCM 8649^T is able to utilize D-sorbitol, but unable to utilize L-arabinose, D-galactose, D-mannose, citric acid, D-gluconic acid or α-D-glucose 1-phosphate. The type strain CCM 8649^T (=LMG 29441^T=P5239^T) was isolated from lichens on stone while strain CCM 8647 (=LMG 29439=P5059) was isolated from stone fragments on James Ross Island, Antarctica.

DESCRIPTION OF *HYMENOBACTER LAPIDARIUS* SP. NOV.

Hymenobacter lapidarius sp. nov. (la.pi.da′ri.us. L. masc. adj. *lapidarius* belonging to stones).

Description of the species is based on one strain. Cells are Gram-stain-negative, non-spore-forming rods, non-motile and non-gliding, occasionally curved and longer, occurring singly or in irregular clusters. Colonies on R2A agar (Oxoid) are circular with entire margin, flat, smooth, glistening, reddish pigmented and 1 mm in diameter after 3 days at 15 °C. Carotenoid pigments are produced while flexirubin-type pigments are absent. Resistant to UVC irradiation. Growth occurs on R2A agar in an aerobic atmosphere, but no growth is observed on BHI, PCA, TSA, MacConkey agar or nutrient agar at 15 °C. There is no growth on R2A agar under anaerobic conditions. Growth is observed at 1 °C (weakly), 5 °C and 25 °C, but not at 30 °C. Cells grow within the range of pH 7.0 to 9.0. The presence of 0.5 % NaCl (w/v) inhibits growth. Glucose is not fermented to acid in OF test medium. Catalase, phosphatase, esterase lipase (C8) (weakly), leucine arylamidase, valine arylamidase, trypsin, α-glucosidase (weakly) and *N*-acetyl-β–glucosaminidase are positive by API ZYM. Urease, oxidase, lysine and ornithine decarboxylase, arginine dihydrolase, esterase (C4), lipase (C14), cystine arylamidase, chymotrypsin, naphthol-AS-BI-phosphohydrolase, α-galactosidase, β-galactosidase, β-glucuronidase, β-glucosidase, α-mannosidase and α-fucosidase are negative by API ZYM. Aesculin, casein and gelatin hydrolysis is positive. Nitrate and nitrite reduction, fluorescein (King B medium), Simmons' citrate, acetamide and malonate utilization are negative. Hydrolysis of Tween 80, starch, ONPG, DNA, tyrosine and lecithin is negative. Acid is not produced (API 50 CH) from glycerol, erythritol, D-arabinose, L-arabinose, ribose, D-xylose, L-xylose, adonitol, methyl β-D-xyloside, galactose, D-glucose, D-fructose, D-mannose, sorbose, rhamnose, dulcitol, inositol, mannitol, sorbitol, methyl α-D-mannoside, methyl α-D-glucoside, *N*-acetylglucosamine, amygdalin, arbutin, salicin, cellobiose, maltose, lactose, melibiose, sucrose, trehalose, inulin, melezitose, raffinose, starch, glycogen, xylitol, β-gentiobiose, turanose, D-lyxose, D-tagatose, D-fucose, L-fucose, D-arabitol, L-arabitol, gluconate, 2 ketogluconate or 5 ketogluconate.

Able to utilize Tween 40 as a carbon source via respiration (Biolog GN2 Micro Plate). Negative in utilization of α-cyclodextrin, dextrin, glycogen, Tween 80, *N*-acetyl-D-galactosamine, *N*-acetyl-D-glucosamine, adonitol, L-arabinose, D-arabitol, cellobiose, erythritol, D-fructose, L-fucose, D-galactose, gentiobiose, α-D-glucose, *myo*-inositol, lactose, lactulose, maltose, D-mannitol, D-mannose, melibiose, methyl β-D-glucoside, D-psicose, raffinose, L-rhamnose, D-sorbitol,

sucrose, trehalose, turanose, xylitol, pyruvic acid methyl ester, succinic acid monomethyl ester, acetic acid, *cis*-aconitic acid, citric acid, formic acid, D-galactonic acid lactone, D-galacturonic acid, D-gluconic acid, D-glucosaminic acid, D-glucuronic acid, α-hydroxybutyric acid, β-hydroxybutyric acid, γ-hydroxybutyric acid, *p*-hydroxyphenylacetic acid, itaconic acid, α-ketobutyric acid, α-ketoglutaric acid, α-ketovaleric acid, D,L-lactic acid, malonic acid, propionic acid, quinic acid, D-saccharic acid, sebacic acid, succinic acid, bromosuccinic acid, succinamic acid, glucuronamide, L-alaninamide, D-alanine, L-alanine, L-alanyl-glycine, L-asparagine, L-aspartic acid, L-glutamic acid, glycyl-L-aspartic acid, glycyl-L-glutamic acid, L-histidine, hydroxy-L-proline, L-leucine, L-ornithine, L-phenylalanine, L-proline, L-pyroglutamic acid, D-serine, L-serine, L-threonine, D,L-carnitine, γ-aminobutyric acid, urocanic acid, inosine, thymidine, uridine, phenyethylamine, putrescine, 2-aminoethanol, 2,3-butanediol, glycerol, α-D,L-glycerol phosphate, α-D-glucose 1-phosphate and D-glucose 6-phosphate. Sensitive to ampicillin, carbenicillin, cefixim, cefalotin, ciprofloxacin, chloramphenicol, imipenem, kanamycin, kotrimoxazol, piperacillin, polymyxin B, streptomycin and tetracycline. Resistant to ceftazidime and gentamicin, and shows intermediate resistance to aztreonam.

Contains summed feature 3 ($C_{16:1}\omega7c/C_{16:1}\omega6c$) and $C_{16:1}\omega5c$ as major cellular fatty acids. The polar lipid profile contains phosphatidylethanolamine as the major compound and moderate to minor amounts of phosphatidylserine, 11 unidentified lipids (L1-L8, L12-L14), an unidentified phospholipid, two unidentified glycolipids (GL1, GL2), an unidentified aminoglycolipid (AGL1), and an unidentified aminolipid (AL). The quinone system contains predominantly menaquinone MK-7, and the major polyamine is *sym*-homospermidine.

The type strain is CCM 8643^T (=LMG 29435^T=$P3150^T$). The DNA G+C content of the type strain is 61.0 mol%. Isolated from small stones in Marsovske valley, James Ross Island, Antarctica.

DESCRIPTION OF *HYMENOBACTER GLACIALIS* SP. NOV.

Hymenobacter glacialis sp. nov. (gla.ci.a'lis. L. masc. adj. *glacialis* referring to a polar region).

Description of the species is based on one strain. Cells are Gram-stain-negative, non-spore forming rods, non-motile and non-gliding, occasionally curved and longer, occurring singly or in irregular clusters. Colonies on R2A agar (Oxoid) are circular with entire margin, flat, smooth, glistening, reddish-pigmented and 1.5 mm in diameter after 3 days at 15 °C. Carotenoid pigments are produced while flexirubin-type pigments are absent. Resistant to UVC irradiation. Growth occurs on R2A, PCA (weakly) and TSA agars in an aerobic atmosphere, but no growth is observed on BHI agar, MacConkey agar or nutrient agar at 15 °C. There is no growth on R2A agar under anaerobic conditions. Growth is observed at temperatures between 5 and 25 °C, but neither at 1 °C nor at 30 °C. Cells grow within the range of pH 7.0 to 8.0. Grows on R2A medium in the presence of 0.5 % NaCl (w/v); the presence of 1.0 % NaCl inhibits growth. Glucose is not fermented to acid in OF test medium. Catalase, phosphatase, esterase (C4) (weakly), leucine arylamidase, valine arylamidase, chymotrypsin, naphthol-AS-BI-phosphohydrolase (weakly), α-glucosidase and *N*-acetyl-β-glucosaminidase are positive by API ZYM. Urease, oxidase, lysine and ornithine decarboxylase, arginine dihydrolase, esterase lipase (C8), lipase (C14), cystine arylamidase, trypsin, α-galactosidase, β-galactosidase, β-glucuronidase, β-glucosidase, α-mannosidase and α-fucosidase are negative by API ZYM. Aesculin, Tween 80, starch, casein, DNA and gelatin hydrolysis is positive. Nitrate and nitrite reduction, fluorescein (King B medium), Simmons' citrate, acetamide and malonate utilization are negative. Hydrolysis of ONPG, tyrosine and lecithin is negative. Acid is not produced (API 50 CH) after 4 days from glycerol, erythritol, D-arabinose, L-arabinose, ribose, D-xylose, L-xylose, adonitol, methyl β-D-xyloside, galactose, D-glucose, D-fructose, D-mannose, sorbose, rhamnose, dulcitol, inositol, mannitol, sorbitol, methyl α-D-mannoside, methyl α-D-glucoside, *N*-acetylglucosamine, amygdalin, arbutin, salicin, cellobiose, maltose, lactose, melibiose, sucrose, trehalose, inulin, melezitose, raffinose, starch, glycogen, xylitol, β-gentiobiose, turanose, D-lyxose, D-tagatose, D-fucose, L-fucose, D-arabitol, L-arabitol, gluconate, 2 ketogluconate or 5 ketogluconate.

Able to utilize dextrin (weakly), Tween 40 and L-glutamic acid as a carbon source via respiration (Biolog GN2 Micro Plate). Negative in utilization of α-cyclodextrin, glycogen, Tween 80, *N*-acetyl-D-galactosamine, *N*-acetyl-D-glucosamine, adonitol, L-arabinose, D-arabitol, cellobiose, erythritol, D-fructose, L-fucose, D-galactose, gentiobiose, α-D-glucose, *myo*-inositol, lactose, lactulose, maltose, D-mannitol, D-mannose, melibiose, methyl β-D-glucoside, D-psicose, raffinose, L-rhamnose, D-sorbitol, sucrose, trehalose, turanose, xylitol, pyruvic acid methyl ester, succinic acid monomethyl ester, acetic acid, *cis*-aconitic acid, citric acid, formic acid, D-galactonic acid lactone, D-galacturonic acid, D-gluconic acid, D-glucosaminic acid, D-glucuronic acid, α-hydroxybutyric acid, β-hydroxybutyric acid, γ-hydroxybutyric acid, *p*-hydroxyphenylacetic acid, itaconic acid, α-ketobutyric acid, α-ketoglutaric acid, α-ketovaleric acid, D,L-lactic acid, malonic acid, propionic acid, quinic acid, D-saccharic acid, sebacic acid, succinic acid, bromosuccinic acid, succinamic acid, glucuronamide, L-alaninamide, D-alanine, L-alanine, L-alanyl-glycine, L-asparagine, L-aspartic acid, glycyl-L-aspartic acid, glycyl-L-glutamic acid, L-histidine, hydroxy-L-proline, L-leucine, L-ornithine, L-phenylalanine, L-proline, L-pyroglutamic acid, D-serine, L-serine, L-threonine, D,L-carnitine, γ-aminobutyric acid, urocanic acid, inosine, thymidine, uridine, phenyethylamine, putrescine, 2-aminoethanol, 2,3-butanediol, glycerol, α-D,L-glycerol phosphate, α-D-glucose 1-phosphate and D-glucose 6-phosphate. Sensitive to ampicillin, carbenicillin, cefixim, cefalotin, ciprofloxacin, chloramphenicol, imipenem, kanamycin, kotrimoxazol, piperacillin, polymyxin B, streptomycin and tetracycline. Resistant

to ceftazidime and gentamicin, and shows intermediate resistance to aztreonam.

Contains summed feature 3 ($C_{16:1}\omega7c/C_{16:1}\omega6c$) and $C_{16:1}\omega5c$ as major cellular fatty acids. The polar lipid profile contains phosphatidylethanolamine and phosphatidylserine as the major compounds. In addition, several unidentified lipids are present including an aminoglycolipid (AGL1), a phospholipid (PL1), a glycolipd (GL1), an aminolipid (AL1) and ten lipids for which no functional group was detected (L1-L10). The quinone system contains predominantly menaquinone MK-7, and the major polyamine is *sym*-homospermidine.

The type strain is CCM 8648^T (=LMG 29440^T=P5086^T). The DNA G+C content of the type strain is 60.5 mol%. Isolated from fragments of volcanic tuff in James Ross Island, Antarctica.

Funding information
Ministry of Education, Youth and Sports of the Czech Republic project LM2015078. S.K. is a holder of Brno PhD Talent financial aid.

Acknowledgements
The authors thank the scientific infrastructure of the J. G. Mendel Czech Antarctic Station as a part of the Czech Polar Research Infrastructure (CzechPolar2) and its crew for their assistance, supported by the Ministry of Education, Youth and Sports of the Czech Republic (LM2015078), as well as the Czech Antarctic Foundation for their support. Dr Daniel Krsek (NRL for Diagnostic Electron Microscopy of Infectious Agents, National Institute of Public Health, Prague, Czech Republic) is acknowledged for transmission electron microscopy, Bernhard Schink (University of Konstanz, Germany) for name correction and Jana Bajerová (Czech Collection of Microorganisms) for excellent technical assistance.

Conflicts of interest
The authors declare that there are no conflicts of interest.

References

1. Chang X, Zheng J, Jiang F, Liu P, Kan W *et al.* *Hymenobacter arcticus* sp. nov., isolated from glacial till. *Int J Syst Evol Microbiol* 2014;64:2113–2118.
2. Dai J, Wang Y, Zhang L, Tang Y, Luo X *et al.* *Hymenobacter tibetensis* sp. nov., a UV-resistant bacterium isolated from Qinghai-Tibet plateau. *Syst Appl Microbiol* 2009;32:543–548.
3. Han L, Wu SJ, Qin CY, Zhu YH, Lu ZQ *et al.* *Hymenobacter qilianensis* sp. nov., isolated from a subsurface sandstone sediment in the permafrost region of Qilian Mountains, China and emended description of the genus *Hymenobacter*. *Antonie van Leeuwenhoek* 2014;105:971–978.
4. Kang JY, Chun J, Choi A, Moon SH, Cho JC *et al.* *Hymenobacter koreensis* sp. nov. and *Hymenobacter saemangeumensis* sp. nov., isolated from estuarine water. *Int J Syst Evol Microbiol* 2013;63:4568–4573.
5. Klassen JL, Foght JM. Characterization of *Hymenobacter* isolates from Victoria Upper Glacier, Antarctica reveals five new species and substantial non-vertical evolution within this genus. *Extremophiles* 2011;15:45–57.
6. Liu L, Zhou EM, Jiao JY, Manikprabhu D, Ming H *et al.* *Hymenobacter latericoloratus* sp. nov. and *Hymenobacter luteus* sp. nov., isolated from freshwater sediment. *Antonie van Leeuwenhoek* 2015;107:165–172.
7. Reddy GS, Garcia-Pichel F. Description of *Hymenobacter arizonensis* sp. nov. from the southwestern arid lands of the United States of America. *Antonie van Leeuwenhoek* 2013;103:321–330.
8. Zhang G, Niu F, Busse HJ, Ma X, Liu W *et al.* *Hymenobacter psychrotolerans* sp. nov., isolated from the Qinghai-Tibet plateau permafrost region. *Int J Syst Evol Microbiol* 2008;58:1215–1220.
9. Zhang DC, Busse HJ, Liu HC, Zhou YG, Schinner F *et al.* *Hymenobacter psychrophilus* sp. nov., a psychrophilic bacterium isolated from soil. *Int J Syst Evol Microbiol* 2011;61:859–863.
10. Hirsch P, Ludwig W, Hethke C, Sittig M, Hoffmann B *et al.* *Hymenobacter roseosalivarius* gen. nov., sp. nov. from continental Antarctic soils and sandstone: bacteria of the *Cytophaga/Flavobacterium/Bacteroides* line of phylogenetic descent. *Syst Appl Microbiol* 1998;21:374–383.
11. Buczolits S, Denner EB, Kämpfer P, Busse HJ. Proposal of *Hymenobacter norwichensis* sp. nov., classification of '*Taxeobacter ocellatus*', '*Taxeobacter gelupurpurascens*' and '*Taxeobacter chitinovorans*' as *Hymenobacter ocellatus* sp. nov., *Hymenobacter gelipurpurascens* sp. nov. and *Hymenobacter chitinivorans* sp. nov., respectively, and emended description of the genus *Hymenobacter* Hirsch *et al.* 1999. *Int J Syst Evol Microbiol* 2006;56:2071–2078.
12. Reddy GS. Phylogenetic analyses of the genus *Hymenobacter* and description of *Siccationidurans* gen. nov., and *Parahymenobacter* gen. nov. *J Phylogenetics Evol Biol* 2013;01:122.
13. Buczolits S, Busse HJ. *Hymenobacter*. 1-11. In: Whitman WB (editor). *Bergey's Manual of Systematics of Archaea and Bacteria*. John Wiley & Sons, Inc; 2015.
14. Parte AC. LPSN—list of prokaryotic names with standing in nomenclature. *Nucleic Acids Res* 2014;42:D613–D616.
15. Klassen JL, Foght JM. Differences in carotenoid composition among *Hymenobacter* and related strains support a tree-like model of carotenoid evolution. *Appl Environ Microbiol* 2008;74:2016–2022.
16. Chung AP, Lopes A, Nobre MF, Morais PV. *Hymenobacter perfusus* sp. nov., *Hymenobacter flocculans* sp. nov. and *Hymenobacter metalli* sp. nov. three new species isolated from an uranium mine waste water treatment system. *Syst Appl Microbiol* 2010;33:436–443.
17. Buczolits S, Denner EB, Vybiral D, Wieser M, Kämpfer P *et al.* Classification of three airborne bacteria and proposal of *Hymenobacter aerophilus* sp. nov. *Int J Syst Evol Microbiol* 2002;52:445–456.
18. Collins MD, Hutson RA, Grant IR, Patterson MF. Phylogenetic characterization of a novel radiation-resistant bacterium from irradiated pork: description of *Hymenobacter actinosclerus* sp. nov. *Int J Syst Evol Microbiol* 2000;50:731–734.
19. Su S, Chen M, Teng C, Jiang S, Zhang C *et al.* *Hymenobacter kanuolensis* sp. nov., a novel radiation-resistant bacterium. *Int J Syst Evol Microbiol* 2014;64:2108–2112.
20. Zhang Q, Liu C, Tang Y, Zhou G, Shen P *et al.* *Hymenobacter xinjiangensis* sp. nov., a radiation-resistant bacterium isolated from the desert of Xinjiang, China. *Int J Syst Evol Microbiol* 2007;57:1752–1756.
21. Edwards U, Rogall T, Blöcker H, Emde M, Böttger EC. Isolation and direct complete nucleotide determination of entire genes. characterization of a gene coding for 16S ribosomal RNA. *Nucleic Acids Res* 1989;17:7843–7853.
22. Yoon SH, Ha SM, Kwon S, Lim J, Kim Y *et al.* Introducing EzBioCloud: a taxonomically united database of 16S rRNA gene sequences and whole-genome assemblies. *Int J Syst Evol Microbiol* 2017;67:1613–1617.
23. Kumar S, Stecher G, Tamura K. MEGA7: molecular evolutionary genetics analysis version 7.0 for bigger datasets. *Mol Biol Evol* 2016;33:1870–1874.
24. Sedláček I, Kwon SW, Švec P, Mašlaňová I, Kýrová K *et al.* *Aquitalea pelogenes* sp. nov., isolated from mineral peloid. *Int J Syst Evol Microbiol* 2016;66:962–967.
25. Meier-Kolthoff JP, Auch AF, Klenk HP, Göker M. Genome sequence-based species delimitation with confidence intervals and improved distance functions. *BMC Bioinformatics* 2013;14:60.

26. **Lee I, Ouk Kim Y, Chun J, Park S-C.** OrthoANI: an improved algorithm and software for calculating average nucleotide identity. *Int J Syst Evol Microbiol* 2016;66:1100–1103.
27. **Wayne LG, Moore WEC, Stackebrandt E, Kandler O, Colwell RR *et al.*** Report of the ad hoc committee on reconciliation of approaches to bacterial systematics. *Int J Syst Evol Microbiol* 1987;37:463–464.
28. **Richter M, Rosselló-Móra R.** Shifting the genomic gold standard for the prokaryotic species definition. *Proc Natl Acad Sci USA* 2009;106:19126–19131.
29. **Carlone GM, Valadez MJ, Pickett MJ.** Methods for distinguishing gram-positive from gram-negative bacteria. *J Clin Microbiol* 1983; 16:1157–1159.
30. **Bernardet JF, Nakagawa Y, Holmes B, Subcommittee on the taxonomy of Flavobacterium and Cytophaga-like bacteria of the International Committee on Systematics of Prokaryotes.** Proposed minimal standards for describing new taxa of the family *Flavobacteriaceae* and emended description of the family. *Int J Syst Evol Microbiol* 2002;52:1049–1070.
31. **Burns J, Fraser PD, Bramley PM.** Identification and quantification of carotenoids, tocopherols and chlorophylls in commonly consumed fruits and vegetables. *Phytochem* 2003;62:939–947.
32. **Hirsch P, Gallikowski CA, Siebert J, Peissl K, Kroppenstedt R *et al.*** *Deinococcus frigens* sp. nov., *Deinococcus saxicola* sp. nov., and *Deinococcus marmoris* sp. nov., low temperature and draught-tolerating, UV-resistant bacteria from continental Antarctica. *Syst Appl Microbiol* 2004;27:636–645.
33. **Da X, Fang C, Deng S, Zhang Y, Chang X *et al.*** *Pedobacter ardleyensis* sp. nov., isolated from soil in Antarctica. *Int J Syst Evol Microbiol* 2015;65:3841–3846.
34. **Hugh R, Leifson E.** The taxonomic significance of fermentative versus oxidative metabolism of carbohydrates by various gram-negative bacteria. *J Bacteriol* 1953;66:24–26.
35. **Christensen WB.** Urea decomposition as a means of differentiating *Proteus* and paracolon cultures from each other and from *Salmonella* and *Shigella* types. *J Bacteriol* 1946;52:461–466.
36. **Brooks K, Sodeman T.** A rapid method for determining decarboxylase and dihydrolase activity. *J Clin Pathol* 1974;27:148–152.
37. **Barrow GL, Feltham RKA.** *Cowan and Steel's Manual for the Identification of Medical Bacteria*, 3 ed. Great Britain: Cambridge University Press; 1993.
38. **Páčová Z, Kocur M.** New medium for detection of esterase and gelatinase activity. *Zb Bakt Hyg* 1984;258:69–73.
39. **Kurup VP, Babcock JB.** Use of casein, tyrosine, and hypoxanthine in the identification of nonfermentative gram-negative bacilli. *Med Microbiol Immunol* 1979;167:71–75.
40. **Owens JJ.** The egg yolk reaction produced by several species of bacteria. *J Appl Bacteriol* 1974;37:137–148.
41. **Lowe GH.** The rapid detection of lactose fermentation in paracolon organisms by the demonstration of beta-D-galactosidase. *J Med Lab Technol* 1962;19:21–25.
42. **Oberhofer TR, Rowen JW.** Acetamide agar for differentiation of nonfermentative bacteria. *Appl Microbiol* 1974;28:720–721.
43. **Ewing WH.** *Enterobacteriaceae. Biochemical Methods for Group Differentation.* Atlanta: Public Health Service Publication no 734 CDC; 1960.
44. **EUCAST-European committee on antimicrobial susceptibility testing.** *EUCAST Clinical Breakpoints - Bacteria*. Version 5.0 http://www.eucast.org. 2015
45. **CLSI.** *Performance Standards for Antimicrobial Susceptibility Testing; Twenty-Fifth Informational Supplement (M100-S25)*, vol. 35; 2015. ISBN 1-56238-989-0.
46. **Sasser M.** *Identification of Bacteria by Gas Chromatography of Cellular Fatty Acids*, MIDI Technical Note 101. Newark, DE: MIDI Inc; 1990.
47. **Altenburger P, Kämpfer P, Makristathis A, Lubitz W, Busse H-J.** Classification of bacteria isolated from a medieval wall painting. *J Biotechnol* 1996;47:39–52.
48. **Stolz A, Busse HJ, Kämpfer P.** *Pseudomonas knackmussii* sp. nov. *Int J Syst Evol Microbiol* 2007;57:572–576.
49. **Tindall BJ.** Lipid composition of *Halobacterium lacusprofundi*. *FEMS Microbiol Lett* 1990a;66:199–202.
50. **Tindall BJ.** A comparative study of the lipid composition *of Halobacterium saccharovorum* from various sources. *Syst Appl Microbiol* 1990b;13:128–130.
51. **Busse HJ, Auling G.** Polyamine pattern as a chemotaxonomic marker within the proteobacteria. *Syst Appl Microbiol* 1988;11:1–8.
52. **Busse HJ, Bunka S, Hensel A, Lubitz W.** Discrimination of members of the family *Pasteurellaceae* based on polyamine patterns. *Int J Syst Bacteriol* 1997;47:698–708.

International Journal of Systematic and Evolutionary Microbiology

Supplementary materials

Red-pink pigmented *Hymenobacter coccineus* sp. nov., *Hymenobacter lapidarius* sp. nov., and *Hymenobacter glacialis* sp. nov. isolated from rocks in Antarctica

Ivo Sedláček*[1], Stanislava Králová[1], Kamila Kýrová[1], Ivana Mašlaňová[2], Hans-Jürgen Busse[3], Eva Staňková[1], Veronika Vrbovská[1,2], Miroslav Němec[4], Miloš Barták[5], Pavla Holochová[1], Pavel Švec[1], and Roman Pantůček[2]

[1]Czech Collection of Microorganisms, Department of Experimental Biology, Faculty of Science, Masaryk University, Kamenice 5, 625 00 Brno, Czech Republic

[2]Section of Genetics and Molecular Biology, Department of Experimental Biology, Faculty of Science, Masaryk University, Kotlářská 2, 611 37 Brno, Czech Republic

[3]Institut für Bakteriology, Mykology und Hygiene, Veterinärmedizinische Universität Wien, Veterinärplatz 1, A-1210 Wien, Austria

[4]Section of Microbiology and Molecular Biotechnology, Department of Experimental Biology, Faculty of Science, Masaryk University, Kamenice 5, 625 00 Brno, Czech Republic

[5]Section of Plant Physiology and Anatomy, Department of Experimental Biology, Faculty of Science, Masaryk University, Kamenice 5, 625 00 Brno, Czech Republic

*Corresponding author:

Ivo Sedláček; E-mail: ivo@sci.muni.cz; Tel.: +420-549496922; Fax: +420-549498289

Table S1. Cellular fatty acid contents (%) of strains CCM 8649^T, CCM 8647, CCM 8643^T and CCM 8648^T, and the closest *Hymenobacter* spp. type strains.

All data were taken from this study using cells grown to the late exponencial phase (72 h) on R2A agar medium at 20 °C with exception of CCM 8583^T and CCM 8582^T which were grown for 96 h. TR, traces (< 1.0%); ND, not detected. CCM, Czech Collection of Microorganisms; KCTC, Korean Collection of Type Cultures.

Fatty acid	CCM 8649^T	CCM 8647	CCM 8643^T	CCM 8648^T	*H. ruber* KCTC 32477^T	*H. terrae* KCTC 32554^T	*H. soli* KCTC 12607^T	*H. arizonensis* CCM 8581^T	*H. antarcticus* CCM 8582^T	*H. glaciei* CCM 8583^T
iso-$C_{14:0}$	TR	TR	TR	1.6	TR	1.5	TR	TR	TR	TR
iso-$C_{15:1}$ G	ND	ND	TR	TR	3.3	1.3	12.6	2.4	2.0	11.0
anteiso-$C_{15:1}$ A	ND	ND	TR	ND	TR	TR	TR	1.0	TR	3.1
iso-$C_{15:0}$	13.8	14.1	5.4	7.4	24.4	16.0	21.7	12.4	13.8	14.9
anteiso-$C_{15:0}$	6.7	7.2	6.2	7.7	7.2	15.5	8.5	12.4	11.7	16.2
$C_{15:1}$ $\omega 6c$	TR	1.0	TR	1.2	ND	TR	TR	TR	TR	ND
iso-$C_{16:1}$ H	ND	2.1	5.2	8.4	TR	2.5	ND	1.7	1.0	TR
iso-$C_{16:0}$	ND	1.0	2.0	2.6	TR	TR	ND	1.4	ND	ND
$C_{16:1}$ $\omega 5c$	20.5	20.3	15.2	16.6	9.4	10.1	8.6	17.6	15.6	9.6
$C_{16:0}$	1.2	1.0	5.4	3.9	3.8	2.3	1.4	1.3	2.7	TR
iso-$C_{15:0}$ 3OH	2.1	1.8	1.7	1.6	2.2	2.0	2.7	1.2	2.2	1.8
iso-$C_{16:0}$ 3OH	TR	TR	2.7	2.6	TR	1.2	TR	1.0	1.6	TR
$C_{16:0}$ 3OH	1.1	TR	TR	TR	1.3	TR	1.6	TR	1.6	TR
iso-$C_{17:0}$	TR	1.8	1.1	2.1	1.5	1.0	TR	1.0	TR	4.3
$C_{17:1}$ $\omega 6c$	TR	1.4	TR	1.6	TR	1.0	TR	TR	TR	TR
iso-$C_{17:0}$ 3OH	TR	TR	1.0	TR	1.9	TR	1.6	TR	TR	1.7
$C_{17:0}$ 2OH	ND	TR	1.6	1.1	TR	1.0	TR	TR	TR	2.0
$C_{18:1}$ $\omega 9c$	ND	ND	1.4	TR	TR	ND	TR	TR	TR	TR
*Summed Feature 1	1.1	TR	TR	1.2	ND	TR	ND	TR	TR	ND
*Summed Feature 2	1.7	ND	ND	ND	TR	ND	TR	ND	TR	TR
*Summed Feature 3	39.0	37.1	34.2	24.6	33.2	33.2	28.8	30.8	35.5	21.4
*Summed Feature 4	8.1	6.2	9.5	10.3	5.1	4.0	6.0	9.6	6.7	6.5

*As indicated by Montero-Calasanz *et al.* (*Int J Syst Evol Microbiol* 2013; 63:4386-4395) summed features are groups of two or three fatty acids that are treated together for the purpose of evaluation in the MIDI system and include both peaks with discrete ECLs as well as those where the ECLs are not reported separately. Summed feature 1 was listed as iso-$C_{15:0}$ H/ $C_{13:0}$ 3OH, Summed Feature 2 was listed as $C_{14:0}$ 3OH/ iso-$C_{16:1}$ I, Summed Feature 3 was listed as $C_{16:1}$ $\omega 7c$ /$C_{16:1}$ $\omega 6c$ Summed feature 4 was listed as anteiso-$C_{17:1}$ B/iso I

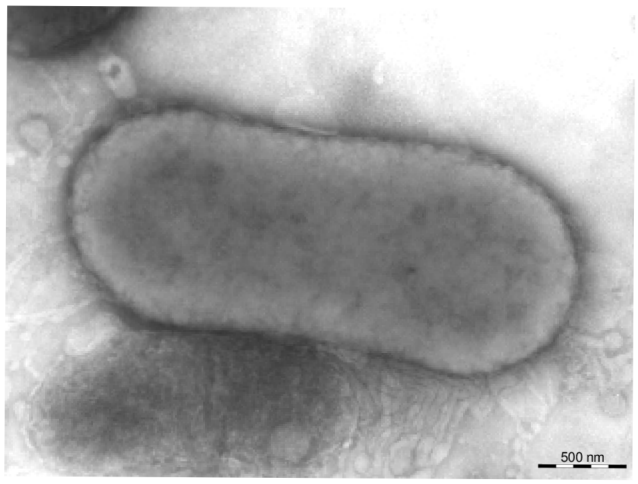

Hymenobacter coccineus CCM 8649^{T}

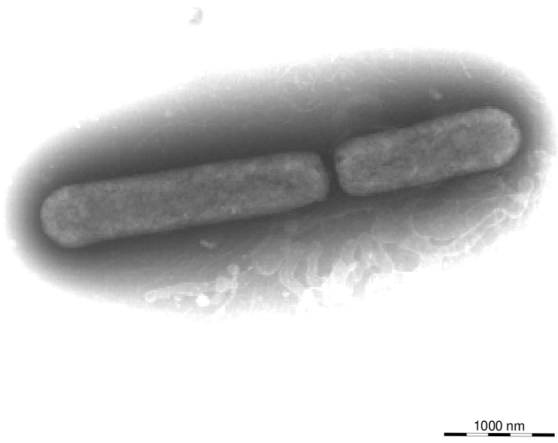

Hymenobacter lapidarius CCM 8643^{T}

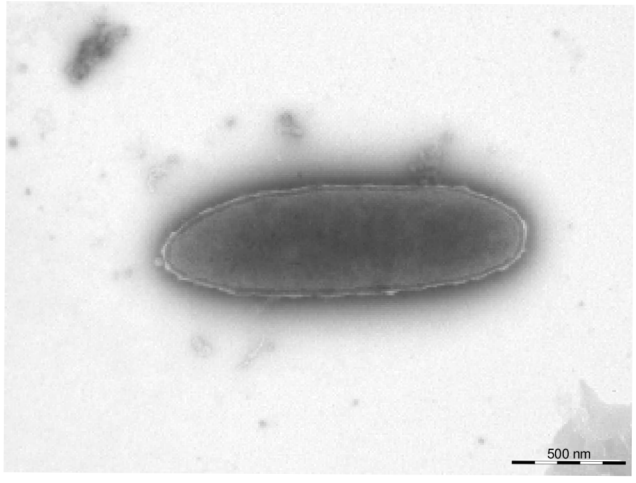

Hymenobacter glacialis CCM 8648^{T}

Fig. S1. Transmission electron microscopy of *Hymenobacter coccineus* CCM 8649^{T}, *Hymenobacter lapidarius* CCM 8643^{T} and *Hymenobacter glacialis* CCM 8648^{T} performed with a Morgagni 268D Philips (FEI Company, USA) electron microscope. Negative staining with 2% ammonium molybdate. Original magnification ×10 000.

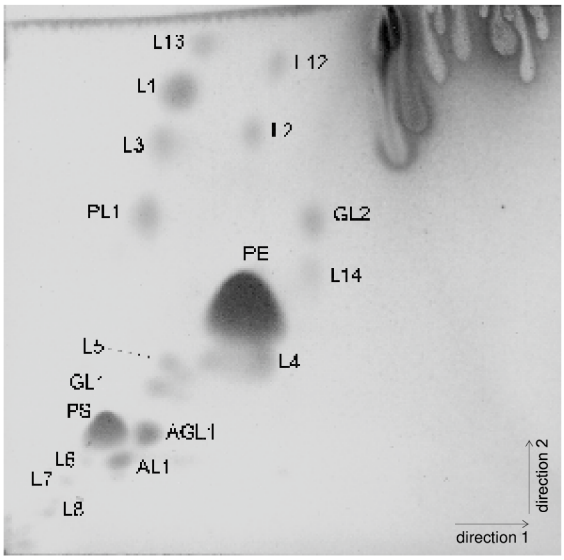

Hymenobacter lapidarius CCM 8643^{T}

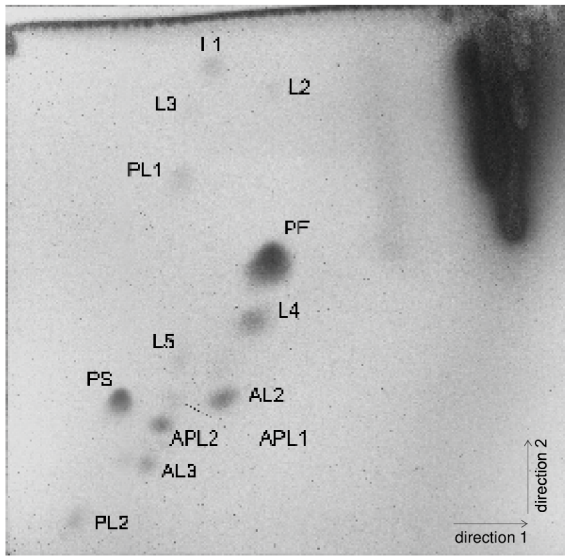

Hymenobacter coccineus CCM 8647

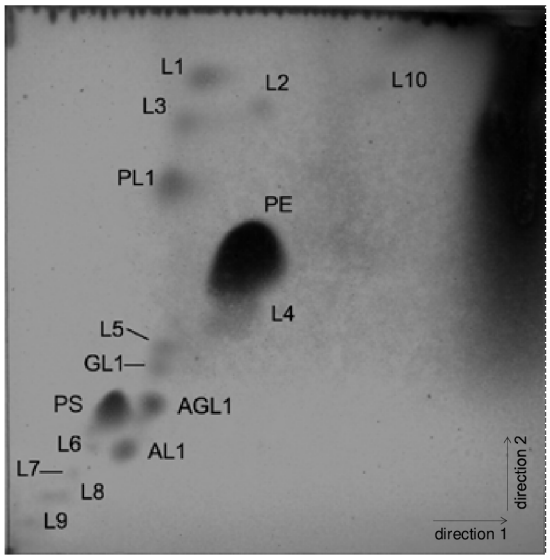

Hymenobacter glacialis CCM 8648^{T}

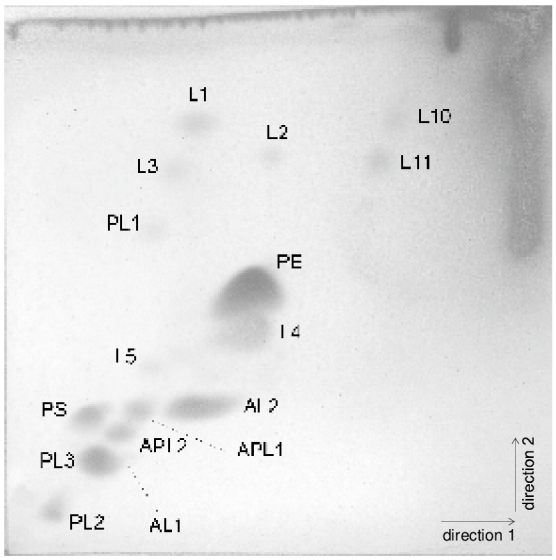

Hymenobacter coccineus CCM 8649^{T}

Fig. S2. Two dimensional TLC showing the total polar lipids of strains *Hymenobacter lapidarius* CCM 8643^{T}, *Hymenobacter coccineus* CCM 8649^{T} and CCM 8647 and *Hymenobacter glacialis* CCM 8648^{T}. Abbreviations: L1-L14, unidentified polar lipids; AL1-AL3, unidentified aminolipids; GL1 and GL2, unidentified glycolipids; AGL1, unidentified aminoglycolipid; APL1 and APL2, unidentified aminophospholipid; PL1-PL3, unidentified phospholipids; PS, phosphatidylserine; PE, phosphatidylethanolamine.

Príloha č. 5.

Sedláček I., Pantůček R., Králová S., Mašlaňová I., Holochová P., Staňková E., Sobotka R., Barták M., Busse H.-J., Švec P. (2017, v tlači) *Mucilaginibacter terrae* sp. nov., isolated from Antarctic soil. *Int. J. Syst. Evol. Microbiol*. 67: 1-6. Doi:10.1099/ijsem.0.002240.

INTERNATIONAL JOURNAL OF **SYSTEMATIC AND EVOLUTIONARY MICROBIOLOGY**

TAXONOMIC DESCRIPTION
Sedláček *et al.*, *Int J Syst Evol Microbiol* 2017;67:1–6
DOI 10.1099/ijsem.0.002240

MICROBIOLOGY SOCIETY

Mucilaginibacter terrae sp. nov., isolated from Antarctic soil

Ivo Sedláček,[1] Roman Pantůček,[2] Stanislava Králová,[1] Ivana Mašlaňová,[2] Pavla Holochová,[1] Eva Staňková,[1] Roman Sobotka,[3] Miloš Barták,[4] Hans-Jürgen Busse[5] and Pavel Švec[1,*]

Abstract

A bacterial strain designated CCM 8645^T was isolated from a soil sample collected nearby a mummified seal carcass in the northern part of James Ross Island, Antarctica. The cells were short rods, Gram-stain-negative, non-motile, catalase and oxidase positive, and produced a red-pink pigment on R2A agar. A polyphasic taxonomic approach based on 16S rRNA gene sequencing, extensive biotyping using conventional tests and commercial identification kits and chemotaxonomic analyses were applied to clarify its taxonomic position. Phylogenetic analysis based on the 16S rRNA gene placed strain CCM 8645^T in the genus *Mucilaginibacter* with the closest relative being *Mucilaginibacter daejeonensis* Jip 10^T, exhibiting 96.5 % 16S rRNA pairwise similarity which was clearly below the 97 % threshold value recommended for species demarcation. The major components in fatty acid profiles were Summed feature 3 ($C_{16:1}\omega7c$/$C_{16:1}\omega6c$), $C_{15:0}$ iso and $C_{17:0}$ iso 3OH. The cellular quinone content was exclusively menaquinone MK-7. The major polyamine was *sym*-homospermidine and predominant polar lipids were phosphatidylethanolamine and phosphatidylserine. Based on presented results, we propose a novel species for which the name *Mucilaginibacter terrae*sp. nov. is suggested, with the type strain CCM 8645^T (=LMG 29437^T).

The genus *Mucilaginibacter* is a member of the family *Sphingobacteriaceae* [1, 2] within the phylum *Bacteroidetes*. The genus *Mucilaginibacter* was proposed by Pankratov *et al.* [2] and subsequently the genus description was emended by Urai *et al.* [3], Baik *et al.* [4], and Chen *et al.* [5]. In recent years numerous novel *Mucilaginibacter* spp. have been discovered worldwide among environmental bacteria and described as novel species [5–13]. Members of the genus *Mucilaginibacter* are known to hydrolyse organic matter such as xylan, pectin and laminarin, and produce large amounts of extracellular polymeric substances [2, 14, 15]. Representatives of *Mucilaginibacter* spp. have been isolated from various habitats of environment, e.g. from rhizosphere of plants [14–16], fresh water [4, 6, 10], soil [8, 17, 18], marine sand [19] or moss [5]. The majority of mucilaginibacters are psychrotolerant organisms revealing good growth at 4 °C. However, they have not been reported to be found in polar regions, except for *Mucilaginibacter soli* isolated from Arctic tundra soil [17]. In the present taxonomic study we report classification of strain CCM 8645^T representing a novel species of the genus *Mucilaginibacter*.

Strain CCM 8645^T was isolated from a soil sample collected nearby a mummified seal carcass on James Ross Island, Antarctica (63°49′52″ S, 57°49′55″ W) in 2012. The seal carcass was located at the bottom of V-shaped valley well supplied by thawing water [20]. Thanks to local microclimate and availability of nutrients, a small-in-area vegetation spot (about 16 m^2) rich in terrestrial algae, lichens and mosses had developed in the neighbourhood of the carcass. Sampling was carried out by dispersing 1 g of soil sample in 5 ml of sterile saline solution and 100 µl of the suspension was spread on R2A agar (Oxoid) plate and cultivated at 15 °C for 4 days. Afterwards, individual red-pink pigmented colonies were purified by repeated streaking on R2A plates and incubation at 15 °C, and the final pure strain CCM 8645^T was stored in R2A broth supplemented with 15 % glycerol (v/v) and maintained at −70 °C until analysed.

Extraction of DNA for molecular analyses by FastPrep Lysing Matrix type B and FastPrep Homogenizer (MP Biomedicals), 16S rRNA gene amplification by PCR and partial 16S rRNA gene sequencing (1472 bp) was performed as described previously [21]. The 16S rRNA gene sequences

Author affiliations: [1]Czech Collection of Microorganisms, Department of Experimental Biology, Faculty of Science, Masaryk University, Kamenice 5, 625 00 Brno, Czech Republic; [2]Section of Genetics and Molecular Biology, Department of Experimental Biology, Faculty of Science, Masaryk University, Kotlářská 2, 611 37 Brno, Czech Republic; [3]Centre Algatech, Institute of Microbiology, Academy of Sciences, Novohradská 237, 379 81 Třeboň, Czech Republic; [4]Section of Plant Physiology, Department of Experimental Biology, Faculty of Science, Masaryk University, Kamenice 5, 625 00 Brno, Czech Republic; [5]Institut für Mikrobiologie, Veterinärmedizinische Universität Wien, Veterinärplatz 1, A-1210 Wien, Austria.
***Correspondence:** Pavel Švec, mpavel@sci.muni.cz
Keywords: *Mucilaginibacter terrae* sp. nov.; James ross island; Antarctica; soil; taxonomy.
The GenBank/EMBL/DDBJ accession number for the 16S rRNA gene sequence of *Mucilaginibacter terrae* CCM 8645^T is KY171988.
Four supplementary figures are available with the online Supplementary Material.

with the highest scores were identified by the calculation of pairwise sequence similarity with strain CCM 8645^T using a global alignment algorithm, which was implemented at the EzBioCloud (http://www.ezbiocloud.net/; [22]). Resulting 16S rRNA gene sequence similarities demonstrated that strain CCM 8645^T is a member of the genus *Mucilaginibacter* and identified *Mucilaginibacter daejeonensis* Jip 10^T as its closest relative (96.5 %). Other *Mucilaginibacter* species did not show higher sequence similarities than 95.5 %. Since the nearest neighbours exhibited similarity scores of <97 %, strain CCM 8645^T was considered a candidate for a new species. Phylogenetic analysis was performed using MEGA version 6 software [23]. Genetic distances were calculated using Tamura and Nei [24] model and the evolutionary history was inferred using the maximum-likelihood and neighbor-joining methods. Maximum-likelihood analysis (Fig. 1) matched the tree topology obtained by the neighbor-joining clustering (Fig. S1, available in the online Supplementary Material) except the position of *Mucilaginibacter koreensis* which was placed in different clusters. Phylogenetically, strain CCM 8645^T formed a common branch with *M. daejeonensis* which is in accordance with the highest value of 16S rRNA gene sequence similarity.

The cell morphology of strain CCM 8645^T was observed by Gram-staining and by transmission electron microscopy (Morgagni 268D Philips, FEI Company) using a sample stained with 2 % ammonium molybdate (Fig. S2). The presence of flexirubin-type pigments was investigated using a 20 % (w/v) KOH solution [25]. Spectrophotometric characterization of carotenoid pigments was done from the cells grown on R2A agar for 72 h at 20 °C [21]. The basic phenotypic classification was performed using key tests relevant for Gram-negative rods. Catalase (ID colour Catalase, bioMérieux) and oxidase (OXItest, Erba-Lachema) activity was tested according to manufacturers' instructions. Further tests were done as follows: oxidation-fermentation (OF) test [26], arginine dihydrolase, ornithine and lysine decarboxylase [27], urease [28], hydrolysis of aesculin, starch [29], gelatin, Tween 80 [30], casein, tyrosine [31], and DNA (CM321, Oxoid), egg-yolk reaction [32], ONPG [33], nitrate and nitrite reduction, growth on Simmon's citrate agar [29], utilization of acetamide [34] and sodium malonate [35]. Motility was observed in a glucose oxidation tube. Cells grown at 20 °C for 48–72 h on R2A agar were used to inoculate all tests during all experiments. Liquid culture was not used because of the poor growth of the isolate CCM 8645^T in broth media. Growth on several media such as Plate

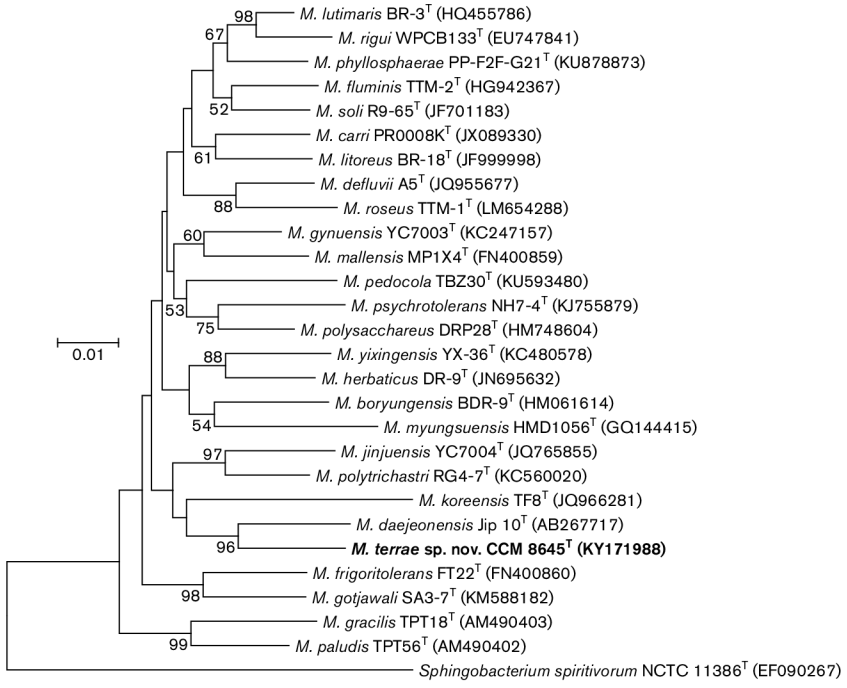

Fig. 1. Phylogenetic tree based on 16S rRNA gene sequence comparison showing the position of strain CCM 8645^T within the genus *Mucilaginibacter*. The evolutionary history was inferred by using the Maximum Likelihood method based on the Tamura-Nei model. The tree with the highest log likelihood is shown. Bootstrap probability values (percentages of 500 tree replications) greater than 50 % are indicated at branch points. There were a total of 1465 positions in the final dataset. Bar indicates number of substitutions per nucleotide position. *Sphingobacterium spiritivorum* was used as an outgroup.

count agar (Oxoid), Tryptone soya agar (Oxoid), Nutrient agar CM03 (Oxoid), MacConkey agar (Becton Dickinson) and Brain heart infusion agar (Oxoid) at 20 °C was evaluated. Anaerobic growth on R2A agar was tested using the Anaerocult A system (Merck) at 20 °C for 72 h and compared with those cultivated in the ambient atmosphere. Growth at different temperatures (1, 5, 10, 15, 20, 25, 30 and 35 °C) and tolerance to various NaCl concentrations (0.5, 1, 2, 3, 4 and 5 % w/v) were determined based on cultivation on R2A agar plates for up to 4 days. The pH range for growth was tested on R2A agar plates adjusted to pH 5.0–10.0 by using the buffer system (pH 5.0–8.0, 0.1M KH_2PO_4/0.1M NaOH; pH 9.0–10.0, 0.1M $NaHCO_3$/0.1M Na_2CO_3; at interval of 1 pH unit) for one week at 20 °C [36]. Further extended phenotyping using identification test kits API ZYM (bioMérieux) and GN2 MicroPlate (Biolog) was performed according to the manufacturers' instructions and enabled detailed characterization of the isolate. Inoculated kits were incubated at 20 °C, and the results were read after 18 h (API ZYM) or 24 and 48 h (GN2 MicroPlate). Antibiotic resistance pattern was assessed by the disc diffusion method on R2A agar for 2 days at 20 °C. Sixteen antibiotic discs generally used for Gram-negative rods [37, 38] were chosen: ampicillin (10 µg), aztreonam (30 µg), carbenicillin (100 µg), cefixim (5 µg), ceftazidime (10 µg), cephalothin (30 µg), ciprofloxacin (5 µg), gentamicin (10 µg), chloramphenicol (30 µg), imipenem (10 µg), kanamycin (30 µg), co-trimoxazole (25 µg), piperacillin (30 µg), polymyxin B (300 U), streptomycin (10 µg) and tetracycline (30 µg). EUCAST/CLSI standards were strictly followed for cultivation and inhibition zone diameter reading.

Strain CCM 8645^T represented psychrotolerant (growing in the temperature range 5–25 °C), Gram-stain-negative, aerobic, catalase and oxidase positive non-fermenting short rods and formed slimy colonies with a pink-red colour. The extracted pigments were separated by HPLC, which revealed at least five different compounds with absorbance properties typical for carotenoids (Fig. S3). The red-shifted spectrum of the most abundant pigment in CCM 8645^T resembled major carotenoid species of the recently described *Rufibacter ruber* CCM 8646^T strain [21] with maxima at 482 and 506 nm and a shoulder at 450 nm. Nonetheless, HPLC mobility and absorbance spectra of these pigments were slightly shifted, which suggests that these carotenoids are similar but not identical (Fig. S3). Strain CCM 8645^T was susceptible to ciprofloxacin, imipenem, co-trimoxazole, streptomycin and tetracycline, resistant to ampicillin, aztreonam, carbenicillin, cefixim, ceftazidime, gentamicin, chloramphenicol, kanamycin, piperacillin and polymyxin B and intermediate result was revealed for cephalothin.

Comprehensive morphological, biochemical and physiological traits of strain CCM 8645^T are summarized in the species description given below. The tests distinguishing strain CCM 8645^T from the phylogenetically closest *Mucilaginibacter* spp. are shown in Table 1.

Fatty acids methyl ester (FAME) analysis was performed using cells grown on R2A agar (Difco) incubated at 20±1 °C for 72 h, where the bacterial communities reached the late-exponential stage of growth according to the four quadrants steak method [39]. The extraction of fatty acids methyl esters was performed according to a standard protocol of Sherlock Microbial Identification System [39]. Cellular fatty acid extract was analysed by GC (model 7890B, Agilent) by using the rapid Sherlock Identification system (MIS, version 6.2B, MIDI database: RTSBA6, MIDI Inc.). The predominant fatty acids of CCM 8645^T were Summed feature 3 ($C_{16:1}\omega7c$/$C_{16:1}\omega6c$) (37.0 %), $C_{15:0}$ iso (22.6 %) and $C_{17:0}$ iso 3OH (13.4 %). Cellular contents of remaining fatty acids detected in strain CCM 8645^T were as follows: $C_{16:1}\omega5c$, Summed Feature 9 ($C_{17:1}$ 10-methyl/iso $\omega9c$), $C_{15:0}$ iso 3OH, $C_{18:1}\omega9c$, Summed Feature 4 ($C_{17:1}$ anteiso B/iso I), $C_{17:0}$ iso, and $C_{16:0}$. The FAME profile of CCM 8645^T was similar to profiles of other *Mucilaginibacter* species [2, 4].

Quinones and polar lipids were extracted from freeze-dried biomass grown on R2A medium and analysed as described previously [40–43]. The major respiratory quinone was menaquinone MK-7, which is in agreement with the description of the genus *Mucilaginibacter* [44]. The predominant polar lipids were phosphatidylethanolamine, phosphatidylserine and an unidentified lipid (L4) lacking a detectable functional group. Strain CCM 8645^T also contained moderate to minor amounts of nine unidentified lipids L1, L2, L3, L5, L6, L7, L8, L9 and L10 lacking a functional group, four unidentified aminolipids AL1, AL2, AL3, and AL4, unidentified phospholipid PL1 and unidentified glycolipid GL1 (Fig. S4). These chemotaxonomic data were in agreement with the emended description of the genus *Mucilaginibacter* [5]. The presence of sphingolipids in strain CCM 8645^T was investigated by applying the method of Kato *et al.* [44]. After mild alkaline hydrolysis, one-dimensional thin layer chromatography and detection with ninhydrin one positive lipid spot was detected which was negative after detection with molybdenum blue. These results demonstrate that this alkaline-stable lipid is not a sphingophospholipid as known to be present in members of the genus *Sphingobacterium*. However, this observation is in agreement with findings in *Mucilaginibacter litoreus*, *Mucilaginibacter sabulilitorius* and *Mucilaginibacter gallii* [19, 45, 46]. The biomass subjected to polyamine analysis was grown on R2A agar, scrapped off the surface, freeze dried and then extracted according to Busse and Auling [47] and analysed by HPLC as reported by Busse *et al.* [48]. The HPLC equipment applied was described by Stolz *et al.* [41]. Strain CCM 8645^T contained *sym*-homospermidine [26.5 µmol (g dry weight)$^{-1}$] as the main polyamine. Moreover, spermine [0.4 µmol (g dry weight)$^{-1}$], spermidine [1.7 µmol (g dry weight)$^{-1}$] and putrescine [0.1 µmol (g dry weight)$^{-1}$] were present in smaller amounts. Similar polyamine patterns with the major compound *sym*-homospermidine have also been detected in *Mucilaginibacter phyllosphaerae*, *Mucilaginibacter auburnensis* and *M. gallii* [7, 46].

Table 1. Phenotypic characteristics that differentiate *Mucilaginibacter terrae* sp. nov. from closely related *Mucilaginibacter* spp.

Strains: 1, *M. terrae* sp. nov. CCM 8645^T; 2, *M. daejeonensis* Jip 10^T; 3, *M. boryungensis* BDR-9^T; 4, *M. lutimaris* BR-3^T; 5, *M. jinjuensis* YC7004^T; 6, *M. polytrichastri* RG4-7^T. +, positive; w, weakly positive; −, negative; data for reference type strains were obtained from An *et al.* [49]; Kang *et al.* [18]; Kim *et al.* [50]; Khan *et al.* [51] and Chen *et al.* [5].

Characteristics	1	2	3	4	5	6
Pigment	Red-pink	Orange	Light yellow	Light pink	Pale orange	Orange
Growth at 5 °C	+	−	+	+	+	+
Growth at 30 °C	−	+	+	+	+	+
Growth in>1 % NaCl	−	+	−	−	−	+
α−galactosidase	−	+	+	+	w	+
Cystine arylamidase	−	+	−	−	−	−
Esterase (C4)	+	+	−	−	−	+
N-acetyl-βglucosaminidase	−	+	+	+	+	+
α−mannosidase	−	−	−	+	−	−

All phenotypic, genotypic and chemotaxonomic results obtained in the present taxonomic study demonstrated that strain CCM 8645^T isolated from soil in Antarctica represents a novel *Mucilaginibacter* species, for which the name *Mucilaginibacter terrae* sp. nov. is proposed.

DESCRIPTION OF *MUCILAGINIBACTER TERRAE* SP. NOV. (TER′RAE. L. GEN. N. *TERRAE*, OF SOIL)

Cells are Gram-stain-negative short rod-shaped to coccoid cells, occurring predominantly in pairs or in irregular clusters and non-spore forming. Red-pink pigmented colonies on R2A agar are circular, with whole margins, slightly mucous, smooth, glistening, and 2 mm in diameter. Aerobic, non-haemolytic on sheep blood agar. Grows on Plate count agar, but not on Tryptone soya agar, Brain heart infusion agar, MacConkey agar and CM03 agar. No anaerobic growth on R2A agar. Grows in the range from 5 to 25 °C but not at 1 or 30 °C. Grows in the presence of up to 1 % NaCl and at pH range from 5 to 8. No fluorescein pigment on King B medium. Hugh and Leifson of fermentation test negative. Catalase, oxidase (weak), DNase (weak), esterase (C 4), esterase lipase (C 8) (weak), leucine arylamidase, valine arylamidase, naphthol-AS-Bi-phosphohydrolase, β-galactosidase, α-glucosidase (weak), alkaline and acid phosphatase positive. Aesculin, ONPG, casein (weak) and starch hydrolysis positive. Negative Simmons citrate, sodium malonate, acetamide and hydrolysis of Tween 80, gelatine, tyrosine and lecithin (egg-yolk reaction). Urease, arginine dihydrolase, lysine decarboxylase, ornithine decarboxylase, lipase (C 14), cystine arylamidase, trypsin, chymotrypsin, α-galactosidase, β-glucuronidase, β-glucosidase, *N*-acetyl-βglucosaminidase, α-mannosidase, α-fucosidase, nitrate reduction and nitrite reduction negative. Acid is produced from glucose, fructose, xylose and maltose. Acid is not produced from mannitol.

Strain CCM 8645^T has the ability to use the following carbon sources via respiration: α-cyclodextrin, dextrin, Tween 40, cellobiose, D-galactose, α-D-glucose, α-lactose, lactulose, maltose, D-mannose, trehalose, D-glucuronic acid and L-glutamic acid. Negative utilization tests were revealed for glycogen, Tween 80, *N*-acetyl-D-galactosamine, *N*-acetyl-D-glucosamine, adonitol, L-arabinose D-arabitol, erythritol, m-inositol, D-mannitol, melibiose, β-methyl-D-glucoside, D-psicose, raffinose, L-rhamnose, D-sorbitol, sucrose, succinic acid monomethyl ester, acetic acid, cis-aconitic acid, citric acid, formic acid, D-galactonic acid lactone, D-gluconic acid, D-glucosaminic acid, α-hydroxybutyric acid, β-hydroxybutyric acid, γ-hydroxybutyric acid, p-hydroxy phenyl acetic acid, itaconic acid, α-keto butyric acid, α-keto glutaric acid, α-keto valeric acid, D,L-lactic acid, malonic acid, propionic acid, quinic acid, D-saccharic acid, sebacic acid, succinic acid, bromosuccinic acid, succinamic acid, glucuronamide, L-alaninamide, D-alanine, L-alanine, L-alanyl-glycine, L-asparagine, L-aspartic acid, glycyl-L-aspartic acid, L-histidine, hydroxy-L-proline, L-leucine, L-ornithine, L-phenylalanine, L-pyroglutamic acid, D-serine, D,L-carnitine, γ-aminobutyric acid, urocanic acid, inosine, uridine, thymidine, phenyl ethylamine, putrescine, 2-aminoethanol, 2,3-butanediol, glycerol, D,L-α-glycerol phosphate, α-D-glucose-1-phosphate and D-glucose-6-phosphate. The borderline results were obtained for utilization of D-fructose, L-fucose, gentiobiose, turanose, xylitol, pyruvic acid methyl ester, D-galacturonic acid, glycyl-L-glutamic acid, L-proline, L-serine and L-threonine.

The quinone system cosists exclusively of menaquinone MK-7 and the major compound in the polyamine pattern is *sym*-homospermidine. In the polar lipid profile phosphatidylethanolamine, phosphatidylserine and an unidentified lipid (L4) are predominant. In addition moderate to minor amounts of nine unidentified lipids (L1, L2, L3, L5, L6, L7, L8, L9, L10) lacking a functional group, four unidentified aminolipids (AL1, AL2, AL3, AL4), unidentified phospholipid PL1 and unidentified glycolipid GL1 are present. One alkali-stable aminolipid is present. The fatty acid profile contains as major components Summed feature 3 ($C_{16:1}\omega7c$/$C_{16:1}\omega6c$), $C_{15:0}$ iso and $C_{17:0}$ iso 3OH.

The type strain CCM 8645^T (=LMG 29437^T) was isolated on James Ross Island, Antarctica, from a soil sample collected nearby a mummified seal carcass.

Funding information
Ministry of Education, Youth and Sports of the Czech Republic projects LM2015078 and LO1416.

Acknowledgements
The authors thank to the scientific infrastructure of the J. G. Mendel Czech Antarctic Station as a part of the Czech Polar Research Infrastructure (CzechPolar2) and its crew for their assistance, supported by Ministry of Education, Youth and Sports of the Czech Republic (LM2015078) and the Czech Antarctic Foundation for their support. S. K. is a holder of Brno Ph.D. Talent financial aid. R. S. was supported by the National Programme of Sustainability I (LO1416). Dr Daniel Krsek (National Reference Laboratory for Diagnostic Electron Microscopy of Infectious Agents, National Institute of Public Health, Prague, Czech Republic) is acknowledged for transmission electron microscopy, Jana Bajerová for an excellent technical assistance and Bernhard Schink for the name correction.

Conflicts of interest
The authors declare that there are no confilcts of interest.

References

1. **Lambiase A.** The family *Sphingobacteriaceae*. In: Rosenberg E, DeLong EF, Lory S, Stackebrandt E, Thompson F *et al.* (editors). *The Prokaryotes*, 4 ed. Heidelberg, Germany: Springer; 2014. pp. 907–9014.
2. **Pankratov TA, Tindall BJ, Liesack W, Dedysh SN.** *Mucilaginibacter paludis* gen. nov., sp. nov. and *Mucilaginibacter gracilis* sp. nov., pectin-, xylan- and laminarin-degrading members of the family *Sphingobacteriaceae* from acidic *Sphagnum* peat bog. *Int J Syst Evol Microbiol* 2007;57:2349–2354.
3. **Urai M, Aizawa T, Nakagawa Y, Nakajima M, Sunairi M.** *Mucilaginibacter kameinonensis* sp., nov., isolated from garden soil. *Int J Syst Evol Microbiol* 2008;58:2046–2050.
4. **Baik KS, Park SC, Kim EM, Lim CH, Seong CN.** *Mucilaginibacter rigui* sp. nov., isolated from wetland freshwater, and emended description of the genus *Mucilaginibacter*. *Int J Syst Evol Microbiol* 2010;60:134–139.
5. **Chen XY, Zhao R, Tian Y, Kong BH, Li XD *et al.*** *Mucilaginibacter polytrichastri* sp. nov., isolated from a moss (*Polytrichastrum formosum*), and emended description of the genus *Mucilaginibacter*. *Int J Syst Evol Microbiol* 2014;64:1395–1400.
6. **Joung Y, Kang H, Lee BI, Kim H, Joh K *et al.*** *Mucilaginibacter aquaedulcis* sp. nov., isolated from fresh water. *Int J Syst Evol Microbiol* 2015;65:698–703.
7. **Kämpfer P, Busse HJ, Mcinroy JA, Glaeser SP.** *Mucilaginibacter auburnensis* sp. nov., isolated from a plant stem. *Int J Syst Evol Microbiol* 2014;64:1736–1742.
8. **Lee KC, Kim KK, Eom MK, Kim JS, Kim DS *et al.*** *Mucilaginibacter gotjawali* sp. nov., isolated from soil of a lava forest. *Int J Syst Evol Microbiol* 2015;65:952–958.
9. **Hwang YM, Baik KS, Seong CN.** *Mucilaginibacter defluvii* sp. nov., isolated from a dye wastewater treatment facility. *Int J Syst Evol Microbiol* 2014;64:565–571.
10. **Joung Y, Kim H, Kang H, Lee BI, Ahn TS *et al.*** *Mucilaginibacter soyangensis* sp. nov., isolated from a lake. *Int J Syst Evol Microbiol* 2014;64:413–419.
11. **Joung Y, Kim H, Lee BI, Kang H, Kim TS *et al.*** *Mucilaginibacter flavus* sp. nov., isolated from wetland. *Int J Syst Evol Microbiol* 2014;64:1304–1309.
12. **Park CS, Han K, Ahn TY.** *Mucilaginibacter koreensis* sp. nov., isolated from leaf mould. *Int J Syst Evol Microbiol* 2014;64:2274–2279.
13. **Paiva G, Abreu P, Proença DN, Santos S, Nobre MF *et al.*** *Mucilaginibacter pineti* sp. nov., isolated from *Pinus pinaster* wood from a mixed grove of pines trees. *Int J Syst Evol Microbiol* 2014;64:2223–2228.
14. **Han SI, Lee HJ, Lee HR, Kim KK, Whang KS.** *Mucilaginibacter polysaccharеus* sp. nov., an exopolysaccharide-producing bacterial species isolated from the rhizoplane of the herb *Angelica sinensis*. *Int J Syst Evol Microbiol* 2012;62:632–637.
15. **Madhaiyan M, Poonguzhali S, Lee JS, Senthilkumar M, Lee KC *et al.*** *Mucilaginibacter gossypii* sp. nov. and *Mucilaginibacter gossypiicola* sp. nov., plant-growth-promoting bacteria isolated from cotton rhizosphere soils. *Int J Syst Evol Microbiol* 2010;60:2451–2457.
16. **Kim BC, Poo H, Lee KH, Kim MN, Kwon OY *et al.*** *Mucilaginibacter angelicae* sp. nov., isolated from the rhizosphere of *Angelica polymorpha* Maxim. *Int J Syst Evol Microbiol* 2012;62:55–60.
17. **Jiang F, Dai J, Wang Y, Xue X, Xu M *et al.*** *Mucilaginibacter soli* sp. nov., isolated from Arctic tundra soil. *Int J Syst Evol Microbiol* 2012;62:1630–1635.
18. **Kang SJ, Jung YT, Oh KH, Oh TK, Yoon JH.** *Mucilaginibacter boryungensis* sp. nov., isolated from soil. *Int J Syst Evol Microbiol* 2011;61:1549–1553.
19. **Yoon JH, Kang SJ, Park S, Oh TK.** *Mucilaginibacter litoreus* sp. nov., isolated from marine sand. *Int J Syst Evol Microbiol* 2012;62:2822–2827.
20. **Nývlt D, Fišáková MN, Barták M, Stachoň Z, Pavel V *et al.*** Death age, seasonality, taphonomy and colonization of seal carcasses from Ulu Peninsula, James ross island, Antarctic Peninsula. *Antarct Sci* 2016;28:3–16.
21. **Kýrová K, Sedláček I, Pantůček R, Králová S, Holochová P *et al.*** *Rufibacter ruber* sp. nov., isolated from fragmentary rock. *Int J Syst Evol Microbiol* 2016;66:4401–4405.
22. **Jeon YS, Lee K, Park SC, Kim BS, Cho YJ *et al.*** EzEditor: a versatile sequence alignment editor for both rRNA- and protein-coding genes. *Int J Syst Evol Microbiol* 2014;64:689–691.
23. **Tamura K, Stecher G, Peterson D, Filipski A, Kumar S.** MEGA6: molecular evolutionary genetics analysis version 6.0. *Mol Biol Evol* 2013;30:2725–2729.
24. **Tamura K, Nei M.** Estimation of the number of nucleotide substitutions in the control region of mitochondrial DNA in humans and chimpanzees. *Mol Biol Evol* 1993;10:512–526.
25. **Bernardet JF, Nakagawa Y, Holmes B.** Proposed minimal standards for describing new taxa of the family *Flavobacteriaceae* and emended description of the family. *Int J Syst Evol Microbiol* 2002;52:1049–1070.
26. **Hugh R, Leifson E.** The taxonomic significance of fermentative versus oxidative metabolism of carbohydrates by various gram negative bacteria. *J Bacteriol* 1953;66:24–26.
27. **Brooks K, Sodeman T.** A rapid method for determining decarboxylase and dihydrolase activity. *J Clin Pathol* 1974;27:148–152.
28. **Christensen WB.** Urea decomposition as a Means of Differentiating *Proteus* and paracolon cultures from each other and from *Salmonella* and *Shigella* types. *J Bacteriol* 1946;52:461–466.
29. **Barrow GL, Cowan F.** *Steel's Manual for the Identification of Medical Bacteria*, 3rd ed. Great Britain: Cambridge University Press; 1993.
30. **Pácová Z, Kocur M.** New medium for detection of esterase and gelatinase activity. *Zentralbl Bakteriol Mikrobiol Hyg A* 1984;258:69–73.
31. **Kurup VP, Babcock JB.** Use of casein, tyrosine, and hypoxanthine in the identification of nonfermentative gram-negative bacilli. *Med Microbiol Immunol* 1979;167:71–75.
32. **Owens JJ.** The egg yolk reaction produced by several species of bacteria. *J Appl Bacteriol* 1974;37:137–148.
33. **Lowe GH.** The rapid detection of lactose fermentation in paracolon organisms by the demonstration of β-D-galactosidase. *J Med Lab Technol* 1962;19:21–25.

34. **Oberhofer TR, Rowen JW.** Acetamide Agar for differentiation of nonfermentative bacteria. *Appl Microbiol* 1974;28:720–721.
35. **Ewing WH.** *Enterobacteriaceae. Biochemical Methods for Group Differentation*. Atlanta: Public Health Service Publication No 734 CDC; 1960.
36. **Da X, Fang C, Deng S, Zhang Y, Chang X *et al.*** *Pedobacter ardleyensis* sp. nov., isolated from soil in Antarctica. *Int J Syst Evol Microbiol* 2015;65:3841–3846.
37. **EUCAST.** *European Committee on Antimicrobial Susceptibility Testing. EUCAST Clinical Breakpoints - Bacteria*; 2015. (version 5.0; http://www.eucast.org).
38. **CLSI.** *Performance Standards for Antimicrobial susceptibility testing;* Twenty-Fifth Informational Supplement (M100-S25). Vol. 35 No. 3. Wayne, PA: Clinical and Laboratory Standards Institute; 2015.
39. **Sasser M.** *Identification of Bacteria by Gas Chromatography of Cellular Fatty Acids*, MIDI Technical Note 101. Newark, DE: Microbial IDentification Inc.; 1990.
40. **Altenburgera P, Kämpferb P, Makristathisc A, Lubitza W, Bussea H-J.** Classification of bacteria isolated from a medieval wall painting. *J Biotechnol* 1996;47:39–52.
41. **Stolz A, Busse HJ, Kämpfer P.** *Pseudomonas knackmussii* sp. nov. *Int J Syst Evol Microbiol* 2007;57:572–576.
42. **Tindall BJ.** Lipid composition of *Halobacterium lacusprofundi*. *FEMS Microbiol Lett* 1990;66:199–202.
43. **Tindall BJ.** A comparative study of the lipid composition *of Halobacterium saccharovorum* from various sources. *Syst Appl Microbiol* 1990;13:128–130.
44. **Kato M, Muto Y, Tanaka-Bandoh K, Watanabe K, Ueno K.** Sphingolipid composition in *Bacteroides* species. *Anaerobe* 1995;1:135–139.
45. **Kang CH, Jung YT, Yoon JH.** *Mucilaginibacter sabulilitoris* sp. nov., isolated from marine sand in a firth. *Int J Syst Evol Microbiol* 2013; 63:2865–2871.
46. **Aydogan EL, Busse HJ, Moser G, Müller C, Kämpfer P *et al.*** Proposal of *Mucilaginibacter galii* sp. nov. isolated from leaves of *Galium album*. *Int J Syst Evol Microbiol* 2017;67:1318–1326.
47. **Busse J, Auling G.** Polyamine pattern as a chemotaxonomic marker within the *Proteobacteria*. *Syst Appl Microbiol* 1988;11:1–8.
48. **Busse H-J, Bunka S, Hensel A, Lubitz W.** Discrimination of members of the Family *Pasteurellaceae* based on polyamine patterns. *Int J Syst Bacteriol* 1997;47:698–708.
49. **An DS, Yin CR, Lee ST, Cho CH.** *Mucilaginibacter daejeonensis* sp. nov., isolated from dried rice straw. *Int J Syst Evol Microbiol* 2009; 59:1122–1125.
50. **Kim JH, Kang SJ, Jung YT, Oh TK, Yoon JH.** *Mucilaginibacter lutimaris* sp. nov., isolated from a tidal flat sediment. *Int J Syst Evol Microbiol* 2012;62:515–519.
51. **Khan H, Chung EJ, Kang DY, Jeon CO, Chung YR.** *Mucilaginibacter jinjuensis* sp. nov., with xylan-degrading activity. *Int J Syst Evol Microbiol* 2013;63:1267–1272.

International Journal of Systematic and Evolutionary Microbiology

Supplementary materials

Mucilaginibacter terrae sp. nov., isolated from Antarctic soil

Ivo Sedláček[1], Roman Pantůček[2], Stanislava Králová[1], Ivana Mašlaňová[2], Pavla Holochová[1], Eva Staňková[1], Roman Sobotka[3], Miloš Barták[4], Hans-Jürgen Busse[5] and Pavel Švec*[1]

[1]Czech Collection of Microorganisms, Department of Experimental Biology, Faculty of Science, Masaryk University, Kamenice 5, 625 00 Brno, Czech Republic

[2]Section of Genetics and Molecular Biology, Department of Experimental Biology, Faculty of Science, Masaryk University, Kotlářská 2, 611 37 Brno, Czech Republic

[3]Centre Algatech, Institute of Microbiology, Academy of Sciences, Novohradská 237, 379 81 Třeboň, Czech Republic

[4]Section of Plant Physiology, Department of Experimental Biology, Faculty of Science, Masaryk University, Kamenice 5, 625 00 Brno, Czech Republic

[5]Institut für Mikrobiologie, Veterinärmedizinische Universität Wien, Veterinärplatz 1, A-1210 Wien, Austria

*Corresponding author: Pavel Švec, E-mail: mpavel@sci.muni.cz

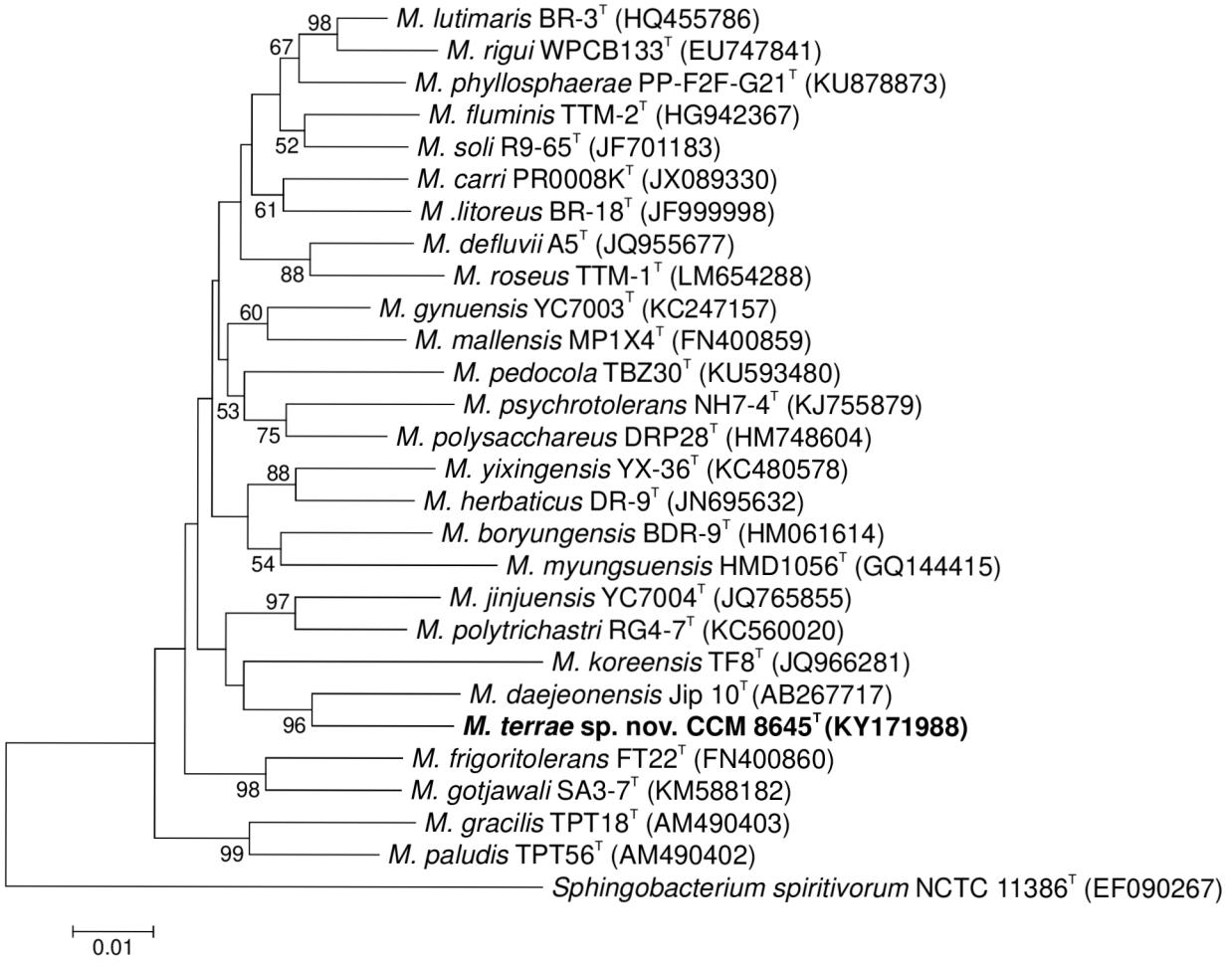

Fig. S1. Neighbour-Joining tree based on 16S rRNA gene sequence comparison showing the phylogenetic position of strain CCM 8645^T within the genus *Mucilaginibacter*. Bootstrap probability values (percentages of 500 tree replications) greater than 50 % are shown at branch points. Bar indicates number of substitutions per nucleotide position. *Sphingobacterium spiritivorum* was used as an outgroup.

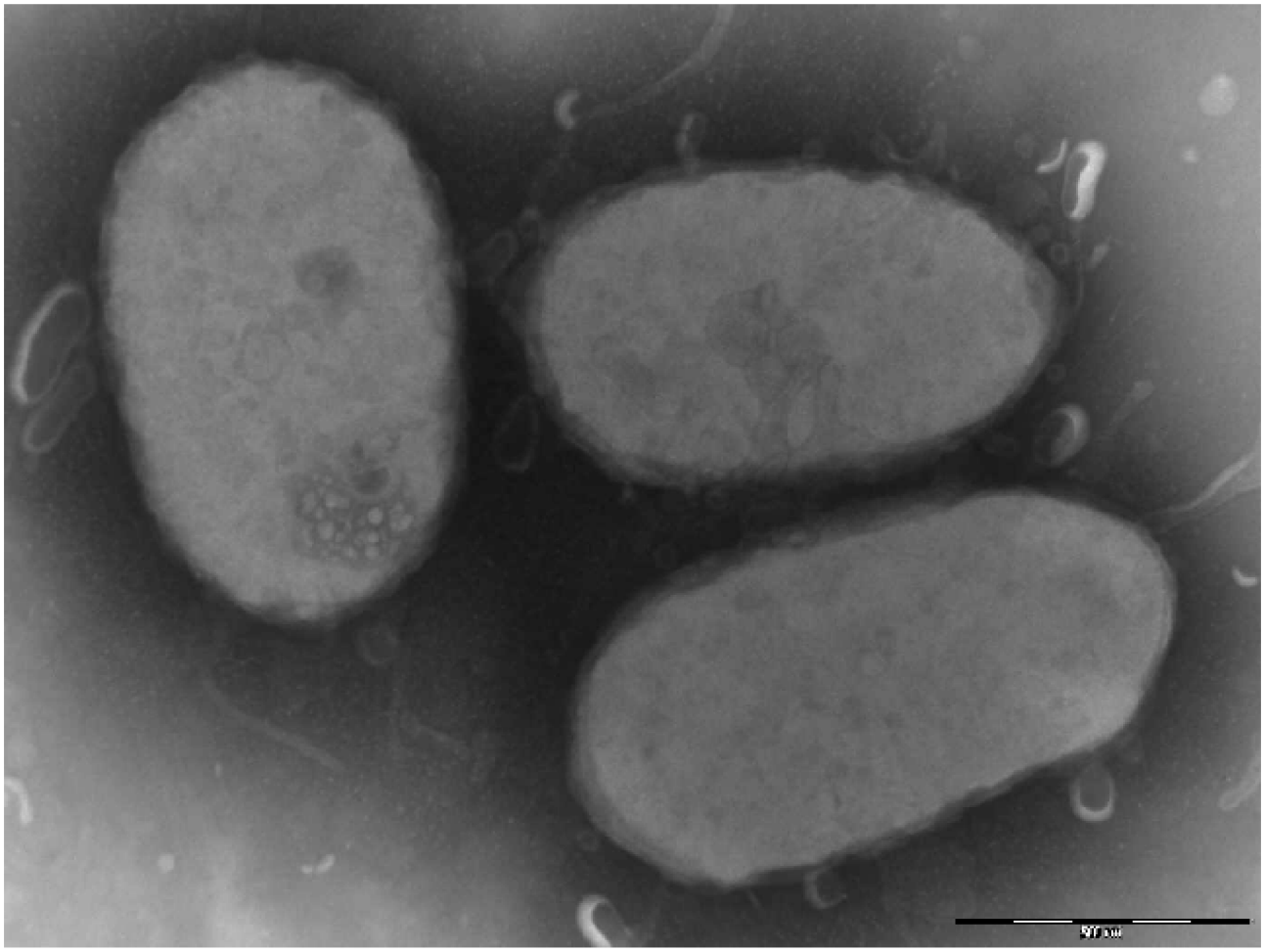

Fig. S2. Transmission electron microscopy of *Mucilaginibacter terrae* CCM 8645^{T} performed with a Morgagni 268D Philips (FEI Company, USA) electron microscope. Negative staining with 2% amonium molybdate. Bar represents 500 nm (original magnification ×10 000).

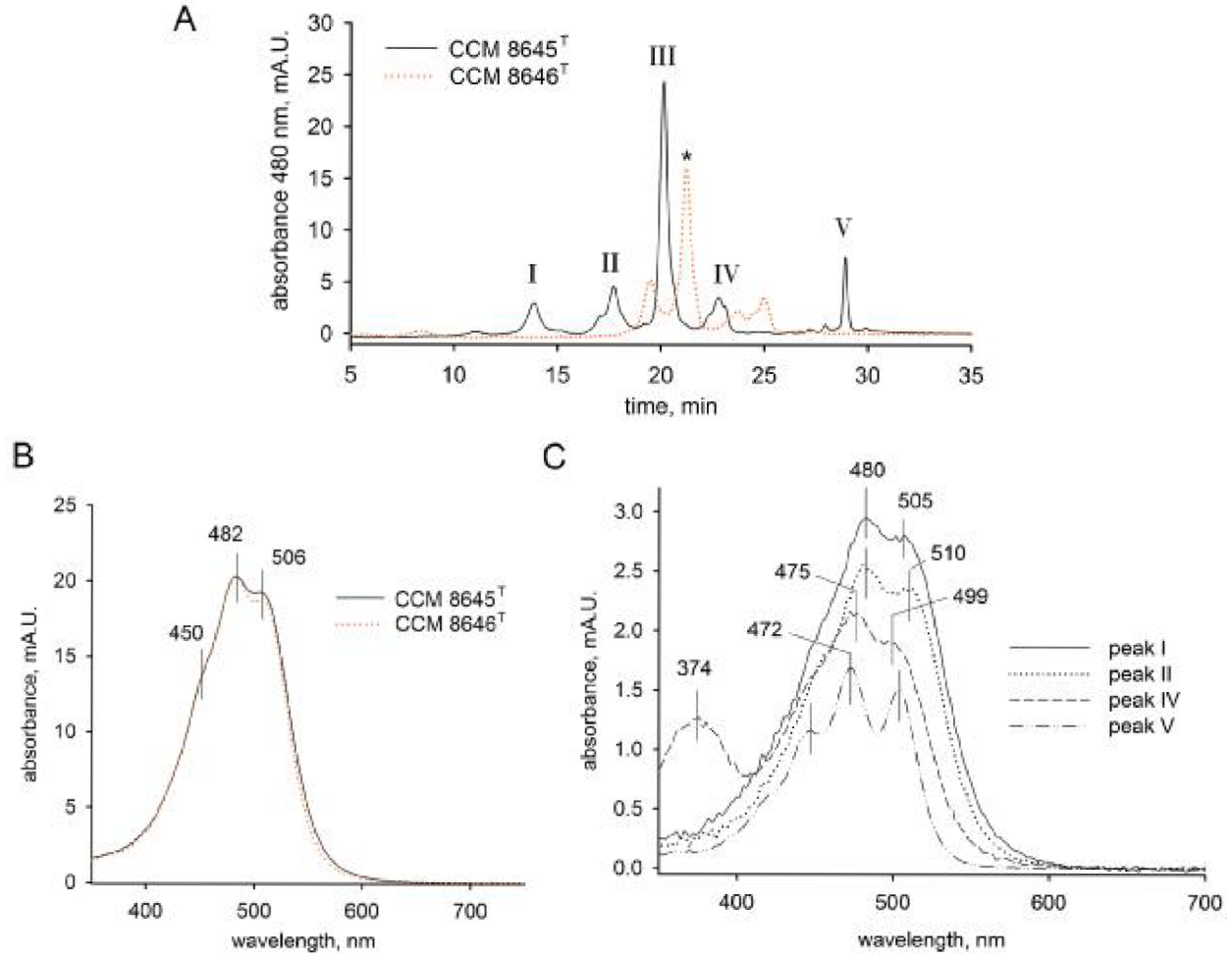

Fig. S3. Analysis of pigments extracted from the *Mucilaginibacter terrae* CCM 8645^T.

A) Methanol extract was separated by HPLC and pigments detected at 480 nm. Five major peaks are marked (I-V) and the chromatogram is compared with separated pigments from the *Rufibacter ruber* CCM 8646^T strain (dotted; see main text). B) Absorbance spectra of the most abundant pigments from the *Mucilaginibacter terrae* CCM 8645^T (III) and from the *Rufibacter ruber* CCM 8646^T (*) recorded by a diode-array detector. C) Absorbance spectra for peaks I, II, IV and V.

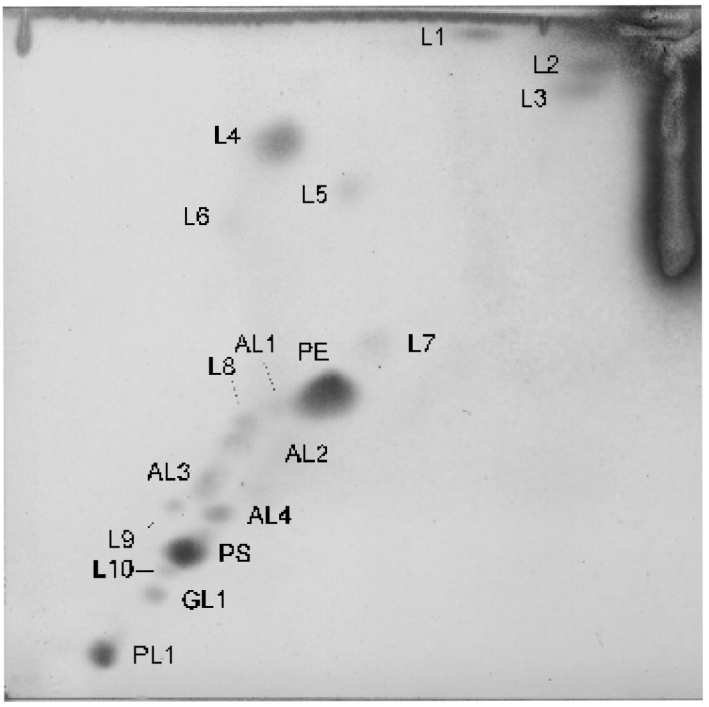

Fig. S4. Two dimensional TLC showing the total polar lipids of strains *Mucilaginibacter terrae* CCM 8645^{T}. Abbreviations: L1-L10, unidentified polar lipids; AL1-AL4, unidentified aminolipids; PE, phosphatidylethanolamine; PL1, unidentified phospholipid; PS, phosphatidylserine; GL1, unidentified glykolipid.

Príloha č. 6.

Kýrová K., Sedláček I., Pantůček R., Králová S., Holochová P., Mašlaňová I., Staňková E., Kleinhagauer T., Gelbíčová T., Sobotka R., Švec P., Busse H.-J. (2016) *Rufibacter ruber* sp. nov., isolated from fragmentary rock. *Int. J. Syst. Evol. Microbiol*. 66(11): 4401–5. Doi: 10.1099/ijsem.0.001364.

Rufibacter ruber sp. nov., isolated from fragmentary rock

Kamila Kýrová,[1] Ivo Sedláček,[1] Roman Pantůček,[2] Stanislava Králová,[1] Pavla Holochová,[1] Ivana Mašlaňová,[2] Eva Staňková,[1] Tanita Kleinhagauer,[3] Tereza Gelbíčová,[1] Roman Sobotka,[4] Pavel Švec[1] and Hans-Jürgen Busse[3]

Correspondence
Kamila Kýrová
kyrova@sci.muni.cz

[1]Czech Collection of Microorganisms, Department of Experimental Biology, Faculty of Science, Masaryk University, Kamenice 5, 625 00 Brno, Czech Republic

[2]Section of Molecular Biology, Department of Experimental Biology, Faculty of Science, Masaryk University, Kamenice 5, 625 00 Brno, Czech Republic

[3]Institut für Mikrobiologie, Veterinärmedizinische Universität Wien, Veterinärplatz 1, Wien A-1210, Austria

[4]Centre Algatech, Institute of Microbiology, Academy of Sciences, Novohradská 237, 379 81, Třeboň, Czech Republic

A red-pigmented, Gram-stain-negative, rod-shaped, aerobic bacterium, designated strain CCM 8646^T, was isolated from stone fragments in James Ross Island, Antarctica. Strain CCM 8646^T was able to grow from 10 to 40 °C, in the presence of up to 1 % (w/v) NaCl and at pH 7.0–11.0. Analysis of the 16S rRNA gene sequence placed strain CCM 8646^T in the genus *Rufibacter* with the closest relative being *Rufibacter roseus* H359^T (97.07 % 16S rRNA gene sequence similarity). The digital DNA–DNA hybridization values between strain CCM 8646^T and *R. roseus* H359^T were low (21.30±2.34 %). The major quinone was menaquinone MK-7. The polar lipids comprised phosphatidylethanolamine, an unknown aminoglycolipid and six unknown polar lipids. The G+C content of strain CCM 8646^T was 51.54 mol%. On the basis of phenotypic, chemotaxonomic and genotyping results, strain CCM 8646^T is considered to represent a novel species within the genus *Rufibacter*, for which the name *Rufibacter ruber* sp. nov. is proposed. The type strain is CCM 8646^T (=LMG 29438^T).

The genus *Rufibacter* is a member of the family *Cytophagaceae* and comprises four species with validly published names. *Rufibacter tibetensis* isolated from soil was described as the type species of the genus (Abaydulla *et al.*, 2012). Later, *Rufibacter roseus* from radiation-polluted soil (Zhang *et al.*, 2015), *Rufibacter immobilis* from saline lake (Polkade *et al.*, 2015) and *Rufibacter glacialis* from glacier soil (Liu *et al.*, 2016) were assigned to the genus. Bacteria of the genus *Rufibacter* are aerobic, psychrotolerant, Gram-stain-negative, catalase-positive and non-spore-forming with red carotenoid pigments. The major respiratory quinone is menaquinone 7 (MK-7) and phosphatidylethanolamine is the predominant polar lipid of the genus *Rufibacter*.

Strain CCM 8646^T was isolated from fragmentary rock in James Ross Island, Antarctica (57° 48′ 32.036″ W 63° 47′ 34.888″ S). Phenotypic classification of CCM 8646^T was performed using key tests applicable for Gram-negative rods, such as those for oxidase, catalase and urease, nitrate reduction, oxidation–fermentation (OF), arginine dihydrolase, ornithine and lysine decarboxylase, and production of hydrolytic enzymes (Atlas, 2010; Barrow & Feltham, 1993; Kosina *et al.*, 2013). The temperature range for growth (1–40 °C in increments of 5.0 °C) and NaCl concentration tolerance (0, 1, 2 and 3 %, w/v) were tested on R2A agar (Oxoid) adjusted accordingly. The pH range for growth was

The GenBank/EMBL/DDBJ accession number for the 16S rRNA gene sequence of *Rufibacter ruber* CCM 8646 T is KU603607.

The Whole Genome Shotgun projects have been deposited at DDBJ/EMBL/GenBank under the accession LRML00000000 (*Rufibacter roseus* CCM 8621) and LRMM00000000 (*Rufibacter ruber* sp. nov. CCM 8646). The version described in this paper is version LRML01000000 and LRMM01000000, respectively.

Abbreviations: dDDH, digital DNA-DNA hybridization; FAME, fatty acid methyl ester; ANI, average nucleotide identity.

Four supplementary figures and two supplementary tables are available with the online Supplementary Material.

tested on R2A agar adjusted to pH 6.0–11.0 (in increments of 1 pH unit) by using the buffer system (pH 6.0–8.0, 0.1 M KH_2PO_4/0.1 M NaOH; pH 9.0–10.0, 0.1 M $NaHCO_3$/0.1 M Na_2CO_3; pH 11.0, 0.05 M Na_2HPO_4/0.1 M NaOH) as described by Da *et al.* (2015). Further extended phenotyping was achieved by using GN2 MicroPlate (Biolog) and API ZYM (bioMérieux) identification test kits. The morphology of the isolate was observed by Gram staining and transmission electron microscopy (Morgagni 268D Philips; FEI) using samples stained with 2 % ammonium molybdate (Fig. S1, available in the online Supplementary Material). Differences in the antibiotic resistance patterns were tested by the disc diffusion method on R2A agar (Oxoid). Sixteen antibiotic discs generally used for Gram-negative rods (EUCAST v5.0., 2015 ; CLSI, 2015) were chosen: ampicillin (10 μg), aztreonam (30 μg), carbenicillin (100 μg), cefixim (5 μg), ceftazidim (10 μg), cephalothin (30 μg), ciprofloxacin (5 μg), gentamicin (10 μg), chloramphenicol (30 μg), imipenem (10 μg), kanamycin (30 μg), cotrimoxazol (25 μg), piperacillin (30 μg), polymyxin B (300 U), streptomycin (10 μg) and tetracycline (30 μg). EUCAST/CLSI standards were strictly followed for cultivation and inhibition zone diameter reading. Strain CCM 8646^T was susceptible to the majority of tested antibiotics. It was resistant to aztreonam, gentamicin and polymyxin B only. The biochemical/physiological data of CCM 8646^T are presented in the species description. The characterization of CCM 8646^T using GN2 MicroPlates is detailed in Table S1. The strain was grown at 20 °C for 48–72 h on R2A medium (Oxoid) during all experiments. Reference strain *R. roseus* CCM 8621^T was obtained from the Czech Collection of Microorganisms (http://www.sci.muni.cz/ccm/).

Genomic DNA was extracted for phylogenetic analysis using a FastPrep Lysing Matrix type B and FastPrep Homogenizer (MP Biomedicals) and purified using a High Pure PCR Template Preparation Kit (Roche Diagnostics). A fragment of the 16S rRNA gene corresponding to positions 8–1542 (*Escherichia coli* nomenclature) was amplified by PCR with FastStart PCR Master (Roche Diagnostics) and using conserved primers forward pA (AGAGTTTGATCCTGGCTCAG) and reverse pH (AAGGAGGTGATCCAGCCGCA) (Edwards *et al.*, 1989) and purified using a QIA quick PCR Purification Kit (Qiagen). Sequencing was performed using PCR primers and custom primers F1 (GTGGGGAKCRAACAGGATTAG), F2 (CGTCARGTCMTCATGGCCCTT), R1 (ATTACCGCGGCTGCTGGCAC) and R2 (CACATSMTCCMCCRC TTGT) in the Eurofins MWG Operon sequencing facility. The obtained partial 16S rRNA gene sequence of strain CCM 8646^T was compared with corresponding sequences of type strains using the EZtaxon database (Kim *et al.*, 2012). Preliminary 16S rRNA gene sequence analysis identified *R. roseus* H359^T as its closest relative (97.07 % similarity). To determine the taxonomic position of this novel strain in more detail, whole genome sequencing was performed.

The purified genomic DNA of strain CCM 8646^T and *R. roseus* CCM 8621^T was used for 400 bp sequencing library preparation as described previously (Sedláček *et al.*, 2016). The sample was loaded on a 316 v2 chip and sequenced using the Ion PGM Hi-Q sequencing kit (Life Technologies) on an Ion PGM system (Life Technologies). Quality trimming and error correction of the reads were performed with the Ion Torrent Suite Software (version 5.0.2). The assembly computation was performed using the plug-in Assembler SPAdes (v5.0.0). The total length of the assembly comprised 5 502 314 bp (CCM 8646^T) and 5 117 794 bp (*R. roseus* CCM 8621^T). Assembled contigs larger than 200 bp were used for subsequent analysis.

The complete 16S rRNA gene sequence extracted from whole genome sequence data using the RNAmmer 1.2. server (Lagesen *et al.*, 2007) showed similarity to that obtained by Sanger sequencing and therefore was used for further phylogenetic analysis. Pairwise similarities were calculated with the BioNumerics version 7.5 software (Applied Maths) and showed that strain CCM 8646^T shared 95.4–97.1 % 16S rRNA gene sequence similarity with other members of the genus *Rufibacter*. Phylogenetic analysis was performed using MEGA version 6 software (Tamura *et al.*, 2013). Genetic distances were corrected using Kimura's two-parameter model (Kimura, 1980) and the evolutionary history was inferred using the maximum-likelihood (Fig. 1) and neighbour-joining algorithms using a bootstrap test based on 5000 replications. Neighbour-joining clustering confirmed the tree topology obtained by the maximum-likelihood analysis (data not shown).

To evaluate the mean level of nucleotide sequence similarity at the genome level among strain CCM 8646^T and *R. roseus* CCM 8621^T, average nucleotide identity (ANI) and digital DNA–DNA hybridization (dDDH) values were determined. The dDDH values were calculated using the web-based genome-to-genome distance calculator (GGDC) version 2.1. (Meier-Kolthoff *et al.*, 2013) and the recommended formula 2 was taken into account to interpret the results. To calculate the ANI value, the algorithm implemented at the EzGenome server was used (http://www.ezbiocloud.net/ezgenome; Goris *et al.*, 2007). The dDDH values (21.30 ±2.34 %) and ANI (74.5465 %; reciprocal value 74.5491 %) were well below the cut-off values recommended for delineation of species (70 % and 95–96 %, respectively) (Richter & Rossello-Mora, 2009; Meier-Kolthoff *et al.*, 2013).

To estimate the DNA G+C content, the draft genome sequence was used. The G+C content was 51.54 mol%, which falls in the range 43.9–52.8 % observed in other *Rufibacter* species (Abaydulla *et al.*, 2012; Zhang *et al.*, 2015; Polkade *et al.*, 2015; Liu *et al.*, 2016).

Colonies of strain CCM 8646^T exhibited a pink–red colour and the whole absorbance spectra with three maxima (458, 487 and 518 nm; Fig. S2) suggested the presence of a red-shifted carotenoid. Pigments were extracted with an excess of methanol and the extract was injected into an Agilent-1200 HPLC system. Separation was performed on a reversed-phase column (Kinetex C8, 2.6 μm particle size, 3.9×150 mm; Phenomenex) with 35 % methanol and 15 % acetonitrile in 0.25 M pyridine (solvent A) and 20 %

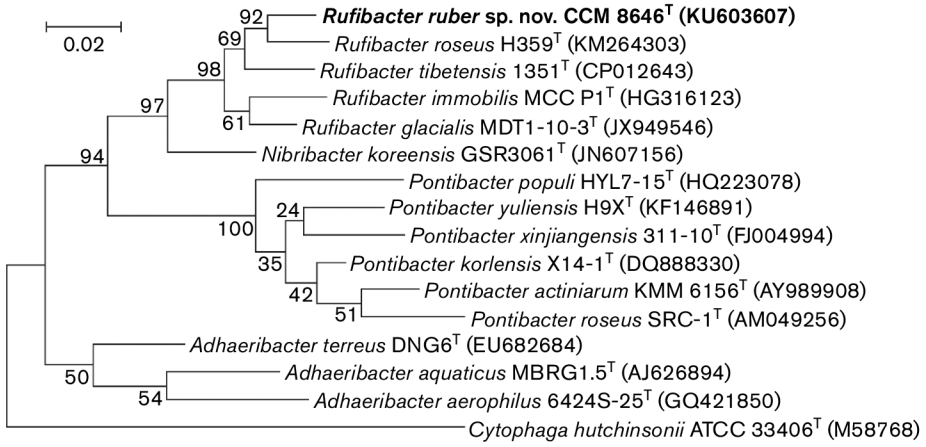

Fig. 1. Molecular phylogenetic analysis of 16S rRNA gene sequences by the maximum-likelihood method based on the Kimura two-parameter model showing the relationships among strain CCM 8646^T, the type strains of *Rufibacter* species and related taxa of the family *Cytophagaceae*. The percentage of trees in which the associated taxa clustered together is shown next to the branches. The tree is drawn to scale, with branch lengths measured in the number of substitutions per site. There were a total of 1543 positions in the final dataset. Bar, 0.02 substitutions per nucleotide position.

methanol and 20 % acetone in acetonitrile (solvent B). Pigments were eluted with a linear gradient of solvent B (30 to 95 % in 25 min) followed by 95 % of solvent B at a flow rate of 0.8 ml min^{-1} at 40 °C.

As shown by HPLC separation of extracted pigments,cells of strain CCM 8646^T contained three major and several minor pigments (Fig. S3a). All major pigment absorbances resembled those of carotenoids; the spectrum of the most abundant pigment is shown in Fig. S3(b). It is of note that this red-shifted spectrum did not correspond to any typical carotenoid and it might represent a new, relatively polar carotenoid.

The analysis of fatty acid methyl esters (FAMEs) was performed with cells grown on R2A agar (Oxoid) incubated at 20 ±2 °C for 72 h (late log-phase). Extraction of FAMEs was performed according to the standard protocol of the Sherlock Microbial Identification System (Sasser, 1990). Cellular fatty acid extracts were analysed by GC (model 7890B; Agilent) by using the rapid Sherlock Identification system (MIS, version 6.2B, MIDI database: RTSBA6, MIDI). The FAME profile of strain CCM 8646^T is shown in Table S2. The predominant fatty acids of strain CCM 8646^T were summed feature 4 (iso-$C_{17:1}$ I/anteiso-$C_{17:1}$ B) (27.2 %), iso-$C_{15:0}$ (16.8 %), $C_{17:1}\omega6c$ (11.2 %) and summed feature 3 ($C_{16:1}\omega7c$/$C_{16:1}\omega6c$) (10.1 %), which is in agreement with the FAME data for the type strains of *Rufibacter* species (Abaydulla *et al.*, 2012; Liu *et al.*, 2016; Polkade *et al.*, 2015; Zhang *et al.*, 2015).

Quinones and polar lipids were extracted from freeze-dried biomass and analysed as previously described (Altenburger *et al.*, 1996; Stolz *et al.*, 2007; Tindall, 1990a, b). The major respiratory menaquinone was MK-7 and the major component in the polar lipid profile was phosphatidylethanolamine, which is in agreement with the description of the genus *Rufibacter* (Abaydulla *et al.*, 2012; Liu *et al.*, 2016; Polkade *et al.*, 2015; Zhang *et al.*, 2015). In addition, an unidentified aminoglycolipid and six unidentified polar lipids were also present (Fig. S4).

Based on 16S rRNA gene sequence similarities, strain CCM 8646^T was related most closely to members of the genus *Rufibacter* within the family *Cytophagaceae*. Further investigation by a polyphasic taxonomic approach differentiated strain CCM 8646^T from the type strains of recognized *Rufibacter* species and revealed strain CCM 8646^T as a representative of a novel species of the genus *Rufibacter*, for which the name *Rufibacter ruber* sp. nov. is proposed.

Description of *Rufibacter ruber* sp. nov.

Rufibacter ruber (ru′ber. L. masc. adj. *ruber* red, referring to the colour of the colonies).

Cells are Gram-stain-negative, short rods, occurring predominantly in pairs or in irregular clusters and are non-spore-forming. Colonies on R2A agar are circular, with whole margin, slightly convex, smooth, glistening and 1–2 mm in diameter. Aerobic; non-haemolytic on sheep blood agar. Grows at 10–37 °C but not at 5 or 42 °C. Growth is observed in the presence of up to 1 % (w/v) NaCl and at pH 7.0–11.0 on R2A medium. Most abundant growth is observed on R2A agar without NaCl, at pH 8.0 and at 25 °C. No fluorescein pigment on King B medium. Grows on plate count agar (Oxoid), tryptone soya agar (Oxoid) and brain infusion agar (Oxoid) but not on MacConkey agar (Oxoid) or CM03 agar (Oxoid). No anaerobic growth is observed on R2A agar. OF test is negative. Positive for catalase, DNase, esterase lipase (C8), leucine arylamidase, valine arylamidase, α-glucosidase, α-galactosidase (weak), *N*-acetyl-β-glucosaminidase, alkaline phosphatase and acid phosphatase.

Table 1. Differential characteristics between strain CCM 8646^T and *R. roseus* CCM 8621^T

All presented data were obtained in this study. +, Positive; −, negative; w, weakly positive.

Characteristic	CCM 8646^T	*R. roseus* CCM 8621^T
Growth in the presence of 3 % (w/v) NaCl	−	+
Growth at 5 °C	−	+
Oxidase	−	+
Enzyme activity of (API ZYM):		
α-Galactosidase	w	−
β-Galactosidase	−	w

Negative for urease, oxidase, arginine dihydrolase, lysine decarboxylase, ornithine decarboxylase, esterase (C4), lipase (C14), cystine arylamidase, trypsin, chymotrypsin, naphthol-AS-BI-phosphohydrolase, β-galactosidase, β-glucuronidase, β-glucosidase, α-mannosidase, α-fucosidase, nitrate reduction and nitrite reduction. Aesculine, gelatine, ONPG and starch hydrolysis are positive. Negative for Simmons citrate, sodium malonate, acetamide, and hydrolysis of Tween 80, tyrosine, casein and lecithin (egg-yolk reaction). Acid is produced from glucose, fructose, xylose and maltose (King's modified OF medium with phenol red). Acid is not produced from mannitol.

The type strain, CCM 8646^T (=LMG 29438^T), was isolated from fragmentary rock in Antarctica. The DNA G+C content of the type strain is 51.54 mol%. Basic tests distinguishing the type strain from its phylogenetically closest related species, *Rufibacter roseus*, are shown in Table 1.

Acknowledgements

The authors thank the scientific infrastructure of the J. G. Mendel Czech Antarctic Station as a part of the Czech Polar Research Infrastructure (CzechPolar2) and its crew for their assistance, supported by the Ministry of Education, Youth and Sports of the Czech Republic (LM2015078). S.K. is a holder of Brno PhD Talent Financial Aid. R.S. was supported by the National Programme of Sustainability I (LO1416). Daniel Krsek (NRL for Diagnostic Electron Microscopy of Infectious Agens, National Institute of Public Health, Prague, Czech Republic) is acknowledged for transmission electron microscopy. The authors would also like to thank Jana Bajerová for excellent technical assistance and Bernhard Schink for help with the species name correction.

References

Abaydulla, G., Luo, X., Shi, J., Peng, F., Liu, M., Wang, Y., Dai, J. & Fang, C. (2012). *Rufibacter tibetensis* gen. nov., sp. nov., a novel member of the family *Cytophagaceae* isolated from soil. *Antonie Van Leeuwenhoek* **101**, 725–731.

Altenburgera, P., Kämpferb, P., Makristathisc, A., Lubitza, W. & Bussea, H.-J. (1996). Classification of bacteria isolated from a medieval wall painting. *J Biotechnol* **47**, 39–52.

Atlas, R. M. (2010). *Handbook of Microbiological Media*, 4th edn, Washington, D.C.: ASM Press.

Barrow, G. I. & Feltham, R. K. A. (1993). *Cowan and Steel's Manual for the Identification of Medical Bacteria*, 3rd edn, Great Britain: Cambridge University Press.

CLSI. (2015). *Performance Standards for Antimicrobial Susceptibility Testing*. Twenty-Fifth Informational Supplement (M100-S25), vol. 35, No. 3.

Da, X., Jiang, F., Chang, X., Ren, L., Qiu, X., Kan, W ., Deng, S., Fang, C., Zhang, Y. & other authors (2015). *Pedobacter ardleyensis* sp. nov., isolated from soil in Antarctica. *Int J Syst Evol Microbiol* **65**, 3841–3846.

Edwards, U., Rogall, T., Blöcker, H., Emde, M. & Böttger, E. C. (1989). Isolation and direct complete nucleotide determination of entire genes. characterization of a gene coding for 16S ribosomal RNA. *Nucleic Acids Res* **17**, 7843–7853.

EUCAST (2015). European Committee on Antimicrobial Susceptibility Testing. EUCAST Clinical Breakpoints – Bacteria (Version 5.0;). http://www.eucast.org.

Goris, J., Konstantinidis, K. T., Klappenbach, J. A., Coenye, T., Vandamme, P. & Tiedje, J. M. (2007). DNA-DNA hybridization values and their relationship to whole-genome sequence similarities. *Int J Syst Evol Microbiol* **57**, 81–91.

Kim, O. S., Cho, Y. J., Lee, K., Yoon, S. H., Kim, M., Na, H., Park, S. C., Jeon, Y. S., Lee, J. H. & other authors (2012). Introducing EzTaxon-e: a prokaryotic 16S rRNA gene sequence database with phylotypes that represent uncultured species. *Int J Syst Evol Microbiol* **62**, 716–721.

Kimura, M. (1980). A simple method for estimating evolutionary rates of base substitutions through comparative studies of nucleotide sequences. *J Mol Evol* **16**, 111–120.

Kosina, M., Barták, M., Mašlaňová, I., Pascutti, A. V., Šedo, O., Lexa, M. & Sedláček, I. (2013). *Pseudomonas prosekii* sp. nov., a novel psychrotrophic bacterium from Antarctica. *Curr Microbiol* **67**, 637–646.

Lagesen, K., Hallin, P. F., Rødland, E., Stærfeldt, H. H., Rognes, T. & Ussery, D. W. (2007). RNAmmer: consistent annotation of rRNA genes in genomic sequences. *Nucleic Acids Res* **35**, 3100–3108.

Liu, Q., Liu, H. C., Zhang, J. L., Zhou, Y. G. & Xin, Y. H. (2016). *Rufibacter glacialis* sp. nov., a psychrotolerant bacterium isolated from glacier soil. *Int J Syst Evol Microbiol* **66**, 315–318.

Meier-Kolthoff, J. P., Auch, A. F., Klenk, H. P. & Göker, M. (2013). Genome sequence-based species delimitation with confidence intervals and improved distance functions. *BMC Bioinformatics* **14**, 60.

Polkade, A. V., Ramana, V. V., Joshi, A., Pardesi, L. & Shouche, Y. S. (2015). *Rufibacter immobilis* sp. nov., isolated from a high-altitude saline lake. *Int J Syst Evol Microbiol* **65**, 1592–1597.

Richter, M. & Rosselló-Móra, R. (2009). Shifting the genomic gold standard for the prokaryotic species definition. *Proc Natl Acad Sci U S A* **106**, 19126–19131.

Sasser, M. (1990). *Identification of Bacteria by Gas Chromatography of Cellular Fatty Acids*, MIDI Technical Note 101. Newark, DE: MIDI Inc.

Sedláček, I., Kwon, S.-W., Černohlávková, J., Mašlaňová, I., Kýrová, K., Švec, P., Holochová, P., Busse, H.-J., Švec, P. & other authors (2016). *Aquitalea pelogenes* sp. nov., isolated from mineral peloid. *Int J Syst Evol Microbiol* **66**, 962–967.

Stolz, A., Busse, H.-J. & Kämpfer, P. (2007). *Pseudomonas knackmussii* sp. nov. *Int J Syst Evol Microbiol* **57**, 572–576.

Tamura, K., Stecher, G., Peterson, D., Filipski, A. & Kumar, S. (2013). MEGA6: molecular evolutionary genetics analysis version 6.0. *Mol Biol Evol* **30**, 2725–2729.

Tindall, B. J. (1990a). Lipid composition of *Halobacterium lacusprofundi*. *FEMS Microbiol Lett* **66**, 199–202.

Tindall, B. J. (1990b). A comparative study of the lipid composition *of Halobacterium saccharovorum* from various sources. *Syst Appl Microbiol* **13**, 128–130.

Zhang, Z. D., Gu, M. Y., Zhu, J., Li, S. H., Zhang, L. J., Xie, Y. Q., Shi, Y. H., Wang, W. & Li, W. J. (2015). *Rufibacter roseus* sp. nov., isolated from radiation-polluted soil. *Int J Syst Evol Microbiol* **65**, 1572–1577.

International journal of Systematic and Evolutionary Microbiology

Rufibacter ruber sp. nov., isolated from Antarctic fragmentary rock

Supplementary Data

Kamila Kýrová*[1], Ivo Sedláček[1], Roman Pantůček[2], Stanislava Králová[1], Pavla Holochová[1], Ivana Mašlaňová[2], Eva Staňková[1], Tanita Kleinhagauer[4], Tereza Gelbíčová[1], Roman Sobotka[3], Pavel Švec[1] and Hans-Jürgen Busse[4]

[1]Czech Collection of Microorganisms, Department of Experimental Biology, Faculty of Science, Masaryk University, Kamenice 5, 625 00 Brno, Czech Republic

[2]Section of Molecular Biology, Department of Experimental Biology, Faculty of Science, Masaryk University, Kamenice 5, 625 00 Brno, Czech Republic

[3]Centre Algatech, Institute of Microbiology, Academy of Sciences, Novohradská 237, 379 81 Třeboň, Czech Republic

[4]Institut für Bakteriology, Mykology und Hygiene, Veterinärmedizinische Universität Wien, Veterinärplatz 1, A-1210 Wien, Austria

*Corresponding author:

Kamila Kýrová: E-mail: kyrova@sci.muni.cz; Tel.: +420-549494399; Fax: +420-549498289

Table S1: Metabolic fingerprint of *Rufibacter ruber* sp. nov. CCM 8646^T obtained by the Biolog GN 2 MicroPlate.

Positive for utilization of:	**Negative for utilization of:**	
dextrin	α-cyclodextrin	propionic acid
glycogen	Tween 40	quinic acid
N-acetyl-D-glucosamine	Tween 80	D-saccharic acid
D-fructose	N-acetyl-D-galactosamine	sebacic acid
gentiobiose	adonitol	succinic acid
α-D-glucose	D-arabitol	bromosuccinic acid
maltose	D-cellobiose	succinamic acid
D-mannose	erythritol	glucuronamide
D-melibiose	L-fucose	L-alaninamide
D-raffinose	m-inositol	D-alanine
sucrose	α-D-lactose	L-alanine
D-trehalose	lactulose	L-alanyl-glycine
	D-mannitol	L-asparagine
	β-methyl-D-glucoside	L-aspartic acid
	D-psicose	glycyl-L-aspartic acid
	L-rhamnose	glycyl-L-glutamic acid
	D-sorbitol	L-histidine
Borderline for:	turanose	hydroxy-L-proline
L-arabninose	xylitol	L-leucine
succinic acid monomethyl ester	pyruvic acid methyl ester	L-ornithine
acetic acid	cis-aconitic acid	L-phenylalanine
L-glutamic acid	citric acid	L-pyroglutamic acid
L-proline	formic acid	D-serine
α-D-glucose-1-phosphate	D-galactonic acid lactone	L-serine
	D-galacturonic acid	L-threonine
	D-gluconic acid	D,L-carnithine
	D-glucosaminic acid	γ-aminobutyric acid
	D-glucuronic acid	urocanic acid
	α-hydroxybutyric acid	inosine, uridine
	β-hydroxybutyric acid	thymidine
	γ-hydroxybutyric acid	phenylethylamine
	p-hydroxy phenylacetic acid	putrescine
	itaconic acid	2-aminoethanol
	α-keto butyric acid	2,3-butanediol
	α-keto glutaric acid	glycerol
	α-keto valeric acid	D,L-α-glycerolphosphate
	D,L-lactic acid	D-glucose-6-phosphate
	malonic acid	

Table S2: Cellular fatty acid composition (as the percentage of the total) of strain CCM 8646^T. Cells were grown on R2A at 20 °C for 72 hrs.

Fatty acid	%
C $_{15:1}$ iso G	4.4
C $_{15:0}$ iso	16.8
C $_{15:0}$ anteiso	4.5
C $_{15:1}$ ω6*c*	3.1
C $_{16:1}$ iso H	1.7
C $_{16:0}$ iso	1.6
C $_{16:1}$ ω5*c*	2.6
C $_{15:0}$ iso 3OH	3.2
C $_{17:1}$ ω8*c*	1.0
C $_{17:1}$ ω6*c*	11.2
C $_{16:0}$ iso 3OH	1.4
C $_{16:0}$ 3OH	1.1
C $_{17:0}$ iso 3OH	3.7
Summed Feature 1*	1.6
Summed Feature 3†	10.1
Summed Feature 4‡	27.2

*Summed feature 1 represents C $_{13:0}$ 3OH/ C $_{15:1}$ iso H
†Summed feature 3 represents C $_{16:1}$ ω7*c*/ C $_{16:1}$ ω6*c*
‡Summed feature 4 represents C $_{17:1}$ iso I/ C $_{17:1}$ anteiso B

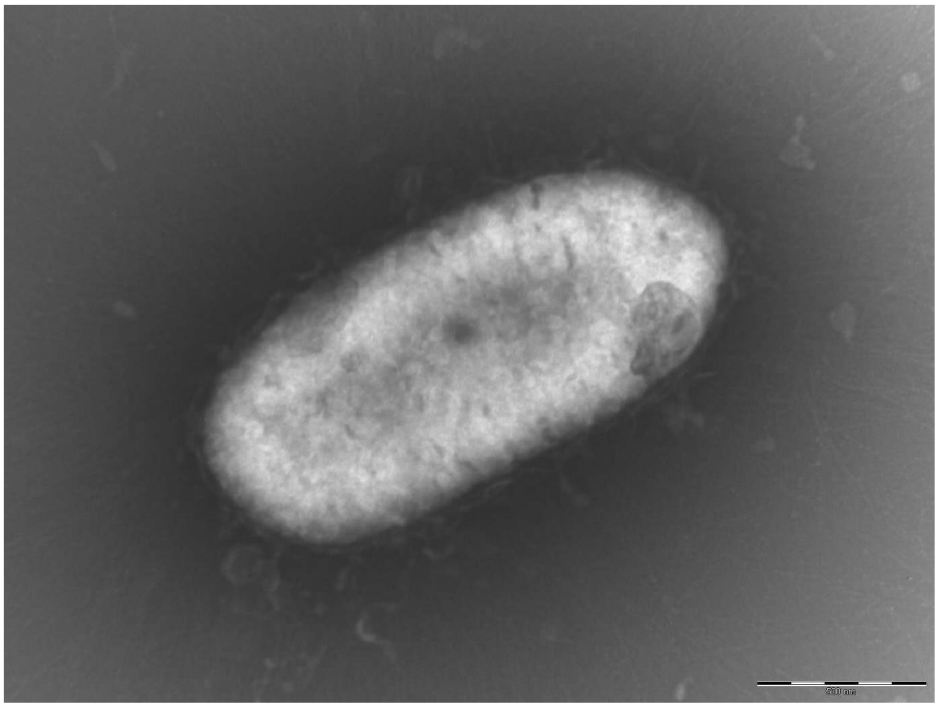

Figure S1. Transmission electron micrographs of the strain CCM 8646^{T} cultured on R2A at 30 °C for 72 hours. Bar represents 500 nm (original magnification ×10 000).

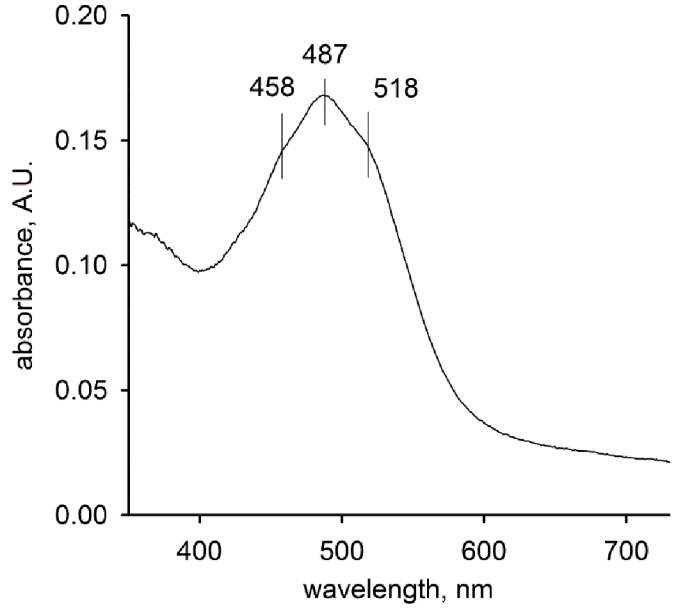

Figure S2. Whole-cell spectra of strain CCM 8646^{T}. Spectra were measured with a Shimadzu UV-3000 spectrophotometer; absorbance maxima suggest prevalence of a carotenoid(-like) pigment(s).

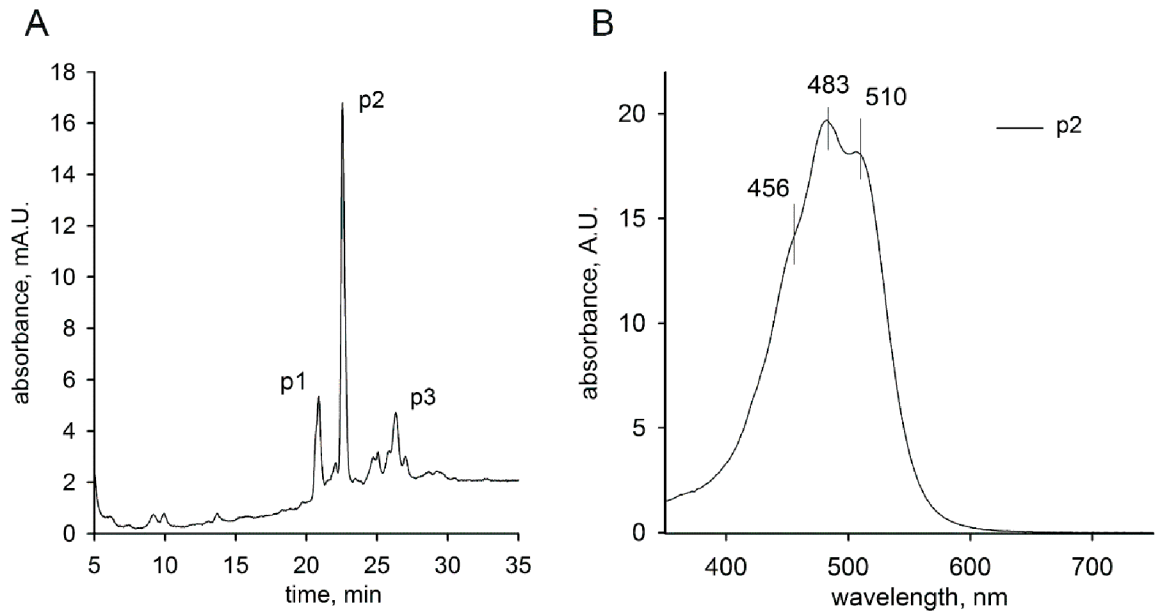

Figure S3. Analysis of pigments extracted from strain CCM 8646^T. A) Methanol extract was separated by HPLC and pigments detected at 460 nm. B) Absorbance spectra of the most abundant (p2) pigment as recorded by a diode-array detector.

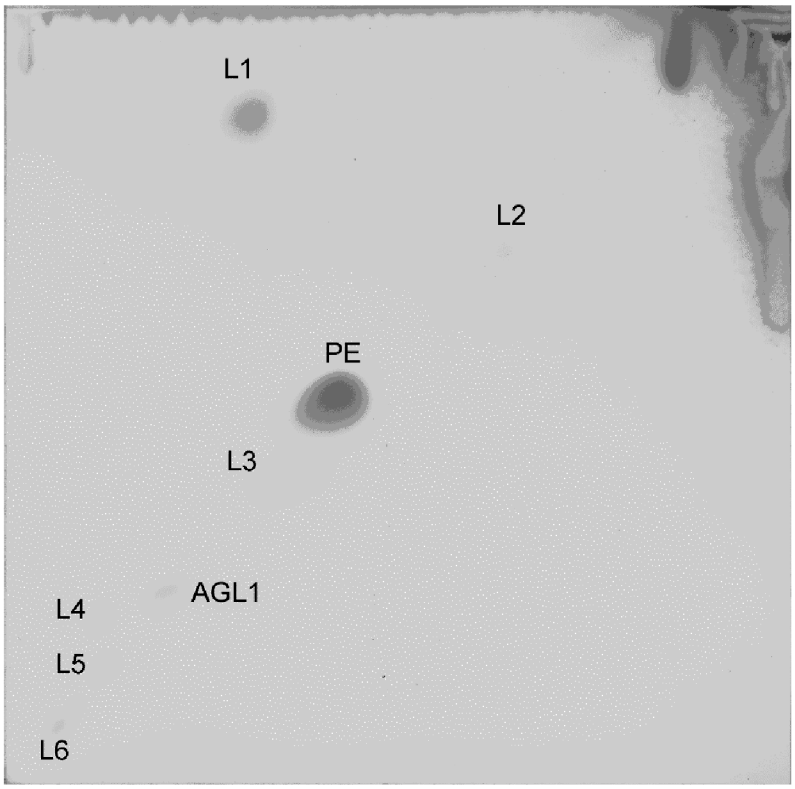

Figure S4. Two dimensional TLC showing the total polar lipids of strain CCM 8646^T: L1-L6: unknown polar lipids, PE-phosphatidylethanolamine, AGL1 – unknown aminoglycolipid.

Príloha č. 7.

Švec P., Černohlávková J., Busse H.-J., Vojtková H., Pantůček R., Cnockaert M., Mašlaňová I., Králová S., Vandamme P., Sedláček I. (2015) Classification of strain CCM 4446^{T} as *Rhodococcus degradans* sp. nov. *Int. J. Syst. Evol. Microbiol*. 65(12): 4381–7. Doi: 10.1099/ijsem.0.000584.

International Journal of Systematic and Evolutionary Microbiology (2015), **65**, 4381–4387 **DOI** 10.1099/ijsem.0.000584

Classification of strain CCM 4446^T as *Rhodococcus degradans* sp. nov.

Pavel Švec,[1] Jitka Černohlávková,[1] Hans-Jürgen Busse,[2] Hana Vojtková,[3] Roman Pantůček,[4] Margo Cnockaert,[5] Ivana Mašlaňová,[4] Stanislava Králová,[1] Peter Vandamme[5] and Ivo Sedláček[1]

Correspondence
Pavel Švec
mpavel@sci.muni.cz

[1]Czech Collection of Microorganisms, Department of Experimental Biology, Faculty of Science, Masaryk University, Kamenice 5, Bld. A25, 625 00 Brno, Czech Republic

[2]Institute for Microbiology, Veterinary University Vienna, Veterinärplatz 1, A-1210 Vienna, Austria

[3]Faculty of Mining and Geology, Institute of Environmental Engineering, VŠB–Technical University of Ostrava, 17. listopadu 15/2172, 708 33 Ostrava–Poruba, Czech Republic

[4]Division of Genetics and Molecular Biology, Department of Experimental Biology, Faculty of Science, Masaryk University, Kotlářská 2, 611 37 Brno, Czech Republic

[5]Department of Biochemistry and Microbiology, Faculty of Sciences, Ghent University, K.L. Ledeganckstraat 35, 9000 Ghent, Belgium

Strain CCM 4446^T, with notable biodegradation capabilities, was investigated in this study in order to elucidate its taxonomic position. Chemotaxonomic analyses of quinones, polar lipids, mycolic acids, polyamines and the diamino acid of the cell-wall peptidoglycan corresponded with characteristics of the genus *Rhodococcus*. Phylogenetic analysis, based on the 16S rRNA gene sequence, assigned strain CCM 4446^T to the genus *Rhodococcus* and placed it in the *Rhodococcus erythropolis* 16S rRNA gene clade. Further analysis of *catA* and *gyrB* gene sequences, automated ribotyping with *Eco*RI restriction endonuclease, whole-cell protein profiling, DNA–DNA hybridization and extensive biotyping enabled differentiation of strain CCM 4446^T from all phylogenetically closely related species, i.e., *Rhodococcus baikonurensis, Rhodococcus qingshengii, Rhodococcus erythropolis* and *Rhodococcus globerulus.* The results obtained show that the strain investigated represents a novel species within the genus *Rhodococcus*, for which the name *Rhodococcus degradans* sp. nov., is proposed. The type strain is CCM 4446^T (=LMG 28633^T).

The genus *Rhodococcus* is an abundant bacterial group widely distributed in various types of environments including soils, sludge, anthropogenic and marine sediments, and fresh and salt waters. Certain species are opportunistic pathogens of plants and animals, including humans. Members of the genus *Rhodococcus* have become important agents in the fields of environmental and industrial biotechnology and bioremediation due to their ability to degrade a remarkable range of substances, such as polycyclic and aliphatic hydrocarbons, steroids, chlorinated phenols, lignin, nitroaromatic compounds and some pesticides or polychlorinated biphenyls (Jones & Goodfellow, 2012; Martínková *et al.*, 2009). The tolerance of members of this genus to diverse and harsh conditions is related to the high complexity, and capacity for modification, of the fatty acid composition of the cell membrane and to the usage of unique transport systems (de Carvalho *et al.*, 2014). Rhodococci are also used for the production of enzymes for biotransformation of a number of polymers and xenobiotics (Bell *et al.*, 1998; Warhurst & Fewson, 1994) and may be utilized as sources of biosurfactants and carotenoid pigments or as biosensors (Lang & Philp, 1998; Roach *et al.*, 2003).

The present taxonomic study deals with strain CCM 4446^T (=HA1^T), assigned tentatively to the genus *Rhodococcus*, but revealing characteristics differentiating it from species of the genus *Rhodococcus* with validly published names. This strain was isolated in Switzerland from a soil contaminated by organic pollutants and was originally assigned as

Abbreviations: GL, glycolipid; L, lipid; PIM, phosphatidylinositol-mannoside.

The GenBank/EMBL/DDBJ accession numbers for the 16S rRNA, *gyrB* and *catA* gene sequences of strain CCM 4446^T are JQ776649, KP663665 and KP663666, respectively.

One supplementary table and three supplementary figures are available with the online Supplementary Material.

Arthrobacter sp. HA1^T (Scholtz *et al.*, 1987b). It was deposited in the Czech Collection of Microorganisms (CCM) public collection in 2002. The biodegradation capacities of strain CCM 4446^T (=HA1^T) have been investigated in a number of earlier studies, which documented its significant physiological capability to reduce organic and inorganic substances from the environment. The strain has been shown to degrade polychlorinated biphenyls and low-molecular polycyclic aromatic hydrocarbons (Janáková & Vojtková, 2012; Kašáková *et al.*, 2012). It produces dehalogenases that break the carbon-halogen bond in halogenated aliphatic compounds via the hydrolytic mechanism (Damborský *et al.*, 1997; Damborský & Koča, 1999; Martínková *et al.*, 2009; Poelarends *et al.*, 2000; Scholtz *et al.*, 1988). The strain was shown to produce 1-chloro halidohydrolase (Scholtz *et al.*, 1987a) and to utilize 1-chloro-, 1-bromo- and 1-iodo-alkanes (Scholtz *et al.*, 1987a, b; Scholtz *et al.*, 1988). Strain CCM 4446^T was also examined for its applicability to treating wastewater from a textile production plant containing multiple toxic metals originating from textile dyeing and pigmentation processes, dispersing agents, inorganic salts, dust-reducing substances, thickening agents and buffers (Vojtková *et al.*, 2012). In the present study we determined the taxonomic position of strain CCM 4446^T.

The type and reference strains included in individual experiments were obtained from the CCM (Masaryk University, Brno, www.sci.muni.cz/ccm/).

The almost complete 16S rRNA gene sequence and sequences of the partial gene coding for the subunit B of DNA gyrase (*gyrB*) and the partial gene for catechol 1,2-dioxygenase (*catA*) involved in the metabolism of monoaromatic compounds, were determined as described by Táncsics *et al.* (2014). DNA amplification was performed with crude boiled cell extracts and sequencing was performed in the Eurofins MWG Operon sequencing facility (Ebersberg, Germany). The sequences obtained were compared with those of other taxa of the genus *Rhodococcus* retrieved from the GenBank/EMBL/DDJB database. Phylogenetic analysis was performed using MEGA version 6 software (Tamura *et al.*, 2013). The evolutionary history was inferred using the neighbour-joining, maximum-likelihood and maximum-parsimony methods and using a bootstrap test based on 1000 replications. Maximum-likelihood and maximum-parsimony clustering confirmed the tree topologies obtained by the neighbour-joining analyses of all three genes (data not shown). The 16S rRNA, *catA* and *gyrB* gene sequence similarities were calculated using BioNumerics software (Applied Maths). Phylogenetic analysis based on the 16S rRNA gene showed that strain CCM 4446^T belongs to the *Rhodococcus erythropolis* 16S rRNA gene clade (Jones & Goodfellow, 2012) and placed it in a subcluster containing *Rhodococcus qingshengii*, *Rhodococcus baikonurensis*, *Rhodococcus erythropolis* and *Rhodococcus globerulus* (100 %, 99.8 %, 99.4 % and 99.0 % 16S rRNA gene sequence similarities, repectively) (Fig. 1). The phylogenetic position of strain CCM 4446^T was further assessed using *catA* and *gyrB* genes, which have been shown to be suitable alternative phylogenetic markers for differentiating between species of the genus *Rhodococcus* (Táncsics *et al.*, 2014). The *catA* (595 bp) and *gyrB* (1059 bp) nucleotide sequence based phylogenetic analysis showed that strain CCM 4446^T is separate from species of the genus *Rhodococcus* with validly published names. The *catA* gene sequence similarities between CCM 4446^T and the closest species phylogenetically ranged from 90.8 % with *R. globerulus* to 99.4 % with *R. qingshengii*. Similarly, the *gyrB* gene sequence similarity values ranged from 88.4 % towards the *R. globerulus* sequence to 99.1 % towards the *R. qingshengii* sequence (Fig. 2).

Automated ribotyping with the *Eco*RI restriction enzyme was performed using the RiboPrinter Microbial Characterization System (DuPont Qualicon) in accordance with the manufacturer's instructions. Numerical analysis and dendrogram reconstruction was carried out using BioNumerics 7.5 software (Applied Maths). The ribotype patterns were exported into the BioNumerics database using a load samples import script provided by the manufacturer. The ribotype pattern obtained from strain CCM 4446^T was clearly separated (72 % similarity) from those of the remaining type strains representing phylogenetically closely related species (Fig. S1, available in the online Supplementary Material).

Comparison of whole-cell protein profiles from strain CCM 4446^T, *R. erythropolis* CCM 277^T, *R. globerulus* CCM 8449^T, *R. baikonurensis* CCM 8450^T and *R. qingshengii* CCM 8451^T was carried out using an Agilent 2100 Bioanalyser system with a Protein 230 kit (Agilent Technologies). Whole-cell proteins were extracted from the cells grown on Tryptone Soya agar (Oxoid) at 30 °C for 48 h. In total, 50 mg of cells were harvested, washed twice in 800 µl of PBS buffer (137 mM NaCl, 10 mM Na_2HPO_4, 2.7 mM KCl, 2 mM KH_2PO_4, pH 7.4) and finally resuspended in 600 µl PBS buffer. Subsequently, the cell suspensions were transferred into tubes containing 1 g of 0.1 mm diameter Zirconia/Silica Beads (BioSpec Products) and treated using a FastPrep-24 homogenizer for 40 s at 6 m s^{-1}. The cell lysates obtained were centrifuged and protein extracts were transferred into clean tubes and analysed immediately. Further processing of the protein extracts and analysis using the Agilent 2100 Bioanalyser system was performed according to the protocol provided by the manufacturer. Numerical analysis of the protein patterns obtained and reconstruction of the dendrogram was carried out using BioNumerics 7.5 software (Applied Maths). Whole-cell protein profiles obtained from individual type strains were visually similar with similarity values ranging from 86 to 73 %. The dendrogram (Fig. S2) showed differentiation of strain CCM 4446^T from phylogenetically related strains of species of the genus *Rhodococcus*. The most similar fingerprint (86 % similarity) was that of *R. globerulus* CCM 8449^T.

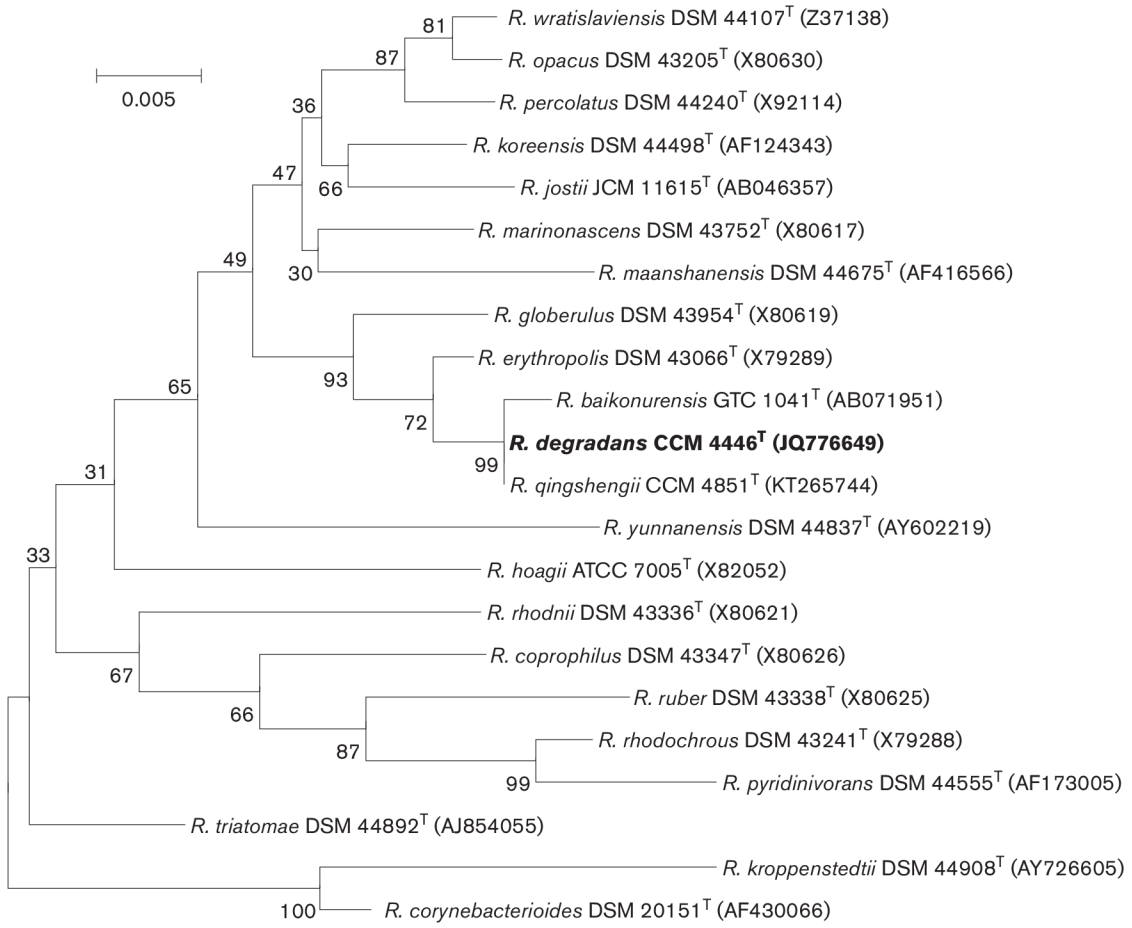

Fig. 1. Unrooted neighbour-joining tree based on 16S rRNA gene sequence comparisons showing the phylogenetic position of CCM 4446^T within the genus *Rhodococcus*. Bootstrap probability values (percentages of 1000 tree replications) are indicated at branch points. The evolutionary distances were computed using the maximum composite likelihood method. There were a total of 1338 positions in the final dataset. Bar, 0.005 substitutions per site.

High molecular mass genomic DNA for DNA–DNA hybridization experiments and DNA G+C content analysis was obtained using the protocol described by Gevers *et al.* (2001). The DNA G+C content of strain CCM 4446^T was determined using the HPLC method described by Mesbah & Whitman (1989) and was 63 mol %.

DNA–DNA hybridization between strain CCM 4446^T and the type strains representing the nearest phylogenetically neighbouring species was performed using the microplate method described by Ezaki *et al.* (1989), according to the protocols described previously (Cleenwerck *et al.*, 2002; Goris *et al.*, 1998). The hybridization temperature calculated from the G+C content of the strains analysed was 48 °C. The DNA–DNA relatedness percentages were calculated as means based on at least three independent hybridizations. Reciprocal reactions were performed and also considered as independent experiments. The standard deviation between reciprocal reactions was approximately 7 %, as reported by Goris *et al.* (1998). The DNA–DNA hybridization levels obtained between strain CCM 4446^T and *R. globerulus* CCM 8449^T, *R. baikonurensis* CCM 8450^T, *R. qingshengii* CCM 8451^T and *R. erythropolis* CCM 277^T were 18 %, 44 %, 47 % and 50 %, respectively. This confirmed that strain CCM 4446^T represented a different species. Similarly, the DNA–DNA hybridization values between *R. erythropolis* CCM 277^T, *R. globerulus* CCM 8449^T, *R. baikonurensis* CCM 8450^T and *R. qingshengii* CCM 8451^T ranged from 15 % to 46 %.

Quinones and polar lipids were extracted from freeze-dried biomass and analysed as described previously (Altenburger *et al.*, 1996; Stolz *et al.*, 2007; Tindall, 1990a, b). The quinone system of strain CCM 4446^T comprised menaquinone MK-8(H_2) as the predominant respiratory quinone (85 %), with minor amounts of MK-7(H_2) (9.4 %), MK-9(H_2) (3.3 %), MK-8 (1.6 %) and MK-7 (0.7 %). The major polar lipids detected in CCM 4446^T were diphosphatidylglycerol, phosphatidylethanolamine, one phosphatidylinositol-mannoside (PIM1), phosphtidylinositol and an

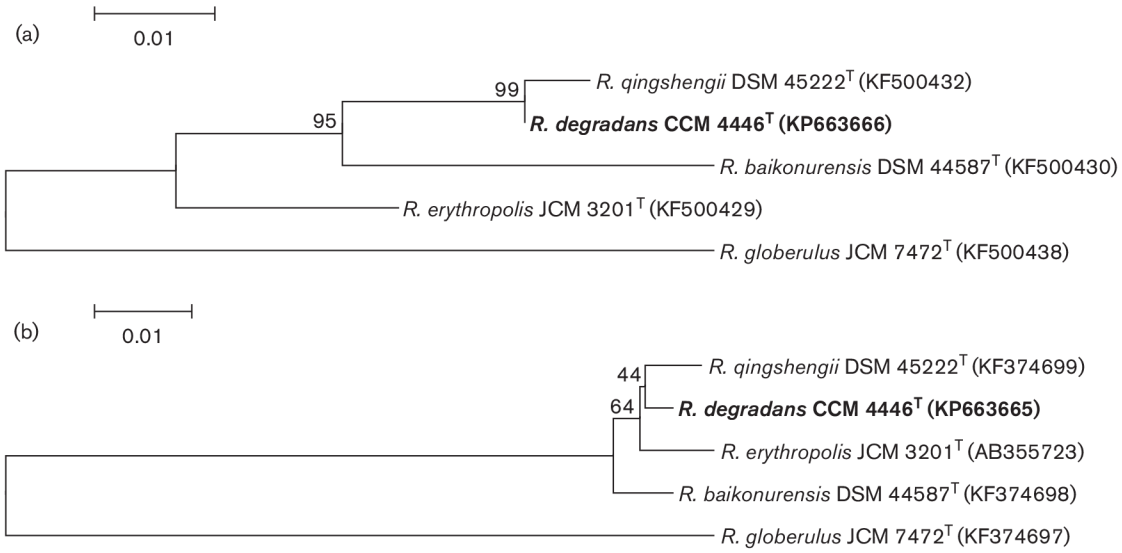

Fig. 2. Neighbour-joining trees reconstructed using partial nucleotide sequences of a) *catA* genes and b) *gyrB* genes showing the relationships of *R. degradans* CCM 4446^T and reference type strains of phylogenetically closely related species of the genus *Rhodococcus*. Bootstrap probability values (percentages of 10 000 tree replications) are indicated at branch points. The evolutionary distances were computed using the maximum composite likelihood method. There were a total of 1239 and 595 positions for *gyrB* and *catA*, respectively, in the final datasets. Bar, 0.01 substitutions per site.

unidentified glycolipid, GL1. Also, moderate amounts of the unidentified glycolipids, GL2 and GL3, and minor amounts of PIM2 and unidentified lipids (L1, L2 and L3) were detected (Fig. S3a). A similar polar lipid profile was detected in *R. qingshengii* CCM 8451^T, but in this strain only PIM1 was detectable and the glycolipids, GL1 and GL2, were absent. In addition two unidentified phospholipids, three polar lipids only detectable after total polar lipid staining (L4, L5 and L6) and one unidentified aminolipid were found (Fig. S3b), which were absent from strain CCM 4446^T. Hence the polar lipid profile distinguishes strain CCM 4446^T unambiguously from its nearest relative, *R. qingshengii* CCM 8451^T.

The diamino acid was determined according the method described by Schumann (2011). The diamino acid of the cell-wall peptidoglycan of strain CCM 4446^T was *meso*-diaminopimelic acid.

Mycolic acids were determined according to the method of Frischmann *et al.* (2012). The chromatographic motility of the mycolic acids of strain CCM 4446^T was slightly lower than that of *R. qingshengii* CCM 8451^T, but slightly higher than that of *Rhodococcus hoagii* DSM 20307 (formerly the type strain of *Rhodococcus equi*; Kämpfer *et al.*, 2014). Since *R. equi* was reported to contain mycolic acids consisting of 30–36 carbons (Klatte *et al.*, 1994) the number of carbons of the mycolic acids of CCM 4446^T is estimated to be 32–38.

Biomass for the detection of polyamines was harvested from the late exponential growth phase. Extraction and analysis was carried out according to Altenburger *et al.* (1996). Strain CCM 4446^T contained (all μmol g^{-1} dry weight) putrescine (0.1), spermidine (0.02), 1,3-diaminopropane (0.01), cadaverine (0.01), *sym*-homospermidine (0.01) and traces of spermine (<0.01). This pattern with very low polyamine content is similar to that reported for *Rhodococcus wratislaviensis* (Altenburger *et al.*, 1996) and a very low polyamine content was also detected in *R. qingshengii* CCM 8451^T (results not shown).

For cellular fatty acid analysis the strains were cultivated on BBL Trypticase Soy Agar plates (BD) at 28 °C for 24 h. The extraction procedure was performed according to Sasser (1990). The fatty acids were analysed by the Agilent 7890B gas chromatograph according to the standard protocol of the Sherlock MIDI Identification System (MIDI Sherlock version 6.2, MIDI database RTSBA 6.21). The fatty acid content of strain CCM 4446^T corresponded with those of phylogenetically related species (Table S1).

The phenotypic characteristics of the strains were determined using conventional tube or plate tests according to Atlas (2010) and MacFaddin (2000). Conventional test characteristics were supplemented with those of the API Coryne and API ZYM microtest systems (bioMérieux). Subsequently, phenotypic fingerprinting using the Biolog system with the Gram-positive identification test panel GP2 MicroPlate (Biolog) was performed to obtain more extensive phenotypic profiles. The phenotypic characteristics of CCM 4446^T are given in the species description.

Table 1. Characteristics differentiating *Rhodococcus degradans* sp. nov., from phylogenetically related species of the genus *Rhodococcus*

Strains: 1, *R. degradans* CCM 4446^T; 2, *R. baikonurensis* CCM 8450^T; 3, *R. erythropolis* CCM 277^T; 4, *R. globerulus* CCM 8449^T; 5, *R. qingshengii* CCM 8451^T. +, Positive; −, negative; w, weak reaction. All data were obtained in this study.

Characteristic	1	2	3	4	5
Nitrate reduction	−	−	−	+	−
Growth in 6.5 % (w/v) NaCl	+	+	+	−	−
Growth at 15 °C	+	+	+	+	−
Hydrolysis of tyrosine	−	w	−	−	w
Hydrolysis of DNA	w	−	w	−	−
Pyrazinamidase	−	+	−	+	w
Esterase (C4)	+	−	−	+	+
Acid from:					
D-Xylose	+	+	−	+	+
Cellobiose	+	+	−	−	+
Lactose	−	+	w	+	+
D-Mannitol	+	+	+	+	−

Strain CCM 4446^T can be differentiated from the type strains of phylogenetically closely related species using the tests listed in Table 1.

In summary, data from the present study showed that strain CCM 4446^T can be distinguished both genotypically and phenotypically from all species of the genus *Rhodococcus* with validly published names, which demonstrates that it represents a novel species within the genus *Rhodococcus*. We, therefore, propose classifying this strain as *Rhodococcus degradans* sp. nov., with strain CCM 4446^T (=LMG 28633^T) as the type strain.

Description of *Rhodococcus degradans* sp. nov.

Rhodococcus degradans (de.gra'dans L. part. adj. *degradans* returning to the original order, referring to the ability of the type strain to degrade several complex organic compounds).

Cells are Gram-stain-variable rods occurring predominantly in pairs and in irregular clusters, non-spore-forming. Aerobic. Colonies on Tryptone Soya agar (Oxoid) are circular with whole margins, flat, matt with pale salmon-pink pigment and reach 1–3 mm in diameter when cultivated at 30 °C for 48 h. No haemolytic activity on sheep blood agar. The species grows at 15 and 30 °C, but it is inhibited at 37 °C. Grows in the presence of 6.5 % (w/v) NaCl, but not in 10 % (w/v) NaCl. Catalase, urease, alkaline phosphatase, acid phosphatase, esterase (C4), esterase lipase (C8), leucine arylamidase, valine arylamidase, α-glucosidase, β-glucosidase and naphthol-AS-biphosphohydrolase-positive. Simmons citrate, DNase and cystine arylamidase are weakly positive. Aesculin and ONPG hydrolysis positive. Acid is aerobically produced from D-glucose, D-fructose, cellobiose, D-xylose, D-mannitol and myo-inositol when tested conventionally in a tube test, but these tests are negative in an API Coryne kit. Oxidase, arginine dihydrolase, pyrazinamidase, pyrrolidonyl arylamidase, lipase (C14), trypsin, chymotrypsin, α-galactosidase, β-galactosidase, β-glucuronidase, *N*-acetyl-β-glucosaminidase, α-mannosidase, α-fucosidase, acetamide, Voges–Proskauer test (acetoin) and nitrate reduction negative. Hydrolysis of Tween 80, gelatin, starch, casein, tyrosine and lecithine are negative. Acid is not produced from lactose. Carbon source utilization ability via respiration, determined in Biolog GP2 MicroPlate test panels, is positive for dextrin, Tween 40, Tween 80, D-fructose, D-gluconic acid, α-D-glucose, maltotriose, D-mannose, D-psicose, D-ribose, trehalose, acetic acid, α-hydroxy-butyric acid, α-ketovaleric acid, L-lactic acid, L-malic acid, pyruvatic acid methyl ester, succinic acid monomethyl ester, propionic acid, pyruvic acid, L-alaninamide, L-asparagine, glycyl-L-glutamic acid and glycerol. Negative utilization tests were for α-cyclodextrin, β-cyclodextrin, glycogen, inulin, mannan, *N*-acetyl-D-glucosamine, *N*-acetyl-β-D-mannosamine, amygdalin, L-arabinose, D-arabitol, arbutin, L-fucose, D-galactose, D-galacturonic acid, gentiobiose, m-inositol, α-lactose, lactulose, maltose, D-mannitol, melezitose, melibiose, α-methyl-D-galactoside, β-methyl-D-galactoside, 3-methyl glucose, α-methyl-D-glucoside, β-methyl-D-glucoside, α-methyl-D-mannoside, palatinose, raffinose, L-rhamnose, salicin, sedoheptulosan, D-sorbitol, stachyose, sucrose, D-tagatose, turanose, xylitol, D-xylose, β-hydroxy-butyric acid, γ-hydroxy-butyric acid, *p*-hydroxy phenylacetic acid, α-ketoglutaric acid, lactamide, D-lactic acid methyl ester, D-malic acid, succinamic acid, succinic acid, D-alanine, L-alanine, L-alanyl-glycine, L-glutamic acid, L-pyroglutamic acid, L-serine, putrescine, 2,3-butanediol, adenosine, 2′-deoxyadenosine, inosine, thymidine, uridine, adenosine-5′-monophosphate, thymidine-5′-monophosphate, uridine-5′-monophosphate, D-fructose-6-phosphate, α-D-glucose-1-phosphate, D-glucose-6-phosphate and DL-α-glycerol-phosphate. Borderline reactions were revealed for the utilization of cellobiose and *N*-acetyl-L-glutamic acid.

Polyamine concentrations are very low consisting of putrescine, spermidine, 1,3-diaminopropane, cadaverine, *sym*-homospermidine (0.01) and spermine. The quinone system contains predominantly menaquinone MK-8(H_2), lesser amounts of MK-7(H_2), MK-9(H_2), MK-8 and MK-7. The major polar lipids are diphosphatidylglycerol, phosphatidylethanolamine, one phosphatidylinositol-mannoside, phosphatidylinositol and one unidentified glycolipid. In addition, moderate amounts of two unidentified glycolipids and minor amounts of phosphatidylinositol-mannoside and three unidentified lipids are present. Mycolic acids are present consisting of approximately 32–38 carbons. The major fatty acids (>3 %) are $C_{16:0}$ (31.7 %), $C_{18:1}\omega9c$ (31.2 %), Summed Feature 3 ($C_{16:1}\omega7c$ and/or $C_{16:1}\omega6c$) (13.3 %), $C_{18:0}$ 10 methyl (TSBA) (11.6 %), and $C_{14:0}$ (3.8 %).

The type strain CCM 4446^T (=LMG 28633^T) was isolated from soil in Switzerland. The DNA G+C content of the type strain is 63 mol %.

Acknowledgements

This work was supported by the Ministry of Education, Youth and Sports of the Czech Republic projects CZ.1.07/2.3.00/20.0183 and Specific University Research (SGS no. SP2015/31).

References

Altenburger, P., Kämpfer, P., Makristathis, A., Lubitz, W. & Busse, H.-J. (1996). Classification of bacteria isolated from a medieval wall painting. *J Biotechnol* **47**, 39–52.

Atlas, R. M. (2010). *Handbook of Microbiological Media*, 4th edn. New York: CRC Press, Taylor & Francis Group.

Bell, K. S., Philp, J. C., Aw, D. W. J. & Christofi, N. (1998). The genus *Rhodococcus*. *J Appl Microbiol* **85**, 195–210.

Cleenwerck, I., Vandemeulebroecke, K., Janssens, D. & Swings, J. (2002). Re-examination of the genus *Acetobacter*, with descriptions of *Acetobacter cerevisiae* sp. nov. and *Acetobacter malorum* sp. nov. *Int J Syst Evol Microbiol* **52**, 1551–1558.

Damborský, J. & Koča, J. (1999). Analysis of the reaction mechanism and substrate specificity of haloalkane dehalogenases by sequential and structural comparisons. *Protein Eng* **12**, 989–998.

Damborský, J., Nyandoroh, M. G., Němec, M., Holoubek, I., Bull, A. T. & Hardman, D. J. (1997). Some biochemical properties and the classification of a range of bacterial haloalkane dehalogenases. *Biotechnol Appl Biochem* **26**, 19–25.

de Carvalho, C. C., Costa, S. S., Fernandes, P., Couto, I. & Viveiros, M. (2014). Membrane transport systems and the biodegradation potential and pathogenicity of genus *Rhodococcus*. *Front Physiol* **5**, 133.

Ezaki, T., Hashimoto, Y. & Yabuuchi, E. (1989). Fluorometric deoxyribonucleic acid-deoxyribonucleic acid hybridization in microdilution wells as an alternative to membrane filter hybridization in which radioisotopes are used to determine genetic relatedness among bacterial strains. *Int J Syst Bacteriol* **39**, 224–229.

Frischmann, A., Knoll, A., Hilbert, F., Zasada, A. A., Kämpfer, P. & Busse, H.-J. (2012). *Corynebacterium epidermidicanis* sp. nov., isolated from skin of a dog. *Int J Syst Evol Microbiol* **62**, 2194–2200.

Gevers, D., Huys, G. & Swings, J. (2001). Applicability of rep-PCR fingerprinting for identification of *Lactobacillus* species. *FEMS Microbiol Lett* **205**, 31–36.

Goris, J., Suzuki, K., De Vos, P., Nakase, T. & Kersters, K. (1998). Evaluation of a microplate DNA-DNA hybridization method compared with the initial renaturation method. *Can J Microbiol* **44**, 1148–1153.

Janáková, I. & Vojtková, H. (2012). Application of flotation and biodegradation to eliminate persistent organic pollutants in the influent stream of Cerny Prikop. In *Microbes in Applied Research*, pp. 28–32. Edited by A. Mendez-Vilas. Singapore: World Scientific Publishing.

Jones, A. L. & Goodfellow, M. (2012). Genus IV. *Rhodococcus* (Zopf 1891) emend. Goodfellow, Alderson and Chun 1998a. In *Bergey's Manual of Systematic Bacteriology, The Actinobacteria, Part A*, **vol. 5**, pp. 437–464. Edited by W. Whitman, M. Goodfellow, P. Kämpfer, H.-J. Busse, M. E. Trujillo, W. Ludwig, K.-i. Suzuki & A. Parte. New York: Springer.

Kämpfer, P., Dott, W., Martin, K. & Glaeser, S. P. (2014). *Rhodococcus defluvii* sp. nov., isolated from wastewater of a bioreactor and formal proposal to reclassify [*Corynebacterium hoagii*] and *Rhodococcus equi* as *Rhodococcus hoagii* comb. nov. *Int J Syst Evol Microbiol* **64**, 755–761.

Kašáková, H., Vojtková, H. & Jablonka, R. (2012). Biodegradation of oil sludge using bacterial organisms. In *12th International Multidisciplinary Scientific GeoConference SGEM*, SGEM Conference Proceedings, vol. 2. Sofia STEF92 Technology, pp. 435–440. Albena, Bulgaria: IJSEM.

Klatte, S., Kroppenstedt, R. M. & Rainey, F. A. (1994). *Rhodococcus opacus* sp. nov., an unusual nutritionally versatile *Rhodococcus* species. *Syst Appl Microbiol* **17**, 355–360.

Lang, S. & Philp, J. C. (1998). Surface-active lipids in *rhodococci*. *Antonie van Leeuwenhoek* **74**, 59–70.

MacFaddin, J. F. (2000). *Biochemical Tests for Identification of Medical Bacteria*, 3rd edn. USA: Lippincott Williams & Wilkins.

Martínková, L., Uhnáková, B., Pátek, M., Nešvera, J. & Křen, V. (2009). Biodegradation potential of the genus *Rhodococcus*. *Environ Int* **35**, 162–177.

Mesbah, M. & Whitman, W. B. (1989). Measurement of deoxyguanosine/thymidine ratios in complex mixtures by high-performance liquid chromatography for determination of the mole percentage guanine + cytosine of DNA. *J Chromatogr A* **479**, 297–306.

Poelarends, G. J., Zandstra, M., Bosma, T., Kulakov, L. A., Larkin, M. J., Marchesi, J. R., Weightman, A. J. & Janssen, D. B. (2000). Haloalkane-utilizing *Rhodococcus* strains isolated from geographically distinct locations possess a highly conserved gene cluster encoding haloalkane catabolism. *J Bacteriol* **182**, 2725–2731.

Roach, P. C. J., Ramsden, D. K., Hughes, J. & Williams, P. (2003). Development of a conductimetric biosensor using immobilised *Rhodococcus ruber* whole cells for the detection and quantification of acrylonitrile. *Biosens Bioelectron* **19**, 73–78.

Sasser, M. (1990). *Identification of bacteria by gas chromatography of cellular fatty acids*, MIDI Technical Note 101. Newark, DE: MIDI Inc.

Scholtz, R., Leisinger, T., Suter, F. & Cook, A. M. (1987a). Characterization of 1-chlorohexane halidohydrolase, a dehalogenase of wide substrate range from an *Arthrobacter* sp. *J Bacteriol* **169**, 5016–5021.

Scholtz, R., Schmuckle, A., Cook, A. M. & Leisinger, T. (1987b). Degradation of eighteen 1-monohaloalkanes by *Arthrobacter* sp. strain HA1. *J Gen Microbiol* **133**, 267–274.

Scholtz, R., Messi, F., Leisinger, T. & Cook, A. M. (1988). Three dehalogenases and physiological restraints in the biodegradation of haloalkanes by *Arthrobacter* sp. strain HA1. *Appl Environ Microbiol* **54**, 3034–3038.

Schumann, P. (2011). Peptidoglycan structure. In *Taxonomy of Prokaryotes, Methods in Microbiology*, **vol. 38**, pp. 101–129. Edited by F. Rainey & A. Oren. London: Academic Press.

Stolz, A., Busse, H.-J. & Kämpfer, P. (2007). *Pseudomonas knackmussii* sp. nov. *Int J Syst Evol Microbiol* **57**, 572–576.

Tamura, K., Stecher, G., Peterson, D., Filipski, A. & Kumar, S. (2013). MEGA6: molecular evolutionary genetics analysis version 6.0. *Mol Biol Evol* **30**, 2725–2729.

Táncsics, A., Benedek, T., Farkas, M., Máthé, I., Márialigeti, K., Szoboszlay, S., Kukolya, J. & Kriszt, B. (2014). Sequence analysis of 16S rRNA, *gyr*B and *cat*A genes and DNA-DNA hybridization reveal that *Rhodococcus jialingiae* is a later synonym of *Rhodococcus qingshengii*. *Int J Syst Evol Microbiol* **64**, 298–301.

Tindall, B. J. (1990a). Lipid composition of *Halobacterium lacusprofundi*. *FEMS Microbiol Lett* **66**, 199–202.

Tindall, B. J. (1990b). A comparative study of the lipid composition *of Halobacterium saccharovorum* from various sources. *Syst Appl Microbiol* **13**, 128–130.

Vojtková, H., Mašlaňová, I., Sedláček, I., Švanová, P. & Janulková, R. (2012). Removal of heavy metals from wastewater by a *Rhodococcus* sp. bacterial strain. In *12th International Multidisciplinary Scientific GeoConference SGEM*, SGEM Conference Proceedings, vol. 5. Sofia STEF92 Technology. pp. 685–691. Albena, Bulgaria.

Warhurst, A. M. & Fewson, C. A. (1994). Biotransformations catalyzed by the genus *Rhodococcus*. *Crit Rev Biotechnol* **14**, 29–73.

International Journal of Systematic and Evolutionary Microbiology

Classification of strain CCM 4446^T as *Rhodococcus degradans* sp. nov.

Supplementary Data

Pavel Švec[1,*], Jitka Černohlávková[1], Hans-Jürgen Busse[2], Hana Vojtková[3], Roman Pantůček[4], Margo Cnockaert[5], Ivana Mašlaňová[4], Stanislava Králová[1], Peter Vandamme[5], Ivo Sedláček[1]

[1]Czech Collection of Microorganisms, Department of Experimental Biology, Faculty of Science, Masaryk University, Kamenice 5, Bld. A25, 625 00 Brno, Czech Republic

[2]Institute for Microbiology, Veterinary University Vienna, Veterinärplatz 1, A-1210 Vienna, Austria

[3]Faculty of Mining and Geology, Institute of Environmental Engineering, VŠB – Technical University of Ostrava, 17 listopadu 15/2172, 708 33 Ostrava – Poruba, Czech Republic

[4]Division of Genetics and Molecular Biology, Department of Experimental Biology, Faculty of Science, Masaryk University, Kotlářská 2, 611 37 Brno, Czech Republic

[5]Department of Biochemistry and Microbiology, Faculty of Sciences, Ghent University, K.L. Ledeganckstraat 35, 9000 Ghent, Belgium

*Corresponding author:
Pavel Švec: E-mail: mpavel@sci.muni.cz; Tel.: +420 - 549 497 601

Table S1. Cellular fatty acid composition (as a percentage of the total) of strain CCM 4446^T and type strains of related *Rhodococcus* spp.

Species: 1, *R. degradans* CCM 4446^T; 2, *R. baikonurensis* CCM 8450^T; 3, *R. erythropolis* CCM 277^T; 4, *R. globerulus* CCM 8449^T; 5, *R. qingshengii* CCM 8451^T. All data were obtained in this study. Values of less than 1 % are not shown. TR, trace amounts (< 1%); ND, not detected.

Fatty acid	1	2	3	4	5
$C_{14:0}$	3.8	5.4	5.0	2.8	5.9
$C_{16:1}\omega9c$	TR	ND	ND	3.1	ND
$C_{16:1}\omega7c/C_{16:1}\omega6c$*	13.3	20.1	17.8	10.1	10.8
$C_{16:0}$	31.7	25.8	27.1	28.7	30.3
$C_{17:1}\omega8c$	TR	3.8	2.6	1.2	2.4
$C_{17:0}$	TR	1.2	TR	1.5	1.8
$C_{17:0}$ 10 methyl	TR	1.1	TR	TR	TR
$C_{18:1}\omega9c$	31.2	26.6	27.4	36.2	32.6
$C_{18:0}$	2.8	1.3	1.1	6.8	7.7
$C_{18:0}$ 10 methyl (TBSA†)	11.6	10.9	13.6	5.9	5.7
$C_{19:1}\omega11c/C_{19:1}\omega9c$‡	TR	1.3	1.7	ND	TR
$C_{19:1}\omega7c/C_{19:1}\omega6c$§	TR	TR	TR	1.8	TR

*Summed feature 3; †Tuberculostearic acid; ‡Summed feature 6; §Summed feature 7

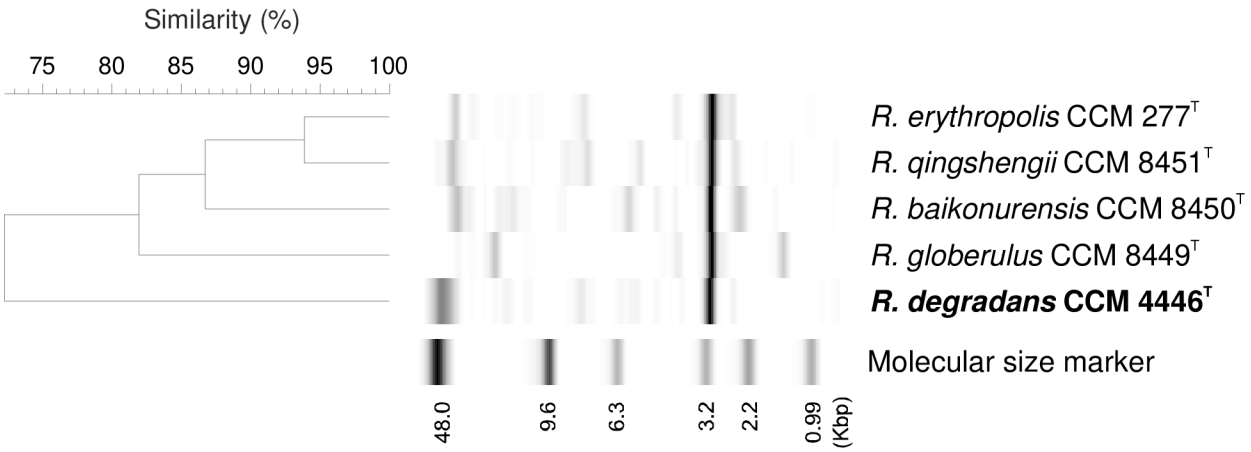

Fig. S1. Dendrogram based on cluster analysis of *Eco*RI ribotype patterns obtained using the RiboPrinter system from *Rhodococcus degradans* CCM 4446^T and the type strains of the phylogenetically related *Rhodococcus* species. The dendrogram was calculated with Pearson's correlation coefficients with UPGMA clustering method (*r*, expressed as percentage similarity values).

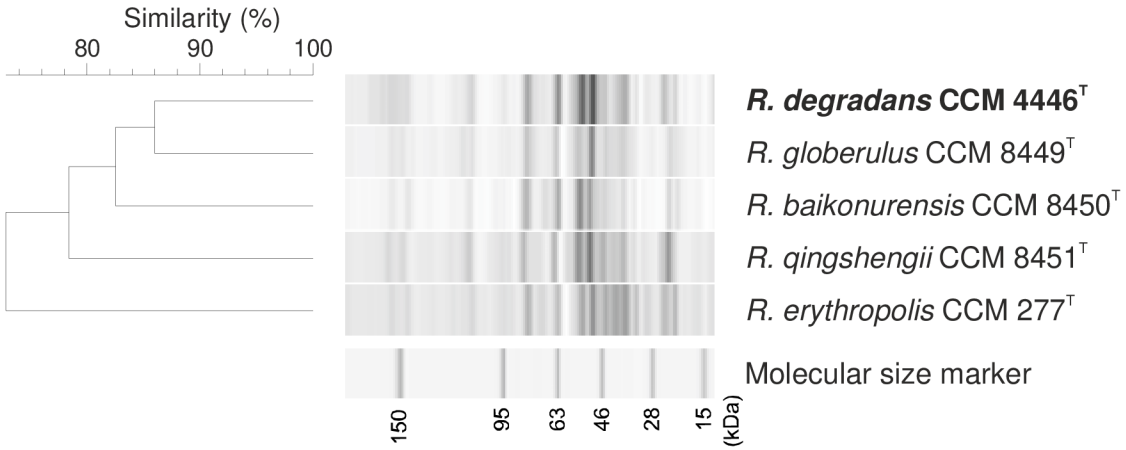

Fig. S2. Dendrogram based on cluster analysis of whole-cell protein profiles obtained using the Agilent 2100 Bioanalyzer system with the Protein 230 kit (Agilent Technologies) from *Rhodococcus degradans* CCM 4446^T and the type strains of the phylogenetically related *Rhodococcus* species. The dendrogram was calculated with Pearson's correlation coefficients with UPGMA clustering method (*r*, expressed as percentage similarity values).

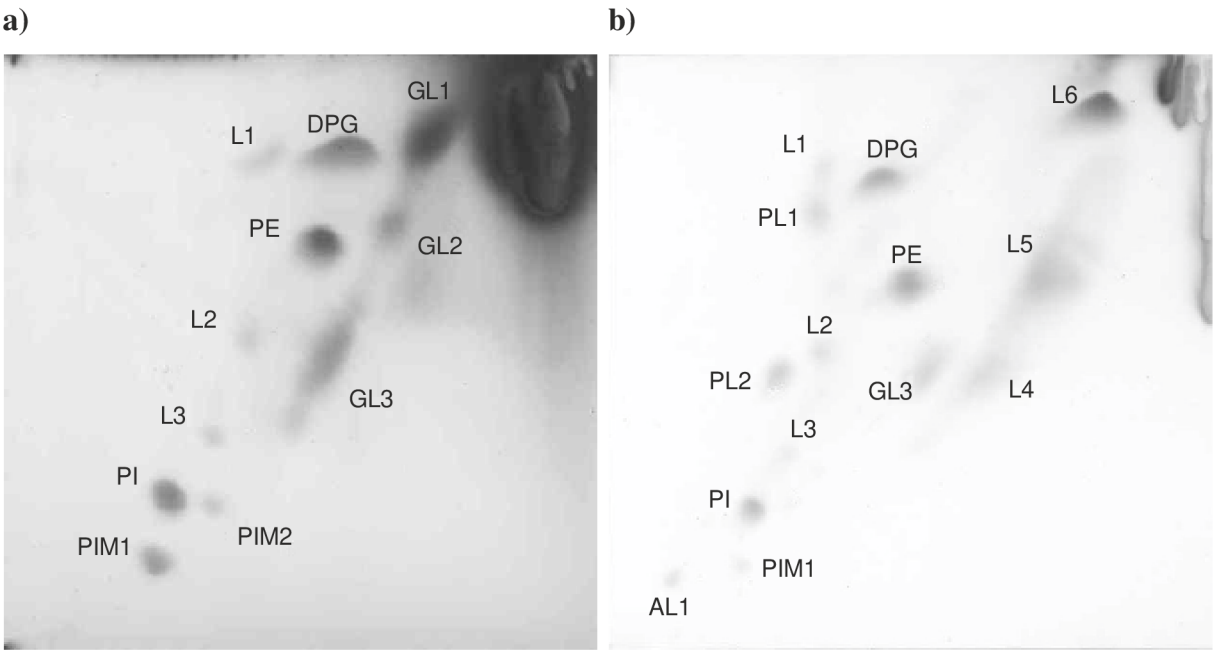

Fig. S3. Two-dimensional thin layer chromatogram of polar lipids from **a)** *Rhodococcus degradans* CCM 4446^{T} and **b)** *Rhodococcus qingshengii* CCM 8451^{T}. DPG, diphosphatidylglycerol; PE, phosphatidylethanolamine; PIM1-2, phosphatidylinositolmannosides; PI, phosphatidylinositol; PL1-2; unidentified phospholipids; AL1, unidentified aminolipid; GL1 - 3, unidentified glycolipids; L1 - 6, unidentified lipids not containg a sugar moiety, an amino group or a phosphate group.

Príloha č. 8.

Pantůček R., Sedláček I., Indráková A., Vrbovská V., Mašlaňová I., Kovařovic V., Švec P., Králová S., Krištofová L., Kekláková J., Petráš P., Doškař J. (zaslané do redakcie). *Staphylococcus edaphicus* sp. nov., isolated in Antarctica, harbours *mecC* gene and genomic islands essential to adaptation to extreme environment. *Appl. Environ. Microbiol.* Rukopis č. AEM01746-17.

Staphylococcus edaphicus sp. nov., isolated in Antarctica, harbours *mecC* gene and genomic islands essential to adaptation to extreme environment

Roman Pantůček[1,*], Ivo Sedláček[2,*], Adéla Indráková[1], Veronika Vrbovská[1,2], Ivana Mašlaňová[1], Vojtěch Kovařovic[1], Pavel Švec[2], Stanislava Králová[2], Lucie Krištofová[2], Jana Kekláková[3], Petr Petráš[3], Jiří Doškař[1]

*These authors contributed equally to this work

[1] Division of Genetics and Molecular Biology, Department of Experimental Biology, Faculty of Science, Masaryk University, Kotlářská 2, 611 37 Brno, Czech Republic

[2] Czech Collection of Microorganisms, Department of Experimental Biology, Faculty of Science, Masaryk University, Kamenice 5, 625 00 Brno, Czech Republic

[3] Reference Laboratory for Staphylococci, National Institute of Public Health, Šrobárova 48, 100 42 Praha 10, Czech Republic

Address correspondence to Roman Pantucek, pantucek@sci.muni.cz.

KEYWORDS

coagulase-negative staphylococci, methicillin resistance, genomics, polyphasic taxonomy, pathogenicity islands, drug resistance evolution

ABSTRACT

Two Gram-stain-positive, coagulase-negative staphylococcal strains were isolated from abiotic sources, stone fragments and sandy soil in James Ross Island, Antarctica. Here we describe properties of novel species of the genus *Staphylococcus* that has near identical 16S rRNA gene sequence to *Staphylococcus saprophyticus*. However, compared to *S. saprophyticus* and the next closest relatives, the new species demonstrates considerable phylogenetic distance at whole genome level, average nucleotide identity <85%, and inferred DNA–DNA hybridization <30%. It forms a separate branch in *S. saprophyticus* phylogenetic clade confirmed by multilocus sequence analysis of six housekeeping genes *rpoB*, *hsp60*, *tuf*, *dnaJ*, *gap*, and *sod*. MALDI-TOF MS and key biochemical characteristics allowed these bacteria to be distinguished from their nearest phylogenetic neighbours. In contrast to *S. saprophyticus* subsp. *saprophyticus*, strains were pyrrolidonyl arylamidase- and β-glucuronidase-positive, β -galactosidase-negative, nitrate was reduced and acid produced aerobically from D-mannose. Whole genome sequencing of 2.75 Mb large chromosome revealed the presence of a number of mobile genetic elements including the 27-kb-long pseudo staphylococcus cassette chromosome *mec* (ψSCC*mec*$_{P5085}$) harboring *mecC* gene, two composite phage-inducible chromosomal islands essential to adaptation to extreme environment, and one complete and one defective prophage. Both strains are resistant to penicillin G, ampicillin, ceftazidin, methicillin, cefoxitin, and fosfomycin. We hypothesize that antibiotic resistance might represent an evolutionary advantage against beta-lactams producers, which are common in a polar environment. Based on these results, a novel species of the genus *Staphylococcus* is described and named *Staphylococcus edaphicus* sp. nov. The type strain is P5085^T (=CCM 8730^T = DSM 104441^T).

IMPORTANCE

The description of *Staphylococcus edaphicus* sp. nov. enables the comparison of multidrug-resistant staphylococci from human and veterinary sources evolved in the globalized world to their geographically distant relative from the extreme Antarctic environment. Although this new species was not exposed to the pressure of antibiotic treatment in human or veterinary practice, mobile genetic elements carrying antimicrobial resistance genes were found in the genome. The presented genomic characteristics elucidate the evolutionary relationships in the *Staphylococcus* genus with a special focus on antimicrobial resistance, pathogenicity and survival traits. Genes encoded on mobile genetic elements were arranged in unique combinations but retained conserved locations for the integration of mobile genetic elements. These findings point to enormous plasticity of the staphylococcal pangenome shaped by horizontal gene transfer. Thus the soil bacterium *S. edaphicus* can act not only as a reservoir of antibiotic resistance in a natural environment, but also as a mediator for the spread and evolution of resistance genes.

INTRODUCTION

Members of the genus *Staphylococcus* are widespread in nature and occupy a variety of niches (1). As a result of their ubiquity and adaptability, staphylococci are a major group of bacteria inhabiting the skin, skin glands, and mucous membranes of humans, other mammals, and birds. Most environmental sources also contain small, transient populations of staphylococci, many of which are probably contaminants disseminated by human, other mammal, or bird host carriers (2, 3). Moreover, *Staphylococcus succinus* subsp. *succinus* was isolated from plant and soil inclusions in Dominican amber (4). Recently, *Staphylococcus argensis* was isolated from river sediments (5). A small number of species such as *Staphylococcus xylosus* and *Staphylococcus sciuri* have been occasionally isolated from soil, beach sand, natural waters, and also from plants (1, 6, 7). They can grow in habitats containing only an inorganic nitrogen source, and thus might be capable of a free-living existence.

The ubiquity of *S. xylosus* might be explained by its ability to adapt to different environments. Its capacity to colonize biotic and abiotic surfaces is probably due to its ability to form a biofilm (8) and genes implicated in ecological fitness (9). It has been considered a non-pathogenic commensal organism (10) and has rarely been reported to be associated with infections (11). On the other hand *Staphylococcus saprophyticus*, the closest phylogenetic relative of *S. xylosus*, is an important opportunistic pathogen, causing human urinary tract infections, wound infections and septicaemia (12). The host range of *S. saprophyticus* varies from humans to lower mammals and birds (6, 13). It has been isolated from the gastrointestinal tract of both humans and animals, as well as from meat and cheese products, vegetables and from the environment (14).

The aim of this study was to investigate the genomic properties and clarify the taxonomic position of two coagulase-negative staphylococcal isolates belonging to *S. saprophyticus* phylogenetic clade that could not be identified to the species level by common diagnostic techniques. The isolates are notable due to their origin from the Antarctic environment and resistance to beta-lactam antibiotics encoded by a novel ψSCC*mec* element.

RESULTS AND DISCUSSION

Two Gram-stain positive isolates were obtained as a by-product in the framework of a project monitoring psychrotolerant bacteria of the phylum *Bacteroidetes* from abiotic sources in James Ross Island, Antarctica (CzechPolar2 project). Strain P5085^T (=CCM 8730^T) was isolated from stone fragments sampled from a hill above Lachman Cape (GPS coordinates 63°46'58"S 57°47'11"W), and strain P5191 (=CCM 8731) was isolated from sandy soil in the Panorama Pass locality (GPS coordinates 63°48'51"S 57°50'45"W). The preliminary identification by sequencing of the 16S rRNA gene assigned both isolates to the *Staphylococcus saprophyticus* species group defined by Takahashi *et al.* (15). The whole genomic sequence of the *S. saprophyticus* type strain (16) even exhibited

indistinguishability from the strain CCM 8730^T 16S rRNA gene in two *rrn* operons and only 1 residue difference (positions 190, 278 or 457) in the others. However, the obtained phenotypic results listed in the species description given below did not include isolates of any known staphylococcal species. The key characteristics differentiating the novel taxon represented by strain CCM 8730^T from the phylogenetically closely related species are shown in Table 1.

The strains were analysed by MALDI-TOF MS and yielded profiles containing signals in the mass range 2 - 15 kDa. They did not exhibit significant similarity (BioTyper log(score) > 1.7) to any of the reference entries belonging to *Staphylococcus* species with valid names included in the BioTyper database version 5989 (Bruker Daltonics) and proved *S. saprophyticus* to be the closest relative (Fig. S1).

Three DNA fingerprinting techniques were used to show the differences between the isolates and similarity to related taxa. Repetitive sequence-based PCR (rep-PCR) fingerprinting using the $(GTG)_5$ primer (Fig. S2) and automated ribotyping with the *Eco*RI restriction enzyme (Fig. S3) showed a high genetic similarity between strains CCM 8730^T and CCM 8731, because they gave visually identical fingerprints. At the same time, both DNA fingerprinting techniques also clearly differentiated analysed strains from the type strains representing the phylogenetically close *Staphylococcus* spp. The strains CCM 8730^T and CCM 8731 were also undistinguishable by *Sma*I macrorestriction analysis resolved by PFGE (Fig. S4).

The fatty acid content of strain CCM 8730^T corresponded with that of phylogenetically related species (Table S1). The fatty acid composition of strains CCM 8730^T and CCM 8731 was found to be very similar. The major fatty acids (> 10%) were $C_{15:0}$ anteiso (51.4%), $C_{15:0}$ iso (13.3%) and $C_{17:0}$ anteiso (12.9%). $C_{15:0}$ and $C_{15:0}$ anteiso, were found to be major fatty acids in all members of the *S. saprophyticus* species group. The amount of $C_{17:0}$ anteiso slightly differed between members of this group, only reaching the highest value of 10% in the CCM 8730^T and CCM 8731 strains, and both subspecies of *S. saprophyticus*. The overall content of other fatty acids was found to be comparable in this clade, with the exception of the *S. succinus* type strain, where $C_{13:0}$ iso and $C_{13:0}$ anteiso were found to be predominant as well (4).

The genome of the strain CCM 8730^T was shot-gun sequenced and the contigs were compared with *S. saprophyticus* ATCC 15305^T and *S. xylosus* CCM 2738^T whole genome sequences (Fig. 1). The size of the draft genome of CCM 8730^T is 2.75 Mb, comprised of 63 contigs with an average G+C content of 33.3 mol%. A total of 2645 genes were predicted. Analysis of the genes identified 2 608 orthologous clusters and singletons. The majority of clusters, up to 2264, are shared with either *S. xylosus* or *S. saprophyticus* (Fig. 2). There are 16 unique clusters, including 39 ORFs and 328 unique singletons localized mainly on variable genetic elements such as the pseudo *Staphylococcus* cassette chromosome *mec* (ψSCC*mec*), two composite phage-inducible chromosomal islands (PICIs), one

complete and one defective prophage (Fig. 1). High heterogeneity in the gene composition compared to related species was detected in the region following ψSCC*mec.* Genes were found for a restriction modification system type II homologous to *Sau*3AI, a thiamine biosynthesis operon, and two predicted protein-coding genes with an LPXTG motif, putative cell anti-adhesin Pls and cardiolipin synthase. The *pls* gene has been associated with virulence (18) and it has been found adjacent to SCCs present in other staphylococci (19). Cardiolipin synthesis can enhance cell survival under acid or salinity stress conditions (20, 21) and mutations in this gene enhance resistance to daptomycin (22).

The 27,158-bp-long pseudo *Staphylococcus* cassette chromosome *mec* (ψSCC*mec*$_{P5085}$) element bordered by imperfectly matched 27-bp-long direct repeats, CCGCATCACTTGTGATA[C/T]GCTTC[C/T]CCC, was identified inserted between the *rlmH* gene encoding rRNA-methyltransferase and the gene for putative threonyl-tRNA synthetase. This ψSCC*mec* contains *mec* gene complex class E (*blaZ-mecC-mecR1-mecI*) reflecting the corresponding IWG-SCC designation (23) and it lacks recombinase genes (*ccr*) or their homologues (Fig. 3). The *mecC* gene shares 99% nucleotide identity with that of *S. aureus* LGA251 (24) and 93% nucleotide identity with the *mecC1* gene of *S. xylosus* S04009 (25) or with the *mecC2* of *S. saprophyticus* 210 (26). Apart from human and livestock staphylococcal isolates (24), the *mecC* gene was previously identified in isolates from wildlife such as birds and mammals (27-29), and in waste and river waters (30, 31), but to our knowledge this is the first time the *mecC* gene was identified in an isolate from soil.

Besides the *mecC* gene, very few genes were conserved among ψSCC*mec*$_{P5085}$ and related SCCs, localized mainly in the *mec* gene complex (Fig. 3). This implies that SCC elements might serve for foreign DNA integration and exchange as suggested for other genomic islands. Downstream of the *mec* gene complex of ψSCC*mec*$_{P5085}$ there are 28 predicted ORFs encoding kinase, hydrolase, oxidoreductase, transcriptional regulators, and several hypothetical proteins, whose homologs were identified predominantly in coagulase-negative staphylococcal species. Furthermore, in the ψSCC*mec*$_{P5085}$ two intact and one truncated *lpl* genes coding for tandem lipoprotein-like proteins that are usually found in νSaα genomic islands (32) were identified. Under certain nutrient limitations and environmental conditions, lipoproteins may be crucial for ion and nutrient transport allowing growth and survival (33).

Noticeably lower G+C content below 29 mol% clearly leads to the identification of two genomic islands (Fig. 1). Both islands resemble the *Staphylococcus aureus* pathogenicity islands (SaPIs). They carry genes necessary for the transfer of the element, namely integrase, primase, terminase, and transcriptional regulators usually found in PICIs (34). However, the two genomic islands are much longer than SaPIs. The first genomic island, designated νSed1 and found in CCM 8730^{T}, is approximately 45 kb long with more than 70 predicted ORFs. The island is integrated into

the tmRNA gene within the attachment sequence site TCCCGCCGTCTCCA[T/C]TATAGAGTCTGCAACC[C/-]AT[T/-]GTGGTTGTGGGCTTTTTATTTTTG that corresponds to the attachment site of SaPIm/νSa3 (35). Two additional copies of the *att* site were found in this island, thus dividing the element into three parts. The first part is 17.9 kb long and it resembles canonical SaPI (νSa3) in its gene composition (36). It encodes integrase and genes necessary for the transfer, *fosB/fosD* fosfomycin resistance gene homologue (91% amino acid identity with *fosB/fosD* family of *S. saprophyticus*) and several proteins of unknown function. So far only plasmid-borne fosfomycin resistance genes have been detected in *Staphylococcus* sp., though the possible localization of the *fosB* on other mobile genetic elements has been discussed (37). The second 15.4-kb-long part of the νSed1 is comprised of phage- and SaPI-(νSa2) related genes, but no integrase has been found. It also carries a remnant of the *fosB* gene and other genes of unknown function. The last part of νSed1 is 11.7 kb with an indistinct left border, because the bracketing sequence of the *att* site is absent. This part consists of genes encoding resistance to arsenic, cadmium, and bleomycin, hypothetical proteins, and a few phage-related genes, such as the transcriptional regulator from the *cro/cI* family, which controls the switch between the lytic and lysogenic cycle of bacteriophages. The mosaic organization of islands suggests that more than one integration event occurred in the locus.

The second genomic island designated νSed2 is about 30 kb with more than 45 predicted ORFs. The attachment site TATATTATTCCCACTCGAT of νSed2 is located within the glutamine-hydrolyzing GMP synthase gene, which matches the attachment site for SaPIbov1/νSa2 (35, 38). This genomic island also enhances the resistance and endurance of the host, because it codes for transporters and transcriptional regulators involved in antibiotic resistance, oxidative stress responses and the synthesis of virulence factors. It also contains the *cspC* gene for cold shock protein C, which has been found to be expressed strongly after antibiotic, arsenate, and peroxide induction (39). In addition, many insertion sequences from the *IS*3 and *IS*1182 family were found in this genomic island.

A prophage designated ϕSED1 located downstream of $tRNA_{Leu}$ gene was identified. The prophage is 44,424 bp long with an average G+C content of 33.36 mol%, which is comparable to the G+C content of the CCM 8730^T strain. The direct repeats of the phage *att* site ATCCCGACCACCGGTAT flank 67 ORFs encoding essential phage genes, which cluster together into functional modules corresponding to staphylococcal *Siphoviridae* (40). The lysogeny module starts with phage integrase, which has a tyrosine recombinase XerD domain, AP2-like DNA binding domain, and N-terminal SAM-like domain. There are genes in the DNA replication and transcription regulation modules encoding a DNA primase, helicase, HNH endonuclease domain protein, and putative single-stranded binding protein. The DNA packaging and head and tail morphogenesis modules share 78% nucleotide identity with a StB20 phage infecting *Staphylococcus capitis* (41). The

holin and amidase from the lysis module exhibit high amino acid identity to *S. saprophyticus* prophage holins and amidases, 95 - 99% and 77 - 85%, respectively. The last encoded protein downstream of the lysis module is a glycosyltransferase family 2 protein. The prophage does not carry any genes encoding tRNA or virulence factors. Another, however, incomplete ϕSED2 prophage 9241 bp long bordered by TAGTGTCCTGGGAGG direct repeats was found in the CCM 8730^T genome. This prophage has an average G+C content of 30.73 mol%, lower than its host.

Although the strain CCM 8730^T comes from a geographically isolated polar environment, it carries genes for a surprisingly high number of antimicrobial resistance factors. Its resistance to beta-lactam antibiotics was unexpected. The class E *mec* complex coding for a beta-lactamase and alternative penicillin-binding MecC protein that is more stable and active at lower temperatures than the MecA protein (42) might represent an evolutionary advantage against beta-lactams producers, which are common in a polar environment. McRae *et al.* (43) documented that penicillia are major decomposers and represent an important element of the terrestrial nutrient cycle of Antarctica, particularly since a limited range of other microbial taxa can tolerate the harsh Antarctic climate. Penicillia-producing β-lactams, such as *Penicillium chrysogenum*, have been isolated from sediments of ponds (44), permafrost (45), subglacial ice (46), and oligotrophic and ornithogenic soil in Antarctica (43, 47). Several studies tested for the extrolite production and confirmed the antibacterial activity of *Penicillium* spp. strains isolated in Antarctica (44, 46, 48). This is consistent with the fact that both localities where the strains were isolated are apical parts of the landscape often visited by birds in austral summer and there is a high probability they are colonized by fungi.

The 16S rRNA analysis had limited discriminatory power for identifying the examined staphylococcal isolates, therefore their phylogenetic position was assessed using the concatenated multilocus sequence data of six routinely used housekeeping genes *rpoB*, *hsp60*, *dnaJ*, *tuf*, *gap* and *sod* commonly used in phylogenetic studies of *Staphylococcus*, as well as the amino acid sequences of their protein products. Neighbour-joining and maximum-likelihood phylogenetic trees for the six housekeeping genes were very similar, and confirmed that the isolates under study represented a well-delineated group within the *S. saprophyticus* phylogenetic clade, clearly separated from known species (Fig. 4).

To evaluate the intergenomic distances between the genome sequences of strain CCM 8730^T and reference type strains belonging to the phylogenetically closest *Staphylococcus* spp., an average nucleotide identity (ANI) and a digital DDH (dDDH) value were determined (Table S2). The calculated ANI and dDDH values are well below the threshold 95 - 96% and 70%, respectively, for species delineation (49). This confirms that the strain CCM 8730^T represents a distinct *Staphylococcus* species.

The data from this study demonstrate that although they have a high similarity to *S. saprophyticus*, the two isolates represented by strain CCM 8730^T belong to a new taxon that can be distinguished both genotypically and phenotypically from established species of the genus *Staphylococcus*. We suggest classifying these isolates as a novel species for which the name *Staphylococcus edaphicus* is proposed, with the strain P5085^T (=CCM 8730^T = DSM 104441^T) as the type strain.

Description of *Staphylococcus edaphicus* sp. nov.

Staphylococcus edaphicus (e.da'phi.cus. Gr. n. edaphos, soil; N. L. masc. adj. *edaphicus*, belonging to soil).

Its cells are Gram-stain-positive, spherical or irregular cocci, 880 ± 60 nm in diameter (Fig. S5), occurring predominantly in clusters, non-spore-forming. Colonies on P agar after 24 h are circular with whole margins, slightly convex, smooth, shiny, whitish, 2 mm in diameter and aerobic. Weak haemolytic activity (production of δ-haemolysin) on blood agar. Good growth at 10 °C, 42 °C and in the presence of 11% NaCl; weak growth in the presence of 12% NaCl or at 5 °C. No growth at 0 or 45 °C. No growth in M9 minimal agar. No growth in thioglycollate medium or in the presence of 14% NaCl on TSA agar plate. Catalase, urease, pyrrolidonyl arylamidase, Voges-Proskauer test (acetoin), nitrate reduction and hydrolysis of Tween 80 positive. Coagulase, clumping factor, hyaluronidase, thermonuclease, oxidase, arginine dihydrolase, ornithine decarboxylase and arginine arylamidase negative. Susceptible to polymyxin B (300 IU) and furazolidone (100 µg), but resistant to bacitracine (0.2 IU) and novobiocin (5 µg). Susceptible to lysostaphin (200 mg l^{-1}) and resistant to lysozyme (400 mg l^{-1}). Hydrolysis of esculin, DNA and gelatine negative. Esterase (C 4), esterase lipase (C 8), lipase (C14) (weak), β-glucuronidase, acid phosphatase (weak), alkaline phosphatase and naphthol-AS-Bi-phosphohydrolase activity is present, but not leucine arylamidase, valine arylamidase, cystine arylamidase, trypsin, α-chymotrypsin, α-galactosidase, β-galactosidase, α-glucosidase, β-glucosidase, N-acetyl-β-glucosaminidase, α-mannosidase and α-fucosidase. Acid is produced from glycerol, ribose, galactose, D-glucose, fructose, mannose, mannitol, sorbitol (weak), N-acetyl glucosamine, salicine, maltose sucrose, trehalose and β-gentiobiose, but not from erythritol, D-arabinose, L-arabinose, D-xylose, L-xylose, adonitol, β-methyl-D-xyloside, sorbose, rhamnose, dulcitol, inositol, α-methyl-D-mannoside, α-methyl-D-glucoside, amygdaline, arbutine, cellobiose, lactose, melibiose, inulin, melezitose, D-raffinose, glycogen, xylitol, turanose, D-lyxose, D-tagatose, D-fucose, L-fucose, D-arabitol, L-arabitol, gluconate, 2 keto-gluconate, or 5 keto-gluconate. The test result was strain-dependent for acid production from amidon (CCM 8730^T positive). The tested strains were susceptible to cephalothin, ciprofloxacin, clindamycin, erythromycin, gentamicin, chloramphenicol, imipenem, kanamycin, neomycin, cotrimoxazol, tetracycline, and vancomycin. Resistant to penicillin G, ampicillin, ceftazidin, methicillin, cefoxitin, fosfomycin and novobiocin. The ability to utilize carbon

sources via respiration as well as chemical sensitivity assays determined by Biolog GEN III MicroPlate test panel are shown in Table S3.

The type strain CCM 8730^T (=P5085^T = DSM 104441^T) was retrieved in January 2013 from fragments of black porous stone at a hill above Cape Lachman, James Ross Island, Antarctica. G+C content 33.3 mol% calculated from whole genomic sequence. The majority of the characteristics of the type strain are in agreement with the general species description; in addition, strain CCM 8730^T produces acid from amidon.

MATERIALS AND METHODS

Sampling and cultivation. Sampling was carried out by dispersing approx. 1 g of stone fragments in 5 ml of sterile saline solution and 100 µl of the suspension was spread on an R2A agar plate (Oxoid) and cultivated at 15 °C for 5 days. Subsequently, individual morphologically diverse colonies were picked up, purified by repeated streaking on R2A medium at 15 °C, and the resulting pure cultures were maintained at -70 °C until analysed. Two Gram-stain positive isolates were obtained. Additional cultivation of these isolates for biotyping and genotyping was performed with cells growing on TSA agar (Oxoid). The type strains of the closely related staphylococcal taxa were obtained from the Czech Collection of Microorganisms (www.sci.muni.cz/ccm) and were simultaneously investigated in all tests.

Phenotypic characterization. Extensive phenotypic characterization using the commercial kits API 50CH, API ID 32 Staph and API ZYM (bioMérieux), phenotypic fingerprinting using the Biolog system with the identification test panel GEN III MicroPlate (Biolog) and conventional biochemical, physiological and growth tests relevant for the genus *Staphylococcus* were done as described previously (50, 51). Transmission electron microscopy was performed with bacterial cells negative stained with 2% ammonium molybdate using a T Morgagni 268D Philips (FEI Company, USA) electron microscope.

The antibiotic resistance pattern was tested by the disc diffusion method on Mueller-Hinton agar (Oxoid). Sixteen discs generally used for Gram-positive cocci were applied: ampicillin (10 µg), ceftazidime (10 µg), cephalothin (30 µg), ciprofloxacin (5 µg), clindamycin (2 µg), erythromycin (15 µg), gentamicin (10 µg), chloramphenicol (30 µg), imipenem (10 µg), kanamycin (30 µg), neomycin (10 µg), novobiocin (5 µg), penicillin G (1 IU), cotrimoxazol (25 µg), tetracycline (30 µg), vancomycin (30 µg). EUCAST/CLSI standards were strictly followed for cultivation and inhibition zone diameter reading (52, 53).

Matrix-assisted laser-desorption/ionization time-of-flight mass spectrometry (MALDI-TOF MS). The strains were analysed using a MALDI-TOF mass spectrometer (Microflex LT, Bruker

Daltonics) in an automatic acquisition mode. Mass spectra were processed using the software Flex Analysis (version 3.4, Bruker Daltonics) and BioTyper (version 3.0, Bruker Daltonics). Signals present in at least eight out of the total of ten replicate analyses of each sample were used as input data. The MALDI-TOF MS-based dendrogram was generated using the correlation distance measure with the unweighted average linkage algorithm.

Fatty acid methyl esters analysis (FAME). The fatty acid methyl esters analysis (FAME) was performed with cells growing on BBL Trypticase Soy Agar plates (BD) at 28 °C ± 1° C for 24 hrs. The extraction of fatty acid methyl esters was performed according to the standard protocol of the Sherlock Microbial Identification System (54). Cellular fatty acid extracts were analysed with an Agilent 7890B gas chromatograph using the rapid Sherlock Identification system (MIS, version 6.2B, MIDI database: RTSBA 6.21, MIDI Inc.).

Genotypic analysis by fingerprinting techniques. Rep-PCR fingerprinting with the $(GTG)_5$ primer was performed as described previously (55). The automatic ribotyping was performed using a RiboPrinter Microbial Characterization System (DuPont Qualicon, USA) in accordance with the manufacturer's instructions. Numerical analysis of obtained fingerprints and dendrogram construction was done using the software BioNumerics 7.6 (Applied Maths, Belgium). The ribotype patterns were imported into the software BioNumerics using the load samples import script provided by the manufacturer. Pulsed-field gel electrophoresis (PFGE) using *Sma*I macrorestriction pattern analysis was performed as previously described (56).

Genome sequencing and bioinformatics analysis. Genomic DNA was extracted using a High Pure PCR Template Preparation Kit (Roche) according to the manufacturer's recommendations. The concentration of extracted DNA was estimated with a Qubit 2.0 Fluometer using a Qubit dsDNA BR assay kit (Invitrogen). The partial 16S rRNA gene was sequenced as described previously (57). Whole-genome shotgun (WGS) sequencing was performed using an Ion Torrent™ Personal Genome Machine (Ion PGM™). The purified genomic DNA was used for preparing a 400-bp sequencing library with an Ion Plus Fragment Library Kit (Thermo Fisher Scientific). The sample was loaded onto a 316v2 chip and sequenced using an Ion PGM Hi-Q View sequencing kit (Thermo Fisher Scientific). Quality trimming and error correction of the reads were performed with the Ion Torrent Suite Software (version 5.0.4). The assembly computation was performed using the Assembler SPAdes 3.9 (58) with default parameters for Ion Torrent data. Contigs were then re-ordered according to the reference genome *S. saprophyticus* ATCC 15305^T; GenBank accession number NC_007350 (16) using MauveContigMover (59). Ordering was evaluated using assembly graph visualized in Bandage (60).

Sequences were manipulated and inspected in the cross-platform bioinformatics software Ugene v1.23.1 (61). For primal analysis, the genome was annotated using RAST (62). Gene content

was further examined by BLASTp (63), ISFinder (64), InterProScan (65), and CD-Search (66). The complete 16S rRNA gene sequence was extracted from WGS data using RNAmmer version 1.2 (67). Phylogenetic analysis from multilocus sequence data was performed using the software MEGA version 7 (68).

The GenBank accession number for the 16S rRNA genes of isolate CCM 8730^T is KY315825. The data from WGS of strains *Staphylococcus edaphicus* CCM 8730^T and *Staphylococcus xylosus* CCM 2738^T were recorded in the GenBank WGS project under the accession numbers MRZN00000000 and MRZO00000000.

DNA homology studies. To calculate the ANI value, the OrthoANI algorithm implemented on the EzBioCloud server (http://www.ezbiocloud.net/tools/ani) was used (69). The dDDH values were calculated using web-based genome-to-genome distance calculator (GGDC) version 2.1 (70) and the recommended formula 2 was taken into account to interpret the results. Whole genome sequences of related staphylococcal species were obtained from the NCBI database (71-74).

SUPPLEMENTAL MATERIAL

Supplemental material for this article may be found online.

ACKNOWLEDGEMENTS

This work was supported by the Ministry of Health of the Czech Republic (NT16-29916A).The authors wish to thank the scientific infrastructure of the J.G. Mendel Czech Antarctic Station as part of the Czech Polar Research Infrastructure (CzechPolar2) and its crew for their assistance, supported by the Ministry of Education, Youth and Sports of the Czech Republic (LM2015078) as well as the Czech Antarctic Foundation for their support. Access to computing and storage facilities owned by parties and projects contributing to the National Grid Infrastructure MetaCentrum provided under the programme "Projects of Large Research, Development, and Innovations Infrastructures" CESNET (LM2015042), is greatly appreciated. Dr. Daniel Krsek (NRL for the Diagnostic Electron Microscopy of Infectious Agents, National Institute of Public Health, Prague, Czech Republic) is gratefully acknowledged for transmission electron microscopy, Dr. Bernhard Schink (University of Konstanz) for name correction. S. K. is a beneficiary of Brno Ph.D. Talent financial aid.

AUTHOR CONTRIBUTIONS

IS isolated and preliminary identified the strains. IS, JK and PP performed phenotypic characterization. Whole genome sequencing was performed by VV, and VK and AI analyzed the data. Phylogenetic analyses were performed by IM and VV. PS performed genotyping by fingerprinting techniques and analysed the data. SK performed FAME analysis. PP and LK performed MALDI-TOF

identification and analysed the data. RP and IS designed the study, RP, IS, AI, VV, IM and JD wrote the manuscript. All the authors approved the final manuscript.

REFERENCES

1. Götz F, Bannerman T, Schleifer K-H. 2006. The Genera *Staphylococcus* and *Macrococcus*, p 5-75. *In* Dworkin M, Falkow S, Rosenberg E, Schleifer K-H, Stackebrandt E (ed), The Prokaryotes, Bacteria: Firmicutes, Cyanobacteria, vol 4. Springer US, New York, NY. https://doi.org/10.1007/0-387-30744-3_1
2. Emmett M, Kloos WE. 1975. Amino acid requirements of staphylococci isolated from human skin. Can J Microbiol 21:729-733. https://doi.org/10.1139/m75-107
3. Emmett M, Kloos WE. 1979. The nature of arginine auxotrophy in cutaneous populations of staphylococci. J Gen Microbiol 110:305-314. https://doi.org/10.1099/00221287-110-2-305
4. Lambert LH, Cox T, Mitchell K, Rossello-Mora RA, Del Cueto C, Dodge DE, Orkand P, Cano RJ. 1998. *Staphylococcus succinus* sp. nov., isolated from Dominican amber. Int J Syst Bacteriol 48:511-518. https://doi.org/10.1099/00207713-48-2-511
5. Hess S, Gallert C. 2015. *Staphylococcus argensis* sp nov., a hovel staphylococcal species isolated from an aquatic environment. Int J Syst Evol Microbiol 65:2661-2665. https://doi.org/10.1099/ijs.0.000319
6. Kloos WE. 1980. Natural populations of the genus *Staphylococcus*. Annu Rev Microbiol 34:559-592. https://doi.org/10.1146/annurev.mi.34.100180.003015
7. Kloos WE, Schleifer KH, Smith RF. 1976. Characterization of *Staphylococcus sciuri* sp. nov. and its subspecies. Int J Syst Bacteriol 26:22-37. https://doi.org/10.1099/00207713-26-1-22
8. Planchon S, Gaillard-Martinie B, Dordet-Frisoni E, Bellon-Fontaine MN, Leroy S, Labadie J, Hebraud M, Talon R. 2006. Formation of biofilm by *Staphylococcus xylosus*. Int J Food Microbiol 109:88-96. https://doi.org/10.1016/j.ijfoodmicro.2006.01.016
9. Dordet-Frisoni E, Dorchies G, De Araujo C, Talon R, Leroy S. 2007. Genomic diversity in *Staphylococcus xylosus*. Appl Environ Microbiol 73:7199-7209. https://doi.org/10.1128/AEM.01629-07
10. Irlinger F. 2008. Safety assessment of dairy microorganisms: coagulase-negative staphylococci. Int J Food Microbiol 126:302-310. https://doi.org/10.1016/j.ijfoodmicro.2007.08.016
11. Giordano N, Corallo C, Miracco C, Papakostas P, Montella A, Figura N, Nuti R. 2016. Erythema nodosum associated with *Staphylococcus xylosus* septicemia. J Microbiol Immunol Infect 49:134-137. https://doi.org/10.1016/j.jmii.2012.10.003
12. Becker K, von Eiff C. 2011. *Staphylococcus*, *Micrococcus*, and Other Catalase-Positive Cocci, p 308-330. *In* Versalovic J, Carroll KC, Funke G, Jorgensen JH, Landry ML, Warnock DW (ed), Manual of Clinical Microbiology, 10th Edition. ASM Press, Washington, DC. https://doi.org/10.1128/9781555816728.ch19
13. Schleifer KH, Kloos WE. 1975. Isolation and characterization of staphylococci from human skin. 1. Amended descriptions of *Staphylococcus epidermidis* and *Staphylococcus saprophyticus* and descriptions of 3 new species - *Staphylococcus cohnii*, *Staphylococcus haemolyticus*, and *Staphylococcus xylosus*. Int J Syst Bacteriol 25:50-61. https://doi.org/10.1099/00207713-25-1-50
14. Widerström M, Wiström J, Sjöstedt A, Monsen T. 2012. Coagulase-negative staphylococci: update on the molecular epidemiology and clinical presentation, with a focus on *Staphylococcus epidermidis* and *Staphylococcus saprophyticus*. Eur J Clin Microbiol Infect Dis 31:7-20. https://doi.org/10.1007/s10096-011-1270-6
15. Takahashi T, Satoh I, Kikuchi N. 1999. Phylogenetic relationships of 38 taxa of the genus *Staphylococcus* based on 16S rRNA gene sequence analysis. Int J Syst Bacteriol 49:725-728. https://doi.org/10.1099/00207713-49-2-725
16. Kuroda M, Yamashita A, Hirakawa H, Kumano M, Morikawa K, Higashide M, Maruyama A, Inose Y, Matoba K, Toh H, Kuhara S, Hattori M, Ohta T. 2005. Whole genome sequence of *Staphylococcus saprophyticus* reveals the pathogenesis of uncomplicated urinary tract

infection. Proc Natl Acad Sci U S A 102:13272-13277. https://doi.org/10.1073/pnas.0502950102

17. Schleifer KH, Bell JA. 2009. Genus I. *Staphylococcus* Rosenbach 1884, 18^{AL} (Nom. Cons. Opin. 17 Jud. Comm. 1958, 153.), p 392-421. *In* De Vos P, Garrity GM, Jones D, Krieg NR, Ludwig W, Rainey FA, Schleifer KH, Whitman WB (ed), Bergey's Manual of Systematic Bacteriology, The Firmicutes, vol 3. Springer-Verlag, New York. https://doi.org/10.1007/978-0-387-68489-5
18. Foster TJ, Geoghegan JA, Ganesh VK, Hook M. 2014. Adhesion, invasion and evasion: the many functions of the surface proteins of *Staphylococcus aureus*. Nat Rev Microbiol 12:49-62. https://doi.org/10.1038/nrmicro3161
19. Wilson LK, Coombs GW, Christiansen K, Grubb WB, O'Brien FG. 2016. Characterization of a novel staphylococcal cassette chromosome composite island from community-associated MRSA isolated in aged care facilities in Western Australia. J Antimicrob Chemother 71:3372-3375. https://doi.org/10.1093/jac/dkw317
20. Ohniwa RL, Kitabayashi K, Morikawa K. 2013. Alternative cardiolipin synthase Cls1 compensates for stalled Cls2 function in *Staphylococcus aureus* under conditions of acute acid stress. FEMS Microbiol Lett 338:141-146. https://doi.org/10.1111/1574-6968.12037
21. Tsai M, Ohniwa RL, Kato Y, Takeshita SL, Ohta T, Saito S, Hayashi H, Morikawa K. 2011. *Staphylococcus aureus* requires cardiolipin for survival under conditions of high salinity. BMC Microbiol 11:13. https://doi.org/10.1186/1471-2180-11-13
22. Peleg AY, Miyakis S, Ward DV, Earl AM, Rubio A, Cameron DR, Pillai S, Moellering RC, Jr., Eliopoulos GM. 2012. Whole genome characterization of the mechanisms of daptomycin resistance in clinical and laboratory derived isolates of *Staphylococcus aureus*. PLoS One 7:e28316. https://doi.org/10.1371/journal.pone.0028316
23. International Working Group on the Classification of Staphylococcal Cassette Chromosome E. 2009. Classification of staphylococcal cassette chromosome mec (SCCmec): guidelines for reporting novel SCCmec elements. Antimicrob Agents Chemother 53:4961-4967. https://doi.org/10.1128/AAC.00579-09
24. García-Álvarez L, Holden MT, Lindsay H, Webb CR, Brown DF, Curran MD, Walpole E, Brooks K, Pickard DJ, Teale C, Parkhill J, Bentley SD, Edwards GF, Girvan EK, Kearns AM, Pichon B, Hill RL, Larsen AR, Skov RL, Peacock SJ, Maskell DJ, Holmes MA. 2011. Meticillin-resistant *Staphylococcus aureus* with a novel *mecA* homologue in human and bovine populations in the UK and Denmark: a descriptive study. Lancet Infect Dis 11:595-603. https://doi.org/10.1016/S1473-3099(11)70126-8
25. Harrison EM, Paterson GK, Holden MT, Morgan FJ, Larsen AR, Petersen A, Leroy S, De Vliegher S, Perreten V, Fox LK, Lam TJ, Sampimon OC, Zadoks RN, Peacock SJ, Parkhill J, Holmes MA. 2013. A *Staphylococcus xylosus* isolate with a new *mecC* allotype. Antimicrob Agents Chemother 57:1524-1528. https://doi.org/10.1128/AAC.01882-12
26. Malyszko I, Schwarz S, Hauschild T. 2014. Detection of a new *mecC* allotype, *mecC2*, in methicillin-resistant *Staphylococcus saprophyticus*. J Antimicrob Chemother 69:2003-2005. https://doi.org/10.1093/jac/dku043
27. Paterson GK, Larsen AR, Robb A, Edwards GE, Pennycott TW, Foster G, Mot D, Hermans K, Baert K, Peacock SJ, Parkhill J, Zadoks RN, Holmes MA. 2012. The newly described *mecA* homologue, *mecA*$_{LGA251}$, is present in methicillin-resistant *Staphylococcus aureus* isolates from a diverse range of host species. J Antimicrob Chemother 67:2809-2813. https://doi.org/10.1093/jac/dks329
28. Monecke S, Gavier-Widen D, Mattsson R, Rangstrup-Christensen L, Lazaris A, Coleman DC, Shore AC, Ehricht R. 2013. Detection of *mecC*-positive *Staphylococcus aureus* (CC130-MRSA-XI) in diseased European hedgehogs (*Erinaceus europaeus*) in Sweden. PLoS One 8:e66166. https://doi.org/10.1371/journal.pone.0066166
29. Loncaric I, Kubber-Heiss A, Posautz A, Stalder GL, Hoffmann D, Rosengarten R, Walzer C. 2013. Characterization of methicillin-resistant *Staphylococcus* spp. carrying the *mecC* gene, isolated from wildlife. J Antimicrob Chemother 68:2222-2225. https://doi.org/10.1093/jac/dkt186

30. Porrero MC, Mentaberre G, Sanchez S, Fernandez-Llario P, Casas-Diaz E, Mateos A, Vidal D, Lavin S, Fernandez-Garayzabal JF, Dominguez L. 2014. Carriage of *Staphylococcus aureus* by free-living wild animals in Spain. Appl Environ Microbiol 80:4865-4870. https://doi.org/10.1128/AEM.00647-14
31. Porrero MC, Valverde A, Fernandez-Llario P, Diez-Guerrier A, Mateos A, Lavin S, Canton R, Fernandez-Garayzabal JF, Dominguez L. 2014. *Staphylococcus aureus* carrying *mecC* gene in animals and urban wastewater, Spain. Emerg Infect Dis 20:899-901. https://doi.org/10.3201/eid2005.130426
32. Babu MM, Priya ML, Selvan AT, Madera M, Gough J, Aravind L, Sankaran K. 2006. A database of bacterial lipoproteins (DOLOP) with functional assignments to predicted lipoproteins. J Bacteriol 188:2761-2773. https://doi.org/10.1128/JB.188.8.2761-2773.2006
33. Shahmirzadi SV, Nguyen MT, Götz F. 2016. Evaluation of *Staphylococcus aureus* lipoproteins: Role in nutritional acquisition and pathogenicity. Front Microbiol 7:1404. https://doi.org/10.3389/fmicb.2016.01404
34. Penadés JR, Christie GE. 2015. The Phage-Inducible Chromosomal Islands: A family of highly evolved molecular parasites. Annu Rev Virol 2:181-201. https://doi.org/10.1146/annurev-virology-031413-085446
35. Baba T, Takeuchi F, Kuroda M, Yuzawa H, Aoki K, Oguchi A, Nagai Y, Iwama N, Asano K, Naimi T, Kuroda H, Cui L, Yamamoto K, Hiramatsu K. 2002. Genome and virulence determinants of high virulence community-acquired MRSA. Lancet 359:1819-1827. https://doi.org/10.1016/S0140-6736(02)08713-5
36. Novick RP, Christie GE, Penadés JR. 2010. The phage-related chromosomal islands of Gram-positive bacteria. Nat Rev Microbiol 8:541-551. https://doi.org/10.1038/nrmicro2393
37. Fu Z, Liu Y, Chen C, Guo Y, Ma Y, Yang Y, Hu F, Xu X, Wang M. 2016. Characterization of fosfomycin resistance gene, *fosB*, in methicillin-resistant *Staphylococcus aureus* isolates. PLoS One 11:e0154829. https://doi.org/10.1371/journal.pone.0154829
38. Fitzgerald JR, Monday SR, Foster TJ, Bohach GA, Hartigan PJ, Meaney WJ, Smyth CJ. 2001. Characterization of a putative pathogenicity island from bovine *Staphylococcus aureus* encoding multiple superantigens. J Bacteriol 183:63-70. https://doi.org/10.1128/JB.183.1.63-70.2001
39. Chanda PK, Mondal R, Sau K, Sau S. 2009. Antibiotics, arsenate and H_2O_2 induce the promoter of *Staphylococcus aureus cspC* gene more strongly than cold. J Basic Microbiol 49:205-211. https://doi.org/10.1002/jobm.200800065
40. Kahánková J, Pantůček R, Goerke C, Růžičková V, Holochová P, Doškař J. 2010. Multilocus PCR typing strategy for differentiation of *Staphylococcus aureus* siphoviruses reflecting their modular genome structure. Environ Microbiol 12:2527-2538. https://doi.org/10.1111/j.1462-2920.2010.02226.x
41. Deghorain M, Bobay LM, Smeesters PR, Bousbata S, Vermeersch M, Perez-Morga D, Dreze PA, Rocha EP, Touchon M, Van Melderen L. 2012. Characterization of novel phages isolated in coagulase-negative staphylococci reveals evolutionary relationships with *Staphylococcus aureus* phages. J Bacteriol 194:5829-5839. https://doi.org/10.1128/JB.01085-12
42. Kim C, Milheirico C, Gardete S, Holmes MA, Holden MT, de Lencastre H, Tomasz A. 2012. Properties of a novel PBP2A protein homolog from *Staphylococcus aureus* strain LGA251 and its contribution to the beta-lactam-resistant phenotype. J Biol Chem 287:36854-36863. https://doi.org/10.1074/jbc.M112.395962
43. McRae CF, Hocking AD, Seppelt RD. 1999. Penicillium species from terrestrial habitats in the Windmill Islands, East Antarctica, including a new species, *Penicillium antarcticum*. Polar Biology 21:97-111. https://doi.org/10.1007/s003000050340
44. Corte AM, Liotta M, Venturi CB, Calegari L. 2000. Antibacterial activity of *Penicillium* spp. strains isolated in extreme environments. Polar Biology 23:294-297. https://doi.org/10.1007/s003000050
45. Zucconi L, Selbmann L, Buzzini P, Turchetti B, Guglielmin M, Frisvad JC, Onofri S. 2012. Searching for eukaryotic life preserved in Antarctic permafrost. Polar Biology 35:749-757. https://doi.org/10.1007/s00300-011-1119-6

46. Sonjak S, Frisvad JC, Gunde-Cimerman N. 2006. *Penicillium* mycobiota in arctic subglacial ice. Microb Ecol 52:207-216. https://doi.org/10.1007/s00248-006-9086-0
47. Godinho VM, Goncalves VN, Santiago IF, Figueredo HM, Vitoreli GA, Schaefer CE, Barbosa EC, Oliveira JG, Alves TM, Zani CL, Junior PA, Murta SM, Romanha AJ, Kroon EG, Cantrell CL, Wedge DE, Duke SO, Ali A, Rosa CA, Rosa LH. 2015. Diversity and bioprospection of fungal community present in oligotrophic soil of continental Antarctica. Extremophiles 19:585-596. https://doi.org/10.1007/s00792-015-0741-6
48. Brunati M, Rojas JL, Sponga F, Ciciliato I, Losi D, Gottlich E, de Hoog S, Genilloud O, Marinelli F. 2009. Diversity and pharmaceutical screening of fungi from benthic mats of Antarctic lakes. Marine Genomics 2:43-50. https://doi.org/10.1016/j.margen.2009.04.002
49. Goris J, Konstantinidis KT, Klappenbach JA, Coenye T, Vandamme P, Tiedje JM. 2007. DNA-DNA hybridization values and their relationship to whole-genome sequence similarities. Int J Syst Evol Microbiol 57:81-91. https://doi.org/10.1099/ijs.0.64483-0
50. Pantůček R, Švec P, Dajcs JJ, Machová I, Černohlávková J, Šedo O, Gelbíčová T, Mašlaňová I, Doškař J, Zdráhal Z, Růžičková V, Sedláček I. 2013. *Staphylococcus petrasii* sp. nov. including *S. petrasii* subsp. *petrasii* subsp. nov. and *S. petrasii* subsp. *croceilyticus* subsp. nov., isolated from human clinical specimens and human ear infections. Syst Appl Microbiol 36:90-95. https://doi.org/10.1016/j.syapm.2012.11.004
51. Mannerová S, Pantůček R, Doškař J, Švec P, Snauwaert C, Vancanneyt M, Swings J, Sedláček I. 2003. *Macrococcus brunensis* sp. nov., *Macrococcus hajekii* sp. nov. and *Macrococcus lamae* sp. nov., from the skin of llamas. Int J Syst Evol Microbiol 53:1647-1654. https://doi.org/10.1099/ijs.0.02683-0
52. The European Committee on Antimicrobial Susceptibility Testing. 2017. Breakpoint tables for interpretation of MICs and zone diameters, version 7.1. http://www.eucast.org/fileadmin/src/media/PDFs/EUCAST_files/Breakpoint_tables/v_7.1_Breakpoint_Tables.pdf
53. CLSI. 2015. Performance Standards for Antimicrobial Disk Susceptibility Tests; Approved Standard - 12th Edition. CLSI document M02-A12. Clinical and Laboratory Standards Institute, Wayne, PA. https://clsi.org/standards/products/microbiology/documents/m02/
54. Sasser M. 1990. Identification of bacteria by gas chromatography of cellular fatty acids, MIDI Technical Note 101. Microbial ID Inc., Newark, DE.
55. Švec P, Pantůček R, Petráš P, Sedláček I, Nováková D. 2010. Identification of *Staphylococcus* spp. using $(GTG)_5$-PCR fingerprinting. Syst Appl Microbiol 33:451-456. https://doi.org/10.1016/j.syapm.2010.09.004
56. Pantůček R, Götz F, Doškař J, Rosypal S. 1996. Genomic variability of *Staphylococcus aureus* and the other coagulase-positive *Staphylococcus* species estimated by macrorestriction analysis using pulsed-field gel electrophoresis. Int J Syst Bacteriol 46:216-222. https://doi.org/10.1099/00207713-46-1-216
57. Pantůček R, Sedláček I, Petráš P, Koukalová D, Švec P, Štětina V, Vancanneyt M, Chrastinová L, Vokurková J, Růžicková V, Doškař J, Swings J, Hájek V. 2005. *Staphylococcus simiae* sp. nov., isolated from South American squirrel monkeys. Int J Syst Evol Microbiol 55:1953-1958. https://doi.org/10.1099/ijs.0.63590-0
58. Nurk S, Bankevich A, Antipov D, Gurevich AA, Korobeynikov A, Lapidus A, Prjibelski AD, Pyshkin A, Sirotkin A, Sirotkin Y, Stepanauskas R, Clingenpeel SR, Woyke T, Mclean JS, Lasken R, Tesler G, Alekseyev MA, Pevzner PA. 2013. Assembling single-cell genomes and mini-metagenomes from chimeric MDA products. J Comput Biol 20:714-737. https://doi.org/10.1089/cmb.2013.0084
59. Rissman AI, Mau B, Biehl BS, Darling AE, Glasner JD, Perna NT. 2009. Reordering contigs of draft genomes using the Mauve aligner. Bioinformatics 25:2071-2073. https://doi.org/10.1093/bioinformatics/btp356
60. Wick RR, Schultz MB, Zobel J, Holt KE. 2015. Bandage: interactive visualization of de novo genome assemblies. Bioinformatics 31:3350-3352. https://doi.org/10.1093/bioinformatics/btv383

61. Okonechnikov K, Golosova O, Fursov M, team U. 2012. Unipro UGENE: a unified bioinformatics toolkit. Bioinformatics 28:1166-1167. https://doi.org/10.1093/bioinformatics/bts091
62. Aziz RK, Bartels D, Best AA, DeJongh M, Disz T, Edwards RA, Formsma K, Gerdes S, Glass EM, Kubal M, Meyer F, Olsen GJ, Olson R, Osterman AL, Overbeek RA, McNeil LK, Paarmann D, Paczian T, Parrello B, Pusch GD, Reich C, Stevens R, Vassieva O, Vonstein V, Wilke A, Zagnitko O. 2008. The RAST Server: rapid annotations using subsystems technology. BMC Genomics 9:75. https://doi.org/10.1186/1471-2164-9-75
63. Altschul SF, Gish W, Miller W, Myers EW, Lipman DJ. 1990. Basic local alignment search tool. J Mol Biol 215:403-410. https://doi.org/10.1016/S0022-2836(05)80360-2
64. Siguier P, Perochon J, Lestrade L, Mahillon J, Chandler M. 2006. ISfinder: the reference centre for bacterial insertion sequences. Nucleic Acids Res 34:D32-D36. https://doi.org/10.1093/nar/gkj014
65. Jones P, Binns D, Chang HY, Fraser M, Li W, McAnulla C, McWilliam H, Maslen J, Mitchell A, Nuka G, Pesseat S, Quinn AF, Sangrador-Vegas A, Scheremetjew M, Yong SY, Lopez R, Hunter S. 2014. InterProScan 5: genome-scale protein function classification. Bioinformatics 30:1236-1240. https://doi.org/10.1093/bioinformatics/btu031
66. Marchler-Bauer A, Derbyshire MK, Gonzales NR, Lu S, Chitsaz F, Geer LY, Geer RC, He J, Gwadz M, Hurwitz DI, Lanczycki CJ, Lu F, Marchler GH, Song JS, Thanki N, Wang Z, Yamashita RA, Zhang D, Zheng C, Bryant SH. 2015. CDD: NCBI's conserved domain database. Nucleic Acids Res 43:D222-D226. https://doi.org/10.1093/nar/gku1221
67. Lagesen K, Hallin P, Rodland EA, Staerfeldt HH, Rognes T, Ussery DW. 2007. RNAmmer: consistent and rapid annotation of ribosomal RNA genes. Nucleic Acids Res 35:3100-3108. https://doi.org/10.1093/nar/gkm160
68. Kumar S, Stecher G, Tamura K. 2016. MEGA7: Molecular Evolutionary Genetics Analysis Version 7.0 for Bigger Datasets. Mol Biol Evol 33:1870-1874. https://doi.org/10.1093/molbev/msw054
69. Lee I, Kim YO, Park SC, Chun J. 2015. OrthoANI: An improved algorithm and software for calculating average nucleotide identity. Int J Syst Evol Microbiol doi:10.1099/ijsem.0.000760. https://doi.org/10.1099/ijsem.0.000760
70. Meier-Kolthoff JP, Auch AF, Klenk HP, Goker M. 2013. Genome sequence-based species delimitation with confidence intervals and improved distance functions. BMC Bioinformatics 14:60. https://doi.org/10.1186/1471-2105-14-60
71. Calcutt MJ, Foecking MF, Hsieh HY, Perry J, Stewart GC, Middleton JR. 2013. Genome sequence analysis of *Staphylococcus equorum* bovine mastitis isolate UMC-CNS-924. Genome Announc 1:e00840-13. https://doi.org/10.1128/genomeA.00840-13
72. Zhou H, Yao Z, Shi H, Wang B, Li D, Hou J, Ma S. 2017. Draft genome sequence of *Staphylococcus succinus* subsp. *succinus* type strain DSM 14617, isolated from plant and soil inclusions within 25- to 35-million-year-old Dominican amber. Genome Announc 5:e01521-16. https://doi.org/10.1128/genomeA.01521-16
73. Shi D, Fang D, Hu X, Li A, Lv L, Guo J, Chen Y, Wu W, Guo F, Li L. 2015. Draft genome sequence of *Staphylococcus gallinarum* DSM 20610^T, originally isolated from the skin of a chicken. Genome Announc 3:e00580-15. https://doi.org/10.1128/genomeA.00580-15
74. Shiroma A, Terabayashi Y, Nakano K, Shimoji M, Tamotsu H, Ashimine N, Ohki S, Shinzato M, Teruya K, Satou K, Hirano T. 2015. First complete genome sequences of *Staphylococcus aureus* subsp. *aureus* Rosenbach 1884 (DSM 20231^T), determined by PacBio single-molecule real-time technology. Genome Announc 3:e00800-15. https://doi.org/10.1128/genomeA.00800-15

FIGURE LEGENDS

Fig. 1. Circular display of *Staphylococcus edaphicus* CCM 8730^T genome (GenBank accession number MRZN00000000) compared to *Staphylococcus saprophyticus* ATCC 15305^T (GenBank accession number NC_007350) and *Staphylococcus xylosus* CCM 2738^T (GenBank accession number MRZO00000000) genomes. The picture shows (from inner to outer) GC skew , mol% G+C, unique regions n CCM 8730^T genome based on BLASTn analysis, orthologous regions in *S. saprophyicus* ATCC 15305^T genome and *S. xylosus* CCM 2738^T genome based on BLASTn analysis. Outer circle depicts location of accessory elements in *Staphylococcus edaphicus* CCM 8730^T genome.

Fig. 2. Venn diagram showing orthologous gene clusters for strain *Staphylococcus edaphicus* CCM 8730^T (GenBank accession number MRZN00000000), *Staphylococcus saprophyticus* ATCC 15305^T (GenBank accession number NC_007350) and *S. xylosus* CCM 2738^T (GenBank accession number MRZO00000000).

Fig. 3. Comparison of genetic structure of SCC*mec* element type XI in *S. aureus* LGA251 (GenBank accession number FR821779), ψSCC*mec*$_{P5085}$ in *Staphylococcus edaphicus* CCM 8730^T and *mecC1* region in *Staphylococcus xylosus* S04009 (GenBank accession number HE993884). Arrows indicate ORFs and their orientation on the genome; *mec* complex is depicted in dark blue, *ccr* complex in green and part of arginine catabolic mobile element (ACME) in orange.

Fig. 4. Unrooted maximum-likelihood trees based on concatenated sequences from six multiple loci showing the phylogenetic position of *Staphylococcus edaphicus* sp. nov. The sections of gene sequences used and their protein products corresponded to the following gene coordinates of *Staphylococcus aureus* subsp. *aureus* NCTC 8325: 949..2748 for *rpoB*, 16..1573 for *hsp60*, 1..1136 for *dnaJ*, 1..1185 for *tuf*, 4..1004 for *gap*, and 1..597 for the *sod* gene. Bootstrap probability values (percentages of 500 tree replications) greater than 70% are shown at branch points. The evolutionary distances are given as the number of substitutions per site (next to the branches). Filled circles indicate that the corresponding nodes are also obtained in the neighbour-joining tree. (**A**) The evolutionary history inferred from nucleotide sequences by using the Maximum Likelihood method based on the Tamura-Nei model. There were a total of 7175 positions in the final dataset. (**B**) The evolutionary history was inferred from amino acid sequences by using the Maximum Likelihood method based on the Poisson correction model. There were a total of 2391 positions in the final dataset.

Table 1. Differentiation of *Staphylococcus edaphicus* sp. nov. from phylogenetically closest *Staphylococcus* spp.

Test	*S. edaphicus* CCM 8730 ^{T}	*S. xylosus* CCM 2738 ^{T}	*S. saprophyticus* subsp. *saprophyticus* CCM 883 ^{T}	*S. saprophyticus* subsp. *bovis* CCM 4410 ^{T}	*S. succinus* subsp. *succinus* CCM 7157 ^{T}	*S. succinus* subsp. *casei* CCM 7194 ^{T}	*S. equorum* subsp. *equorum* CCM 3832 ^{T}	*S. equorum* subsp. *linens* CCM 7278 ^{T}
Nitrate reduction	+	+ / d*	- / -	+ / +	- / -	+ / +	+ / +	+ / +
Pyrrolidonyl arylamidase	+	+ / d	- / -	w / +	- / -	- / -	- / -	- / -
Voges-Proskauer test (acetoin)	+	- / d	+ / +	+ / d	- / -	- / -	- / -	- / -
Esculine hydrolysis	-	- / d	- / -	- / -	+ / +	+ / +	- / d	- / -
β-glucosidase	-	+ / +	- / d	- / d	+ / NT	+ / NT	+ / NT	- / NT
β-glucuronidase	+	+ / +	- / -	- / -	+ / +	+ / +	w / +	+ / +
β-galactosidase	-	+ / +	+ / +	+ / d	+ / +	+ / +	w / d	- / -
Acid from mannose	+	+ / +	- / -	- / -	+ / d	+ / +	- / +	+ / +

Abbreviations: +, positive reaction; w, weakly positive reaction; -, negative reaction; d, variable reaction; NT, not tested

* data obtained from type strains in this study (left) and from species description (right) based on data from Schleifer & Bell (17)

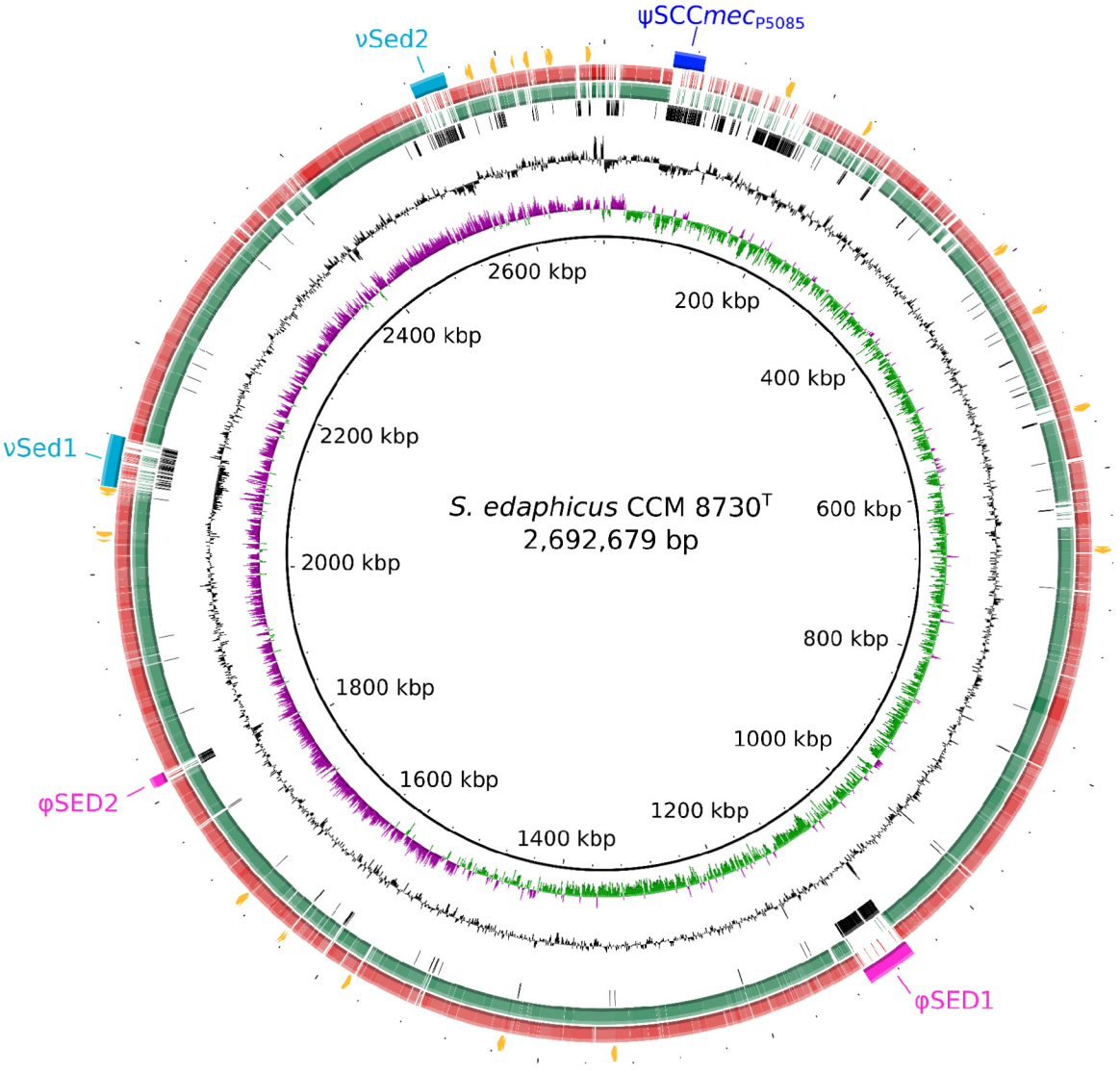
ψSCCmec P5085
νSed2
νSed1
φSED2
φSED1
S. edaphicus CCM 8730T
2,692,679 bp
200 kbp
400 kbp
600 kbp
800 kbp
1000 kbp
1200 kbp
1400 kbp
1600 kbp
1800 kbp
2000 kbp
2200 kbp
2400 kbp
2600 kbp
GC Skew (+)
GC Skew (-)
GC Content
Unique ORFs in CCM 8730T
S. saprophyticus ATCC 15305T
100% identity
75% identity
50% identity
S. xylosus CCM 2738T
100% identity
75% identity
50% identity
S. edaphicus CCM 8730T variable genetic elements
SCCmec
Genomic islands
Prophages
IS Elements

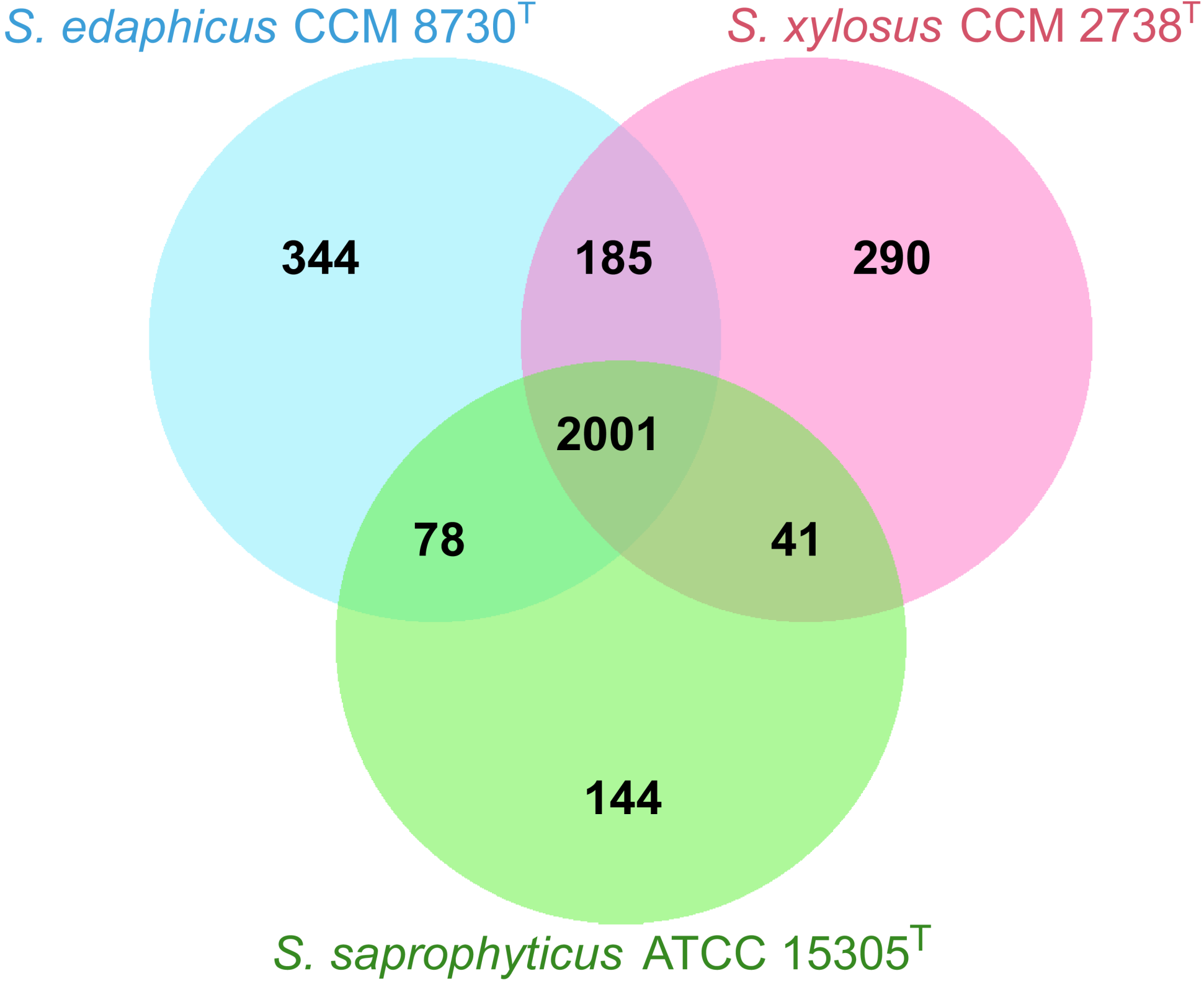
S. edaphicus CCM 8730T
S. xylosus CCM 2738T
344
185
290
2001
78
41
144
S. saprophyticus ATCC 15305T

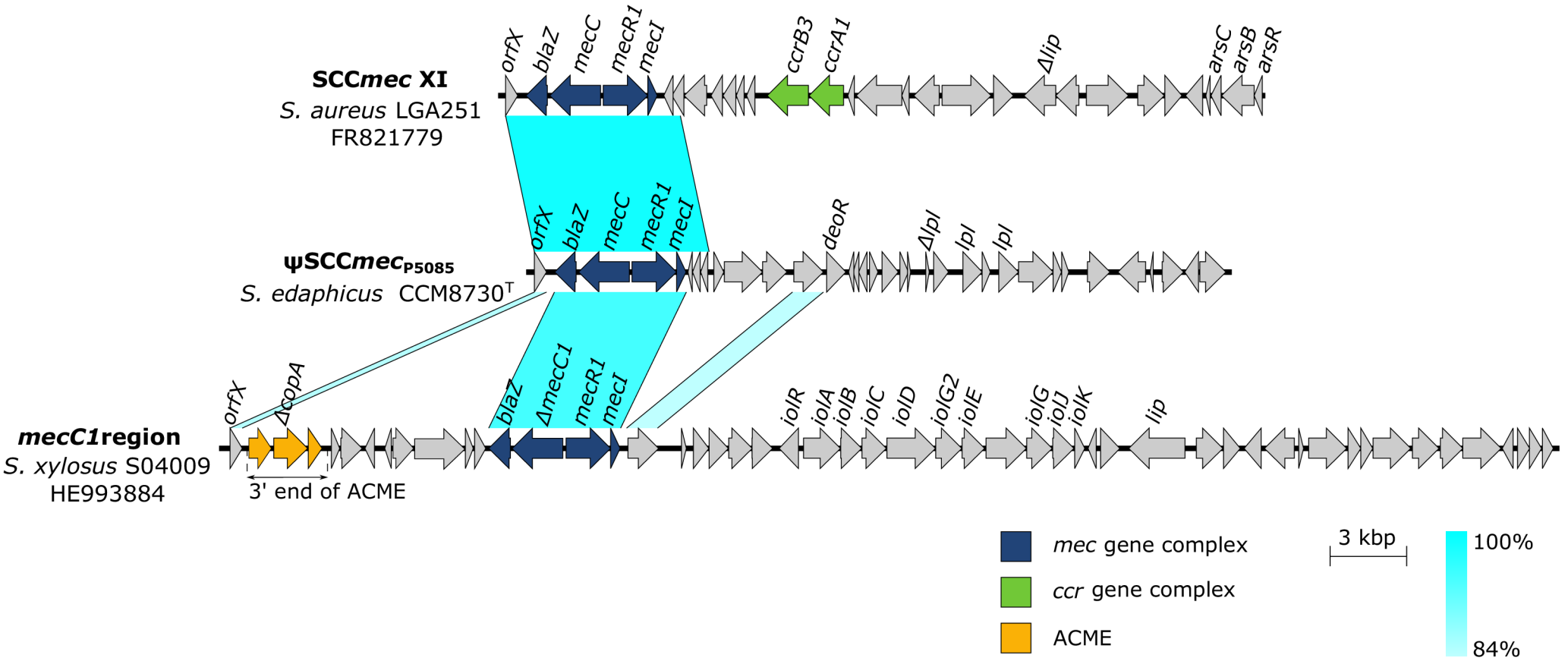
SCCmec XI
S. aureus LGA251
FR821779
orfX
blaZ
mecC
mecR1
mecI
ccrB3
ccrA1
Δlip
arsC
arsB
arsR
ψSCCmecP5085
S. edaphicus CCM8730T
deoR
ΔlplI
lplI
lplI
mecC1region
S. xylosus S04009
HE993884
ΔcopA
ΔmecC1
iolR
iolA
iolB
iolC
iolD
iolG2
iolE
iolG
iolJ
iolK
lip
3' end of ACME
mec gene complex
ccr gene complex
ACME
3 kbp
100%
84%

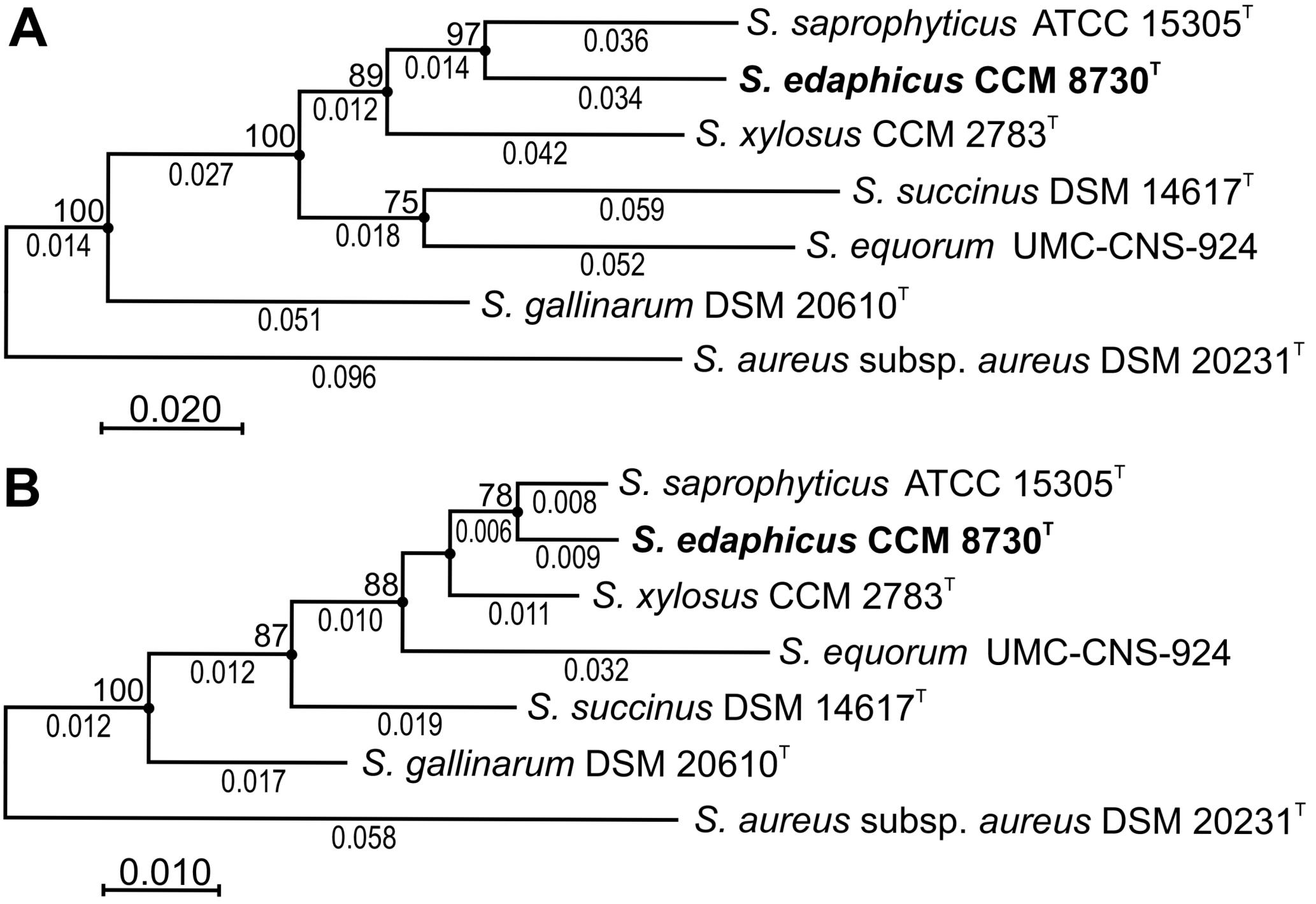
A
S. saprophyticus ATCC 15305T
S. edaphicus CCM 8730T
S. xylosus CCM 2783T
S. succinus DSM 14617T
S. equorum UMC-CNS-924
S. gallinarum DSM 20610T
S. aureus subsp. aureus DSM 20231T
97
0.036
0.014
89
0.034
0.012
100
0.042
0.027
75
0.059
100
0.018
0.014
0.052
0.051
0.096
0.020
B
S. saprophyticus ATCC 15305T
S. edaphicus CCM 8730T
S. xylosus CCM 2783T
S. equorum UMC-CNS-924
S. succinus DSM 14617T
S. gallinarum DSM 20610T
S. aureus subsp. aureus DSM 20231T
78
0.008
0.006
0.009
88
0.010
0.011
87
0.012
0.032
100
0.012
0.019
0.017
0.058
0.010

Staphylococcus edaphicus sp. nov., isolated in Antarctica, harbours *mecC* gene and genomic islands essential to adaptation to extreme environment

Roman Pantůček, Ivo Sedláček, Adéla Indráková, Veronika Vrbovská, Ivana Mašlaňová, Vojtěch Kovařovic, Pavel Švec, Stanislava Králová, Lucie Krištofová, Jana Kekláková, Petr Petráš, Jiří Doškař

Supplemental material

Table S1. Cellular fatty acid composition (as a percentage of the total) of strains CCM 8730^T, CCM 8731, *Staphylococcus saprophyticus* subsp. *saprophyticus* CCM 883 ^{T}, *Staphylococcus saprophyticus* subsp. *bovis* CCM 4410 ^{T}, and *Staphylococcus xylosus* CCM 2738 ^{T}. All data were obtained in this study. Values of less than 1% are not shown. All strains were cultivated on TSBA agar plates for 24 h at 28±1°C.

Fatty acid	CCM 8730^T	CCM 8731	CCM 883 ^{T}	CCM 4410 ^{T}	CCM 2738 ^{T}
$C_{13:0}$ iso	TR	TR	TR	TR	2.2
$C_{13:0}$ anteiso	ND	TR	ND	ND	2.2
$C_{14:0}$ iso	TR	TR	TR	TR	1.4
$C_{14:0}$	TR	TR	TR	1.0	1.3
$C_{15:0}$ iso	13.3	13.2	13.4	14.8	19.6
$C_{15:0}$ anteiso	51.4	51.0	52.8	45.6	42.0
$C_{16:0}$ iso	1.2	1.2	1.2	1.1	1.3
$C_{16:0}$	2.5	2.6	1.4	3.30	2.7
$C_{17:0}$ iso	5.6	5.3	6.3	6.0	5.8
$C_{17:0}$ anteiso	12.9	12.8	12.9	9.9	5.9
$C_{18:1}$ *ω9c*	TR	TR	ND	ND	1.1
$C_{18:0}$	3.5	3.7	2.4	5.5	4.8
$C_{19:0}$ iso	1.2	1.2	2.3	1.8	2.0
$C_{20:1}$ *ω9c*	1.0	1.0	ND	ND	1.6
$C_{20:0}$	5.2	5.6	5.2	8.6	4.9

Legend: TR, trace amounts (< 1%); ND, not detected

Table S2. Intergenomic distances between the genomes of *Staphylococcus edaphicus* CCM 8730^T and reference type strains of phylogenetically closest staphylococcal species represented by average nucleotide identity (ANI) and digitally derived genome-to-genome distances (GGD) emulating DNA-DNA hybridization (DDH) values (%).

Reference genome	*S. edaphicus* CCM 8730^T		*S. saprophyticus* ATCC 15305^T		*S. xylosus* CCM 2783^T		*S. equorum* UMC-CNS-924		*S. succinus* DSM 14617^T		*S. gallinarum* DSM 20610^T	
	ANI (%)	dDDH	ANI (%)	dDDH	ANI (%)	dDDH	ANI (%)	dDDH	ANI (%)	dDDH	ANI (%)	dDDH
		Formula*										
***S. edaphicus* CCM 8730^T** GenBank accession number MRZN00000000	-	1 -	84.78	63.50% [59.7 - 67.1%]	80.37	35.00% [31.7 - 38.6%]	79.49	30.10% [26.7 - 33.7%]	78.53	26.00% [22.7 - 29.7%]	76.9	21.90% [18.7 - 25.6%]
		2 (recom.) -		**29.00% [26.6 - 31.5%]**		**24.00% [21.7 - 26.4%]**		22.90% [20.6 - 25.3%]		**22.20% [19.9 - 24.6%]**		**21.30% [19.1 - 23.8%]**
		3 -		53.00% [49.9 - 56.1%]		31.20% [28.3 - 34.3%]		27.30% [24.4 - 30.5%]		24.20% [21.3 - 27.3%]		20.90% [18.1 - 23.9%]
***S. saprophyticus* ATCC 15305^T** GenBank accession number AP008934	84.78	1 63.50% [59.7 - 67.1%]	-	-	80.61	35.10% [31.7 - 38.6%]	79.71	33.90% [30.5 - 37.4%]	78.72	28.30% [25 - 32%]	77.29	22.60% [19.4 - 26.3%]
		2 (recom.) **29.00% [26.6 - 31.5%]**		-		**24.20% [21.9 - 26.7%]**		23.20% [20.9 - 25.7%]		**22.60% [20.4 - 25.1%]**		**21.90% [19.7 - 24.4%]**
		3 53.00% [49.9 - 56.1%]		-		31.30% [28.4 - 34.4%]		30.10% [27.2 - 33.2%]		26.00% [23.1 - 29.1%]		21.50% [18.7 - 24.6%]
***S. xylosus* CCM 2783^T** GenBank accession number MRZO00000000	80.37	1 35.00% [31.7 - 38.6%]	80.61	35.10% [31.7 - 38.6%]	-	-	79.78	31.50% [28.1 - 35.1%]	78.9	28.10% [24.7 - 31.7%]	77.38	22.50% [19.2 - 26.1%]
		2 (recom.) **24.00% [21.7 - 26.4%]**		**24.20% [21.9 - 26.7%]**		-		23.30% [21 - 25.8%]		**22.70% [20.4 - 25.1%]**		**21.70% [19.5 - 24.2%]**
		3 31.20% [28.3 - 34.3%]		31.30% [28.4 - 34.4%]		-		28.50% [25.5 - 31.6%]		25.80% [22.9 - 28.9%]		21.40% [18.6 - 24.5%]
***S. equorum* UMC-CNS-924** GenBank accession number CP013114	79.49	1 30.10% [26.7 - 33.7%]	79.71	33.90% [30.5 - 37.4%]	79.78	31.50% [28.1 - 35.1%]	-	-	79.86	32.70% [29.4 - 36.3%]	77.445	22.60% [19.3 - 26.3%]
		2 (recom.) 22.90% [20.6 - 25.3%]		23.20% [20.9 - 25.7%]		23.30% [21 - 25.8%]		-		23.30% [21 - 25.8%]		21.70% [19.4 - 24.1%]
		3 27.30% [24.4 - 30.5%]		30.10% [27.2 - 33.2%]		28.50% [25.5 - 31.6%]		-		29.40% [26.4 - 32.5%]		21.50% [18.7 - 24.5%]
***S. succinus* DSM 14617^T** GenBank accession number LCSH00000000	78.53	1 26.00% [22.7 - 29.7%]	78.72	28.30% [25 - 32%]	78.9	28.10% [24.7 - 31.7%]	79.86	32.70% [29.4 - 36.3%]	-	-	78.19	25.70% [22.4 - 29.4%]
		2 (recom.) **22.20% [19.9 - 24.6%]**		**22.60% [20.4 - 25.1%]**		**22.70% [20.4 - 25.1%]**		23.30% [21 - 25.8%]		-		**22.80% [20.5 - 25.2%]**
		3 24.20% [21.3 - 27.3%]		26.00% [23.1 - 29.1%]		25.80% [22.9 - 28.9%]		29.40% [26.4 - 32.5%]		-		24.00% [21.2 - 27.1%]
***S. gallinarum* DSM 20610^T** GenBank accession number JXCF00000000	76.9	1 21.90% [18.7 - 25.6%]	77.29	22.60% [19.4 - 26.3%]	77.38	22.50% [19.2 - 26.1%]	77.45	22.60% [19.3 - 26.3%]	78.19	25.70% [22.4 - 29.4%]	-	-
		2 (recom.) **21.30% [19.1 - 23.8%]**		**21.90% [19.7 - 24.4%]**		**21.70% [19.5 - 24.2%]**		21.70% [19.4 - 24.1%]		**22.80% [20.5 - 25.2%]**		-
		3 20.90% [18.1 - 23.9%]		21.50% [18.7 - 24.6%]		21.40% [18.6 - 24.5%]		21.50% [18.7 - 24.5%]		24.00% [21.2 - 27.1%]		-

Legend: *, recommended formula no. 2 for draft genomes (70)

Table S3. Metabolic fingerprints of *Staphylococcus edaphicus* sp. nov. obtained using Biolog GEN III MicroPlate.

Variable metabolic fingerprints:

Strain	N-Acetyl-D-glucosamine	D-Fucose	L-Rhamnose	D-Serine	D-Fructose-6-PO4	Rifamycin SV	Quanidine HCl	Methyl pyruvate	D-Lactic acid Methyl Ester	Citric acid	α-Keto glutaric acid	L-Malic acid
CCM 8730^T	+	-	+	+	+	b	+	+	+	+	+	+
CCM 8731	-	b	b	-	b	-	-	b	b	b	b	-

Legend: +, positive; -, negative; b, borderline

Positive utilisation of: dextrin, D-maltose, D-trehalose, gentiobiose, sucrose, D-turanose, β-methyl-D-glucoside, D-salicin, N-acetyl-β-D-mannosamine, N-acetyl neuraminic acid, α-D-glucose, D-mannose, D-fructose, D-galactose, inosine, D-mannitol, D-arabitol, glycerol, glycyl-L-proline, L-alanine, L-arginine, L-aspartic acid, L-glutamic acid, L-histidine, L-serine, pectin, D-gluconic acid, D-glucuronic acid, glucuronamide, L-lactic acid, Tween 40, acetoacetic acid, acetic acid and formic acid.

Positive growth: pH 6.0, 1% NaCl, 4% NaCl, 8% NaCl, 1% sodium lactate, nalidixic acid, lithium chloride, potassium tellurite, aztreonam and sodium butyrate.

Negative utilisation of: D-cellobiose, stachyose, D-raffinose, α-D-lactose, D-melibiose, N-acetyl-D-galactosamine, 3-methyl glucose, L-fucose, D-sorbitol, myo-inositol, D-glucose-6-PO4, D-aspartic acid, D-serine, gelatin, L-pyroglutamic acid, D-galacturonic acid, D-galactonic acid lactone, mucic acid, quinic acid, D-saccharic acid, p-hydroxy phenylacetic acid, D-malic acid, bromo-succinic acid, γ-amino-butyric acid, α-hydroxy-butyric acid, β-hydroxy-D,L-butyric acid, α-keto butyric acid and propionic acid.

Negative growth: pH 5.0, fusidic acid, troleandomycin, minocycline, lincomycin, niaproof 4, vancomycin, tetrazolium violet, tetrazolium blue and sodium bromate.

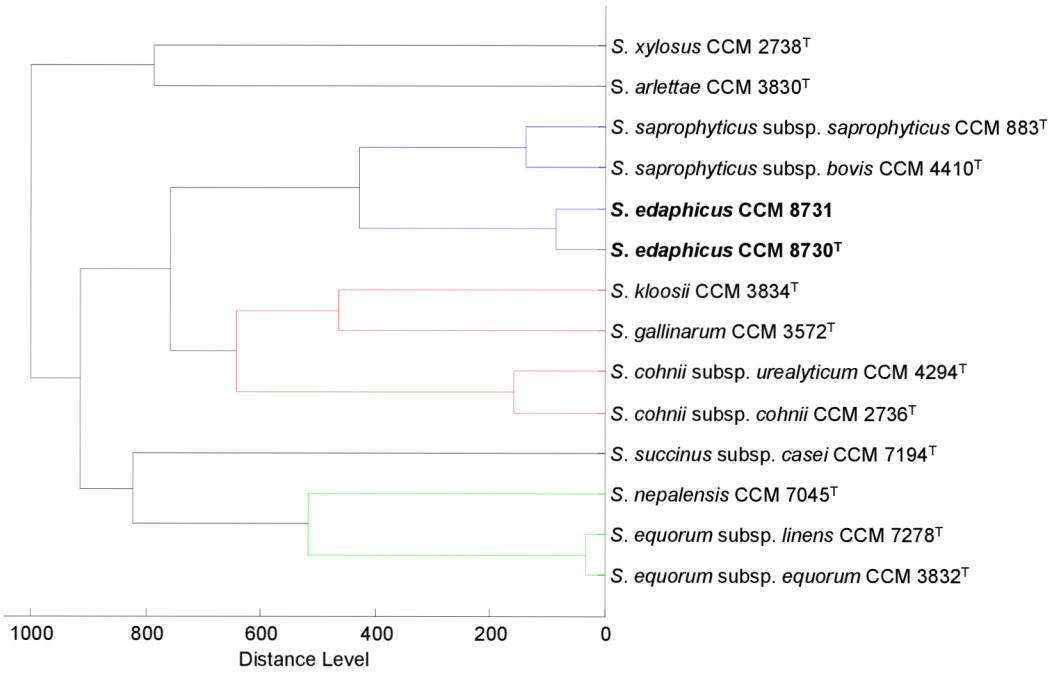

Fig. S1. Dendrogram based on MALDI-TOF MS profiles of *Staphylococcus edaphicus* sp. nov. and other phylogenetically related species. The MALDI-TOF MS profiles were acquired using a Microflex instrument (Bruker Daltonik) and the dendrogram was generated using the correlation distance measure with the average linkage algorithm (UPGMA).

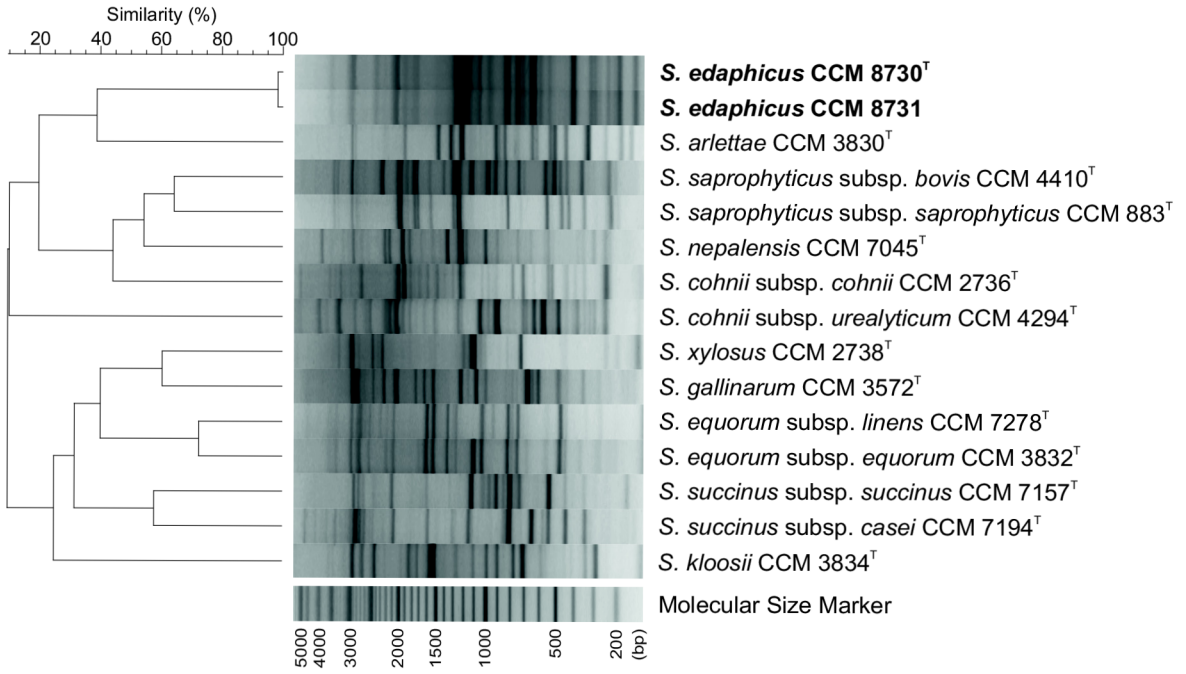

Fig. S2. Dendrogram based on cluster analysis of rep-PCR fingerprints obtained with $(GTG)_5$ primer from novel *Staphylococcus* strains and the type strains of the phylogenetically closely related species. The dendrogram was calculated with Pearson's correlation coefficients with UPGMA clustering method (*r*, expressed as percentage similarity values).

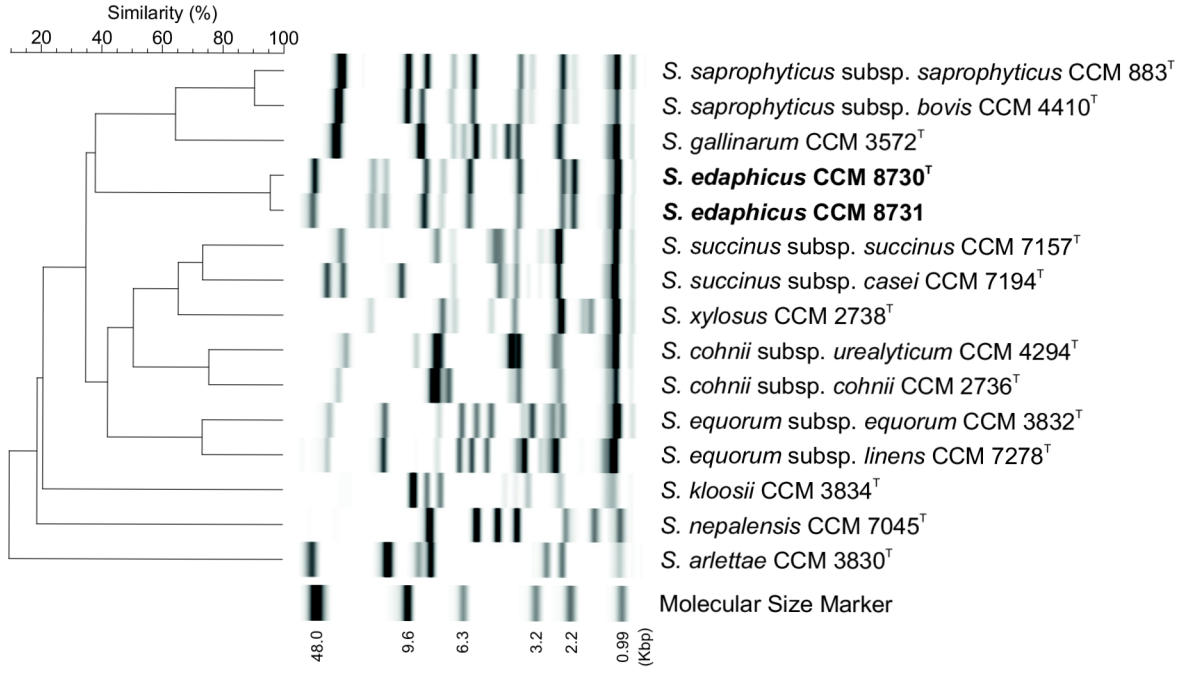

Fig. S3. Dendrogram based on cluster analysis of *Eco*RI ribotype patterns obtained using the RiboPrinter system from novel *Staphylococcus* strains and the type strains of phylogenetically closely related species. The dendrogram was calculated with Pearson's correlation coefficients with the UPGMA clustering method (*r*, expressed as percentage similarity values).

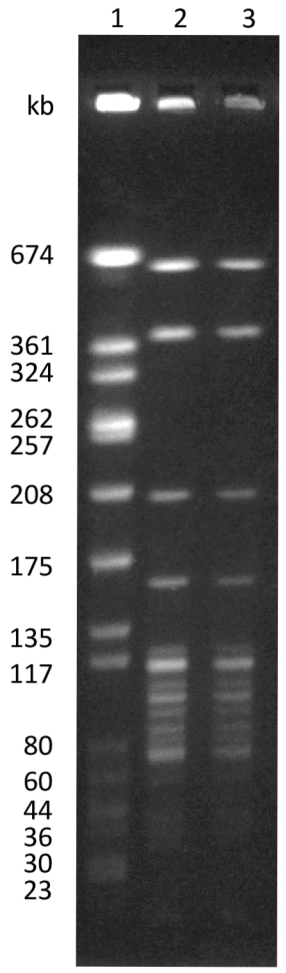

Fig. S4. Pulsed-field gel electrophoresis showing identical *Sma*I macrorestriction patterns of *Staphylococcus edaphicus* sp. nov. strains CCM 8730^T (lane 2) and CCM 8731 (lane 3). *Staphylococcus aureus* NCTC 8325 was used as a size marker (lane 1).

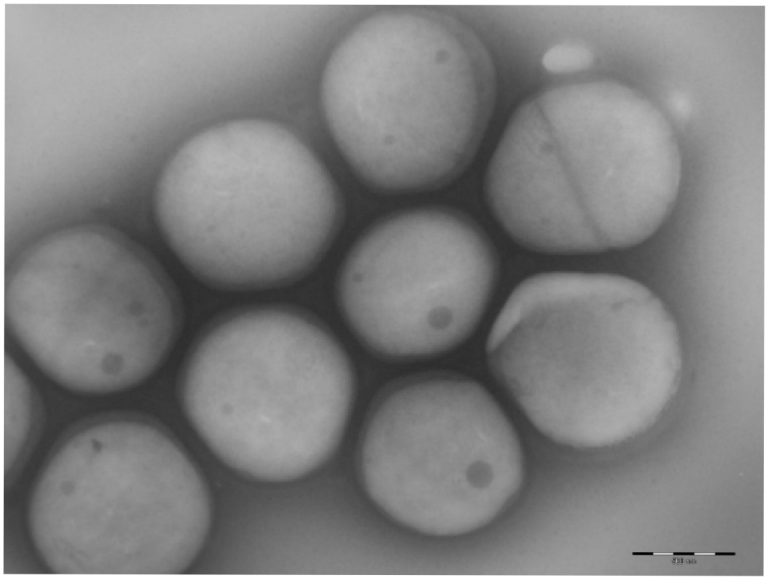

Fig. S5. Transmission electron microscopy of the type strain *Staphylococcus edaphicus* CCM 8730^T performed with a Morgagni 268D Philips (FEI Company, USA) electron microscope. Negative staining with 2% ammonium molybdate. Bar represents 500 nm (original magnification ×10,000).